UNIVERSIDAD DE GRANADA

FACULTAD DE FARMACIA

Departamento de Química Farmacéutica y Orgánica

INTERNATIONAL DOCTORATE DEGREE

PhD THESIS

Synthesis and biological evaluation versus Nitric Oxide Synthase of novel pyrazolines and *N*,*N'*-disubstituted urea and thiourea derivatives

TESIS DOCTORAL

Síntesis y evaluación biológica frente a Óxido Nítrico Sintasa de nuevas pirazolinas y derivados de urea y tiourea *N*,*N'*-disustituidos

Programa de doctorado en Química

Meriem Chayah Ghaddab

Granada, 2015

Editorial: Universidad de Granada. Tesis Doctorales
Autora: Meriem Chayah Ghaddab
ISBN: 978-84-9125-390-7
URI: http://hdl.handle.net/10481/41557

La doctoranda Meriem Chayah Ghaddab y los directores de la tesis Miguel Ángel Gallo Mezo, Mª Encarnación Camacho Quesada y Mª Dora Carrión Peregrino garantizamos, al firmar esta tesis doctoral, que el trabajo ha sido realizado por la doctoranda bajo la dirección de los directores de la tesis y hasta donde nuestro conocimiento alcanza, en la realización del trabajo, se han respetado los derechos de otros autores a ser citados, cuando se han utilizado sus resultados o publicaciones.

Granada, 20 de octubre de 2015

DIRECTORES DE LA TESIS

Miguel Á. Gallo Mezo

Catedrático de Universidad
Facultad de Farmacia
Universidad de Granada

Mª Encarnación Camacho Quesada

Prof. Titular de Universidad
Facultad de Farmacia
Universidad de Granada

Mª Dora Carrión Peregrina

Prof. Titular de Universidad
Facultad de Farmacia
Universidad de Granada

DOCTORANDA

Meriem Chayah Ghaddab

El trabajo presentado en esta Memoria ha sido realizado gracias a la concesión de una beca predoctoral por el Programa de Formación en Investigación en Salud del Instituto de Salud Carlos III - Ministerio de Economía y Competitividad (FI11/00432).

Tres estancias han sido realizadas como complemento de formación durante el periodo predoctoral gracias a las ayudas para estancias breves concedidas dentro del Programa de Formación en Investigación en Salud del Instituto de Salud Carlos III y las subvenciones para la movilidad de estudiantes para la obtención de la mención europea en el título de doctor del Ministerio de Educación:

- Estancia en el Dipartimento di Scienze Chimiche e Farmaceutiche de la Universidad de Ferrara (Ferrara, Italia) durante 3 meses.

- Estancia en el Instituto de Biotecnología del Centro de Investigaciones Biomédicas de la Universidad de Granada (Granada, España) durante 6 meses.

- Estancia en el Laboratorio de Modelado Molecular y Simulación (Departamento de Ciencias Biomédicas, Área de Farmacología) de la Universidad de Alcalá de Henares (Madrid, España) durante 1 mes.

ÍNDICES

ÍNDICE / INDEX

ÍNDICE DE TABLAS Y FIGURAS
LIST OF TABLES AND FIGURES

INTRODUCCIÓN

TABLAS

FIGURAS

SUMMARY

ACRÓNIMOS / ACRONYMS

aMK: N-acetil-5-metoxikinurenamina
ATP: Adenosín Trifosfato
APP: Proteína Precursora de Amiloides
CaM: Calmodulina
CaCaM: Ca-calmodulina
cGMP: Guanosín Monofosfato 3',5'-cíclico
DNA: Ácido desoxirribonucleico
EE.UU: Estados Unidos
EDRF: Factor Relajador derivado del endotelio
eNOS: Óxido Nítrico Sintasa endotelial
FAD: Flavín Adenín Dinucleótido
FMN: FLavín Mononucleótido
GC: Guanilato Cliclasa
IDO: 3-dioxigenasa
iNOS : Óxido Nítrico Sintasa inducible
L-NAA: L-N -aminoarginina
L-NAME: L-N-nitroarginina metilester
L-NIO: L-N-iminoetilornitina
L-NNA: L-N-nitroarginina
L-NPLA: L-N-propilarginina
LPS: Lipopolisacárido
LTD: Depresión a largo plazo
LTP: Potenciación a largo plazo
mtNOS: NOS mitocondrial
NANC: Neuronas no colinérgicas no adrenérgicas
NADPH: Nicotinamida adenín dinucleótido fosfato
NMDA: N-metil-D-aspartato
nNOS: Óxido Nítrico Sintasa neuronal
NO: Óxido Nítrico

NOS: Óxido Nítrico Sintasa

PDZ: acrónimo que combina las primeras letras de tres proteínas: proteína de densidad postsináptica (PSD95), proteína supresora de tumores en Drosophila (DlgA) y la proteína zonula occludens-1 (Zo-1), que fueron las primeras en las cuales se descubrió este dominio.

PIN: Proteína Inhibidora de NOS

PPT: Poro de permeabilidad transitoria

REA: Relación Estructura Actividad

RNS: Especies Reactivas de Nitrógeno

ROS: Especies Reactivas de Oxígeno

SNC: Sistema Nervioso Central

SNP: Sistema Nervioso Periférico

SOD: Superóxido dismutasa

TRIM: Trifluorometilfenilimidazol

1. INTRODUCCIÓN

“Cuando Robert Furchgott, Louis Ignarro y Ferid Murad descubrieron, de manera independiente, que un gas de vida muy breve, el óxido nítrico (NO), se producía endógenamente y actuaba como molécula señalizadora entre células, aquello fue algo inesperado y único. Se inició, así, un nuevo capítulo en la investigación biomédica y se abrieron nuevos horizontes.
Fue Robert Furchgott quién abrió el camino en 1980. Durante los años 70, se había observado que la capa celular interna de los vasos sanguíneos, el endotelio, no sólo tenía propiedades pasivas y protectoras sino que la contracción y la relajación de los vasos sanguíneos dependían de la presencia del endotelio. En un brillante experimento (el llamado experimento sándwich), Furchgott hizo un descubrimiento crucial que sentó las bases para futuras investigaciones científicas.

En este estudio se observaron las respuestas de distintas secciones de la aorta. Una sección tenía la capa endotelial intacta, mientras que en la otra se había eliminado. En ausencia de endotelio, Furchgott registró una contracción que respondía a la estimulación. La sección con endotelio se preparó de tal manera que no se pudieran dar ni la contracción ni la relajación. Cuando juntó las dos secciones en un modelo “sándwich”, observó que esa misma estimulación ya no producía una contracción, sino una relajación. Furchgott concluyó que en el endotelio se producía una sustancia desconocida, un factor, que se transportaba hasta la sección de la aorta sin endotelio y que eso provocaba la relajación.
Fue un gran descubrimiento que dio el pistoletazo de salida en la búsqueda de la identidad de este factor endotelial, una búsqueda que duró seis años.

Se lanzaron diferentes hipótesis. Una de ellas señalaba que debía haber implicados compuestos nitrogenados. En este campo de la investigación se movía Ferid Murad. Sabía que la nitroglicerina activaba una enzima en las células musculares aórticas, la guanilato cliclasa (GC), que aumentaba el cGMP (guanosín monofosfato 3', 5'-cíclico) y provocaba relajación. En este momento Ferid Murad planteó una pregunta importante: ¿Actuaba la nitroglicerina liberando NO? Probó esta hipótesis burbujeando NO gaseoso a través de una preparación de tejido con GC. La producción de cGMP aumentó. Se acababa de descubrir una nueva forma en la que las drogas activaban la función de una enzima. El principio de acción de la nitroglicerina, desconocido hasta ahora a pesar de los más de 100 años de exitosos tratamientos de la angina de pecho, se había descubierto.
Estos experimentos llevados a cabo por Ferid Murad, unos años después del descubrimiento de Furchgott del factor endotelial, crearon un conocimiento nuevo que, posteriormente, se convertiría en la clave de la identificación del factor endotelial.

Fue en este camino en el que el tercer premiado, Louis Ignarro, conducía sus actividades y experiencias científicas. Inspirado por los descubrimientos de Murad, también, observó que el NO relajaba la vasculatura. De manera simultánea e independiente a Robert Furchgott, añadió, durante la primera mitad de los años 80, nuevos descubrimientos sobre este factor. Su identidad era cada vez más clara. La búsqueda del desconocido factor endotelial de Furchgott acabó en un congreso científico en la Clínica Mayo, en Rochester, Minnesota (EE.UU), en el verano de 1986.
En el congreso, Furchgott concluyó, basándose en varios hallazgos, que el factor era idéntico al NO. Ignarro apoyó esta teoría en el mismo congreso, y fue más allá, con un interesante experimento: utilizó el análisis de espectro, lo que significa que cada sustancia emite un espectro único y específico. Encontró espectros idénticos cuando la hemoglobina reactiva reaccionaba con el factor endotelial, y cuando reaccionaba con el NO, y concluyó que el

factor era el NO. La búsqueda había acabado, el misterio del factor endotelial se había resuelto.

Este gas endógeno de vida breve, con capacidad para actuar como una molécula señalizadora entre las células del cuerpo, supuso un fenómeno nuevo. El descubrimiento explicaba el mecanismo de acción de la nitroglicerina al tratar la tensión arterial y la angina, enfermedad que padeció Alfred Nobel… El descubrimiento de que el factor endotelial era el NO también abrió la puerta a nuevas terapias en la medicina clínica, mejoró la capacidad de diagnóstico de enfermedades inflamatorias graves y abrió nuevas posibilidades para el desarrollo de medicamentos. La investigación en el campo del NO desde 1986 hasta nuestros días es enorme.
Profesores Robert Furchgott, Louis Ignarro y Ferid Murad: Sus descubrimientos sobre el NO como molécula señalizadora en el sistema cardiovascular, no sólo han explicado los mecanismos de acción de un antiguo e importante grupo de medicamentos, los nitro- vasodilatadores, sino que además han abierto nuevos caminos para el tratamiento y diagnóstico de muchas enfermedades. Sus descubrimientos han elevado la investigación médica a una nueva era. (…)"[1a]

En la actualidad, el Óxido Nítrico (NO) se encuentra relacionado con infinidad de procesos tanto fisiológicos como patológicos. Su implicación en enfermedades neurodegenerativas, inflamatorias, inmunes o cardiovasculares suscitó mucho interés y promovió la búsqueda de estrategias tanto para luchar contra estas patologías como para entender su fisiopatología.

La familia enzimática de las Óxido Nítrico Sintasas (NOSs) es la responsable de la biosíntesis del NO. Estas isoenzimas tienen distinta localización y están sujetas a una estricta y compleja regulación, lo que hace que cualquier desajuste positivo o negativo conlleva la alteración y el

desorden de todos los procesos fisiológicos relacionados. De este modo, una sobreexpresión de las isoformas neuronal (nNOS) e inducible (iNOS) a nivel del sistema nervioso (SN) causa un exceso de NO que genera un estado progresivo de estrés oxidativo y nitrosativo. Esta situación produce alteraciones a nivel de las células nerviosas induciendo su apoptosis y la consiguiente degeneración neuronal. También el aumento de la expresión de iNOS se ha visto implicado en enfermedades inflamatorias crónicas, varios tipos de tumores, etc. Igualmente una alteración en los niveles de la eNOS contribuye a la patogénesis de ciertas enfermedades vasculares como la aterosclerosis y la hipertensión.

Por todo lo anterior, la regulación farmacológica de la síntesis de NO representa una importante estrategia en el tratamiento de enfermedades neurodegenerativas, inflamatorias, cardiovasculares y en la quimio-prevención del cáncer.

En este sentido se plantea la presente investigación con el fin de desarrollar nuevas moléculas que inhiban la nNOS y la iNOS sin afectar a la eNOS ya que la inhibición de esta última produce efectos adversos a nivel vascular.

En este trabajo se detalla el diseño, síntesis, caracterización y análisis de la actividad biológica de 3 familias de inhibidores de las isoformas neuronal e inducible de la NOS.

1.1 Óxido Nítrico

El óxido nítrico (NO) es un gas diatómico hidrofóbico sintetizado en distintas células del organismo. Es un importante metabolito en el organismo de los mamíferos[1b]. Su pequeño tamaño y su carga neutra le permiten difundir rápidamente (50um/s) de su lugar de formación al de su acción atravesando las membranas biológicas de la mayoría de los tejidos[2]. Es un radical libre con un electrón desapareado que tiene una vida media de 0.5-5 segundos[3] antes de convertirse en nitrato (NO_3^-) o nitrito (NO_2^-)[4]. Estas características junto con los diferentes estados de oxidación del nitrógeno[5] (forma reducida como nitrosilo NO^- y forma oxidada como nitrosonio NO^+) constituyen la base de su implicación en una gran variedad de reacciones. Es capaz de interaccionar con moléculas inorgánicas, grupos prostéticos y proteínas siendo muchos de éstos receptores y moléculas reguladoras[6].

Por todas estas peculiaridades, desde su descubrimiento, en 1980, como el factor relajador derivado del endotelio (EDRF) por parte de Furchgott y Zawadzki[7], se le fueron atribuyendo numerosas funciones fisiológicas e implicando en diversos procesos patológicos[8-11].

En el sistema cardiovascular, el NO interviene en la regulación de la presión arterial controlando el tono vascular y actuando como agente vasodilatador, inhibe la agregación plaquetaria y leucocitaria y mejora la microcirculación gástrica. En los riñones controla la microcirculación glomerular y la secreción de sodio[12]. Además, está muy relacionado con el sistema inmunitario[13,14] al estar implicado en procesos inflamatorios como artritis, miocarditis, colitis, nefritis y, también, con grandes patologías de nuestro tiempo como la diabetes, el cáncer o el sida[15-17].

Por otro lado, además de actuar como un mensajero biológico, el NO interviene a nivel del SN como un neurotransmisor, aunque atípico. A pesar

de que cumple algunos criterios establecidos para este tipo de moléculas (difunde de una neurona a otra y tiene un receptor hierro hemínico en el centro activo de la GC), incumple otros (no se almacena en vesículas sinápticas, no se libera por exocitosis, no se metaboliza por enzimas específicas y su receptor es la GC y no un receptor de membrana)[18-21]. En el sistema nervioso periférico (SNP), el NO controla la secreción hormonal, la visión, la respiración, etc. Mientras, en el sistema nervioso central (SNC), juega un papel crítico en diversas funciones como la memoria y el aprendizaje, la secreción de neurotransmisores, la plasticidad sináptica, la regulación de la expresión de ciertos genes y la percepción del dolor entre otras. Sin embargo, el NO se asocia, también, con la dependencia física a drogas, el daño neuronal causado por el etanol y con multitud de procesos neurodegenerativos como las enfermedades de Párkinson, Alzheimer, Huntington, etc[22].

1.2 Biosíntesis del NO

Inmediatamente después de la identificación del NO, el grupo de Moncada demostró que éste se sintetizaba a partir del amino ácido L-arginina[23] que se encuentra de forma natural a altas concentraciones (60-80 μM) en la sangre y en el fluido extracelular, y a concentraciones todavía más altas dentro de las células[24].

La reacción de síntesis del NO consiste en una serie de oxidaciones y reducciones, catalizada por la familia de las óxido nítrico sintasas (NOSs) y en la que se encuentran implicados varios cofactores que tienen su sitio de unión específico en la enzima. El átomo de nitrógeno del NO proviene del nitrógeno guanidínico de la L-arginina y el átomo de oxígeno del oxígeno molecular (O_2).

La reacción de síntesis se produce en dos fases que combinan la reducción del NADPH (nicotinamida adenín dinucleótido fosfato), uno de los

cofactores, con la oxidación del hierro del grupo hemo presente en el sitio activo. La reacción resulta en la conversión de la L-arginina en L-citrulina y NO. En la primera fase, la arginina se transforma en *N*$^{\omega}$-hidroxi-L-arginina (NHA) consumiendo un mol de O_2 y un mol de NADPH[25,26]. En la segunda fase, se consumen otro mol de O_2 y 0.5 mol de NADPH con los que el intermediario NHA se oxida a L-citrulina y el nitrógeno *N*$^{\omega}$-guanidino se libera en forma de NO[23,27,28]. En líneas generales, por cada mol de NO generado se consumen 2 moles de oxígeno y 1.5 moles de NADPH[29] (Figura 1).

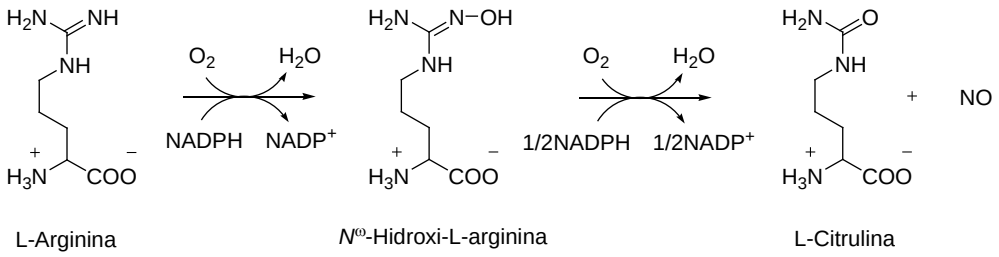

Figura 1. Biosíntesis del NO a partir de L-arginina.

Para la activación del oxígeno molecular, el NADPH actúa como fuente de electrones. Estos electrones se transportan a través de los cofactores FAD (flavín adenín dinucleótido) y FMN (flavín monoleótido) hasta el hierro del grupo hemo que representa el centro catalítico responsable de la unión y reducción de oxígeno y, en consecuencia, la correspondiente oxidación del sustrato L-arginina[30].

Hasta hace poco, se pensaba que las NOSs eran las únicas fuentes de NO en los mamíferos, pero se ha demostrado que hay una ruta alternativa para su formación. Se trata del ciclo de nitrato-nitrito-NO, en el que los iones inorgánicos NO_3^- y NO_2^- se reconvierten en NO a nivel de la sangre y los tejidos. La primera etapa, reducción de NO_3^- a NO_2^-, la realizan bacterias

comensales, mientras que el paso de NO_2^- a NO lo llevan a cabo enzimas[31,32].

Esta ruta destaca por sus condiciones anaeróbicas al contrario de la ruta de la NOS ya que las bacterias no necesitan oxígeno para la reacción de reducción. Se ha demostrado que, a muy bajas concentraciones de oxígeno, se puede generar NO de forma independiente de la NOS y dependiente de NO_2^-. Esto hizo pensar que esta ruta alternativa se puede considerar como un sistema de apoyo complementario a la ruta clásica principalmente en condiciones de hipoxia, cuando las isoformas de la NOS no son funcionales. Y todo ello para garantizar unos niveles adecuados de NO cuando el aporte de oxígeno es limitado[33].

1.3 Óxido Nítrico Sintasas

1.3.1 Visión general y clasificación

La síntesis enzimática del NO a partir de L-arginina está catalizada por una familia de isoenzimas denominada Óxido Nítrico Sintasas (NOSs). En los mamíferos se han descubierto, hasta la actualidad, cuatro isoformas: NOS neuronal (nNOS o NOS-I), NOS inducible (iNOS o NOS-II), NOS endotelial (eNOS o NOS-III)[34] y NOS mitocondrial (mtNOS)[35-37]. Sobre ésta última parece que todavía no hay claro consenso[38].

El nombre de cada isoforma proviene de las células en las que fue descubierta por primera vez y el número indica el orden en el que fueron aisladas. Aunque estas isoenzimas convergen en la biosíntesis del NO, presentan varias diferencias a nivel de sus genes de procedencia, su secuencia de aminoácidos, localización subcelular, regulación y funciones.

Las tres principales isoformas de la NOS son codificadas por genes con distinta localización cromosómica[39] (Tabla 1).

Isoforma humana	Cromosoma	Tipo	Dependencia de Ca
nNOS (NOS-I)	12	Constitutiva	Ca-dependiente
eNOS (NOS-II)	7	Constitutiva	Ca-dependiente
iNOS (NOS-III)	17	Inducible	Ca-independiente

Tabla 1. Características y localización cromosómica de las NOSs humanas[24,39].

Las isoformas nNOS, descubierta por Bredt y Snyder[20], y eNOS, inicialmente identificada por Lamas y Michel[40], son constitutivas bajo la mayoría de las condiciones aunque pueden ser inducidas en situaciones de estrés, daño y/o diferenciación celular[41]. Son calcio-dependientes de manera que requieren altas concentraciones de calcio para activarse. El aumento de los niveles de calcio intracelular (≥100nM) permite la formación del complejo Ca-calmodulina (CaCaM) necesario para la activación de ambas isoformas[42].

La isoforma inducible, aunque se detectó de forma constitutiva en pocos tipos celulares y en muy pequeñas concentraciones, su expresión es inducida transcripcionalmente en todos los tipos celulares en los que se ha probado[43] por endoxinas como el lipopolisacárido (LPS) y mediadores pro-inflamatorios endógenos tales como las citoquinas IFN- γ y TNF-α e interleuquina-1β (IL-1β)[44]. La iNOS, a diferencia de las otras isoformas, no depende del calcio para su activación ya que la CaM se encuentra permanentemente unida a su estructura[45].

La última isoforma descubierta, la mtNOS, ha sido y es un tema controvertido ya que, tras muchos estudios, se pudo observar que compartía muchas características con la isoforma neuronal y algunos la

identificaron como un transcrito de la nNOS, miristoilado y fosforilado, asociado a la membrana mitocondrial[46]. Se encuentra en la membrana interna de la mitocondria próxima a la cadena de transporte electrónico. Es constitutiva y Ca-dependiente. Así, un aumento en la concentración de Ca intramitocondrial aumenta la actividad de la isoenzima y como consecuencia disminuye el consumo de oxígeno y el potencial transmembrana y viceversa. Esto indica que la mtNOS interviene en la modulación de la respiración mitocondrial, la disponibilidad de oxígeno y de energía en las células y la señalización intramitocondrial relacionada con la apoptosis[47].

1.3.2 Estructura

Las NOSs son enzimas voluminosas (Tabla 2) que presentan entre un 50 y 60% de similitud y que se sintetizan como proteínas monoméricas constituidas por dos dominios de plegamiento independiente: un dominio oxigenasa en el extremo *N*-terminal y un dominio reductasa en el extremo C-terminal. Los dos dominios están unidos por un polipéptido con secuencia de unión a CaM[44] (Figura 2).

Isoforma humana	Número de amino ácidos (aa), tamaño	Estructura	Cofactores
nNOS (NOS-I)	1434 aa, 161 kDa	Homodímero	NADPH, FAD, FMN, hemo, BH_4, CaM
eNOS (NOS-II)	1203 aa, 133 kDa	Homodímero	NADPH, FAD, FMN, hemo, BH_4, CaM
iNOS (NOS-III)	1153 aa, 131 kDa	Homodímero	NADPH, FAD, FMN, hemo, BH_4

Tabla 2. Estructura de las NOSs humanas y aspectos relacionados[48].

La forma monomérica de la enzima es inactiva, y tiene que formar una estructura homodimérica mediante la unión de dos monómeros en la región hemo del dominio oxigenasa[49].

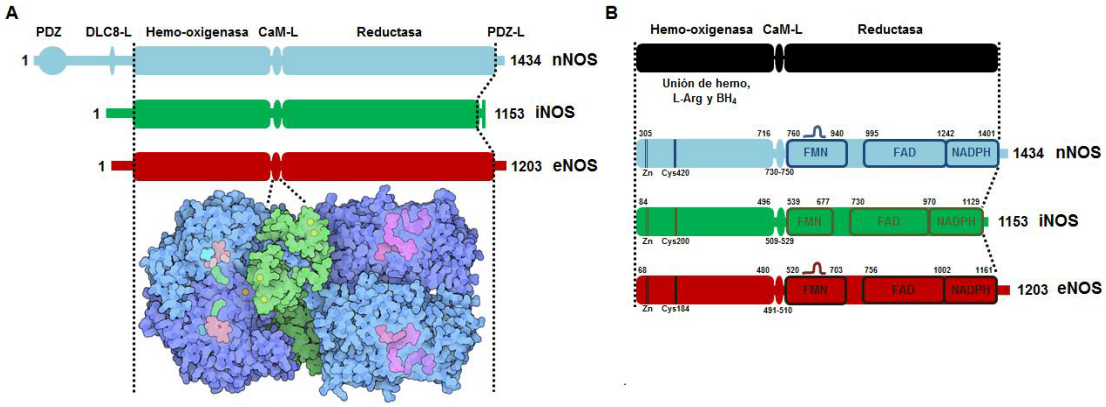

Figura 2. Dominios estructurales de las NOS humanas[49].

La nNOS es la isoforma más voluminosa (Figura 2A). Su mayor tamaño se debe, principalmente, a una extensión *N*-terminal exclusiva que incluye un dominio PDZ y una secuencia polipeptídica, que interacciona con la cadena ligera de dineína DLC8/DYNLL1[50,51], implicados ambos en procesos de localización subcelular y regulación de la nNOS. Mientras la iNOS posee una secuencia de aminoácidos carboxi-terminales que corresponde con un motivo de unión a dominios PDZ[52]. Esta secuencia presenta una variabilidad dependiendo del tipo celular[53,54] pudiendo indicar que diferentes proteínas con dominios PDZ pueden interaccionar específicamente con la iNOS en diferentes tejidos, determinando de esta forma una particular localización subcelular.

El dominio oxigenasa (Figura 2B) es funcionalmente similar, aunque no existe homología, a los citocromos de la familia P450, en tanto en cuanto realiza reacciones de monooxigenación y presenta una cisteína que ejerce de ligando axial del Fe del grupo hemo en su forma de tiolato. Es el dominio catalítico donde se produce la síntesis del NO y donde tienen sitio de unión la L-arginina, la tetrahidrobiopterina (BH_4) y el grupo hemo[43]. En este dominio, existe, además, un grupo zinc-tiolato formado por un átomo de zinc enlazado por puentes de hidrógeno y en conformación tetraédrica con los

grupos tiol (-SH) de dos pares de cisteínas, localizadas simétricamente en la interfase del dímero. Esto es esencial para la estabilidad del dímero y favorece la unión de BH_4[55].

El dominio reductasa alberga sitios de unión para los cofactores redox: NADPH, FAD y FMN. Este dominio de las NOSs presenta alta homología con el de los citocromos P450. Su principal función es permitir que el NADPH (donador de electrones) done electrones al grupo hemo (aceptor de electrones) a través de las flavinas FAD y FMN que actúan como cadena de transporte de electrones (Figura 3)[56]. La unión de la CaM permite la formación del dímero y por tanto la transferencia de los electrones de las flavinas al grupo hemo. El flujo de electrones se entrecruza entre los dos monómeros y los electrones de las flavinas que salen de uno pasan al grupo hemo del otro, lo que podría explicar la inactividad de los monómeros en estado fisiológico[57].

En la zona de unión de la FMN de las isoformas constitutivas (nNOS y eNOS) existe una secuencia de 40-50 aminoácidos que sirven de lazo autoinhibitorio que desestabiliza la unión de CaM a bajas concentraciones de calcio impidiendo la transferencia de electrones de FMN al grupo hemo[58,59]. La NOS inducible no tiene este lazo ya que, cotraduccionalmente, se le une la CaCaM de forma irreversible. Esta irreversibilidad se explica a través de los numerosos contactos entre ambas proteínas mostrados recientemente en una estructura cristalina del complejo[60].

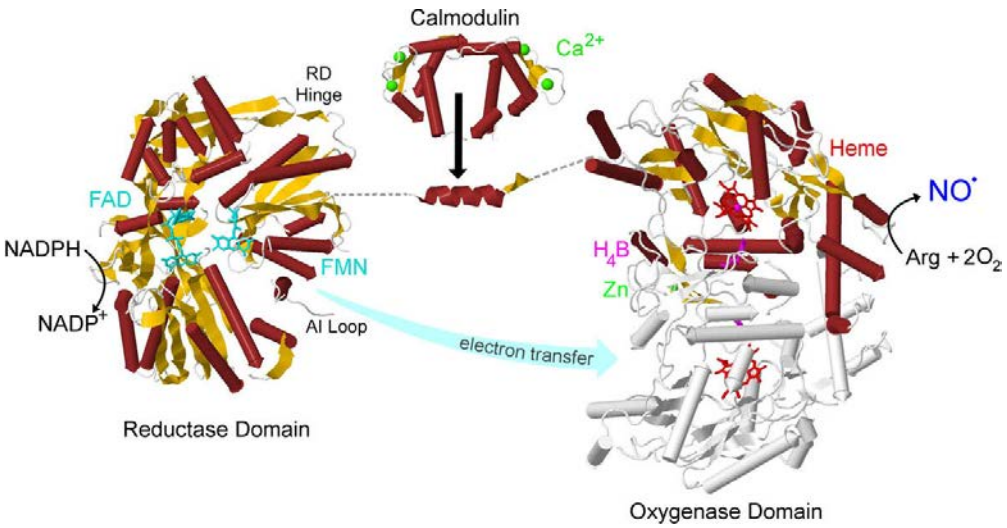

Figura 3. Estructura tridimensional de los dominios de las NOSs alineados según su secuencia de aminoácidos. Domino reductasa, dominio de unión a CaM y dominio oxigenasa dimérico[56].

1.3.2.1 Dimerización

Los homodímeros de las tres isoformas, a pesar de la similitud de los monómeros, presentan una gran diferencia a nivel de la fuerza de asociación de los monómeros, de su interfase y de la influencia de la L-arginina y BH_4 en su formación y estabilidad, dejando una puerta abierta a su regulación[61].

Para ser catalíticamente activas y sintetizar NO, todas las isoenzimas requieren una dimerización (Figura 4)[62a]. Este proceso es esencial porque permite la unión de la BH_4 a las dos subunidades, aumenta la afinidad del sitio de unión de la L-Arg y facilita el flujo electrónico hacia el grupo hemo.

Los monómeros, y los dominios reductasa por sí solos son capaces de transferir los electrones de NADPH a las flavinas FAD y FMN y tienen una capacidad limitada para reducir el oxígeno molecular a O_2^-. Los monómeros

y los dominios reductasa aislados pueden unir CaM, lo que estimula la transferencia de electrones al dominio reductasa. Sin embargo, los monómeros no pueden unir el cofactor BH_4 ni la L-Arg y por lo tanto no pueden catalizar la producción de NO (Figura 4A). La presencia del grupo hemo permite la dimerización de la NOS. El grupo hemo es el único cofactor indispensable para la interacción entre los dominios reductasa y oxigenasa y para la transferencia de electrones de un dominio a otro, desde las flavinas al grupo hemo del monómero opuesto. En ausencia de sustrato, las enzimas con el grupo hemo oxidan NADPH, produciendo O_2^- (Figura 4B).

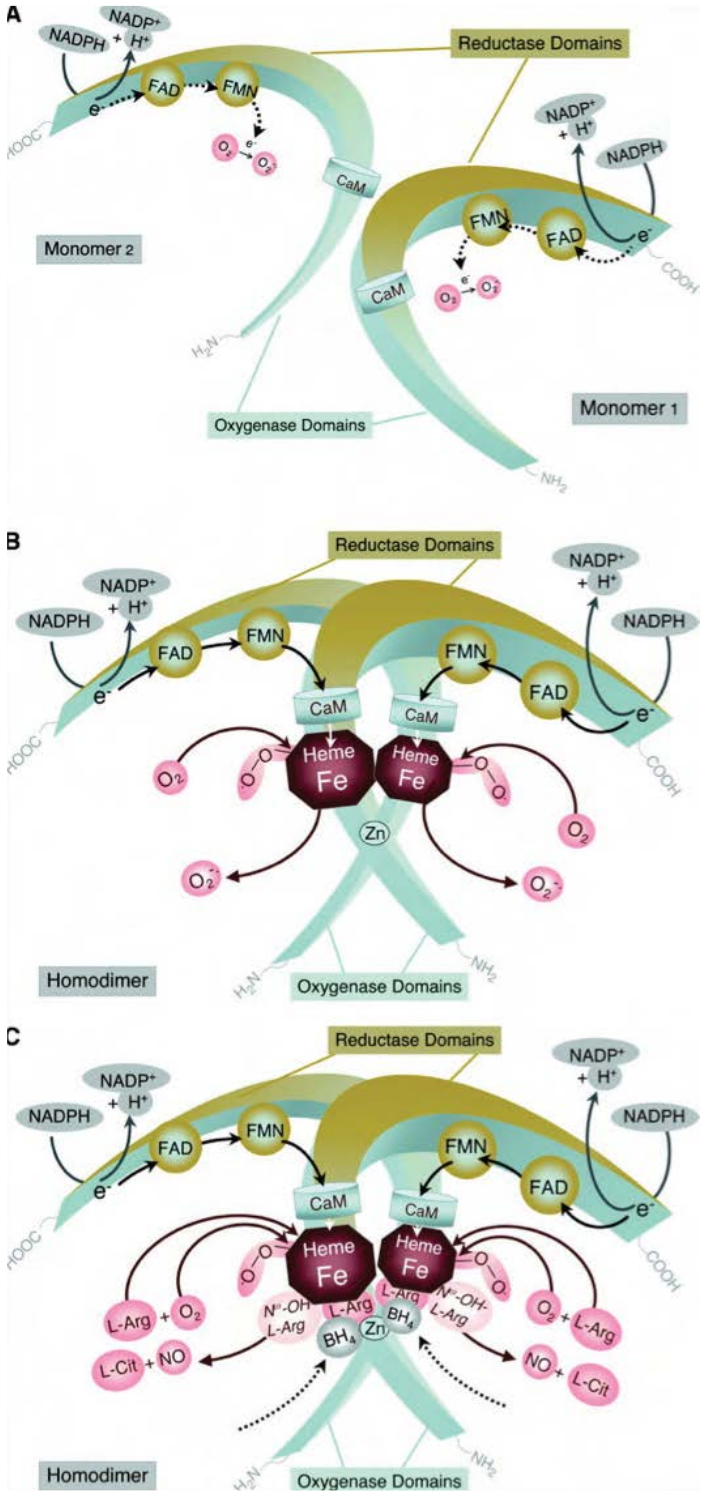

Figura 4. Estructura y dimerización de las NOSs en el proceso de síntesis del NO[62a].

Los electrones donados por el NADPH se transfieren del dominio reductasa al dominio oxigenasa *via* FAD, FMN y CaM[39,63]. El sitio de unión a CaM regula el flujo de electrones entre las dos regiones[64,65]. Cuando aumentan los niveles de calcio intracelular, la CaM se une a él para formar el complejo CaCaM[66], permitiendo el flujo de electrones y la oxidación de la L-arginina para formar L-citrulina y NO. En presencia de cantidades suficientes de sustrato (L-arginina) y cofactor BH_4, los dímeros de NOS acoplan la reducción de oxígeno para sintetizar NO y L-citrulina (Figura 4C, 5)[62a,b].

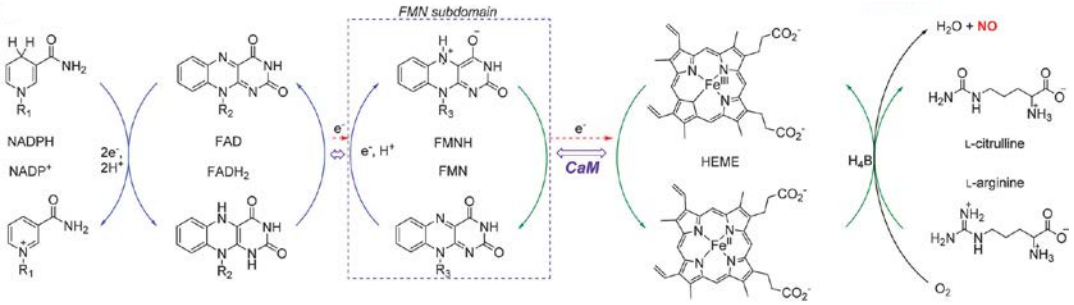

Figura 5. Flujo de electrones desde el NADPH hasta el grupo hemo para la síntesis del NO[62b].

1.3.3 Expresión y localización subcelular

Después de su descubrimiento en determinados tipos celulares, las NOSs se fueron encontrando en más células y tejidos (Tabla 3).

Isoforma humana	Expresión	Localización subcelular
nNOS (NOS-I)	Neuronas Músculo esquelético Músculo cardíaco	Citosol-membrana-núcleo
eNOS (NOS-II)	Células endoteliales	Membrana-aparato Golgi
iNOS (NOS-III)	Cualquier célula	Citosol-membrana

Tabla 3. Tipos celulares en los que se expresan las NOSs y localización subcelular.

La nNOS se expresa mayoritariamente en las neuronas del SNC, aunque también, en nervios nitrérgicos periféricos, en la médula espinal, en los ganglios simpáticos, en glándulas adrenales, en células epiteliales de varios órganos, en células de la mácula densa en el riñón, en células de islotes pancreáticos, en neutrófilos, en el músculo cardíaco, en el músculo liso vascular[44,67], en el músculo liso del tracto gastrointestinal, en los cuerpos cavernosos del pene, en la uretra y la prostata[68] y en el músculo esquelético[69,70]. Su localización subcelular viene determinada por la interacción de su dominio PDZ y la secuencia polipeptídica de su extremo *N*-terminal con muchas otras proteínas celulares[71-73]. Así, se detectó la nNOS tanto en el citosol como asociada a la membrana plasmática[74] y también, recientemente, en el núcleo, lo que puede contribuir a sus diversas funciones[63].

La eNOS se expresa, principalmente, en células endoteliales, si bien también se encuentra en miocitos cardíacos, plaquetas, ciertas neuronas del cerebro, en sincitio-trofoblastos de la placenta humana, en células epiteliales de algunos órganos[75,68], en células tubulares del riñón, fibroblastos, osteoblastos, etc[76]. Intracelularmente, se localiza, específicamente, en el aparato de Golgi y en pequeñas invaginaciones de la membrana plasmática llamadas caveolas, en forma dimérica funcional[48]. Además, una pequeña proporción se encuentra asociada al citoesqueleto en estado inactivo. Se detectó, también, en el citosol pero no se sabe si es activa o activable[77]. En esta localización subcelular intervienen acilaciones del extremo *N*-terminal: la miristoilación (Gly2) y la palmitoilación (Cys15, Cys25)[78], que afectan a la asociación a la membrana y al tráfico subcelular, y al direccionamiento a las caveolas, respectivamente.

La iNOS fue localizada, por primera vez, en macrófagos pero, posteriormente, en hepatocitos, células del músculo liso vascular, miocardio, microglía, astrositos, neuronas, mastocitos, linfocitos, hepatocitos,

cardiomiocitos, músculo esquelético, etc.[44,79,80]. Generalmente, la iNOS no se encuentra anclada a la membrana plasmática pero su presencia está enriquecida en ciertas zonas de la célula[48]. En forma palmitoilada, se puede encontrar anclada a la membrana plasmática aunque no necesariamente a las caveolas[81].

1.3.4 Regulación de la actividad

La regulación de la actividad de la nNOS y eNOS se produce de muchas maneras, a diferencia de la iNOS, que principalmente, se regula a nivel de expresión por mecanismos transcripcionales y post-transcripcionales[39,82,83].

Generalmente, los principales mecanismos que modulan la actividad de las NOSs son la dimerización, la fosforilación, la disponibilidad de sustratos y cofactores y la interacción con otras proteínas. Estos factores pueden afectar positiva o negativamente la actividad.

La dimerización aumenta la actividad de las NOSs al crear sitios de unión de gran afinidad por la BH_4 y la L-arginina, facilitando el flujo de electrones, como se ha comentado previamente. Además, la estabilización de los dímeros protege a las NOSs de la proteólisis[63]. La dimerización de la nNOS se puede inhibir por la PIN (proteína inhibidora de NOS)[84] y la de la iNOS por la kalirina a nivel cerebral[85].

La fosforilación afecta a la actividad de las NOSs de diferentes maneras, algunas aumentan la actividad mientras que otras la disminuyen. La nNOS y la eNOS se fosforilan en residuos de serina por proteínas quinasas[63,86]. La iNOS, también, parece ser regulada por fosforilación ya que hay datos que indican que tirosinas quinasas y fosfatasas regulan iNOS en macrófagos, aunque no se sabe cómo[5].

Como se mencionó anteriormente, las NOSs requieren para su actividad la presencia de cinco cofactores (FAD, FMN, hemo, BH_4 y CaM) y tres sustratos (L-arginina, oxígeno y NADPH). El grupo hemo es indispensable para la dimerización y la interacción entre los dominios reductasa y oxigenasa. En ausencia de sustrato, las enzimas con el grupo hemo oxidan el NADPH produciendo O_2^-. Las flavinas transportan los electrones hasta el hemo a través de la CaCaM que en su ausencia se ralentiza el flujo de electrones y se inactiva el enzima. La CaCaM se asocia a las isoformas constitutivas cuando aumentan los niveles intracelulares de calcio (dos cationes de calcio se unen a la CaM). Cuando vuelven a disminuir, el complejo CaCaM se disocia de las enzimas que se inactivan de nuevo[63]. Por su parte, la iNOS está permanentemente unida a la CaM y de este modo siempre activa, aún a niveles basales de calcio[82].

Las interacciones de las NOSs con otras proteínas se realizan a través de los dominios PDZ de forma alostérica, actuando sobre la unión de la CaM o a través de cascadas de señalización. Algunas de estas interacciones ya se han comentado: la interacción con la CaM (que por sí depende también de los niveles de calcio intracelular, como se ha descrito anteriormente), con la PIN y con la Kalirina. Otros ejemplos de interacciones son las que se producen entre la nNOS o la iNOS y la chaperona Hps90, incrementando su actividad[87] o la que ocurren entre la eNOS y la caveolina-1 o la caveolina-3 que inhiben la unión de CaCaM suprimiendo la actividad[63,88].

1.4 Funciones del NO

Las funciones del NO dependen fundamentalmente de la isoforma que lo sintetiza. La Figura 6 resume las funciones fisiológicas y patológicas en las que está implicado.

El NO producido por la nNOS está principalmente implicado en la señalización neuronal, la plasticidad sináptica, la modulación de rutas implicadas en el aprendizaje, la expresión del dolor y la neurotoxicidad[89].

El NO sintetizado por la eNOS interviene en la regulación de la función vascular. Promueve la vasodilatación, modula la presión arterial y mejora la microcirculación gástrica. Reduce los efectos dañinos de la ateroesclerosis y protege contra la hipoxia pulmonar. Por otro lado, inhibe la agregación plaquetaria y leucocitaria, así como la interacción entre plaquetas y leucocitos en el endotelio vascular. También, atenúa la respiración mitocondrial, regula la apoptosis, y reduce el estrés oxidativo. Los efectos del NO sobre la mitocondria, la muerte celular y el daño oxidativo protegen el corazón y otros tejidos frente a los daños isquémicos. El NO, además, aumenta la respuesta angiogénica tras una isquemia prolongada. En condiciones isquémicas, el NO_2^- se reduce a NO confiriendo citoprotección, mejora del flujo sanguíneo y angiogénesis vascular[90].

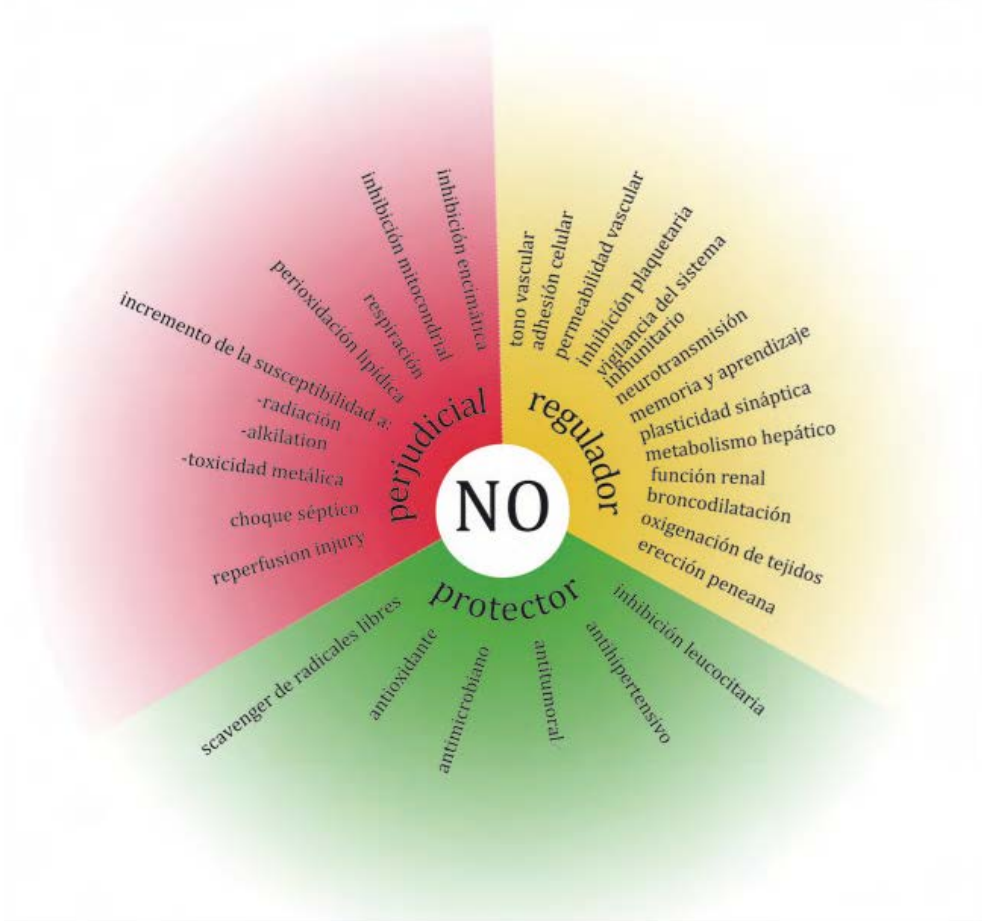

Figura 6. Funciones del NO.

El NO producido por la iNOS forma parte de la inmunidad no específica, ejerciendo acciones citostáticas o citotóxicas frente a microorganismos y células tumorales[91]. Actúa como modulador del sistema inmune y como un mediador proinflamatorio. Sin embargo, el NO posee la dualidad protectora/destructora inherente a los principales componentes del sistema inmune pudiendo causar procesos patológicos[92], como asma artritis, esclerosis múltiple, colitis, enfermedades neurodegenerativas, desarrollo de tumores, rechazo a los trasplantes o choque séptico[93].

1.4.1 NO en el Sistema Nervioso

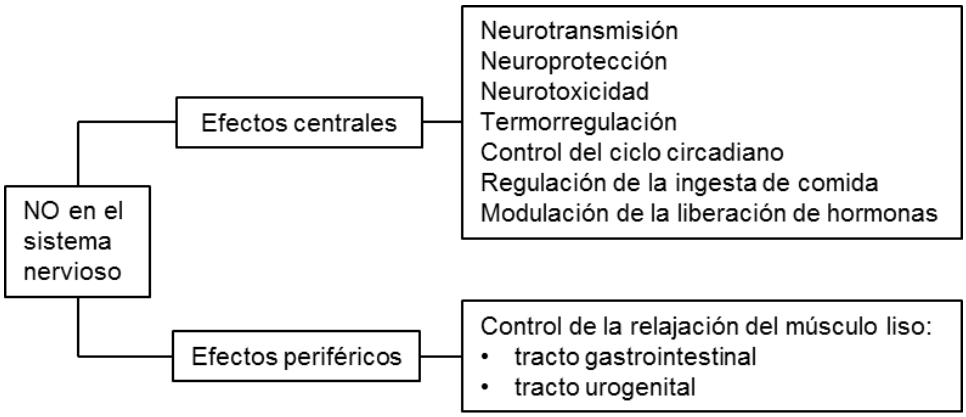

Figura 7. El NO en el sistema nervioso central y periférico[69].

A nivel del SNC (Figura 7), el NO es un mensajero retrógrado que coordina el aumento de los mecanismos pre y post-sinápticos involucrados en las principales formas de plasticidad sináptica, relacionadas con el aprendizaje y memoria: potenciación a largo plazo (LTP) y depresión a largo plazo (LTD)[94-96].

El NO está relacionado con el desarrollo del cerebro, la formación de la memoria y el comportamiento mediante la regulación de la plasticidad sináptica. La inhibición de la síntesis de NO produce amnesia[97] y afecta al aprendizaje espacial ya la memoria olfativa[98,99] y disminuye la actividad locomotora en tareas de habituación[100]. El NO, también, está implicado en la orientación neuronal[101,102], el procesamiento visual[103], el aprendizaje discriminatirio[104], el comportamiento frente a la comida y la bebida[105], la termorregulación[106], la tolerancia y abstinencia a opiáceos[107], el ritmo circadiano[108], el sueño[109] y la generación de patrones respiratorios[110]. La participación del NO en los mecanismos de comportamiento se ha confirmado en ratones deficientes de nNOS[111]. Está implicado, también, en las vías neurales nociceptivas centrales y periféricas[112] y en la

neurogénesis[63]. Además, el NO participa en la regulación de la transmisión nerviosa a nivel del SNC, inhibiendo la respuesta a la dopamina, noradrenalina y serotonina, o estimulando la liberación de acetilcolina[7].

Por otro lado, el NO está relacionado con la etiología de enfermedades neurológicas, como enfermedades neurodegenerativas crónicas y autoinmunes. Las concentraciones de NO presentes en el tejido inflamado bloquean reversiblemente la conducción en axones normales, desmielinizados y remilienizados. En enfermedades que se caracterizan por una pérdida generalizada de mielina, acompañadas de inflamación, como la esclerosis múltiple y el síndrome de Guillain- Barré, las altas concentraciones de NO podrían exacerbar los síntomas neuronales tanto en el SNC como en el SNP.

El NO está implicado en la muerte neuronal tras un trauma. En la médula espinal, tras la avulsión de las raíces de los nervios espinales se observa la expresión de la nNOS y, posteriormente la muerte de las motoneuronas. Un pre-tratamiento con inhibidores de la nNOS aumenta sustancialmente la supervivencia neuronal. La excesiva liberación de glutamato y NO, junto con el estrés oxidativo y la disfunción mitocondrial están relacionadas con varias enfermedades neurodegenerativas. Tras un ataque epiléptico, se induce la nNOS en varias regiones corticales[113].

El Párkinson se asocia con una progresiva pérdida de neuronas dopaminérgicas en la sustancia negra, que conlleva disfunción motora extrapiramidal, con temblores, rigidez y bradiquinesia. Se ha observado que los pacientes con Párkinson presentan una mayor producción de NO y de nitración de tirosinas, así como una sobreexpresión de la nNOS en los ganglios basales[114]. Además, se ha observado en modelos de Párkinson que los ratones knockout para nNOS, y los tratados con inhibidores de las

NOSs son más resistentes a la neurotoxicidad y presentan un efecto protector en modelos de enfermedad de Huntington[115].
En la enfermedad de Alzheimer se ha observado un gran aumento de la expresión de las tres isoformas de las NOSs[63,116].

La administración de metales (aluminio y mercurio) induce cambios en la actividad de la nNOS en el cerebro y el cerebelo, lo que sugiere que la nNOS es un mediador en las enfermedades cerebrales inducidas por metales[113].
El exceso de producción de NO por la iNOS está relacionado con procesos inflamatorios agudos y crónicos en el SNC.

En el sistema nervioso periférico (SNP) (Figura 6), el NO es un importante neurotransmisor inhibitorio de los neuronas no colinérgicas no adrenérgicas (NANC). Los nervios nitrérgicos periféricos se distribuyen ampliamente, y producen la relajación del músculo liso en los sistemas gastrointestinal, respiratorio, vascular y urogenital. Esta relajación inducida por el NO produce en los cuerpos cavernosos del sistema genital la erección peneana. En el sistema gastrointestinal, el NO permite la acomodación de grandes volúmenes de comida en el estómago sin aumentar significativamente la presión intraluminal, regula el tono muscular de los esfínteres intestinales y permite el peristaltismo del tracto gastrointestinal.

En el sistema pulmonar, el NO funciona como broncodilatador. En el sistema vascular la nNOS se encuentra en los nervios perivasculares de varios vasos sanguíneos, y constituye un mecanismo de control regional del flujo de sangre alternativo e independiente de la eNOS. Este NO parece ser particularmente relevante en la regulación del flujo sanguíneo cerebral. En el músculo esquelético hay una gran expresión de la nNOS, principalmente bajo el sarcolema de fibras rápidas, enfatizando el papel del NO como modulador de la fuerza contráctil[113,69].

1.5 Mecanismos de acción del NO

El NO ejerce sus efectos de forma directa o indirecta a través de varios mecanismos pero, probablemente, el mecanismo biológico más significativo es la reacción con metales de transición.

Por sus propiedades como radical, el NO es capaz de donar electrones a los metales y formar aductos metal-nitrosilo. Los metales de transición más importantes en sistemas biológicos son el hierro, el cobre y el zinc. Estos metales son muy abundantes en los sitios catalíticos de los grupos prostéticos de enzimas y proteínas. Las reacciones con el hierro son las más estudiadas[5] (Figura 8).

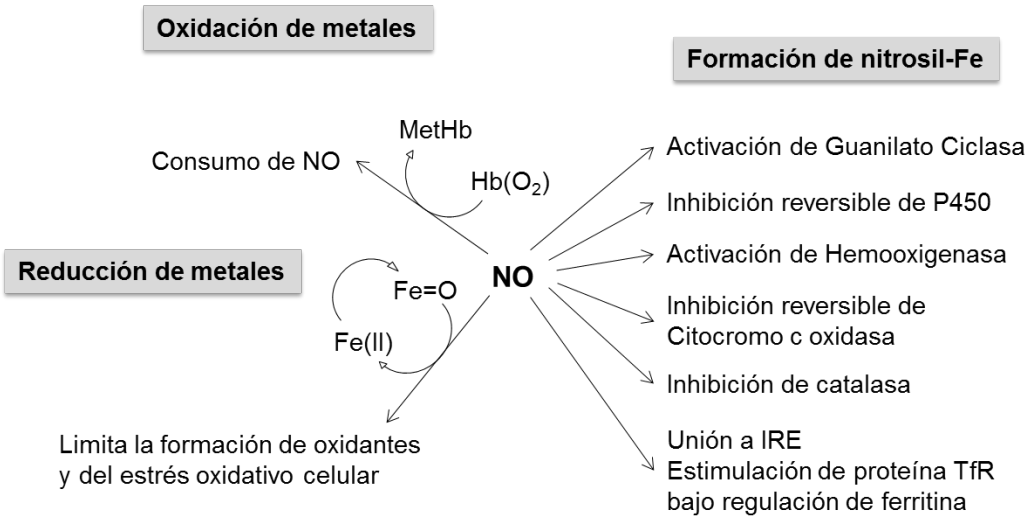

Figura 8. Efectos directos del NO: reacciones con metales de transición[117].

De este modo, la interacción del NO con el grupo hemo de la enzima GC provoca su activación y la producción de GMPc[118]. Esta interacción es la que media muchos efectos fisiológicos del NO y particularmente el efecto vasodilatador que protagonizó su descubrimiento. Al aumentar los niveles del cGMP, se activa una proteína quinasa, generando una cascada de

fosforilaciones de la cual resulta la reducción de la concentración intracelular de calcio y la relajación del músculo liso vascular, la inhibición de la quimiotaxis para polimorfonucleares y el bloqueo de la adhesión y agregación plaquetaria y leucocitaria, entre otros efectos. Por otro lado, el NO tiene otras acciones directas, en virtud de las cuales estimula la ciclooxigenasa en los macrófagos, bloquea varias enzimas mitocondriales (citotoxicidad) y actúa como neurotransmisor en varias áreas del SNC (sistema límbico, áreas olfatorias, nociceptivas y de memoria) y SNP que involucran vías neuronales, como se ha descrito anteriormente.

La S-nitrosilación es, también, otro mecanismo del NO que podría servir de almacenamiento transitorio o vehículo de suministro que guarde el NO o lo transporte cuando sea necesario, además de ser un mecanismo post-traduccional[119] y participar en el sistema de defensa neuronal antioxidativo.

El NO puede actuar indirectamente, tras combinarse con otros radicales libres (Figura 9). Este mecanismo conduce a la formación de especies reactivas de oxígeno (ROS: OH, H_2O_2) y de nitrógeno (RNS: NO_2, N_2O_3,…), ya que el NO puede reaccionar con varios radicales libres entre los cuales destaca el anión superóxido (O_2^-), liberado por la propia NOS y también por NADPH oxidasa, ciclooxigenasa, lipoxigenasa y xantina oxidasa, generando el peroxinitrito ($ONOO^-$)[120,121]. Este último se protona dando el ácido peroxinitroso que se descompone generando el radical hidroxilo ($OH^•$), uno de los radicales más reactivos y tóxicos. En condiciones fisiológicas, el O_2^- es convertido por la superóxido dismutasa (SOD) en peróxido de hidrógeno (H_2O_2) y agua evitando que interaccione con el NO. Puesto que la concentración de la SOD es bastante constante, la producción de peroxinitritos depende, casi exclusivamente, de las concentraciones de sus precursores NO y O_2^- que, a su vez, depende de la actividad de las tres isoformas de la NOS[117].

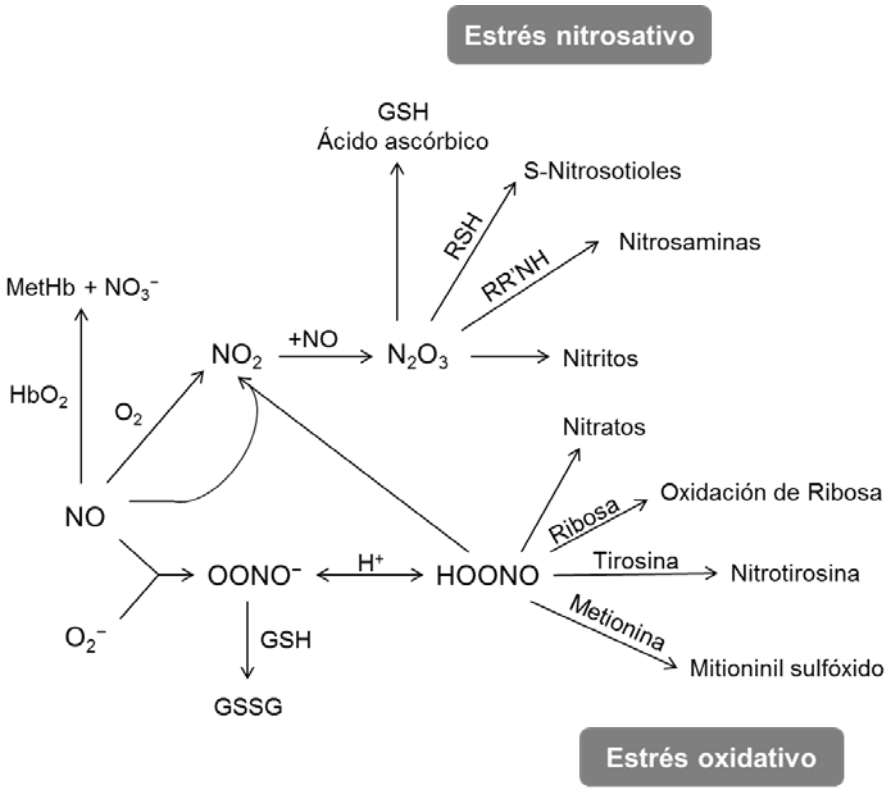

Figura 9. Efectos indirectos del NO: reacciones con radicales libres[117].

A través del $ONOO^-$, principalmente o por sí solo, el NO puede interaccionar con grupos tioles de la lisina, metionina, histidina y, sobre todo, cisteína para formar derivados S-nitrosilados que alteran la conformación y/o la actividad de varias proteínas. También, el peroxinitrito puede nitrar a compuestos heterocíclicos como el triptófano y la guanina, o fenoles como la tirosina. De hecho, la presencia de la nitrotirosina se demostró en las enfermedades de Alzheimer[122], Párkinson[123] y esclerosis lateral amiotrófica[124].

El $ONOO^-$ produce también la peroxidación de los lípidos generando hidroxiperóxidos lipídicos y productos secundarios como los aldehídos, lo que provoca la alteración de la membrana plasmática, pérdida de la homeostasis y finalmente la muerte de la célula.

A nivel de la mitocondria, el NO, por competición con el oxígeno, inhibe reversiblemente la respiración mitocondrial, mientras que el peroxinitrito la inhibe irreversiblemente y participa en la apertura del poro de permeabilidad transitoria (PPT), implicado en la apoptosis y la necrosis celular. Además, el $ONOO^-$ es capaz de interaccionar con el DNA, tanto celular como mitocondrial, provocando su fragmentación. Este evento se ha observado en la isquemia cerebral[125], en la enfermedad de Alzheimer[126], en la esclerosis múltiple[127] y en la degeneración de motoneuronas[128].

1.5.1 Mecanismos de neurotoxicidad del NO

Los cambios positivos o negativos en las concentraciones fisiológicas del NO a nivel neuronal pueden ser la causa o, al menos, contribuir junto con otros factores, a la aparición de estados patológicos. Cuando se produce un aumento en los niveles de NO, el daño que se genera depende tanto de la concentración como de la presencia de otras sustancias reactivas, del tiempo de exposición y de la presencia de dianas.
El NO participa en las neuropatologías a través de su acción a varios niveles: la producción de ROS y RNS e inducción de estrés oxidativo y nitrosativo; nitrosilación de grupos tioles de proteínas y nitración de residuos fenólicos; peroxidación lipídica; daño mitocondrial; daño del DNA; muerte neuronal e inflamación[129].

La neurotoxicidad del NO va acompañada de una excitotoxicidad relacionada con una activación excesiva de los receptores glutamatérgicos. El NO, a través de la activación de la GC, estimula la liberación del glutamato que interacciona con sus receptores postsinápticos *N*-metil-D-aspartato (NMDA), produciendo una entrada masiva de calcio y el aumento de sus niveles intracelulares. El calcio activa la NOS, a través de la CaCaM, estimulando la liberación de NO que difunde fuera de la célula hacia otras células y vuelve a entrar en la misma provocando una nueva síntesis de

glutamato. Este mecanismo retrógrado se produce en condiciones fisiológicas, pero se transforma en neurotóxico cuando existe una activación persistente.

Cuando el aumento de calcio persiste, además de la NOS, se activan proteasas, lipasas y endonucleasas. Las proteasas dañan al citoesqueleto y a las proteínas de membrana. Las lipasas catalizan la hidrólisis de los fosfolípidos de membrana, concretamente, la fosfolipasa A2 libera, tras la hidrólisis, el ácido araquidónico que es el precursor de varios mediadores inflamatorios. Las endonucleasas provocan la fragmentación y destrucción del ADN, conduciendo a la apoptosis (Figura 10).

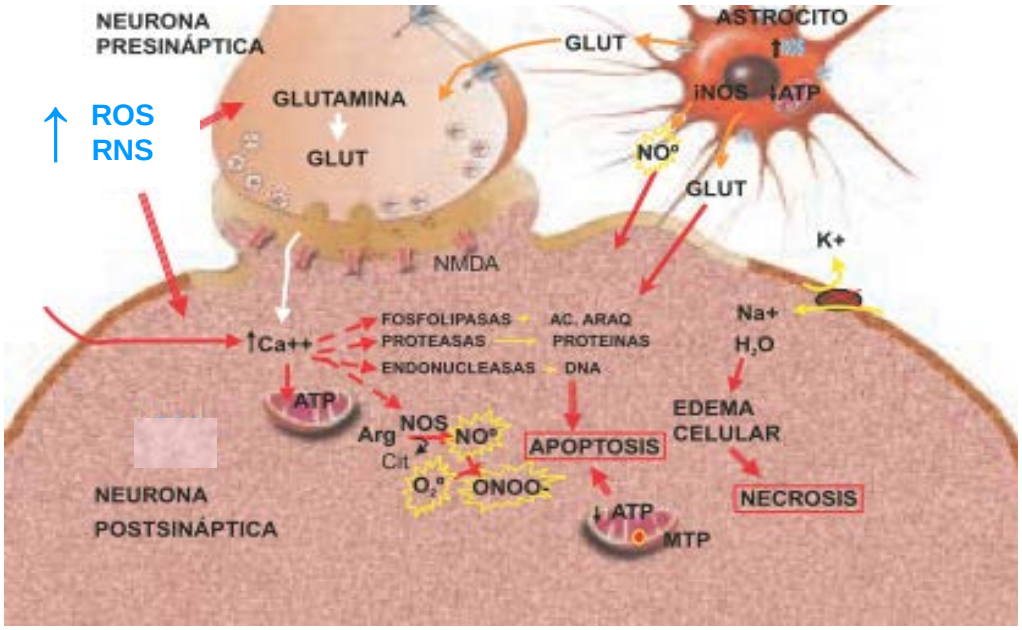

Figura 10. Los eventos que contribuyen a la neurotoxicidad del NO.

El aumento de los niveles de NO y calcio en la mitocondria hace que se reduzca la producción de ATP y que se forme el PPT en la membrana mitocondrial llevando a una mayor disminución de los niveles de ATP y a un aumento de RNS y ROS. La reducción de ATP resulta en una

despolarización de la membrana plasmática, ya que, por un lado, dejan de funcionar las bombas dependientes de ATP, lo que provoca una entrada masiva de agua y sodio y una salida de potasio causando edema celular y, por otro, sigue la entrada de más calcio, creando un círculo vicioso que lleva a la pérdida de la función neuronal y muerte necrótica o apoptótica de la célula[130,131].

Por su parte, los astrositos y la glía activada por los mediadores inflamatorios liberan más NO, producido por la iNOS[132,133], y glutamato junto con otras sustancias proinflamatorias como el H_2O_2, IL-1, TNFα y la proteína precursora de amiloides (APP), lo que provoca un daño neuronal y mayor activación de la microglía. El daño neuronal, a su vez, incrementa la producción ROS y RNS, IL-1 y TNFα produciendo mayor activación de la microglía[129] (Figura 11).

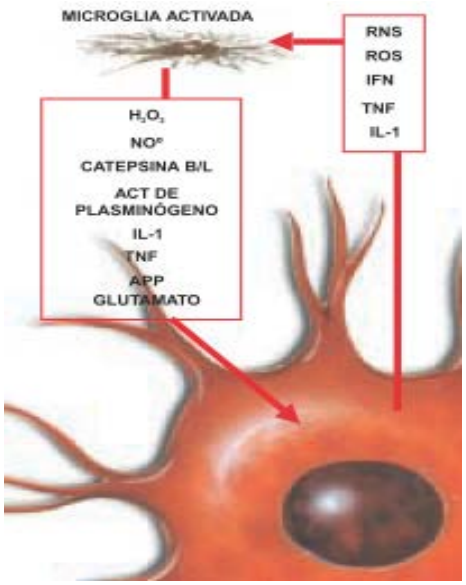

Figura 11. Relación entre microglía activada y neuronas.

De todo lo expuesto anteriormente, se demostró el papel del NO como mediador en la neurodegeneración y en la activación de procesos inflamatorios y se justificó su relación con enfermedades relacionadas con el SN como Alzheimer, Párkinson, esclerosis lateral amiotrófica o corea de Huntington[69,113,131].

1.6 Inhibición de la síntesis del NO

Teniendo en cuenta el potencial neurodestructivo y proinflamatorio de la sobreproducción de NO, la inhibición de la NOS se presenta como una estrategia terapéutica[134] para tratar varios desórdenes de tipo inflamatorio, neurodegenerativo y cáncer[135]. Tratándose del NO esta aproximación no es tan sencilla. Impedir que el NO actúe como segundo mensajero, llegando hasta sus dianas fisiológicas, es perjudicial para el organismo. Una manera de regular sus niveles patológicos sería inhibiendo de forma selectiva las isoformas de la NOS. Experimentos con ratones transgénicos demostraron que la pérdida de cada una de las isoformas produce el esperado efecto de disminución en la concentración de NO en las respectivas células[136-138]. Estos experimentos sugieren que una inhibición selectiva de la nNOS o la iNOS podría proporcionar una solución terapéutica sin los efectos perjudiciales que acarrearía la inhibición de la eNOS en el sistema cardiovascular.

Por otro lado, más allá de su interés terapéutico, el desarrollo de inhibidores selectivos de cada isoforma constituye una herramienta farmacológica útil para seguir estudiando y descubriendo nuevas funciones fisiológicas del NO.

Desde hace más de dos décadas, se emprendió la búsqueda de inhibidores de la NOS. Los primeros inhibidores eran derivados y análogos simples de la L-arginina. Después, se aplicó la teoría del ensayo-error a la hora de

realizar sustituciones y cambios en las estructuras que tenían propiedades inhibitorias de la NOS. Cuando surgieron los métodos computacionales en el panorama del diseño de fármacos, ya se disponía de un amplio arsenal de inhibidores y se empezó a usar ampliamente la teoría del farmacóforo. No fue hasta finales de los noventa cuando se publicó la estructura de los cristales de la iNOS[139,140] y eNOS[141] y en 2002 la de nNOS[142]. A partir de ese momento, se empezaron a diseñar inhibidores mediante el cribado virtual de grandes bibliotecas de compuestos y basándose en la estructura de la enzima[143-145]. Dado que los centros activos de las tres isoformas están muy conservados, el uso del cribado virtual se potenció teniendo en cuenta la plasticidad conformacional de la isoenzima diana[146]. Esto llevó a la técnica llamada "fragment hopping" que permite reducir el farmacóforo a un grupo de átomos, gráficos virtuales y/o vectores. De esta forma, pequeñas diferencias entre las NOSs pueden servir para conseguir inhibidores selectivos[147].

Todo ello hace, que hoy en día se disponga de una variedad desconcertante de inhibidores con diversas estructuras, con diferentes tipos de interacción con la enzima y con distinta selectividad. Estos inhibidores se pueden clasificar de distintas maneras. Atendiendo a la teoría clásica de la enzimología, se puede diferenciar entre inhibidores reversibles (competitivos, no competitivos y mixtos) e inhibidores irreversibles. Sin embargo, la clasificación más adoptada se basa en el sitio de unión del inhibidor a la enzima, pudiendo establecer cuatro clases de inhibidores. La primera clase, y la más amplia, incluye compuestos que interaccionan con el sitio de unión de la L-arginina. La segunda clase la constituyen compuestos que interaccionan directamente con el grupo hemo. La tercera está formada por compuestos que interaccionan con el sitio de unión de la BH_4. La cuarta clase abarca los compuestos que interaccionan con la CaM o las flavinas. Por otro lado, teniendo en cuenta la estructura química de los inhibidores, se pueden formar dos grupos: aminoacídicos y no aminoacídicos.

A continuación, se estudia la unión de la L-arginina a las distintas isoformas de la NOS y las interacciones que se generan. Posteriormente, se hace una descripción de los principales inhibidores descubiertos atendiendo a su estructura química.

1.6.1 Unión del sustrato e interacciones inhibidor-enzima

Los estudios topológicos y cristalográficos de las isoenzimas demuestran una alta conservación de los centros activos, lo que supone un gran desafío en el desarrollo de inhibidores selectivos y competitivos. Sin embargo, la homología entre el resto de las secuencias primarias no supera el 50%. Este hecho hace posible el desarrollo de inhibidores selectivos que interactúan o no con el centro catalítico y con zonas contiguas variables según la isoenzima.

El sustrato L-arginina se une al centro activo mediante una red de puentes de hidrógeno que establecen el grupo guanidínico y el grupo amino. Dos nitrógenos de la guanidina interaccionan con el carboxilato del residuo conservado Glu597 en nNOS humana (Glu377 en iNOS; Glu361 en eNOS) y el otro nitrógeno forma también un puente de hidrógeno con el Trp592 (Trp372 en iNOS; Trp356 en eNOS). El nitrógeno *N*-terminal de la arginina interactúa con un propionato del grupo hemo a través de un enlace de hidrógeno. Estas interacciones son idénticas en todas las isoformas de la NOS (Figura 12).

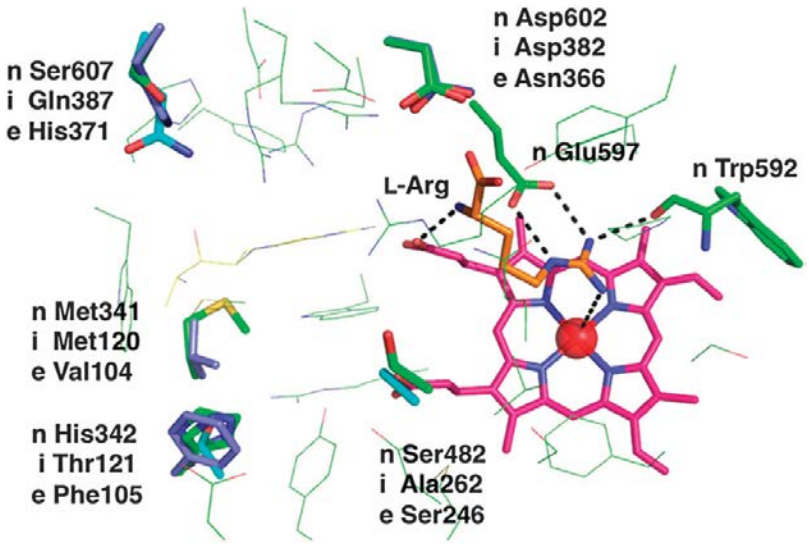

Figura 12. Unión de la L-arginina a las tres isoformas humanas de la NOS. n: nNOS (verde), i: iNOS (azul), e: eNOS (morado). Los puentes de hidrógeno están representados en líneas discontinuas[148].

Las estructuras cristalinas del ligando unido a las isoenzimas permite la comparación de los tres complejos ligando-isoforma, así como el diseño de fármacos por medio de herramientas computacionales. El alineamiento de dichas estructuras tridimensionales revela varios residuos no idénticos en las inmediaciones del sitio activo. Los residuos más diferentes entre las isoformas humanas son la Ser607 y la His342. La Ser607 de nNOS humana es Gln387 en iNOS e His371 en eNOS, mientras la His342 de nNOS humana es Thr121 en iNOS y Phe105 en eNOS. El efecto estérico y electrónico ejercido por estos residuos es bastante diferente, lo que les hace dianas para conseguir selectividad. Además, otros dos residuos son distintos entre la nNOS y la eNOS. Asp602 y Met341 en nNOS son Asn366 y Val104 en eNOS, respectivamente. También, la Ser482 en nNOS es una Ala262 en iNOS. El cambio Asp602/Asn366 en nNOS/eNOS es interesante ya que provoca que el centro activo de nNOS sea más electronegativo que el de eNOS, lo que podría influir en la interacción con un inhibidor. Junto con estas diferencias puntuales, existe, en otros residuos, cierta flexibilidad

conformacional que permite crear nuevos bolsillos de unión específicos de cada isoforma[148] (Figura 12).

1.6.2 Inhibidores de la NOS

La búsqueda de inhibidores enzimáticos parte, generalmente, de la introducción de modificaciones estructurales en la molécula del sustrato, una estrategia que permitió el desarrollo de los primeros inhibidores de la NOS. Progresivamente, y con el avance en los estudios de la estructura enzimática, se han ido diversificando los inhibidores tanto a nivel de estructura química como de lugar de acción.

Desde un punto de vista químico, los inhibidores de la NOS se pueden dividir en dos grupos: inhibidores aminoacídicos e inhibidores no aminoacídicos. Los aminoacídicos son miméticos de la L-arginina y se dividen, a su vez, en análogos de L-arginina, análogos conformacionalmente restringidos de L-arginina y análogos dipeptídicos. Los no aminoacídicos no derivan de aminoácidos y son de naturaleza química muy variada.

1.6.2.1 Inhibidores aminoacídicos análogos de L-arginina

Los primeros Inhibidores análogos de L-arginina **1** tienen una estructura simple con pequeñas modificaciones respecto a la de la L-arginina. De este modo, la mayoría fueron competitivos para el sitio de unión del sustrato, aunque algunos demostraron una inhibición dependiente de la reacción catalítica.

L-N^{ω}-Metilarginina (L-NMA) **2** es un metabolito fisiológico producto de la degradación de arginina metilada de algunas proteínas[149]. Fue uno de los primeros inhibidores utilizados para inhibir la NOS a finales de los

ochenta[23,150,151]. Actúa como un inhibidor competitivo para todas las isoformas aunque frente a nNOS e iNOS puede ejercer una inhibición dependiente de la reacción[152]. Ha demostrado algo de eficacia para reducir la migraña en ensayos efectuados en humanos[153], aunque con efectos adversos a nivel cardiovascular debido a la falta de selectividad[154.155].

Otro de los primeros inhibidores demostrados, a principios de los noventa, es el L-N^{ω}-nitroarginina (L-NNA) **3** y su metilester **4** (L-NAME)[156,157]. Este último se hidroliza en los sistemas biológicos para dar su precursor[158]. Ambos son potentes inhibidores competitivos pero con muy baja selectividad. A pesar de que L-NNA es alrededor de 300 veces más selectivo nNOS que iNOS, ambos producen hipertensión severa en animales de experimentación debido a la inhibición de eNOS[159,160]. El L-NAME presenta la ventaja de ser más soluble por lo que tiene mayor aplicación en experimentos *in vitro* e *in vivo*.

La N^{ω}-alquilación de la arginina con sustituyentes alquilo (ej. dimetilo, etilo, ciclopropilo) ciclos (ej. ciclopropilo) o insaturados (ej. alilo, propargilo) dio lugar a varios compuestos potentes pero desprovistos de selectividad[161-163]. Sin embargo, N^{ω}-propil-L-arginina **5** (L-NPLA) sobresale por tener una potencia de inhibición 3.000 veces mayor frente nNOS que iNOS y 150 veces mayor que eNOS, lo que hace que sea uno de los primeros inhibidores más selectivos[161]. Además de inhibir de forma competitiva reversible, puede inactivar la enzima de forma irreversible.

L-aminoarginina **6** (L-NAA) fue también uno de los primeros inhibidores sintéticos (finales de los ochenta)[164,165]. Es competitivo no selectivo, con buena afinidad por las tres isoformas de la NOS, aunque puede actuar también de forma irreversible[166]. Debido a su efecto convulsionante y su toxicidad irreversible dejó de ser un prototipo atractivo.

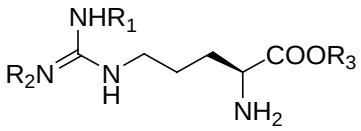

	1	2	3	4	5	6
R_1	H	CH_3	NO_2	NO_2	$CH_2CH_2CH_3$	NH_2
R_2	H	H	H	H	H	H
R_3	H	H	H	CH_3	H	H

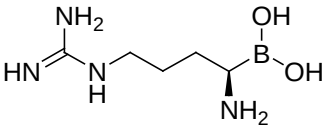

7

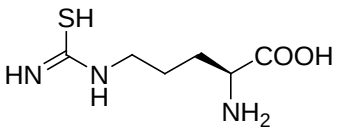

8

En 1998, Lebarbier y colaboradores sintetizaron unos análogos de L-arginina derivados de ácido boránico que actuaban como inhibidores competitivos reversibles. El derivado más destacado **7** presentó una alta selectividad por la isoforma inducible frente a la neuronal con una IC_{50} = 50 µM para iNOS y 300 µM para nNOS[167].

En 1994, el grupo de Griffith sustituyó el oxígeno de la carboxamida de la L-citrulina por un azufre, obteniendo la L-tiocitrulina (L-TC) **8** y otros derivados como L-homotiocitrulina y *S*-metiltiocitrulina. Aunque esta modificación aumentó notablemente la afinidad por las distintas isoformas, no mejoró la selectividad[168]. Sus derivados 3-alquilsustituidos, preparados para estudiar la influencia de un aumento de la lipofilia en la selectividad, mostraron mayor inhibición de iNOS que de nNOS y resultaron poco activos frente a eNOS[169].

En 2009, se publicaron las primeras estructuras cristalinas de los complejos inhibidor-nNOS mostrando la coordinación Fe-tioéter[170] (Figura 13). Una serie de inhibidores fueron diseñados basándose en el esqueleto de L-arginina para permitir su anclaje al sitio de unión del sustrato con una

cabeza amidínica. Tanto la longitud del grupo alquilo en el tioéter como el número de metilenos entre la amidina y el azufre fueron variados para encontrar el puente óptimo para posicionar el tioéter sobre el hemo. De esta serie, el compuesto **9** tenía una buena inhibición de nNOS (K_i = 33 ± 2 µM) y los estudios cristalográficos demostraron una inhibición en la que la distancia Fe-N es de 2.5 Å, los dos metilenos intermedios orientan el azufre hacia el Fe y el grupo tioéter está situado en un bolsillo hidrofóbico formado por Pro565, Val567 y Phe584 lo que proporciona mayor estabilidad. Al contrario de lo que se esperaba, esta fuerte interacción N-Fe no se acompañó de mejora en la potencia[171].

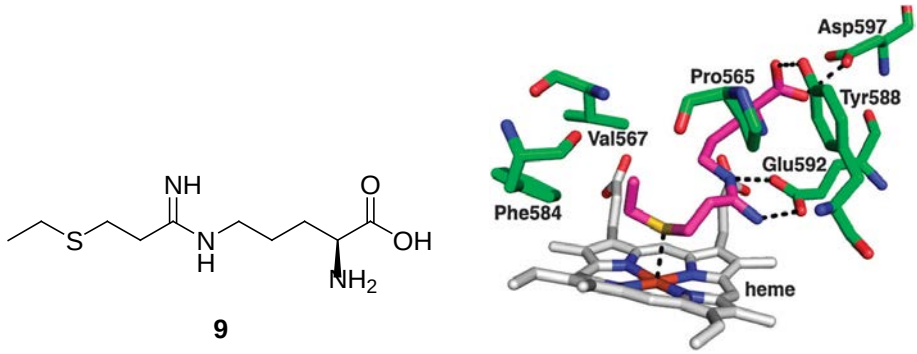

9

Figura 13. Modo de unión del compuesto **9** mostrando la interacción N-Fe. Los puentes de hidrógeno están representados en líneas discontinuas[171].

En un intento de aumentar su actividad y mejorar su selectividad, algunos análogos de L-arginina fueron incorporados en moléculas más largas. Así, una serie de derivados alquilados de isotiocitrulina incorporados en un dipéptido fueron diseñados por Nagano y Higuchi[172]. El compuesto *S*-metil-L-tiocitrulinil-L-fenilalanina **10** demostró la mejor inhibición frente a iNOS y algo menos frente a nNOS con mayor selectividad por estas dos isoformas. Mientras, derivados más pequeños fueron más selectivos frente a nNOS, lo que sugirió que el centro activo tiene diferente tamaño en cada una de las tres isoformas, con lo cual el criterio del tamaño puede servir para orientar la

selectividad (hipótesis que posteriormente fue confirmada por los estudios cristalográficos)[172].

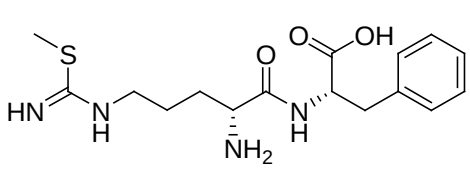

10

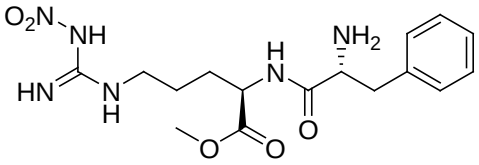

11

L-NNA y L-NAME fueron, también, incorporados a estructuras peptídicas. En un trabajo inicial realizado por Thiemermann y colaboradores se describe la inhibición de la NOS por derivados nitroarginina-dipeptídicos, pero estos compuestos elevaban la presión arterial cuando se administraron a ratas anestesiadas[173]. Posteriormente, el grupo de Silverman demostró que el dipéptido D-Phe-D-Arg-NO_2-OMe **11** inhibe nNOS con una K_i = 2 μM y muestra una selectividad alrededor de 1800 veces para nNOS sobre iNOS[174]. Esto hizo pensar que la selectividad podría mejorar al cambiar las propiedades químicas del otro aminoácido que forma el péptido. Los esfuerzos para aplicar esta hipótesis dieron lugar a un conjunto de 152 dipéptidos con un resto de amida y un aminoácido, distinto de la D-Phe, acoplados a L-NNA. Se observó que compuestos con cadena lateral básica (ej. lisina, histidina) son los que mejor inhibían selectivamente la nNOS (**12**, K_i = 0.13 μM, 1538 veces selectivo nNOS/iNOS)[175]. Esto sugirió una importante interacción electrostática con el centro activo de la nNOS. Modificaciones (introducción de grupos lipofílicos, restricción conformacional o reducción del enlace amida) para reducir las cargas de estos compuestos, aumentar la biodisponibilidad y reforzar el enlace amida, dieron lugar a péptidos y péptidomiméticos todavía más potentes y selectivos (**13**, **14**, **15**)[176-178]. En 2003, el estudio cristalográfico del complejo dipéptidos y péptidomiméticos de arginina con nNOS de rata demostró el origen de la interacción anteriormente mencionada en el residuo Asp597 (Asp602 en

nNOS humana)[179]. Este residuo está mutado en eNOS (bovina) por la Asn368, lo que se traduce en la pérdida de la estabilización electrostática a favor de mayor estabilidad en nNOS. Uno de estos inhbidores **15** con el enlace peptídico reducido ha demostrado ser capaz de proteger a cultivos de neuronas de la apoptosis inducida por hipoxia. Así mismo, este compuesto reduce la neurodegeneración fetal en condiciones de hipoxia en conejos de forma dosis dependiente[144].

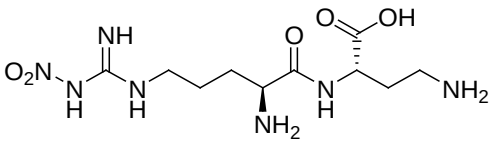

12

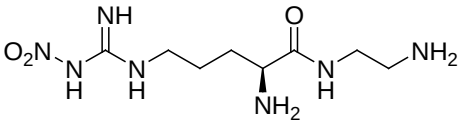

13

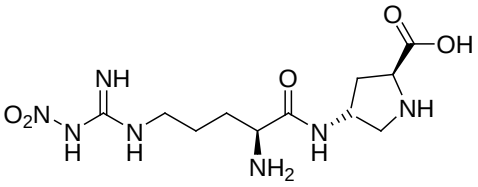

14

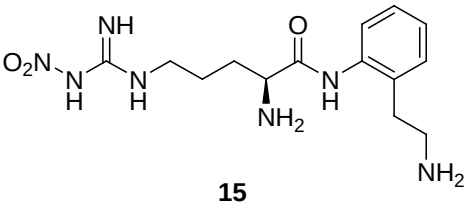

15

Otra familia de análogos aminoacídicos fue diseñada en los noventa a partir de la sustitución del resto de guanidina por uno de amidina. L-N^{ω}-iminoetil-L-ornitina (L-NIO) **16** fue el primer compuesto sintetizado[180]. Actúa de forma competitiva no selectiva frente a las tres isoformas, aunque también puede inactivar la neuronal[181]. Su derivado *N*-(1-imino-3-butenil)-L-ornitina (vinil-L-NIO o L-VNIO) **17** presentó mayor afinidad hacia la nNOS con valores micromolares. Igual que su precursor inactiva fuertemente la nNOS con pérdida del grupo hemo (K_i = 90 nM, K_{inac} = 0.078 min^{-1})[182]. El siguiente compuesto de interés en esta familia es el N^6-(1-iminoetil)-L-lisina (L-NIL) **18** que fue el primer análogo aminoacídico con mayor selectividad por la isoforma iNOS (28 veces) frente a eNOS. Su derivado aminoglicol[183] **19** es 700 veces más selectivo iNOS/eNOS aunque algo menos potente.

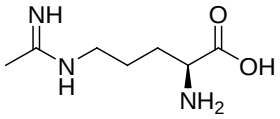

16

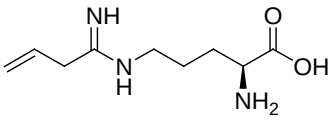

17

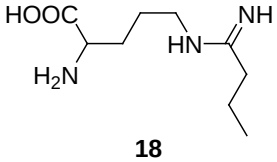

18

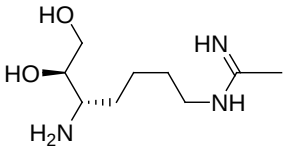

19

Las modificaciones en la cadena metilénica de L-NIL condujeron a una serie de derivados acetamidínicos y heterosustituidos incluyendo sulfonas como el ácido (2*R*)-2-amino-3-((2-(etanimidoilamino)etil)sulfonil)propiónico (GW273629) **20** y sulfuros como el ácido (2*S*)-2-amino-4-((2-(etanimidoilamino)etil)tio)butírico (GW274150) **21** que mostraron igual potencia, pero mucha mayor selectividad frente a iNOS[184,185]. Estos dos inhibidores compiten con la L-arginina. La interacción con eNOS y nNOS es inmediata y reversible, mientras que con iNOS es dependiente del tiempo y parece irreversible en presencia de NADPH[185]. GW274150 está en fase II de los ensayos clínicos para el tratamiento de la migraña y el asma.

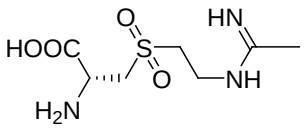

20

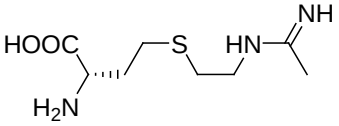

21

En 2005, el grupo de investigación de Higuchi introdujo nuevos inhibidores sintéticos de la NOS basados en los análogos anteriormente mencionados, con sulfuros o sulfonas modificados con un resto de piridina **22** y **23**. Estos compuestos son competitivos y dos de ellos son potentes (K_i del orden de unidades µM) pero sin ninguna selectividad[186].

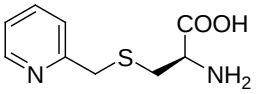

22

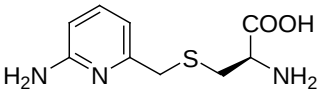

23

Los análogos rígidos de la L-arginina constituyeron otro intento hacia la búsqueda de inhibidores de la NOS. Se presentan bajo tres formas estructurales: el primer tipo de compuestos tiene el grupo guanidínico (o un isóstero equivalente) sustituido con un derivado nitroaromático **24a** o incorporado en un heterociclo, incluyendo derivados tiazólicos **24b**, imidazólicos **24c** o tiazínicos **24d**; los compuestos del segundo tipo tienen el carbono-3 de la cadena con una conformación rígida mediante la introducción de un doble enlace **25** o la inserción en un ciclo **26**; en el tercer tipo se pretende unir un nitrógeno de la función guanidina a un metileno de la cadena **27a-b** partiendo del prototipo L-NIO **16**. En general, estos análogos demostraron ser débiles inhibidores con una selectividad moderada, por lo que la estrategia de aumentar la rigidez de la estructura de la L-arginina no parece favorecer la inhibición selectiva de la NOS[187].

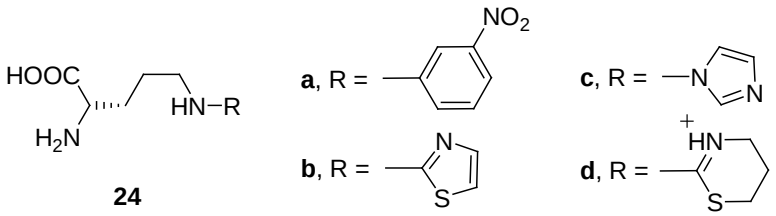

24

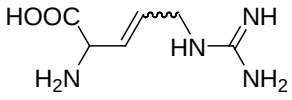

25

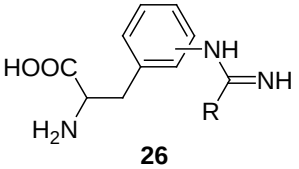

26

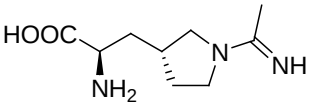

27a

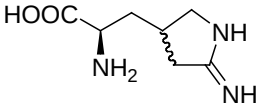

27b

Numerosos derivados aminoacídicos fueron diseñados incorporando un imidazol a la estructura de la ornitina[188] o histidina[189], con la intención de inhibir la nNOS mediante la interacción con el Fe del grupo hemo. La longitud de la cadena intermedia se varió para optimizar la potencia y la selectividad. Dos de estos compuestos, **28** y **29**, con tres y cinco metilenos, respectivamente, fueron potentes pero carecían de selectividad. La sustitución del imidazol por un anillo de triazol o tetrazol mostró inhibiciones más débiles.

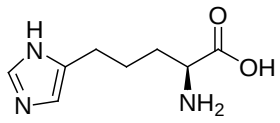

28

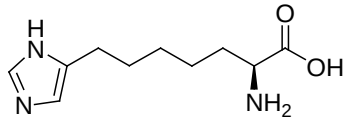

29

1.6.2.2 Inhibidores no aminoacídicos

La disponibilidad de los tres cristales de las NOSs[139,141,142] sentó las bases para varias investigaciones de diseño de fármacos mediante herramientas computacionales. Esto permitió que el grupo de los inhibidores no aminoacídicos se encuentre en continuo crecimiento, abarcando compuestos con diversos grupos funcionales, distintas estructuras químicas y diferentes puntos de interacción con la enzima (centro activo, Fe del grupo hemo, sitio de unión de la BH_4, CaM y dimerización).

1.6.2.2.1 Inhibidores que actúan en el sitio de unión de la L-arginina

Este grupo de inhibidores compiten con la L-arginina por el sitio activo. Interaccionan con la enzima a través de residuos conservados en el centro activo, aunque los más recientes llegan a residuos más a las afueras, en el canal de entrada del sustrato donde la conservación es menor, logrando así mayor selectividad hacia nNOS o iNOS.

Los derivados isotioureicos, entre los cuales aparecen los compuestos con un resto de *N*-fenilisotiourea **30**, son potentes inhibidores de la nNOS[190]. Los estudios de relación estructura-actividad (REA) demostraron que la potencia inhibitoria está estrechamente relacionada con el impedimento estérico del sustituyente *S*-alquilo, encontrándose una potencia máxima para los derivados *S*-etil isotioureicos. También se comprobó que el grupo fenilo es fundamental para la potencia, ya que su sustitución por otros anillos reduce la actividad, aunque se mantiene la selectividad. Además, la sustitución en posición para del fenilo incrementa la selectividad por nNOS en comparación con las posiciones orto y meta. De todos estos derivados destaca el *S*-etil-*N*-(4-(trifluorometil)-fenil)isotiourea (R_1 = 4-CF_3, R_2 = Et, X = Cl).

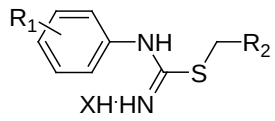

30

R_1 = H, 2-Br, 3-Cl, 4-Cl, 2-OCH_3, 2-CF_3, 3-CF_3, 4-CF_3

R_2 = Me, Et, Pr, CH_2Ph

X = I, Cl

Otra serie de derivados isotioureicos, preparada por el mismo grupo de investigación, incluye compuestos tipo **31** y bisisotioureicos tipo **32**[191]. Los inhibidores tipo **31** presentan una selectividad de dos a seis veces mayor por iNOS que por eNOS. La sustitución con radicales más pequeños mejora la actividad inhibitoria, alcanzándose la máxima potencia con derivados *S*-etilo y *S*-isopropilo. Sin embargo, el cambio en la longitud de la cadena reduce drásticamente la potencia. De la misma forma, los derivados tipo **32** se comportan como potentes inhibidores con mayor afinidad hacia iNOS. Parece que dicha afinidad requiere una región rica en electrones en la zona intermedia del compuesto. El compuesto con R = $(CH_2)_2$-(1,3-Ph)-$(CH_2)_2$ es el que mejor inhibición iNOS presenta.

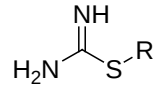

31

R = H, Me, Et, Pr, Bu, CH_2Ph, $(CH_2)_2Ph$, $(CH_2)_3Ph$, $(CH_2)_3Br$, $CH_2CH_2CH_2OH$

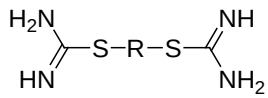

32

R = $(CH_2)_n$, n = 2-8
$(CH_2)_n$-(1,2-Ph)-$(CH_2)_n$,
$(CH_2)_n$-(1,3-Ph)-$(CH_2)_n$,
$(CH_2)_n$-(1,4-Ph)-$(CH_2)_n$, n = 1, 2

Otra clase estructural de compuestos que intenta mimetizar el esqueleto de la L-arginina son los derivados amidínicos cíclicos y acíclicos. Dentro de este grupo, algunos inhibidores muestran interesante selectividad.

La *N*-(3-(aminometil)bencil)acetamidina conocida como 1400W **33** fue presentada por GlaxoWellcome en 1997 y es uno de los inhibidores más

activos y selectivos frente a iNOS[192]. Tiene una selectividad 5.000 y 200 veces mayor por dicha isoforma que por eNOS y nNOS (humanas), respectivamente. Posteriormente, la eliminación del metileno que une el fenilo a la amida dio lugar a los derivados N-fenilamidínicos **34** y **35** que resultaron selectivos frente a nNOS[193]. El compuesto **34** es el más activo y selectivo frente a nNOS con una K_i = 0.006 µM (0.35 µM y 0.16 µM frente a eNOS e iNOS, respectivamente). El compuesto **35** mostró una excelente inhibición de nNOS *in vivo*.

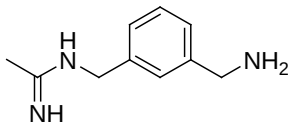

33

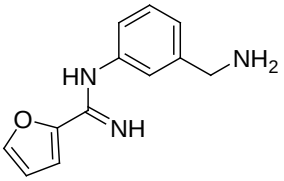

34

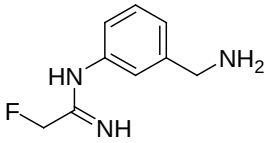

35

Trabajos más recientes llevados a cabo por Maccallini y colaboradores y basados en el compuesto **33** consiguieron una importante mejoría a nivel de potencia. Intentos como eliminar el grupo metilamino[194], unirlo a uno o dos bencilos sustituidos[195] o a un grupo alquilamida o arilamida[196] permitieron obtener compuestos con una IC_{50} < 1 µM y buena selectividad hacia la isoforma inducible, *in vitro*. Así, destacan los compuestos **36** y **37** con una IC_{50} = 0.42 y 0.20 µM y una selectividad iNOS/eNOS de >2300 y 1750, respectivamente.

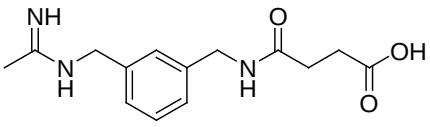

36

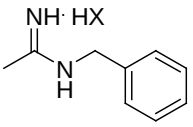

37

Se han descrito también, derivados amidínicos cíclicos que, en general, presentan mayor selectividad por iNOS. Así, en el año 2000, Naka y

colaboradores describen el derivado **38,** conocido como ONO-1714, con una selectividad 10 veces mayor por iNOS (parcialmente purificada) que eNOS[197]. Un año más tarde, el equipo de Moorman sintetiza una serie de amidas heterocíclicas **39** entre las que el derivado con X = O y R = C_4H_9 resultó 10 y 560 veces más selectivo para iNOS que para nNOS y eNOS, respectivamente. En este estudio, se observó que los mejores compuestos son los que llevan un átomo de oxígeno o azufre[198].

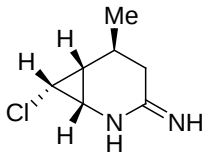

38

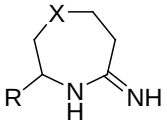

39

R = H, CO_2Et, C_4H_9,
$CH_3(CH_2)_2NH_2$,
$CH_3(CH_2)_2NO_2$,
$CH_3CH_2CH{=}CHCH_3$
X = CH_2, N-CH_3, O, S

Otros inhibidores con amidina cíclica son los derivados 2-iminopiperidínicos entre los cuales destacan los compuestos **40**, **41** y **42**. La introducción del grupo metilo en posición 4 (**40**) y 4 y 6 del anillo iminopiperidínico (**41**) aumenta la potencia inhibitoria pero sin selectividad significativa. Sin embargo, la introducción del grupo ciclohexilmetilo en posición 6 (**42**) produce un notable aumento de la selectividad por iNOS (5 y 64 veces mayor que para nNOS y eNOS, respectivamente).

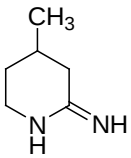

40

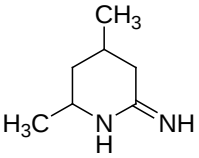

41

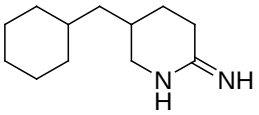

42

En 2002, aparecen inhibidores 2-iminopirrolidínicos de los cuales destacan los compuestos **43** y **44**. A pesar de que el primero es menos potente presenta una selectividad por iNOS tres veces mayor que el segundo que

carece del grupo hidroxilo. El derivado **44** es 35 y 2.540 veces más selectivo para iNOS que para nNOS y eNOS, respectivamente[199].

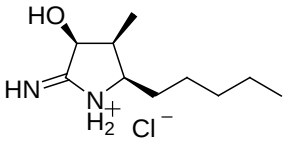

43

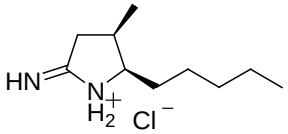

44

Otro tipo estructural de inhibidores son los que llevan un anillo de 2-aminopiridina sustituido **45**[200]. Los derivados 4,6-disustituidos son los más potentes y selectivos frente a iNOS. De todos los compuestos ensayados con este tipo de estructura, sobresalen aquellos que tienen R = 4-CH_3-6-nC_4H_9 y 4-CH_3-6-iC_4H_9. En concreto, este último, que presenta una IC_{50} = 0.028 µM frente a iNOS, es 5 y 3 veces más selectivo para esta isoforma que para eNOS y nNOS, respectivamente.

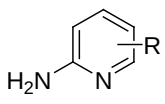

45

R = 3-CH_3, 4-CH_3, 5-CH_3, 6-CH_3, 3,4-$(CH_3)_2$, 4,5-$(CH_3)_2$, 4-Cl, 4-CF_3,...

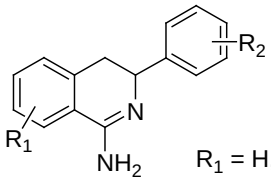

46

R_1 = H, 5-, 6-, 7-, 8-F,

R_2 = H, 2-, 3-, 4-F, 4-Cl

Derivados de 3,4-dihidro-1-isoquinolinamina **46**, también han sido investigados como inhibidores de la NOS, por el grupo de Beaton. Concretamente, el compuesto 3-fenil-3,4-dihidro-1-isoquinolinamina es un débil inhibidor, en cambio variaciones en su estructura permitieron aumentar la potencia y selectividad hacia iNOS. Con un R_1 = 8-F y R_2 = 4-F, se consiguió un inhibidor con IC_{50} = 0.16 µM y una selectividad 100 veces mayor respecto a nNOS y 1000 respecto a eNOS[201]. El cambio del esqueleto de la 3,4-dihidro-1-isoquinolinamina por una 4,5-

tetrahidrotieno[2,3-*c*]piridina no condujo a mejoría, ni a nivel de potencia ni de selectividad[202].

Posteriormente, el mismo grupo publicó otra clase de inhibidores selectivos de iNOS derivados de quinazolinas, 2-sustituidas-1,2-dihidro-4-quinazolinaminas **47** y 4'-aminospiro(piperidin-4,2'(1'*H*)-quinazolin)-4-aminas **48**. Los compuestos de ambas series mostraron, *in vitro*, una potencia nanomolar y alta selectividad para la isoforma inducible con respecto a las isoformas constitutivas. También se ha demostrado la eficacia de estos compuestos en modelos agudos y crónicos de enfermedad inflamatoria en animales tras una administración oral[203].

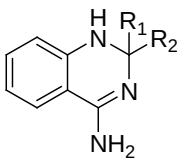

47

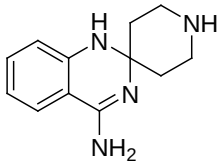

48

Más tarde, el uso de varias técnicas computacionales, entre ellas la llamada "fragment hopping", y la evidencia de la capacidad inhibitoria de determinadas estructuras químicas, permitieron al equipo de Silverman en 2009, el diseño y síntesis de pirrolidinometil-2-aminopiridinas. Así, se descubrió un potente inhibidor **49** con una K_i de 388 nM y una selectividad nNOS/eNOS de 1.000 veces y nNOS/iNOS de 150 veces [204]. Mediante la misma técnica este compuesto fue mejorado introduciendo grupo lipofílicos a la aminopiridina y arilalquilos a la amina secundaria, lo que llevó a dos potentes inhibidores selectivos de la nNOS **50** y **51**[205].

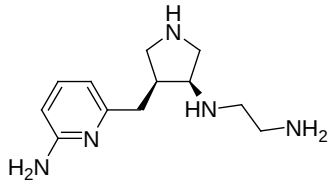

(±)-49

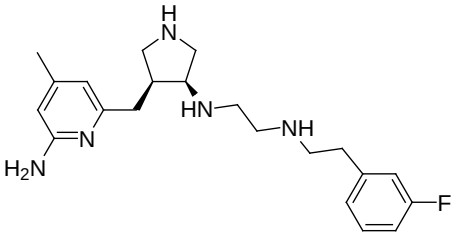

(±)-50

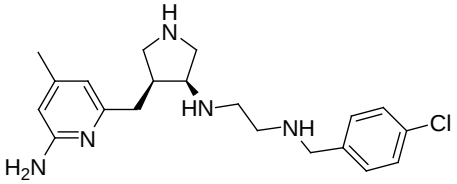

(±)-51

Estos compuestos son especialmente interesantes porque demuestran la influencia de la estereoquímica en el modo de unión del inhibidor a la enzima y, en consecuencia, en la potencia y selectividad hacia las distintas isoformas. La cristalografía por rayos X demostró diferentes modos de unión para los dos isómeros que afectan drásticamente a la actividad inhibitoria hacia nNOS. Los estudios llevaron a comprobar la existencia en nNOS (de rata) de un bolsillo hidrofóbico definido por Leu337, Met336 y Tyr706 que posteriormente se reveló crucial para la selectividad nNOS[206], aunque este bolsillo es algo más pequeño en la nNOS humana. En modelos de neurodegeneración por hipoxia-isquemia en conejos, los compuestos **50** y **51** demostraron alta eficacia en reducir los síntomas de la neurodegeneración sin ninguna toxicidad[207]. A pesar de su eficacia, igual que los análogos de arginina y dipéptidos, estos inhibidores no dejan de tener problemas relacionados con la permeabilidad y biodisponibilidad oral. Sucesivos intentos de mejorar estas características como fluoración de la cadena alquílica[208,209], la introducción de grupos formadores de puentes de hidrógeno internos[210] y de restos lipófilos y colas aromáticas[211], la alquilación y restricción conformacional[212], la introducción de diversos restos de profármacos, el uso de azidas en lugar de amina[213], la sustitución de la

aminopiridina por un aminotiazol menos básico[214], y la sustitución de los grupos amino con amidas y éteres[203,215], resultaron en una reducción de la potencia y selectividad respecto a los compuestos de partida[171], sin mejora a nivel de permeación y biodisponibilidad. Sin embargo, cuando la amina secundaria exocíclica fue sustituida por un oxígeno y los enantiómeros fueron separados, se obtuvo un compuesto **52** muy potente[216]. Dicho compuesto se encuentra entre los inhibidores de la nNOS más potentes descubiertos hasta la fecha, con una K_i = 7 nM (nNOS de rata) y una alta selectividad nNOS/eNOS y nNOS/iNOS de 2.667 y 806 veces, respectivamente, a pesar de que aún muestra los inconvenientes de la poca permeación y biodisponibilidad oral. Intentos de mono y gem-difluoración en la cadena alquílica han mejorado algo la permeación y la biodisponibilidad[217,208].

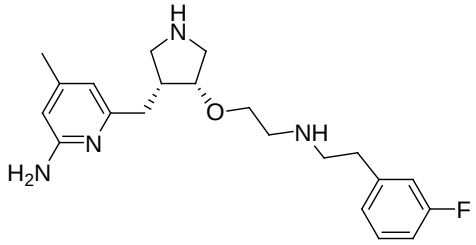

52

El siguiente paso emprendido por el grupo de Silverman fue la simplificación de los anteriores derivados aminopiridínicos mediante el diseño de derivados simétricos con doble cabeza de aminopiridina y en los que el anillo quiral fue remplazado por un grupo arilo o heteroarilo[218] (estos compuestos se encuentran actualmente patentados). Un ejemplo es el compuesto **53** que resultó ser muy potente (K_i = 20 nM) pero con menor selectividad (107 y 58 veces respecto eNOS e iNOS, respectivamente). Aun así, los estudios cristalográficos demostraron que dos moléculas de este inhibidor se pueden unir a la nNOS al mismo tiempo, una en el sitio del grupo hemo y otra en el sitio de la BH_4, donde desplaza a ésta para

interaccionar con un átomo de zinc, dando lugar así a un nuevo tipo de inhibidores duales antagonistas arginina-BH_4. La selectividad de este compuesto se ha mejorado introduciendo un grupo ciano o aminometilo (**54** y **55**, respectivamente) en el anillo central cuya interacción con la nNOS esta mediada por Asp597, permitiendo una alta selectividad nNOS/eNOS (472 veces para **54** y 221 veces para **55**)[219].

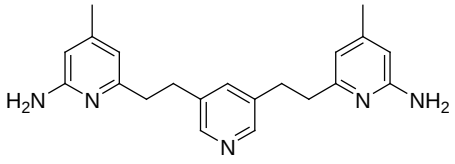

53

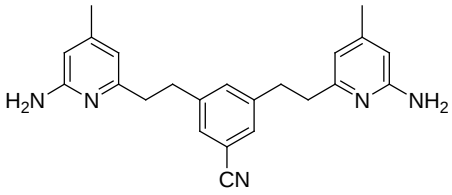

54

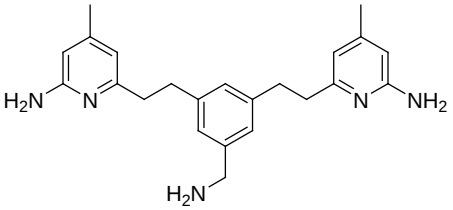

55

Más recientemente, el grupo de Silverman ha patentado[220] una serie de derivados homólogos a los anteriores, pero con el cambio del ciclo central aquiral por otro quiral, mejorando así la selectividad[221]. De esta serie destaca el compuesto **56** con una potencia de 9.7 nM y una selectividad para nNOS 693 y 295 veces mayor que eNOS e iNOS, respectivamente. Además, varios derivados aminopiridínicos α-amino funcionalizados[222] fueron diseñados para estudiar la REA entre el inhibidor, los grupos propionatos del hemo y la BH_4. Entre estos, sobresale el compuesto **57** con una K_i de 24 nM frente a nNOS y una selectividad 273 y 2.822 veces mayor respecto a iNOS y eNOS, respectivamente.

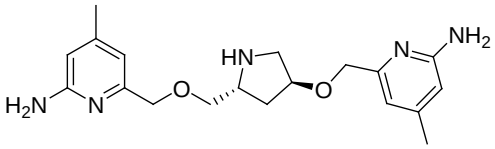

56

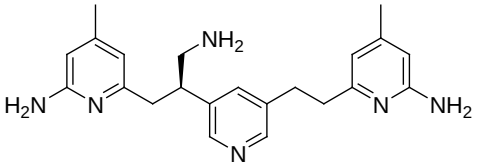

57

Otra de las familias estructurales que se utilizó mucho como prototipo en la búsqueda de inhibidores de la NOS es la de tiofeno-2-carboximidamido. En el año 2000, AstraZeneca describió un potente inhibidor de la isoforma neuronal, AR-R17477 **58** que presenta una IC_{50} = 35 nM. A pesar de tener una selectividad moderada (143 y 100 veces mayor para nNOS que iNOS y eNOS, respectivamente), este compuesto mostró una duración de la inhibición de nNOS excepcionalmente larga en ratas y un interesante perfil neuroprotector[223]. Otro compuesto, el AR-R17338 **59**, tenía cerca del 100% de biodisponibilidad en monos. La estructura cristalina del inhibidor **58** demuestra que el grupo tiofeno-amidínico, igual que el 2-aminopiridínico, mimetiza la L-arginina e interacciona con Glu592, mientras que la amina secundaria forma un puente de hidrógeno con el propionato del grupo hemo y la cola formada por el clorofenilo se proyecta hacia el bolsillo hidrofóbico anteriormente mencionado (Figura 14) [171].

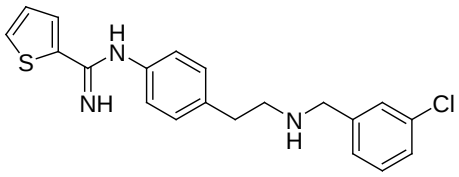

58

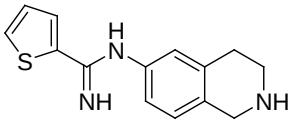

59

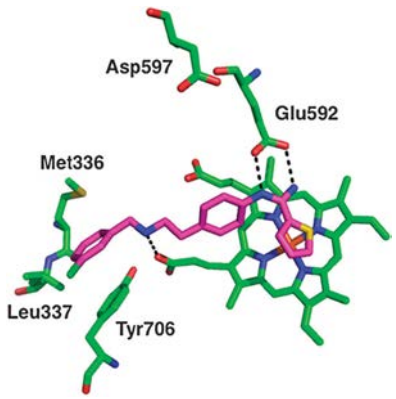

Figura 14. Modo de unión de **58** en el centro activo de nNOS. Los puentes de hidrógeno están representados en líneas discontínuas[171].

Más recientemente, basándose en los datos experimentales de varios complejos cristalográficos inhibidor-enzima, el mismo grupo ha descubierto una nueva serie de potentes y selectivos inhibidores de iNOS[224]. La mayoría de estos compuestos poseen una IC_{50} por debajo de 1 µM. En concreto, el compuesto **60**, en el que el átomo de hidrógeno de C-4 fue sustituido por flúor y se eliminó el grupo N-Me, presentó una interesante inhibición selectiva de iNOS (IC_{50} = 0.006 µM) sobre nNOS y eNOS (IC_{50} = 35 y >10.000 µM, respectivamente) y aumentó su vida media y biodisponibilidad. Además, en el compuesto **61**, el fenilo sustituido fue remplazado por una piridina, con el fin de mejorar la interacción con el grupo hemo, y los valores de IC_{50} fueron 0.004, 28 y >10.000 µM para iNOS, nNOS y eNOS, respectivamente. Sin embargo, todos estos inhibidores tienen limitaciones, tales como la capacidad de antagonizar los transportadores de serotonina o la unión a receptores de noradrenalina, lo que resulta en una falta de selectividad hacia nNOS.

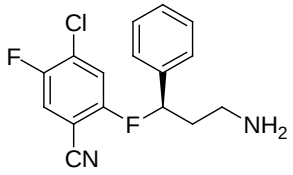

60

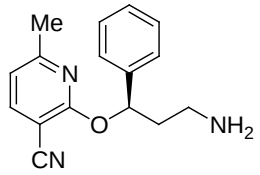

61

Por otro lado, Sanofi-Aventis diseñó inhibidores con el esqueleto de tiofenocarboximidamido unido a una hidroxipiperidina, e introdujo un grupo cloroarilo para alcanzar el bolsillo hidrofóbico del sitio activo de la nNOS. Estas modificaciones mejoraron mucho la potencia y la selectividad, obteniendo el destacable derivado **62** con una IC_{50} = 17 nM y una selectividad 1.664 veces nNOS/eNOS. Desgraciadamente este compuesto se metaboliza rápidamente por el hígado humano (35% en 20 minutos)[225].

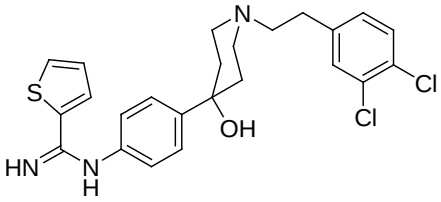

62

La mayoría de los últimos avances realizados en esta familia los llevó a cabo NeurAxon. Los inhibidores sintetizados por esta compañía comparten un farmacóforo: un grupo tiofenoamidínico, un puente central rígido (dihidroquinolonas[226], tetrahidroquinolinas[227,228], aminobenzotiazoles[228], benzazepinas[229] y varios indoles[230-233] e indolinas[234,235] disustituidos han sido empleados) y una cola corta que contiene una amina (ej. dimetilaminoetilo o pirrolidinoetilo). Los avances realizados han permitido llegar a potente inhibidores nNOS selectivos que tienen actividad muy prometedora en varios modelos de dolor en roedor, así como una excelente biodisponibilidad y perfiles de seguridad. Varios compuestos de estas series se encuentran actualmente patentados[220]. Entre estos inhibidores, el compuesto **63**

(derivado de tetrahidroquinolina) posee una IC_{50} = 0.089, 45.6 y 25.7 µM para nNOS, eNOS e iNOS, respectivamente, el compuesto **64** (indolina disustituida) que es el más selectivo de todas las series con unas IC_{50} para nNOS = 0.37, eNOS = 195 e iNOS = 83 µM y el compuesto **65** (indol 3,5-disustituido) que ejerce una ihnibición doble, de la nNOS y del transportador de norepinefrina (NET) con una IC_{50} = 0.56 y 1 µM, respectivamente, junto con una moderada selectividad de 88 veces n/eNOS y 12 veces n/iNOS.

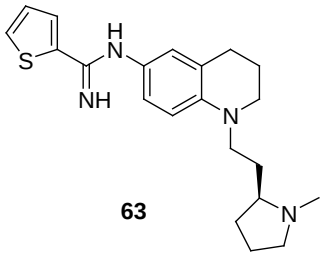

63

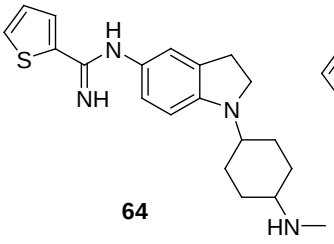

64

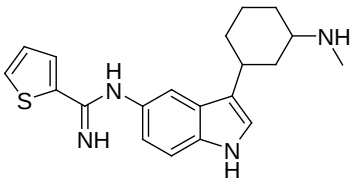

65

El esqueleto de dihidroaminoquinolina fue utilizado para formar derivados amidínicos tricíclicos. La unión de colas con aminas secundarias y grupos de halofenilo **66** permitió aumentar la potencia y selectividad hacia nNOS (IC_{50} = 42 nM). Esta observación está en concordancia con la REA de las pirrolidinometil-2-aminopiridinas y las tiofenoamidinas de Sanofi (**62**)[171].

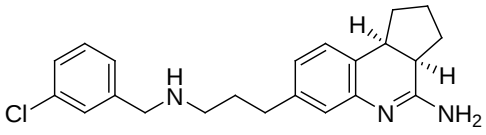

66

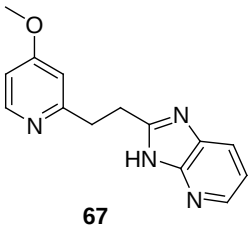

67

En los últimos años, Nycomed presentó una serie de análogos de L-arginina iNOS selectivos con una estructura imidazolopiridínica. Entre estos, el compuesto **67** que demostró buena afinidad iNOS (pIC_{50} = 7.09) y buen perfil de selectividad (nNOS: pIC_{50} = 4.86, eNOS: pIC_{50} = 3.95)[236]. Durante

los últimos 3 años, Nycomed ha sintetizado nuevos derivados basados en la estructura del compuesto **67**, sin embargo, no se identificaron mejores compuestos.

Otros tipos estructurales se han utilizado para desarrollar inhibidores de la iNOS, entre ellos derivados del ácido glicirretínico **68**, derivados de triazolopiridazina **69** y derivados 3-triazolil-cumarinas **70**[220]. Todos presentan inhibiciones de unas unidades del orden µM frente a iNOS, sin embargo faltan los datos de selectividad y de actividad frente a las demás isoformas.

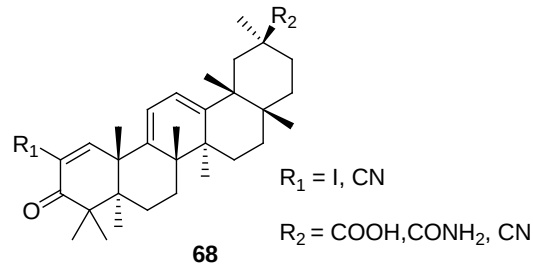

68

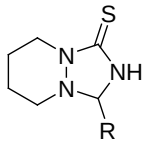

R = CH=CHPh, CH=CH(2-NO_2Ph)
2-NO_2-C_6H_4, 3-NO_2-C_6H_4
4-NO_2-C_6H_4

69

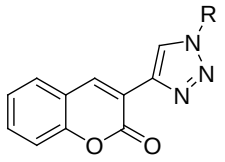

R = $(CH_2)_nCH_3$, n = 5, 7, 9
C_6H_{11}, Ph, CH_2Ph,
2-NO_2-4-CH_3Ph

70

1.6.2.2.2 Inhibidores que interaccionan con el Fe del grupo hemo

Aparte de los análogos de arginina, otra aproximación para la síntesis de inhibidores competitivos de la NOS, aunque menos estudiada, es la interacción con el Fe del grupo hemo.

Ligandos como los imidazoles **71** que producen esta interacción pueden, también, competir con la L-arginina para unirse al sitio activo. En efecto, el imidazol es un inhibidor débil de la nNOS bovina (IC_{50} = 200 µM). Sin embargo, la potencia del imidazol mejora sustancialmente con un fenilo en la posición 1 (**72**, IC_{50} = 25 µM) pero menos en la posición 2 (**73**, IC_{50} = 100 µM) y empeora cuando el fenilo está en posición 4 (**74**, IC_{50} = 600 µM). Esta diferencia podría achacarse a un impedimento estérico o una mejor deslocalización de la densidad electrónica desde el anillo de imidazol por la sustitución 4-fenilo, lo que debilita la unión Fe-N[171].

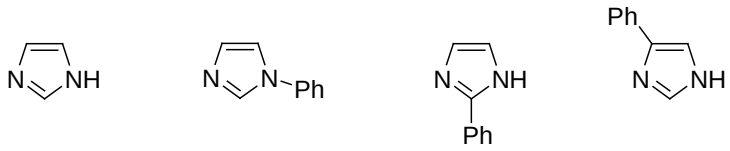

71 **72** **73** **74**

Otros inhibidores aminoacídicos con un imidazol incorporado han sido tratados en la sección correspondiente a este tipo de inhibidores (sección 1.6.2.1).

1.6.2.2.3 Inhibidores que interaccionan con el sitio de BH_4

Debido al importante papel que desempeña la BH_4 en el proceso de síntesis del NO y en la estabilización del dímero de NOS, su sitio de unión ha sido objetivo de varios inhibidores. Algunos compiten, a la vez, con la BH_4 y la L-arginina mientras que otros actúan exclusivamente en el sitio de unión de la BH_4.

Uno de los primeros inhibidores no aminoacídicos de la NOS y de los más estudiados es el 7-nitoindazol (7-NI) **75**. Este inhibidor presenta una alta selectividad hacia la isoforma neuronal *in vivo* pero no *in vitro*. A principios de los noventa, los estudios sobre su mecanismo de acción, con BH_4

marcada (en nNOS bovina), demostraron que compite con esta con una K_i = 0.12 µM, además de competir con L-arginina, mientras que, en la isoforma inducible y endotelial sólo compite con la BH_4. Sus propiedades antinociceptivas y neuroprotectoras animaron a la búsqueda de derivados más potentes. Sin embargo, los cambios estructurales en el 7-NI, como la bromación en posición 3 o nitración en 2, no produjeron mejora en la actividad inhibitoria y confirmaron que el grupo nitro en posición 7 es crucial para la potencia[237-239].

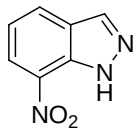

75

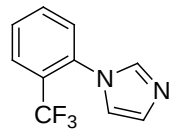

76

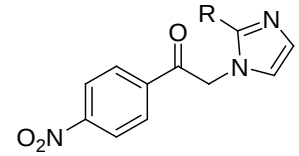

77 (R = H)

78 (R = Me)

Otros derivados que actúan a este nivel los representa el 1-(2-trifluorometilfenil)imidazol (TRIM) **76**. Este compuesto compite por el sitio de unión de L-arginina y BH_4. Demuestra efecto antinociceptivo *in vivo* y mayor afinidad hacia nNOS e iNOS *in vitro*[240]. Otros dos derivados *N*-fenacil imidazoles **77** y **78** antagonizan el sitio de unión de BH_4 pero no compiten con L-arginina. Además, han demostrado tener una actividad antioxidante por lo que se han propuesto como prototipo para futuras investigaciones ya que actúan a nivel de la nNOS y de los ROS[241].

Otros inhibidores diseñados en los noventa son los análogos biopterínicos. El análogo 4-amino-BH_4 **79** es un potente inhibidor de nNOS (IC_{50} = 1 µM, K_i = 13.2 nM, en nNOS de rata)[242]. Estudios posteriores de REA permitieron el diseño de **80** mediante una dialquilación del grupo amino en posición 4 y arilación en la posición 6 de la 2,4-diaminopteridina. Este compuesto resultó ser selectivo nNOS (IC_{50} = 3 µM)[243].

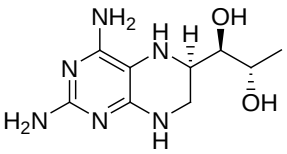

79

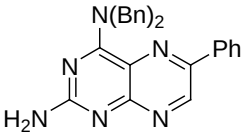

80

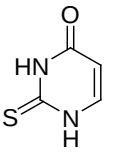

81

El 2-tiouracilo **81**, un fármaco antitiroideo, demostró ser un inhibidor selectivo de la isoforma neuronal con una K_i = 20 µM. Al ser redox-estable no participa en la formación de L-citrulina y NO y no estabiliza el dímero formado[244].

1.6.2.2.4 Inhibidores que actúan a nivel de la dimerización nNOS/iNOS

La NOS, como se ha descrito previamente, bajo sus tres isoformas, solamente puede catalizar la síntesis del NO en forma de dímero. Por otro lado, la implicación de iNOS en procesos inflamatorios y de dolor y la de nNOS en neurodegeneración y la estrecha relación entre la neurodegeneración, la inflamación y el dolor neuropático hace que los inhibidores duales selectivos nNOS/iNOS sean importantes candidatos terapéuticos.

Un potente inhibidor de la dimerización de iNOS, derivado de imidazol, conocido como BBS-1 **82**, fue diseñado a partir de una biblioteca combinatoria y mostró una elevada potencia para iNOS (IC_{50} = 28 µM), mayor selectividad para nNOS que eNOS (i/n = 5, i/e = 1000), y se demostró que interfiere, también, con la dimerización de nNOS[245]. *In vitro*, inhibe reversiblemente la nNOS en células DLD-1 e *in vivo* resultó muy efectivo en ratas al reducir de forma dosis-dependiente los niveles de nitritos en sangre[246]. Los estudios cristalográficos indican que el BBS-1 se une al centro activo de iNOS generando una deslocalización de algunos residuos

lo que provoca un cambio alostérico a nivel de la hélice 7a que desestabiliza la interfaz del dímero (Figura 15)[245].

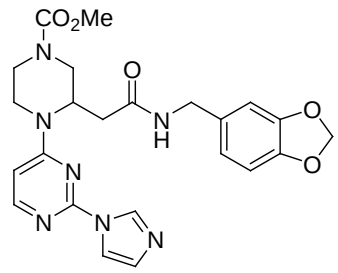

82

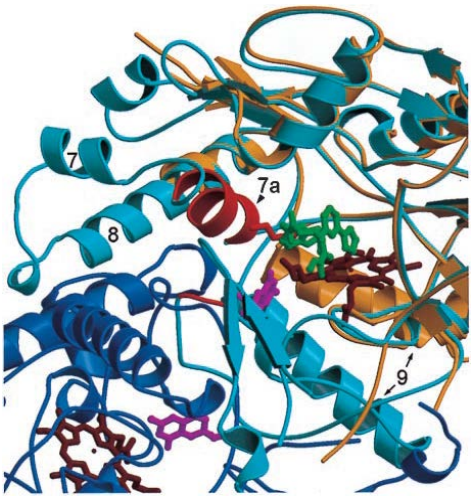

Figura 15. Modo de unión de BBS-1 a la iNOS[245]. Comparación del complejo Δ114 2-iNOS con el dominio oxigenasa del dímero de iNOS de murino. BBS-1 ocupa el sitio de unión de arginina. Los monómeros del dímero iNOS en azul oscuro y claro. La estructura 2-iNOS Δ114 (amarillo) se ha alineado con un monómero (azul claro); los grupos hemo en rojo oscuro. El hemo iNOS Δ114 y el hemo dímero se alinean muy cerca (para mayor claridad sólo se muestra el de iNOS Δ114).

Más recientemente, Kalypsis aportó una nueva clase de inhibidores con estructura quinolinona amídica que resultó muy potente, con alta selectividad para iNOS y nNOS respecto a eNOS y activa, vía oral, en modelos de dolor en roedores (ej. **83**, iNOS humana: EC_{50} = 0.11 μM, i/n = 210, i/e = 2.300)[247]. Sin embargo, *in vivo*, tenían alto aclaramiento y vida media corta en ratones. Para solucionar este problema se cambió la función amida y se introdujo restricción conformacional con un resto de benzimidazol-quinolinona. Se obtuvo el derivado 4-((2-ciclobutil-1H-imidazo[4,5-b]pirazin-1-il)metil)-7,8-difluoroquinolin-2(1H)-ona (KD7332)[248] **84** que inhibe la dimerización y la actividad de la iNOS y nNOS humanas, de primate y de murino (IC_{50} entre 50 y 400 nM), con una marcada selectividad respecto a eNOS (IC_{50}> 15.000 nM). El compuesto **84** mostró alta eficacia en varios modelos de inflamación y dolor en ratones y primates, presentó

alta estabilidad hepática y su perfil farmacocinético le hace un buen candidato clínico[249]. Esta serie de derivados se encuentra actualmente patentada[219].

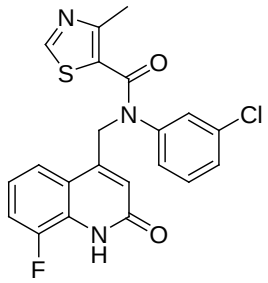

83

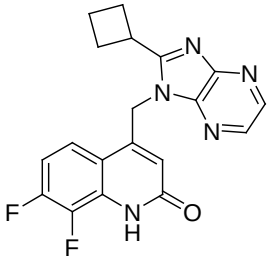

84

1.6.2.2.5 Inhibidores que actúan a nivel de la calmodulina

Al igual que los inhibidores que se unen al centro activo de la NOS e interaccionan, además, con BH_4, existen otros de tipo imidazolínico que se unen competitivamente al hemo y también interactúan con el sitio de unión de la CaM. Miconazol **85**, ketoconazol **86** y clotrimazol **87** son antifúngicos con estructura imidazolínica que mostraron inhibición competitiva en nNOS bovina con valores de K_i de 7, 44 y 19 µM, respectivamente, además de una inhibición competitiva dependiente de calmodulina[250]. Estos productos tenían mayor selectividad hacia las isoformas constitutivas[251].

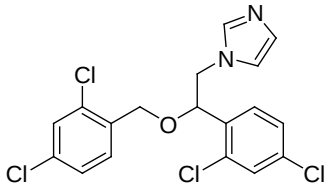

85

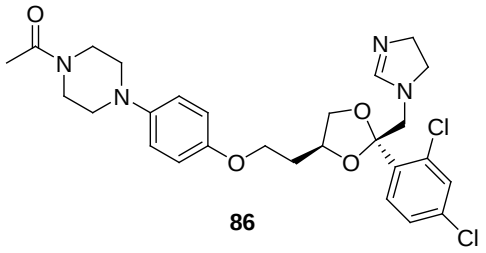

86

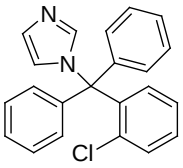

87

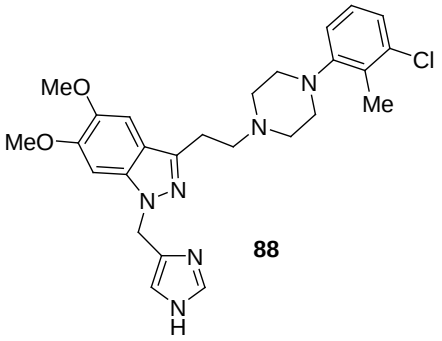

88

DY-9706e **88** es otro antagonista de la CaM que mostró importantes efectos neuroprotectores en isquemia cerebral focal transitoria en ratas[252-254]. Igual que los derivados imidazolínicos mostró mayor afinidad, *in vitro*, hacia las isoformas constitutivas y mayoritariamente la nNOS (K_i = 0.9 µM).

La melatonina **89** es una neurohormona producida en el cerebro por la glándula pineal (epífisis) a partir del triptófano. Se produce también, pero en menor medida, en otros tejidos y órganos dónde actúa como hormona paracrina. A nivel del SNC, presenta efectos inhibitorios que dan origen a sus propiedades anticonvulsivantes y neuroprotectoras[255]. Varios estudios[256-258] sugirieron que la melatonina reduce la respuesta glutamatérgica a través de la inhibición de la nNOS (IC_{50} = 0.1 µM, nNOS de rata). Otros demostraron que dicha inhibición es dosis dependiente y CaM dependiente[259]. En el cerebro, la melatonina, bajo la acción de la indolamina-2,3-dioxigenasa (IDO), se metaboliza a N^1-acetil-N^2-formil-5-metoxikinurenina que luego pasa a *N*-acetil-5-metoxikinurenamina (aMK), el principal metabolito cerebral de la melatonina[260]. El tiempo de latencia de la melatonina, en el que tarda en aparecer el efecto inhibidor, condujo a la

conclusión de que la melatonina ejerce su acción a través de uno de dichos metabolitos[258].

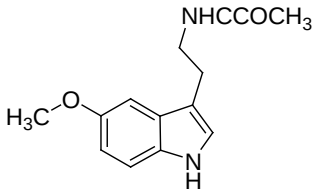

89

Basándose en este hecho y en el potencial neuroprotector que presenta el ácido kinurénico (un metabolito neuroactivo de la vía metabólica del triptófano), nuestro grupo de investigación sintetizó y ensayó varias series de kinureninas.

Los derivados kinurenínicos[261,262] pueden ser diésteres derivados del ácido amidomalónico sustituido en posición 2 **90** o derivados de ácidos carboxílicos α-amido-ω-benzoilsustituidos **91**.

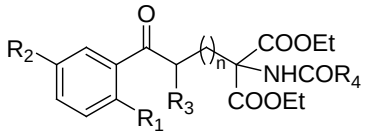

90

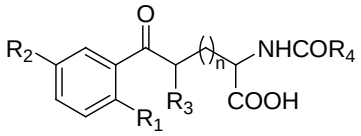

91

R_1 = H, NH_2, $N(CH_3)_2$, $NHCH_2Ph$
R_2 = H, OCH_3, NO_2
R_3 = H, CH_3
R_4 = CH_3, CH_2CH_2, $(CH_2)_2CH_3$, Ph, $CH{=}CHCH_3$, c-C_3HH_5, C_6H_{11}
n = 0, 1.

De todos los compuestos ensayados, resalta, por su potencia inhibitoria tanto de la excitabilidad NMDA como de la enzima nNOS, el ácido **91** con $R_1 = NH_2$, $R_2 = OCH_3$, R_3 = H, $R_4 = CH_3$, n = 0, con una IC_{50} = 40 μM. La actividad inhibitoria de los compuestos desprovistos del grupo amino aromático o en los que este grupo está sustituido es muy limitada o nula.

Esta observación demuestra que el grupo amino libre es imprescindible para la actividad inhibitoria.

Los estudios conformacionales de estas kinureninas[261] concluyen que la presencia del grupo amino restringe la flexibilidad de la molécula al establecer un enlace de hidrógeno intramolecular con el grupo cetónico, favoreciendo así un cambio conformacional que mimetiza la conformación preferente y farmacófora de la melatonina (Figura 16). Por otro lado, el grupo amino establece otro enlace de hidrógeno con la NOS.

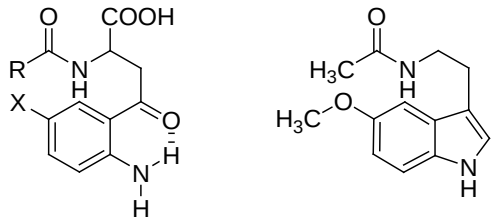

91 **89**

Figura 16. Conformación preferente de kinureninas con grupo amino libre y melatonina.

Las kinurenaminas **92** constituyen el segundo tipo de inhibidores de nNOS sintetizados por nuestro grupo de investigación. Entre estos derivados destaca el principal metabolito cerebral de la melatonina aMK (R_1 = OCH_3, R_2 = CH_3) que presentó una inhibición máxima[263].

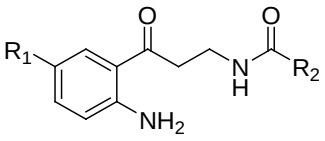

R_1 = Cl, OCH_3

R_2 = alquilo, cicloalquilo, fenilo

92

En general, todos los compuestos ensayados presentan una buena actividad inhibitoria. Se pudo constatar que un aumento en el volumen de la cadena lateral (R_2) conduce a una disminución de la actividad, mientras que

los compuestos con R_1 = OCH_3 son dos veces más activos que los que llevan R_1 = Cl, demostrando la necesidad de un sustituyente electrón-donante. Por otro lado, igual que con las kinureninas, se observó que el grupo amino es imprescindible para la actividad inhibitoria.

1.6.2.2.6 Otros inhibidores

Basándose en las observaciones anteriores, nuestro grupo decidió introducir mayor rigidez estructural lo que llevó al diseño de otras series, los derivados pirazólicos[264-266] entre ellos se encuentran las moléculas tipo **93** (inhibición máxima de nNOS de 70% a una concentración de 1 mM). Los mejores resultados de inhibición se obtuvieron en compuestos con c-Pr y Ph en R_2 y OMe y Cl en R_1.

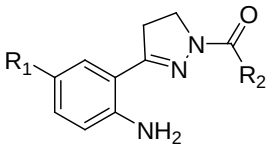

R_1 = H, Cl, OCH_3

R_2 = alquilo, cicloalquilo, fenilo

93

En los últimos años, nuestro grupo de investigación diseñó y sintetizó otras series como los derivados fenil pirrólicos **94** con un resto de carboxamida en posición 2. A pesar de que *in vitro* fueron débiles inhibidores, tanto de nNOS como de iNOS, *in vivo* (modelo de Párkinson inducido por MPTP in ratones) demostraron una fuerte inhibición de la isoforma inducible, tanto a nivel de citosol como de mitocondria. Aunque se piensa que ejercen una inhibición no competitiva, no se llegó a determinar su mecanismo de acción, estipulando que podría ser a través de un metabolito o modificando la expresión de la iNOS[267].

Posteriormente, el anillo de pirrol se sustituyó por uno de tiadiazol **95** obteniéndose unos inhibidores potentes y selectivos de iNOS con una IC_{50}, *in vitro*, entre 20 y 40 µM. Los estudios de docking realizados para estas estructuras acompañan la hipótesis de que estos inhibidores podrían unirse adecuadamente al centro activo de la enzima y por tanto actuar como inhibidores competitivos. Aun así, se requieren más estudios biológicos para confirmarlo[268].

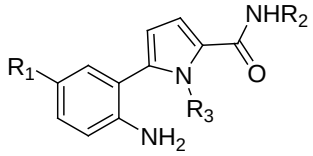

R_1 = H, Cl, OCH_3

R_2 = H, alquilo, cicloalquilo,bencilo

R_3 = H, Me

94

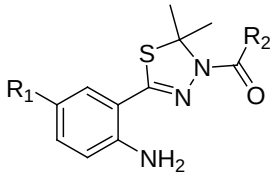

R_1 = H, Cl, OCH_3

R_2 = alquilo, cicloalquilo,bencilo

95

2. OBJETIVOS

El propósito general de este trabajo de investigación es la síntesis y evaluación biológica frente a las isoformas nNOS e iNOS de nuevas pirazolinas y derivados de urea y tiourea *N*,*N'*-disustituidos, con el fin de encontrar inhibidores más potentes y selectivos de la NOS.

Para lograr dicho propósito, se plantean los siguientes objetivos específicos:

1. Basándose en los resultados obtenidos con los derivados pirazolínicos, previamente sintetizados por nuestro grupo de investigación, se propone la síntesis de nuevos compuestos con la estructura general que se muestra en la Figura 17, introduciendo sustituyentes de distinta naturaleza (electrón donante como OCH_3, electrón neutro como H o electrón atrayente como Cl) en distintas posiciones del anillo aromático y cambiando el radical acilo en R_2 para estudiar la influencia tanto de la activación y desactivación del anillo aromático como del tamaño y flexibilidad del sustituyente en R_2 en la inhibición de la enzima.

2. Síntesis de nuevas kinurenaminas con la estructura general que se muestra en la Figura 17. En estos derivados, el grupo de urea (X = O) o tiourea (X = S) mimetiza al de guanidina presente en la L-arginina, sustrato natural de la enzima. Distintos sustituyentes se introducen en R_1 (OCH_3, H, Cl) y en R_2 (Me, Et, Pr) para poder estudiar la relación estructura actividad.

3. Síntesis de derivados 3-hidroxipropil urea y tiourea (Figura 17) en los cuales, en base al estudio de docking, el grupo carbonilo de la cadena intermedia se intercambia por un grupo hidroxilo, tratando de comprobar la influencia de este cambio en la actividad inhibitoria de los compuestos.

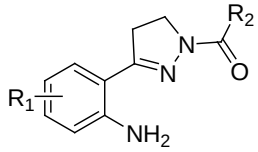

Derivados pirazolínicos

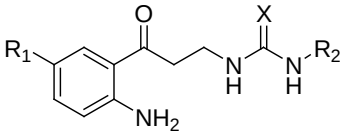

Derivados kinurenamínicos con restos de urea y tiourea

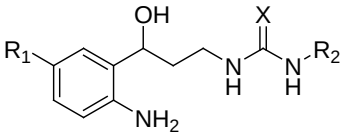

Derivados 3-hidroxipropil urea y tiourea

Figura 17. Estructura general de los compuestos sintetizados

4. Establecimiento de una nueva ruta sintética para obtención de los derivados 3-hidroxipropil urea y tiourea.

5. Purificación e identificación inequívoca de las moléculas sintetizadas mediante los estudios de resonancia magnética nuclear (RMN) mono (^{1}H, ^{13}C, DEPT) y bidimensionales (HSQC, HMBC), espectrometría de masas de alta resolución (HRMS) y análisis elemental.

6. Determinación de la actividad biológica, frente a nNOS e iNOS, de todos los derivados sintetizados y, frente a eNOS, de los más activos.

7. Análisis de la influencia de las modificaciones estructurales sobre la actividad inhibitoria en las tres familias de compuestos.

8. Realización de estudios teóricos de modelado molecular, utilizando estructuras cristalinas de la nNOS e iNOS disponibles en el RCSB PDB. Dichos estudios permiten, por un lado, el diseño de la familia de las 3-hidroxipropil ureas y tioureas, y por otro, una aproximación del modo de unión de los compuestos al centro activo de la enzima y la justificación de los resultados biológicos.

3. RESULTADOS

3.1 Artículo 1

Bioorganic & Medicinal Chemistry 21 (2013) 4132–4142

Contents lists available at SciVerse ScienceDirect

Bioorganic & Medicinal Chemistry

journal homepage: www.elsevier.com/locate/bmc

Synthesis and biological evaluation of 4,5-dihydro-1*H*-pyrazole derivatives as potential nNOS/iNOS selective inhibitors. Part 2: Influence of diverse substituents in both the phenyl moiety and the acyl group

M. Dora Carrión [a], Mariem Chayah [a], Antonio Entrena [a], Ana López [b], Miguel A. Gallo [a], Darío Acuña-Castroviejo [b], M. Encarnación Camacho [a,*]

[a] Departamento de Química Farmacéutica y Orgánica, Facultad de Farmacia, Universidad de Granada, Spain
[b] Centro de Investigación Biomédica, Parque Tecnológico de Ciencias de La Salud, Universidad de Granada, Spain

ARTICLE INFO

Article history:
Received 12 March 2013
Revised 30 April 2013
Accepted 8 May 2013
Available online 17 May 2013

Keywords:
4,5-Dihydro-1*H*-pyrazoles
Inhibition
Neuronal nitric oxide synthase (nNOS)
Inducible nitric oxide synthase (iNOS)

ABSTRACT

In a preliminary article, we reported a series of 4,5-dihydro-1*H*-pyrazole derivatives as neuronal nitric oxide synthase (nNOS) inhibitors. Here we present the data about the inhibition of inducible nitric oxide synthase (iNOS) of these compounds. In general, we can confirm that these pyrazoles are nNOS selective inhibitors. In addition, taking these compounds as a reference, we have designed and synthesized a series of new derivatives by modification of the heterocycle in 1-position, and by introduction of electron-donating or electron-withdrawing substituents in the aromatic ring. These derivatives have been evaluated as nNOS and iNOS inhibitors in order to identify new compounds with improved activity and selectivity. Compound **3r**, with three methoxy electron-donating groups in the phenyl moiety, is the most potent nNOS inhibitor, showing good selectivity nNOS/iNOS.

1. Introduction

Nitric oxide (NO) is an inorganic free radical that has diverse physiological roles, including regulation of blood pressure, neurotransmission and macrophage defense systems.[1] NO is synthesized from the enzyme catalysis of L-arginine to L-citrulline in several cell types by a family of nitric oxide synthase (NOS) isoenzymes, with consumption of molecular oxygen, nicotinamide adenine dinucleotide phosphate (NADPH) and other cofactors such as flavin adenine dinucleotide (FAD), flavin mononucleotide (FMN), tetrahydrobiopterin (BH_4) and iron protoporphyrin (heme). The NOS enzymes are homodimeric proteins consisting of a C-terminal reductase domain and a N-terminal catalitic oxigenase domain connected by a calmodulin-binding linker. The C-terminal reductase domain transfers electrons from NADPH through FAD and FMN, to the N-terminal oxygenase domain, which binds L-arginine, BH_4 and heme.[2] Several distinct isoforms of NOS have been discovered. Two of them, neuronal NOS (nNOS) and endothelial NOS (eNOS) are constitutively expressed in different tissues and are activated by Ca^{2+}, and they play a role in neurotransmission[3] and blood-vessel dilation,[4] respectively; inducible NOS (iNOS) is expressed by macrophages and microglia in response to inflammatory stimuli and it is not Ca^{2+} dependent;[5] finally, a mitochondrial-localized NOS isoform situated in the internal membrane of mitochondria (mtNOS) has been discovered,[6] and the existence of constitutive (c-mtNOS) and inducible (i-mtNOS) has been proved.[7,8]

While eNOS-generated NO plays a role in vascular regulation, the potential therapeutic utility of NOS inhibitors is restricted to the selective inhibition of the neuronal or inducible isoforms.[9] In particular, an overproduction of NO by nNOS has been associated with strokes,[10] migraine headaches,[11] or neurodegenerative disorders such as Parkinson[12] and Alzheimer's diseases.[13] On the other hand, an overproduction of NO by iNOS causes inflammatory bowel disease, arthritis, and neuropathic pain.[14,15] Also, inflammatory reaction in Parkinson's disease is associated with iNOS[16] and i-mtNOS induction.[17] Thus nNOS and iNOS represent a therapeutic target since inhibition of these enzymes can help in the treatment of several disorders, and a selective inhibition of one of these isoforms would be desired.

Previously, we have described a series of nNOS inhibitors with a kynurenine **1**,[18] kynurenamine **2**,[19] or 4,5-dihydro-1*H*-pyrazole structure **3**.[20] Furthermore, we have published 3-benzoyl-1-acyl-4,5-dihydro-1*H*-pyrazole **4**,[21] 3-benzoyl-1-alkyl-1*H*-pyrazole **5**[22] and 5-phenyl-1*H*-pyrrole-2-carboxamide derivatives **6**.[23] These compounds show moderate inhibition values of nNOS and iNOS,

* Corresponding author. Tel.: +34 958 243844; fax: +34 958 243845.
E-mail address: ecamacho@ugr.es (M.E. Camacho).

0968-0896/$ - see front matter © 2013 Elsevier Ltd. All rights reserved.
http://dx.doi.org/10.1016/j.bmc.2013.05.016

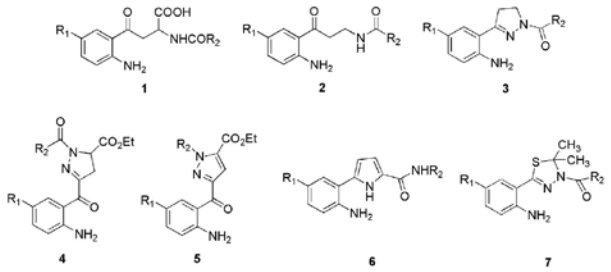

Figure 1. nNOS and iNOS inhibitors synthesized by our research group.

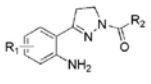

Figure 2. Structure of new 4,5-dihydro-1*H*-pyrazole derivatives **3a**–**r**.

although in some cases iNOS selectivity is observed. Finally, we have reported a group of selective iNOS/nNOS inhibitors wearing a 4,5-dihydro-1,3,4-thiadiazole ring **7** (see Fig. 1).[24]

In this paper we describe a new group of 3-phenyl-4,5-dihydro-1*H*-pryrazole compounds, and we evaluate their in vitro inhibition by both neuronal and inducible NOS. In these compounds, we have increased the activation and deactivation of the aromatic ring keeping the cyclopropyl and phenyl groups, as well as the size and flexibility of the phenyl moiety, with the aim of finding new and more potent and selective nNOS inhibitors. Thus, the benzene ring has been substituted with one or several electron-withdrawing (5-Cl and 4,5-Cl_2) or electron-donating [5-OMe, 4,5-$(OMe)_2$ and 2,3,4-$(OMe)_3$] substituents in order to analyse the influence of the aromatic ring charge distribution on the inhibitory activity. In addition, the size of the R_2 substituent has also been increased (Ph, CH_2Ph and CH_2CH_2Ph) to test the importance of the steric effects in the NOS inhibition and selectivity.

2. Results and discussion

2.1. Chemistry

3,4-Dichlorobenzaldehyde **8** was transformed into the 4,5-dichloro-2-nitrobenzaldehyde **12** by treatment with a mixture of fuming nitric acid (100%) and concentrated H_2SO_4.[25] 2,3,4-Trimethoxy-6-nitrobenzaldehyde **15** was obtained by reaction of 2,3,4-trimethoxybenzaldehyde **9** with a mixture of HNO_3 and AcOH.[26] These nitroderivatives and the commercially available 2-nitrobenzaldehyde **10**, 5-chloro-2-nitrobenzaldehyde **11**, 5-methoxy-2-nitrobenzaldehyde **13** and 4,5-dimethoxy-2-nitrobenzaldehyde **14** were transformed into the final compounds **3a**–**r**.[20] Therefore, these derivatives were treated with vinyl-magnesium bromide to yield the corresponding allylic alcohols **16**–**21**[20,27] quantitatively, which were further oxidized (Jones reagent) to obtain the enone derivatives **22**–**27**. Reaction of the enones **22**–**27** with hydrazine in ethanol produced the 4,5-dihydro-1*H*-pyrazoles **28**–**33** which, in situ, were transformed with the acyl chloride into derivatives **34a**–**r**. Finally, reduction of the nitro group with $SnCl_2$ in ethanol yielded the final compounds **3a**–**r** (see Scheme 1).[28]

2.2. Biological data

The biological activity of the new compounds **3a**–**r** as inhibitors of both iNOS and nNOS has been evaluated by means of in vitro assays using recombinant isoenzymes. We have made the assays using a 1 mM concentration of each compound in order to identify the more potent and selective derivatives.

Figure 3 shows the percentages of residual nNOS and iNOS activity in the presence of each compound in relation to the control, and Table 1 shows the inhibition percentages versus both isoenzymes.

In general, compounds **3a**–**r** behave as weak inhibitors against iNOS, since only two compounds (**3g** and **3h**) show an inhibition of around 50% at the concentration of 1 mM. Nevertheless, some conclusions can be inferred from the experimental data. From a qualitative point of view, the influence of R_1 and R_2 over the iNOS activity is variable. When R_2 = *c*-C_3H_5, compounds with the best inhibitory activity have electron-donating substituents in R_1, and the activity increases with the number of these substituents, **3o** (30.1%) being one of the best iNOS inhibitors with three methoxy groups in the aromatic ring. On the other hand, when R_2 = Ph, CH_2Ph or CH_2CH_2Ph, the most potent compounds wear two electron-withdrawing groups in the aromatic ring, and therefore **3g** (49.2%, $R_2 = CH_2Ph$) and **3h** (50.2%, $R_2 = CH_2CH_2Ph$) are the best iNOS inhibitors.

Table 1 also shows the nNOS inhibition values in presence of 1 mM concentration of compounds **3a**–**r**. These compounds behave as better inhibitors against nNOS, since five molecules show an inhibition percentage higher than 48%. In general, molecules with electron-donating groups in R_1 behave as good nNOS inhibitors, with the exception of compounds **3i** and **3o**, which are inactive. In this series, **3n** (R_1 = 4,5-$(OMe)_2$, $R_2 = CH_2CH_2Ph$) and **3q** (R_1 = 2,3,4-$(OMe)_3$, $R_2 = CH_2Ph$) show moderate inhibition values (55.3% and 48.4%, respectively), **3p** (R_1 = 2,3,4-$(OMe)_3$, R_2 = Ph) shows good percentage of inhibition (62.9%), and compound **3r** (R_1 = 2,3,4-$(OMe)_3$, $R_2 = CH_2CH_2Ph$) is the best nNOS inhibitor (82.5%). In the series with electron-withdrawing substituents, the most potent molecule is **3e** (R_1 = 4,5-Cl_2, R_2 = *c*-C_3H_5) with a moderate inhibition (50.5%). As shown, compounds with electron-donating groups in R_1 are better nNOS inhibitors than those with electron-withdrawing ones, and a non-substituted benzene moiety

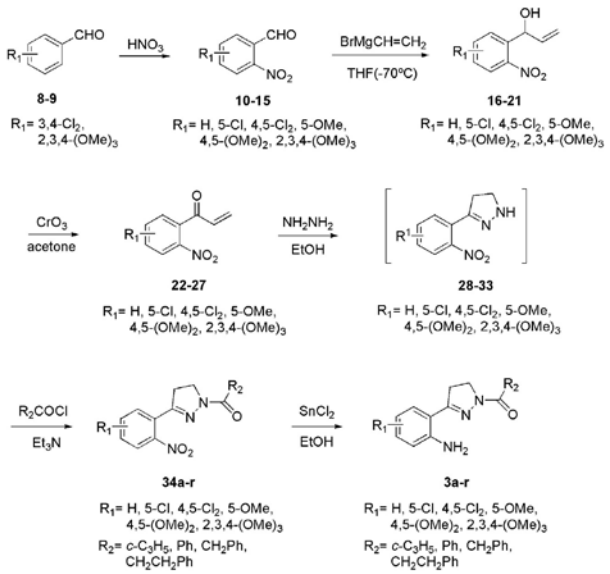

Scheme 1. General synthetic pathway followed in the preparation of compounds **3a–r**.

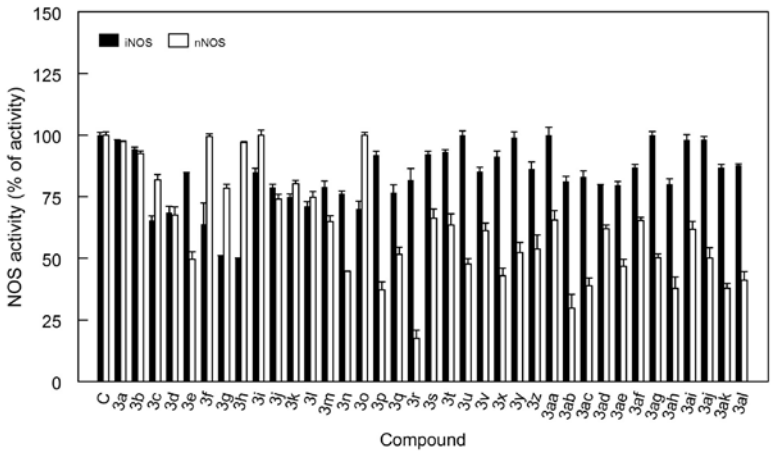

Figure 3. Percentages of the nNOS and iNOS activities in the presence of 1 mM of the 4,5-dihydro-1*H*-pyrazole derivatives assayed (compounds **3a–al**) compared to control. Each value is the mean of three experiments performed in triplicate in the presence of recombinant iNOS or nNOS.

is not beneficial for the nNOS inhibitory activity. Moreover, with regard to the acyl group, the increase of size and flexibility improves the nNOS inhibition in most cases, being the phenylpropanoyl groups one of the most interesting.

Regarding the nNOS/iNOS selectivity, it can be observed that the most active compounds which have electron-donating groups in R_1, show better selectivity versus nNOS than compounds with electron-withdrawing or neutral substituents, and **3p** (R_1 = 2,3,4-$(OMe)_3$, R_2 = Ph) is the most selective one of all the tested compounds. Furthermore, compound **3r**, with three electron-donating groups in the phenyl moiety is the most potent nNOS inhibitor, showing good selectivity versus nNOS. On the other hand, compound **3h** (R_1 = 4,5-Cl_2, R_2 = CH_2CH_2Ph) behaves as a selective iNOS/nNOS inhibitor, with a moderate iNOS inhibition (50.2%).

Table 1
In vitro nNOS and iNOS inhibition (%) observed in the presence of 1 mM concentration of compounds **3a–r**

Compound	R_1	R_2	% Inhib. iNOS[a]	% Inhib. nNOS[a]
3a	H	CH_2Ph	2.31 ± 0.31	2.68 ± 0.27
3b	H	CH_2CH_2Ph	5.64 ± 0.74	7.36 ± 0.96
3c	5-Cl	CH_2Ph	34.62 ± 1.73	18.24 ± 2.35
3d	5-Cl	CH_2CH_2Ph	31.37 ± 2.43	32.36 ± 3.23
3e	4,5-Cl_2	c-C_3H_5	15.53 ± 0.23	50.48 ± 3.12
3f	4,5-Cl_2	Ph	36.10 ± 8.50	0.62 ± 1.13
3g	4,5-Cl_2	CH_2Ph	49.22 ± 0.38	21.59 ± 1.67
3h	4,5-Cl_2	CH_2CH_2Ph	50.17 ± 0.24	2.97 ± 0.32
3i	5-OMe	CH_2Ph	15.0 ± 1.58	0.03 ± 2.03
3j	5-OMe	CH_2CH_2Ph	21.19 ± 1.33	25.93 ± 2.04
3k	4,5-$(OMe)_2$	c-C_3H_5	25.21 ± 1.38	19.65 ± 1.23
3l	4,5-$(OMe)_2$	Ph	28.9 ± 1.97	25.14 ± 2.17
3m	4,5-$(OMe)_2$	CH_2Ph	21.0 ± 2.38	35.07 ± 2.28
3n	4,5-$(OMe)_2$	CH_2CH_2Ph	23.72 ± 1.04	55.33 ± 0.21
3o	2,3,4-$(OMe)_3$	c-C_3H_5	30.07 ± 3.21	0.05 ± 1.25
3p	2,3,4-$(OMe)_3$	Ph	8.14 ± 1.56	62.87 ± 3.25
3q	2,3,4-$(OMe)_3$	CH_2Ph	23.39 ± 3.23	48.36 ± 2.87
3r	2,3,4-$(OMe)_3$	CH_2CH_2Ph	18.29 ± 4.74	82.45 ± 3.26

[a] Data represent the percentage of nNOS and iNOS inhibition produced by 1 mM concentration of each compound. Each value is the mean of three experiments performed by triplicate using recombinant iNOS and nNOS enzymes.

Table 2
In vitro nNOS and iNOS inhibition (%) observed in the presence of 1 mM concentration of compounds **3s–al**

Compound	R_1	R_2	% Inhib. iNOS[a]	% Inhib. nNOS[b]
3s	H	Me	7.73 ± 1.16	33.69 ± 3.62
3t	H	Et	6.88 ± 0.95	36.47 ± 4.52
3u	H	Pr	0.35 ± 1.75	52.39 ± 2.24
3v	H	c-C_3H_5	14.80 ± 1.64	38.79 ± 3.18
3x	H	Ph	8.7 ± 2.18	57.05 ± 3.13
3y	5-Cl	Me	1.03 ± 2.31	47.58 ± 4.01
3z	5-Cl	Et	13.72 ± 2.88	46.15 ± 5.66
3aa	5-Cl	Pr	0.29 ± 3.26	34.43 ± 3.70
3ab	5-Cl	c-C_3H_5	18.89 ± 2.16	70.24 ± 5.60
3ac	5-Cl	Ph	17.04 ± 2.55	61.12 ± 3.11
3ad	5-OMe	Me	20.39 ± 0.42	38.04 ± 1.53
3ae	5-OMe	Et	20.39 ± 1.53	53.27 ± 2.83
3af	5-OMe	Pr	13.09 ± 1.2	34.70 ± 1.32
3ag	5-OMe	Bu	0.18 ± 1.4	49.76 ± 1.53
3ah	5-OMe	c-C_3H_5	19.90 ± 2.11	62.24 ± 4.68
3ai	5-OMe	c-C_6H_7	1.91 ± 2.1	38.30 ± 3.33
3aj	5-OMe	c-C_5H_9	1.85 ± 1.2	49.87 ± 4.13
3ak	5-OMe	c-C_6H_{11}	13.25 ± 1.32	62.20 ± 1.91
3al	5-OMe	Ph	12.18 ± 0.55	58.92 ± 3.55

[a] Data represent the percentage of nNOS and iNOS inhibition produced by 1 mM concentration of each compound. Each value is the mean of three experiments performed by triplicate using recombinant iNOS and nNOS enzymes.
[b] See Ref. 20.

In addition, Figure 3 also shows the data of the iNOS activity of compounds **3s–al**, and Table 2 includes the data of the iNOS inhibition for these compounds (not published before), as well as their nNOS values previously described,[20] in order to compare them. These compounds have weak values of iNOS inhibition and they can be considered as selective inhibitors of nNOS versus iNOS.

In general, the best nNOS inhibition values of derivatives **3s–al** were obtained with the c-C_3H_5 and Ph groups in R_2, **3ab** (R_1 = 5-Cl, R_2 = c-C_3H_5) being the most active compound of this group, showing good selectivity versus nNOS.

When we carried out different modifications in both, the aromatic moiety and the acyl group, we observed that the deactivation of the aromatic ring in the dichloro derivatives in relation to the monochloro ones produced a considerable loss of activity. Moreover, although the greatest activation of the aromatic ring in compounds with R_2 = c-C_3H_5 produced a drastic loss of activity, the increase of size and flexibility of the R_2 radical led us to the preparation of compound **3r**, which is more potent than **3ab**, previously described.

As regards iNOS inhibition of all tested compounds, the best results have been obtained with the deactivation of the aromatic ring (R_1 = 4,5-Cl_2) and the increase of size and flexibility of the phenyl ring (R_2 = CH_2Ph and CH_2CH_2Ph) (derivatives **3g** and **3h**). However, derivatives **3a–al** are, in general, inactive versus iNOS and, as a result, they can be considered inhibitors with good nNOS selectivity.

Table 3 shows the IC_{50} values measured for the nNOS inhibition of derivatives **3n**, **3p** and **3r** observed in the initial in vitro assay, which ranges between 0.40 and 0.88 mM, being **3r** the most potent inhibitor of all compounds of the series.

2.3. Docking studies

nNOS and iNOS crystal structures have been obtained from the Brookhaven protein databank (PDB ID: 1QW6 and 1QW4,[29] respectively). Schrödinger software[30] has been used for the docking studies. The preparation of the enzyme and the ligands has been done following standard procedures included in the Schrödinger suite. The protein preparation is performed using the Protein Preparation Wizard module,[31] and 3D structures of compounds **3a–r** were generated from fragment libraries, and optimized using the Macromodel module. The LigPrep[32] program suite was used for the ligands preparation, and Glide program was utilized for docking the ligands using the SP option.

Glide's Gscore values obtained for compounds **3a–r** complexes in both nNOS and iNOS binding sites are small (between −3.00 and −5.50 kcal/mol) indicating that these complexes are weak, and consequently the compounds are moderated inhibitors.

Three different poses have been obtained for compounds **3a–r** inside the nNOS binding site. Figure 4[33] illustrates, as an example, the preferred pose observed for compounds **3r**, **3p** and **3d**, respectively. In compound **3r** (pose a), the phenyl moiety is situated below the heme group establishing a π–π interaction. The trimethoxyphenyl ring adopts a position that allows the interaction of 4′-OMe and 5′-OMe groups with Arg481 through two hydrogen bonds. The 2′-NH_2 group forms a hydrogen bond with one of the carboxylate moieties of the heme group. The coplanar disposition of the pyrazoline and the amide carbonyl group reinforces the conjugation between both moieties contributing to the stability of the conformation. Moreover, this conformation increases the length of the molecule, which allows the methoxy groups to establish van der Waals (vdW) interactions with Ala497.

Compounds that are not able to interact with Arg481 remain in an intermediate position between the heme group and this amino-acid. This is the case of **3p**. In pose b, the ligand is orientated in a similar manner as pose a showed for the compound **3r**. The phenyl ring is situated below the heme group but interact, by means of one hydrogen bond, with Asn569. Another hydrogen bond is established between 2′-NH_2 and one of the carboxylate moieties of the heme group. The conformation of the ligand **3p** seems to be also stable since C = O and the pyrazoline are coplanar which favors the conjugation between them.

Table 3
IC_{50} values (mM) for the inhibition of nNOS activity by the pyrazoline derivatives **3n**, **3p** and **3r**

Compound	R_1	R_2	IC_{50} (mM)
3n	4,5-$(OCH_3)_2$	CH_2CH_2Ph	0.88
3p	3,2,4-$(OCH_3)_3$	Ph	0.53
3r	3,2,4-$(OCH_3)_3$	CH_2CH_2Ph	0.40

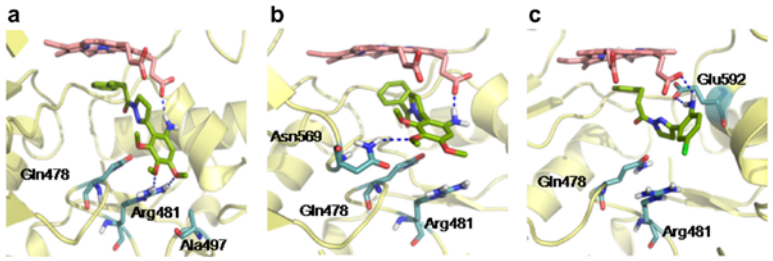

Figure 4. Detailed view of the main poses obtained for compounds **3r** (pose a), **3p** (pose b) and **3d** (pose c) in the nNOS binding site. Dotted lines indicate hydrogen bond interactions between the ligand and the residues of the enzyme.

Finally, Figure 4 also shows the preferred pose for compound **3d** (pose c). In this pose, there are two hydrogen bonds established by the 2′-NH_2 group. One of them implies Glu592 and the other one implies one of the carboxylate moieties of the heme group. The phenyl ring is also situated, as in poses a and b, below the heme group.

Regarding iNOS, docking studies indicate the existence of three different poses for compounds **3a**–**r**. As an example, Figure 5 shows the preferred poses for compounds **3h**, **3f** and **3q**, respectively.

The rotation of Arg260 in iNOS in relation to Arg481 in nNOS diminished the volume available bellow this residue, and forces compound **3h** to adopt a totally different orientation inside iNOS in relation to nNOS. Pose a shows a hydrogen bond between 2′-NH_2 and Ser256 whose conformation changes respect to the conformation of Ser477 in nNOS because of the Arg260 rotation mentioned above. The phenyl and the pyrazoline rings are in a coplanar disposition which reinforces the conjugation between C=N double bond and the phenyl ring, and allows the formation of an intramolecular hydrogen bond between the 2′-NH_2 group and the pyrazoline N-2 atom. This situation contributes to the stability of this conformation. Furthermore, 4′- and 5′-Cl atoms interact by means of vdW interactions with Tyr485 and Asn115 favoring the stability of the conformation.

In pose b, **3f** is orientated towards the opposite side of the binding cavity. The –NH_2 group forms a hydrogen bond with Glu371. The phenyl Cl atoms interact with the guanidinium groups of the Arg375, Arg382 and Arg260. However, the ligand conformation seems to be not too stable since the conjugation between the phenyl ring and the C=N bond is very weak due to the fact that the pyrazoline and the phenyl rings are not coplanar. Compound **3h** cannot adopt this pose because the pocket formed by the three arginine residues does not allow the accommodation of molecules longer than compound **3f**. These aminoacids represent a steric impediment.

The third pose in iNOS for compound **3q** is represented in Figure 5c. This pose is similar to the pose of compound **3r** inside nNOS binding side (Fig. 4a). However, the conformation of Arg260 in iNOS reduces the available volume under the carboxylate heme moieties forcing the ligand **3q** to remain in an intermediate plane without any interaction with the enzyme.

It is clear that the volume of R_1 and the volume and length of R_2 influence the orientation and the disposition of the ligands inside the binding site. Additionally, the conformation of Arg260 in iNOS and Arg481 in nNOS, and consequently, the conformation of other residues in both binding sites, seem to be decisive on the interaction with the protein as well as on the orientation of the ligands inside the binding cavity (Fig. 6).

2.4. Discussion

The substrate binding sites of the NOS isoforms oxygenase domains present a high level of aminoacids conservation and structural similarity. However, some differences outside the active site and a conformational flexibility inside allow the adoption of different conformations and the establishment of different interactions which explains the preference of the compound for one or another isoenzyme.

The main difference between both nNOS and iNOS binding site is the orientation of the side-chain of Arg481 (or Arg260 in iNOS) which controls the orientation of Gln478 (or Gln257 in iNOS), and which in turn depends on the mutation of Asn498 in nNOS by Thr277 in iNOS. Therefore, the difference in the side-chain

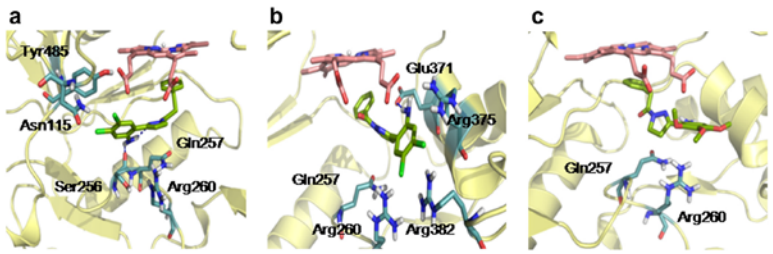

Figure 5. Detailed view of the main poses obtained for compounds **3h** (pose a), **3f** (pose b) and **3q** (pose c) in the iNOS binding site. Dotted lines indicate hydrogen bond interactions between the ligand and the residues of the enzyme and the intramolecular hydrogen bond.

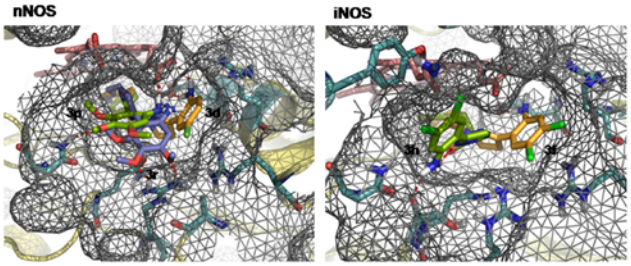

Figure 6. View of the surface of nNOS and iNOS binding site and the orientation of the compounds inside.

orientation of Arg481 in nNOS with regard to Arg260 in iNOS could explain the selectivity and potency observed in some 4,5-dihydro-1*H*-pyrazole derivatives described in this paper.

In poses b and c (Fig. 4) obtained for these molecules inside the nNOS binding site, ligands adopt a conformation that allows the formation of two hydrogen bonds. The first one, usually, formed by the $-NH_2$ group with one of the carboxylate moieties of the heme group. The second bond, in all –OMe derivatives, is formed between –OMe group and the nearest residue. In the case of compounds with R_1 = H, Cl, this second H-bond cannot be formed or is established by the $-NH_2$ group such is the case in compound **3d** (pose c, Fig. 4). In pose a, two –OMe groups interact by mean of two hydrogen bonds with Arg482, the main difference in the binding cavity between nNOS and iNOS. This fact, together with vdW interactions with Ala497, could explain the highest selectivity and potency observed in compound **3r**. Besides, the coplanar disposition of R_2 phenyl ring below the heme group enables a π–cation interaction with Fe^{3+} ion. Also, the conjugation between the pyrazoline and C=O double bond as a consequence of the coplanarity provides more stability to the conformation of the ligands as shown in pose a and b (Fig. 2).

In iNOS, the available volume for binding the ligand is smaller compared with nNOS,[29] as it is illustrated in Fig. 6. The rotation of iNOS Arg260 side-chain in relation to the nNOS Arg481 side-chain is involved in this fact. In pose a and b (Fig. 5), the ligands have an opposite disposition in the binding site. In pose b, one hydrogen bond is formed between the $-NH_2$ group and Glu371. π–cation interaction between the R_2 phenyl ring and heme group Fe^{3+} is weak due to the lack of coplanarity of both rings. The disubstituted phenyl ring is aimed towards the pocket formed by Arg375, Arg382 and Arg260. This pocket represents a steric impediment, for compounds with bulky R_2, to adopt pose b. Therefore, compounds like **3h** is orientated to the opposite site of the binding cavity (Fig. 6). In pose a (Fig. 5), the ligand establishes a hydrogen bond with Ser256 across the $-NH_2$ group. Another intramolecular hydrogen bond, between $-NH_2$ and the pyrazoline N-2, stabilizes the conformation. This orientation allows the Cl atoms to interact by means of vdW interaction with Tyr485 and Asn115 which is mutated by Leu337 in nNOS. The conformational stability and the particular orientation of this compound could explain its higher iNOS selectivity and potency compared with the rest of the compounds.

On the other hand, iNOS poses a and c (Fig. 5) are the preferred ones for most of the pyrazolines with methoxy groups. In both cases, these compounds have weak interactions with the enzyme. This fact could explain the lack of iNOS activity in these derivatives.

3. Conclusions

In summary, as an extension of the 4,5-dihydro-1*H*-pyrazole derivatives **3s**–**al** previously synthesized, in the present study we have reported the results on iNOS and nNOS inhibition of compounds **3a**–**r**, by means of an activation and deactivation of the aromatic ring, and an increase of the size and flexibility of the R_2 group in this type of structures. In this report, the increase of size of R_2 substituent improves the iNOS, as well as the nNOS inhibitory activity. Nevertheless, regarding the R_1 substituent in the aromatic ring, electron-withdrawing groups are good for iNOS inhibition, whereas electron-donating substituents improve the values of nNOS inhibition. This fact is confirmed by docking studies which show the better orientation of **3h** in iNOS and **3r** in nNOS. In addition, structures **3s**–**al** exhibit a nNOS/iNOS selectivity. Among all compounds, **3g** and **3h** are the best iNOS inhibitors (about 50% of inhibition), and derivative **3r** is the most potent nNOS inhibitor of all the tested compounds, with a good nNOS/iNOS selectivity. Thus, such a compound as **3r** can be an interesting starting point for possible new alternatives in neurodegenerative diseases such as Alzheimer or Parkinson.

4. Experimental section

4.1. Chemistry

4.1.1. Material and methods

Melting points were determined using an Electrothermal-1A-6301 apparatus and are uncorrected. ^1H and ^{13}C NMR spectra were recorded on a Bruker AMX 300 spectrometer operating at 75.49 MHz for ^{13}C and 300.20 for ^1H and on a Bruker ARX 400 spectrometer operating at 400.17 MHz for ^1H and 125.69 MHz for ^{13}C, in $CDCl_3$ (at concentration of ca. 27 mg mL^{-1} in all cases) The center of each peak of $CDCl_3$ [7.26 ppm (^1H) and 77.0 ppm (^{13}C)] was used as internal reference in a 5 mm $^{13}C/^1H$ dual probe (Wilmad, No. 528-PP). The temperature of the sample was maintained at 297 K. The peaks are reported in ppm (δ). High-resolution mass spectroscopy (HRMS) was carried out on a VG AutoSpec Q high-resolution mass spectrometer (Fision Instruments). Flash chromatography was carried out using silica gel 60, 230–240 mesh (Merk), and the solvent mixture reported within parentheses was used as eluent.

4.1.2. Preparation of 1-(2-nitrophenyl-substituted)prop-2-en-1-ol (18, 21) general method

To a −70 °C solution of 4.75 mmol of the corresponding 2-nitrobenzaldehyde (**12**, **15**) in 20 mL of THF was added 6.65 mmol of vinylmagnesium bromide. After being stirred for 3.5 h, the mixture was quenched with 20 mL of 0.010 N HCl and diluted with 100 mL of ethyl acetate and extracted. The separated organic phase was washed with brine, dried, then concentrated in vacuo to obtain a residue that was purified by column chromatography (EtOAc/hexane 1:10).

4.1.2.1. 1-(4,5-Dichloro-2-nitrophenyl)prop-2-en-1-ol (18). Mp: 40–41 °C. Yield: 65%; ^{1}H NMR (400.17 MHz, $CDCl_3$) δ: 8.07 (s, 1H, H-3′), 7.91 (s, 1H, H-6′), 6.05–5.97 (m, 1H, H-2), 5.84 (d, 1H, J_{1-2} = 5.5 Hz, H-1), 5.42 (dd, 1H, J_{3a-3b} = 1.2 Hz, J_{3a-2} = 17.2 Hz, H-3a), 5.28 (dd, 1H, J_{3b-3a} = 1.2 Hz, J_{3b-2} = 11.8 Hz, H-3b). ^{13}C NMR (125.69 MHz, $CDCl_3$) δ: 141.35 (C-2′), 140.37 (C-5′), 139.83 (C-2), 135.18 (C-4′), 134.15 (C-1′), 133.11 (C-6′), 129.11 (C-3′), 119.81 (C-3), 71.90 (C-1). MS (ESI): $[M+1]^+$ = 2475.9832.

4.1.2.2. 1-(6-Nitro-2,3,4-trimethoxyphenyl)prop-2-en-1-ol (21). Mp: 90–93 °C. Yield: 100%; ^{1}H NMR (400.17 MHz, $CDCl_3$) δ: 7.24 (s, 1H, H-5′), 6–19–6.15 (m, 1H, H-2), 5.63 (d, 1H, J_{1-2} = 4.1 Hz, H-1), 5.33–5.02 (m, 2H, H-3a, H-3b), 3.99, 3.97, 3.96 (3s, 9H, 2′-OCH_3, 3′-OCH_3, 4′-OCH_3).^{13}C NMR (75.49 MHz, $CDCl_3$) δ: 155.94 (C-2′), 153.46 (C-4′); 152.77 (C-3′), 146.84 (C-6′), 139.52 (C-2), 121.25 (C-1′), 114.75 (C-3), 104.49 (C-5′), 69.03 (C-1), 63.03 (3′-OCH_3), 61.26 (2′-OCH_3), 56.93 (4′-OCH_3). MS (LSIMS): $[M+Na]^+$ = 292.0792.

4.1.3. Preparation of 1-(2-nitrophenyl-substituted)prop-2-en-1-one (24, 26, 27) general method

Freshly prepared Jones reagent (1.1 mL, 2.67 M) was added dropwise to 2 mmol of the corresponding alcohol in 4 mL of acetone at room temperature. After 10 min, ice-water (5 mL) was added followed by 1 mL of saturated $NaHSO_3$. The resulting mixture was extracted with ethyl acetate. The extracts were dried (Na_2SO_4) filtered, and concentrated to afford a residue that was purified by column chromatography (EtOAc/hexane 1:10).

4.1.3.1. 1-(4,5-Dichloro-2-nitrophenyl)prop-2-en-1-one (24). Mp: 68–70 °C. Yield: 78%; ^{1}H NMR (400.17 MHz, $CDCl_3$) δ: 8.26 (s, 1H, H-3′), 7.53 (s, 1H, H-6′), 6.62 (m, 1H, H-2), 6.09 (dd, 1H, J_{3a-3b} = 1.6 Hz, J_{3a-2} = 10.6 Hz, H-3a), 5.91 (dd, 1H, J_{3b-3a} = 1.6 Hz, J_{3b-2} = 17.6 Hz, H-3b,). ^{13}C NMR (75.49 MHz, $CDCl_3$) δ: 190.87 (C-1), 142.50 (C-2′), 139.74 (C-5′), 136.17 (C-6′), 135.46 (C-4′), 134.80 (C-1′), 132.17 (C-3), 130.61 (C-2), 126.59 (C-3′). MS (ESI): $[M+H]^+$ = 245.9722.

4.1.3.2. 1-(4,5-Dimethoxy-2-nitrophenyl)prop-2-en-1-one (26). Mp: 138–140 °C. Yield: 80%; ^{1}H NMR (400.17 MHz, $CDCl_3$) δ: 7.64 (s, 1H, H-3′), 6.79 (s, 1H, H-6′), 6.58 (m, 2H, H-2), 5.94 (d, 1H, J_{3a-2} = 10.6 Hz, H-3a), 5.82 (d, 1H, J_{3b-2} = 17.6 Hz, H-3b,), 3.99 (5′-OCH_3), 3.96 (4′-OCH_3). ^{13}C NMR (125.69 MHz, $CDCl_3$) δ: 193.56 (CO), 154.09 (C-4′), 150.05 (C-5′), 139.91 (C-2′), 137.00 (C-2), 130.31 (C-3), 130.03 (C-1′), 110.25 (C-6′), 107.11 (C-3′), 56.96 (4′-OCH_3, 5′-OCH_3). MS (LSIMS): $[M+Na]^+$ = 260.0540.

4.1.3.3. 1-(6-Nitro-2,3,4-trimethoxyphenyl)prop-2-en-1-one (27). Mp: 143–145 °C. Yield: 70%; ^{1}H NMR (400.17 MHz, $CDCl_3$) δ: 7.55 (s, 1H, H-5′), 6.64 (dd, 1H, J_{2-3a} = 10.6 Hz, J_{2-3b} = 17.6 Hz, H-2), 6.08–5.67 (m, 2H, H-3a, H-3b), 4.09–3.91 (3s, 9H, 2′-OCH_3, 3′-OCH_3, 4′-OCH_3). ^{13}C NMR (125.69 MHz, $CDCl_3$) δ: 187.07 (CO), 155.88 (C-4′), 153.82 (C-2′), 150.91 (C-6′), 148.17 (C-3′), 137.83 (C-2), 130.39, (C-3), 124.48 (C-1′), 104.05 (C-5′), 63.05, 62.45 (2′-OCH_3, 3′-OCH_3), 56.78 (4′-OCH_3). MS (LSIMS): $[M+Na]^+$ = 290.0646.

4.1.4. Preparation of 1-acyl-3-(2-nitrophenyl-substituted)-4,5-dihydro-1*H*-pyrazoles (34a–n) and 1-acy-3-(6-nitro-2,3,4-trimethoxyphenyl)-4,5-dihydro-1*H*-pyrazole (34o–r) general method

The corresponding substituted-phenyl vinyl ketone (1.4 mmol) was added to a solution of hydrazine monohydrate in ethanol (15 mL), and the mixture was refluxed during 3 h. After this period, the mixture was cooled, extracted with diethyl ether (4 × 10 mL), dried Na_2SO_4, filtered and concentrated to dryness. Without isolation, the pyrazoline was dissolved in dry CH_2Cl_2, and triethylamine (1.5 mmol) and the acyl chloride (1.4 mmol) were added at room temperature under nitrogen atmosphere. The reaction mixture was stirred for 3 h, filtered and washed with 10% HCl, 2 M NaOH, H_2O, and brine. The organic phase was dried and filtered. Evaporation of the solvent rendered a residue that was purified by column chromatography (EtOAc/hexane 1:2).

4.1.4.1. 3-(2-Nitrophenyl)-1-phenylacetyl-4,5-dihydro-1*H*-pyrazole (34a). Mp: 116–117 °C. Yield: 75%; ^{1}H NMR (400.17 MHz, $CDCl_3$) δ: 7.93–7.17 (3 m, 9H, –CH–$_{arom}$), 4.09 (t, 2H, J_{5-4} = 10.2 Hz, H-5), 4.01 (s, 2H, CO-CH_2), 3.20 (t, 2H, J_{4-5} = 10.2 Hz, H-4). ^{13}C NMR (75.49 MHz, $CDCl_3$) δ: 170.18 (CO), 152.81 (C-3), 148.59 (C-2′), 132.58 (C-1″), 130.73, 130.41, 130.23 (C-4′, C-5′, C-6′), 129.62, 128.48, 126.80 (C-2″–C-6″), 124.54 (C-1′), 124.26 (C-3′), 44.65 (C-5), 40.91 (CO-CH_2), 33.63 (C-4). MS (ESI): $[M+H]^+$ = 310.1102.

4.1.4.2. 3-(2-Nitrophenyl)-1-phenylpropanoyl-4,5-dihydro-1*H*-pyrazole (34b). Mp: 120–121 °C. Yield: 70%; ^{1}H NMR (300.20 MHz, $CDCl_3$) δ: 7.74 -7.09 (3 m, 9H, –CH–$_{arom}$), 3.99 (t, 2H, J_{4-5} = 10.2 Hz, H-5), 3.08 (t, 2H, J_{4-5} = 10.2 Hz, H-4), 2.91 (m, 4H, CO-CH_2–CH_2). ^{13}C NMR (75.49 MHz, $CDCl_3$): δ 171.64 (CO), 152.72 (C-3), 148.84 (C-2′), 141.46 (C-1″), 132.63 (C-4′), 130.66 (C-5′), 130.25 (C-6′), 128.78, 128.59, 126.35 (C-2″ to C-6″), 126.23 (C-1′), 124.44 (C-3′), 44.58 (C-5), 36.02 (CO–CH_2–CH_2), 33.57 (C-4), 31.34 (CO–CH_2–CH_2). MS (ESI): $[M+Na]^+$ = 346.1166.

4.1.4.3. 3-(5-Chloro-2-nitrophenyl)-1-phenylacetyl-4,5-dihydro-1*H*-pyrazole (34c). Mp: 154–156 °C. Yield: 50%; ^{1}H NMR (400.17 MHz, $CDCl_3$) δ: 7.81 (d, 1H, $J_{3′-4′}$ = 7.8 Hz, H-3′), 7.54–7.22 (m, 7H, H-4′, H-6′, H-2″ to H-6″), 4.07 (t, 2H, J_{4-5} = 10.2 Hz, H-5), 3.98 (s, 2H, CO-CH_2) 3.15 (t, 2H, J_{4-5} = 10.2 Hz, H-4). ^{13}C NMR (75.49 MHz, $CDCl_3$) δ: 170.21 (CO), 151.77 (C-3), 145.56 (C-2′), 139.13 (C-5′), 135.18 (C-1″), 130.58 (C-4′), 130.48 (C-6′), 129.77, 128.70 (C-2″, C-3″, C-5″, C-6″), 128.25 (C-1′), 127.05 (C-4″), 125.95 (C-3′), 44.87 (C-5), 40.99 (CO-CH_2), 33.52 (C-4). MS (LSIMS): $[M+H]^+$ = 344.0798.

4.1.4.4. 3-(5-Chloro-2-nitrophenyl)-1-phenylpropanoyl-4,5-dihydro-1*H*-pyrazole (34d). Mp: 160–162 °C. Yield: 60%; ^{1}H NMR (400.17 MHz, $CDCl_3$) δ: 7.75 (d, 1H, H-3′, $J_{3′-4′}$ = 8.4 Hz), 7.47–7.08 (m, 7H, H-4′, H-6′, H-2″ to H-6″), 4.01 (t, 2H, J_{4-5} = 10.2 Hz, H-5), 3.05 (t, 2H, J_{4-5} = 10.2 Hz, H-4), 2.84–2.60 (m, 4H, COCH_2–CH_2). ^{13}C NMR (75.49 MHz, $CDCl_3$) δ: 171.75 (CO), 151.83 (C-3), 146.85 (C-2′), 141.35 (C-1″), 139.22 (C-5′), 130.55 (C-4′), 130.37 (C-6′), 128.79, 128.55 (C-2″, C-3″, C-5″, C-6″), 128.99 (C-1″), 126.36 (C-4″), 125.97 (C-3′), 44.76 (C-5), 35.96 (C-4), 33.51 (CO–CH_2–CH_2), 31.51 (CO–CH_2–CH_2). MS (LSIMS): $[M+H]^+$ = 358.0957.

4.1.4.5. 1-Cyclopropylcarbonyl-3-(4,5-dichloro-2-nitrophenyl)-4,5-dihydro-1*H*-pyrazole (34e). Mp: 164–166 °C. Yield: 60%; ^{1}H NMR (400.17 MHz, $CDCl_3$) δ: 7.94 (s, 1H, H-3′), 7.72 (s, 1H, H-6′), 4.09 (t, 2H, J_{5-4} = 10.6 Hz, H-5), 3.13 (t, 2H, J_{4-5} = 10.6 Hz, H-4), 2.49–2.44 (m, 1H, H-1″), 1.13–0.86 (m, 4H, H-2″, H-3″). ^{13}C NMR (125.69 MHz, $CDCl_3$) δ: 173.01 (CO), 150.36 (C-3), 146.82 (C-2′), 137.54 (C-5′), 134.68 (C-4′), 131.62 (C-6′), 126.33 (C-3′), 126.18 (C-1′), 45.25 (C-5), 33.06 (C-4), 11.81 (C-1″), 8.82 (C-2″, C-3″). MS (LSIMS): $[M+Na]^+$ = 350.0077.

4.1.4.6. 1-Benzoyl-3-(4,5-dichloro-2-nitrophenyl)-4,5-dihydro-1*H*-pyrazole (34f). Mp: 130–132 °C. Yield: 50%; ^{1}H NMR (400.17 MHz, $CDCl_3$) δ: 7.90 (s, 1H, H-3′), 7.80 (d, 2H, H-2″, H-6″, $J''_{2-3} = J''_{6-5}$ = 7.2 Hz), 7.63 (s, 1H, H-6′), 7.45–7.38 (m, 3H, H-3″, H-4″, H-5″), 4.29 (t, 2H, H-5, J_{5-4} = 10.1 Hz), 3.18 (t, 2H, H-4,

J_{4-5} = 10.1 Hz). ^{13}C NMR (75.49 MHz, $CDCl_3$) δ: 167.52 (CO), 151.22 (C-3), 137.38 (C-1″), 134.70 (C-5′), 133.41 (C-4′), 131.43 (C-6′), 131.36 (C-4″), 129.74–127.88 (C-2″-C-6″), 126.25 (C-3′), 125.91 (C-1′), 45.81 (C-5), 32.54 (C-4). MS (ESI): $[M+H]^+$ = 364.0256.

4.1.4.7. 3-(4,5-Dichloro-2-nitrophenyl)-1-phenylacetyl-4,5-dihydro-1*H*-pyrazole (34g). Mp: 128–130 °C. Yield: 40%; ^{1}H NMR (300.20 MHz, $CDCl_3$) δ: 7.93 (s, 1H, H-3′), 7.63 (s, 1H, H-6′), 7.42–7.26 (m, 5H, H-2″ to H-6″), 4.08 (t, 2H, J_{5-4} = 10.4 Hz, H-5), 3,97 (s, 2H, $COCH_2$), 3.13 (t, 2H, J_{4-5} = 10.5 Hz, H-4). ^{13}C NMR (75.49 MHz, $CDCl_3$) δ: 170.23 (CO), 150.62 (C-3), 148.05 (C-2′), 137.53 (C-1″), 135.07 (C-5′), 134.91 (C-4′), 131.64 (C-6′), 129.73, 128.71 (C-2″, C-3″, C-5″, C-6″), 127.08 (C-4″), 126.39 (C-3′), 125.8 (C-1′), 44.93 (C-5), 40.99 ($COCH_2$), 33.25 (C-4). MS (ESI): $[M+H]^+$ = 378.0412.

4.1.4.8. 3-(4,5-Dichloro-2-nitrophenyl)-1-phenylpropanoyl-4,5-dihydro-1*H*-pyrazole (34h). Mp: 126–128 °C. Yield: 41%; ^{1}H NMR (300.20 MHz, $CDCl_3$) δ: 7.86 (s, 1H, H-3′), 7.54 (s, 1H, H-6′), 7.34–7.20 (m, 5H, H-2″ to H-6″), 4.00 (t, 2H, J_{5-4} = 10.2 Hz, H-5), 3.04 (t, 2H, J_{4-5} = 10.2, H-4), 3.02–2.91 (m, 4H, $COCH_2CH_2$). ^{13}C NMR (75.49 MHz, $CDCl_3$) δ: 171.72 (CO), 150.57 (C-3), 148.04 (C-2′), 141.29 (C-1″), 137.60 (C-5′), 134.85 (C-4′), 131.63 (C-6′), 128.77 (C-2″-C-6″), 126.38 (C-3′),126.33 (C-1′), 44.84 (C-5), 35.92 ($COCH_2CH_2$), 33.20 (C-4), 31.34 ($COCH_2CH_2$). MS (ESI): $[M+H]^+$ = 392.0569.

4.1.4.9. 3-(5-Methoxy-2-nitrophenyl)-1-phenylacetyl-4,5-dihydro-1*H*-pyrazole (34i). Mp: 116–117 °C. Yield: 75%; ^{1}H NMR (400.17 MHz, $CDCl_3$) δ: 8.05 (d, 1H, H-3′ $J_{3'-4'}$ = 9.0 Hz), 7.40–7.19 (m, 5H, H-2″ to H-6″), 7.02 (dd, 1H, $J_{4'-3'}$ = 9.0 Hz, $J_{4'-6'}$ = 2.8 Hz, H-4′), 6.95 (d, 1H, $J_{6'-4'}$ = 2.8 Hz, H-6′), 4.09 (t, 2H, H-5, J_{5-4} = 10.6 Hz), 4.00 (s, 2H, $COCH_2$), 3.93 (s, 3H, OCH_3), 3.13 (d, 2H, J_{4-5} = 10.6 Hz, H-4,). ^{13}C NMR (125.69 MHz, $CDCl_3$) δ: 172.41 (CO), 165.76 (C-5′), 157.33 (C-3), 141.40 (C-2′), 137.91 (C-1″), 132.68, 132.16, 131.06 (C-2″ to C-6″), 129.94 (C-1′), 129.32 (C-3′), 118.40 (C-6′), 117.54 (C-4′), 58.78 (OCH_3), 47.24 ($COCH_2$), 43.43 (C-5), 36.99 (C-4). MS (LSIMS): $[M+H]^+$ = 340.1297.

4.1.4.10. 3-(5-Methoxy-2-nitrophenyl)-1-phenylpropanoyl-4,5-dihydro-1*H*-pyrazole (34j). Mp: 117–118 °C. Yield: 81%; ^{1}H NMR (400.17 MHz, $CDCl_3$) δ: 8.05 (d, 1H, $J_{3'-4'}$ = 9.0 Hz, H-3′), 7.32–7.13 (m, 5H, H-2″ to H-6″), 7.02 (dd, 1H, $J_{4'-3'}$ = 9.0 Hz, $J_{4'-6'}$ = 2.8 Hz, H-4′), 6.93 (d, 1H, $J_{6'-4'}$ = 2.8 Hz, H-6′), 4.08 (t, 2H, J_{5-4} = 10.6 Hz, H-5), 3.92 (s, 3H, OCH_3), 3.12 (d, 2H, J_{4-5} = 10.6 Hz, H-4), 3.01–2.99 (m, 4H, $COCH_2CH_2$). ^{13}C NMR (125.69 MHz, $CDCl_3$) δ: 173.87 (CO), 165.81 (C-5′), 157.24 (C-3), 143.95 (C-2′), 137.91 (C-1″), 132.80, 131.15, (C-2″ to C-6″), 130.97 (C-1′), 128.62 (C-3′), 118.45 (C-6′), 117.40 (C-4′), 58.80 (OCH_3), 47.14 (C-5), 38.35 ($COCH_2CH_2$), 36.99 ($COCH_2CH_2$), 33.64 (C-4). MS (LSIMS): $[M+H]^+$ = 354.1453.

4.1.4.11. 1-Cyclopropylcarbonyl-3-(4,5-dimethoxy-2-nitrophenyl)-4,5-dihydro-1*H*-pyrazole (34k). Mp: 144–146 °C. Yield: 80%; ^{1}H NMR (400.17 MHz, $CDCl_3$) δ: 7.60 (H-3′), 6.98 (H-6′), 4.09 (t, 2H, J_{5-4} = 10.2 Hz, H-5), 4.00 (5′-OCH_3), 3.98 (4′-OCH_3), 3.11 (t, 2H, J_{4-5} = 10.2 Hz, H-4), 2.55–2.51 (m, 1H, H-1″), 1.08–0.83 (m, 4H, H-2″, H-3″). ^{13}C NMR (125.69 MHz, $CDCl_3$) δ: 172.66 (CO), 155.15 (C-3), 153.22 (C-5′), 149.96 (C-4′), 141.90 (C-2′), 122.39 (C-1′), 112.13 (C-6′), 108.07 (C-3′), 56.89, 56.78 (4′-OCH_3, 5′-OCH_3), 45.14 (C-5), 34.40 (C-4), 11.89 (C-1″), 8.56 (C-2″, C-3″). MS (LSIMS): $[M+H]^+$ = 320.1246.

4.1.4.12. 1-Benzoyl-3-(4,5-dimethoxy-2-nitrophenyl)-4,5-dihydro-1*H*-pyrazole (34l). Mp: 186–188 °C. Yield: 60%; ^{1}H NMR (300.20 MHz, $CDCl_3$) δ: 7.92–7.89 (m, 2H, H-2″, H-6″), 7.59 (s, 1H, H-3′), 7.48–7.42 (m, 3H, H-3″ to H-5″), 7.29 (s, 1H, H-6′), 4.33 (t, 2H, J_{5-4} = 9.9 Hz, H-5), 4.00, 3.99 (2s, 6H, 4′-OCH_3, 5′-OCH_3), 3.21 (t, 2H, J_{4-5} = 9.9 Hz, H-4). ^{13}C NMR (75.49 MHz, $CDCl_3$) δ: 165.71 (CO), 151.28 (C-3), 148.24 (C-5′), 144.08 (C-4′), 139.72 (C-2′), 132.49 (C-1″), 129.43 (C-2″, C-6″), 128.24 (C-4″), 126.16 (C-3″, C-5″), 120.25 (C-1′), 110.23 (C-6′), 106.29 (C-3′), 55.02 (4′-OCH_3, 5′-OCH_3), 44.18 (C-5), 32.29 (C-4). MS (LSIMS): $[M+Na]^+$ = 378.1064.

4.1.4.13. 3-(4,5-Dimethoxy-2-nitrophenyl)-1-phenylacetyl-4,5-dihydro-1*H*-pyrazole (34m). Mp: 60–62 °C. Yield: 52%; ^{1}H NMR (300.20 MHz, $CDCl_3$) δ: 7.58 (s, 1H, H-3′), 7.37–7.35 (m, 2H, H-2″, H-6″), 7.30–7.27 (m, 2H, H-3″, H-5″), 7.22 (m, 1H, H-4″), 6.88 (s, 1H, H-6′), 4.07 (t, 2H, J_{5-4} = 10.2 Hz, H-5), 4.01–3.93 (m, 8H, 4′-OCH_3, 5′-OCH_3, CO–CH_2), 3.10 (t, 1H, 2H, J_{4-5} = 10.2 Hz, H-4). ^{13}C NMR (75.49 MHz, $CDCl_3$) δ: 165.17 (CO), 150.64 (C-3), 148.37 (C-5′), 145.33 (C-4′), 136.70 (C-2′), 130.86 (C-1″), 124.98 (C-3″, C5″), 123.87 (C-2″, C-6″); 122.17 (C-4″), 117.21 (C-1′), 107.39 (C-6′), 103.32 (C-3′), 52.10 (4′-OCH_3, 5′-OCH_3), 40.14 (C-5), 36.42 (CO-CH_2), 29.71 (C-4). MS (LSIMS): $[M+H]^+$ = 370.1402.

4.1.4.14. 3-(4,5-Dimethoxy-2-nitrophenyl)-1-phenylpropanoyl)-4,5-dihydro-1*H*-pyrazole (34n). Mp: 165–167 °C. Yield 30%; ^{1}H NMR (400.17 MHz, $CDCl_3$) δ: 7.58 (s, 1H, H-3′), 7.27–7.25 (m, 4H, H-2″, H-3″, H-5″, H-6″), 7.18 (m, 1H, H-4″), 6.89 (s, 1H, H-6′), 4.08 (t, 2H, J_{5-4} = 10.2 Hz, H-5), 3.99, 3.98 (2s, 4′-OCH_3, 5′-OCH_3), 3.09 (t, 2H, J_{4-5} = 10.2 Hz, H-4), 3.01–2.98 (m, 4H, CO–CH_2–CH_2). ^{13}C NMR (125.69 MHz, $CDCl_3$) δ: 173. 76 (CO), 157. 64 (C-3), 155.59 (C-5′), 152.42 (C-4′), 144.01 (C-2′), 143.77 (C-1″), 131.15 (C-2″, C-6″), 130.98 (C-3″, C-5″), 128.62 (C-4″), 124.57 (C-1′), 114.41 (C-6′), 110.48 (C-3′), 59.30, 59.22 (4′-OCH_3, 5′-OCH_3), 47.16 (C-5), 38.37 (C-4), 36.98 (CO–CH_2–CH_2), 33.62 (CO–CH_2–CH_2). MS (LSIMS): $[M+H]^+$ = 384.1559.

4.1.4.15. 1-Cyclopropylcarbonyl-3-(6-nitro-2,3,4-trimethoxyphenyl)-4,5-dihydro-1*H*-pyrazole (34o). Mp: 100–103 °C. Yield: 30%; ^{1}H NMR (400.17 MHz, $CDCl_3$) δ: 7.42 (s, 1H-5′), 4.07 (t, 2H, H-5, J_{5-4} = 10.2 Hz), 3.96, 3.95, 3.90 (3s, 2′-OCH_3, 3′-OCH_3, 4′-OCH_3), 3.18 (t, 2H, H-4, J_{4-5} = 10.2 Hz), 2.41–2.38 (m, 1H, H-1″), 1.04–0.83 (m, 4H, H-2″, H-3″). ^{13}C NMR (75.49 MHz, $CDCl_3$) δ: 172.66 (CO), 154.14 (C-3), 153.12 (C-4′), 152.58 (C-3′), 147.13 (C-6′), 143.69 (C-2′), 116.82 (C-1′), 104.58 (C-5′), 62.45, 61.46 (2′-OCH_3, 3′-OCH_3), 56.81 (4′-OCH_3), 44.83 (C-5), 35.93 (C-4), 11.90 (C-1″), 8.41 (C-2″, C-3″). MS (LSIMS): $[M+H]^+$ = 350.1306.

4.1.4.16. 1-Benzoyl-3-(6-nitro-2,3,4-trimethoxyphenyl)-4,5-dihydro-1*H*-pyrazole (34p). Mp: 102–106 °C. Yield: 20%; ^{1}H NMR (400.17 MHz, $CDCl_3$) δ: 7.70–7.67 (m, 2H, H-2″, H-6″), 7.33–7.25 (m, 3H, H-3″ to H-5″), 7.18 (s, 1H, H-5′), 4.23 (t, 2H, J_{4-5} = 9.9 Hz, H-4), 3.87, 3.86, 3.79 (3s, 2′-OCH_3, 3′-OCH_3, 4′-OCH_3), 3.18 (t, 2H, J_{4-5} = 9.9 Hz, H-4). ^{13}C NMR (75.49 MHz, $CDCl_3$) δ: 168.91 (CO), 155.35 (C-3), 154.91 (C-4′), 153.80 (C-3′), 148.12 (C-6′), 145.12 (C-2′), 135.71 (C-4″), 132.19 (C-3″, C-5″), 130.19 (C-1″), 129.08 (C-2″, C-6″), 117.19 (C-1′), 105.71 (C-5′), 63.47, 62.59 (2′-OCH_3, 3′-OCH_3), 57.06 (4′-OCH_3), 46.87 (C-5), 36.71 (C-4). MS (LSIMS): $[M+H]^+$ = 386.1312.

4.1.4.17. 1-Phenylacetyl-3-(2,3,4-trimethoxy-6-nitrophenyl)-4,5-dihydro-1*H*-pyrazole (34q). Mp: 100–102 °C. Yield: 21%; ^{1}H NMR (400.17 MHz, $CDCl_3$) δ: 7.45–7.10 (m, 6H, H-2″ to H-6″, H-5′), 4.08 (t, 2H, H-5, J_{5-4} = 10.0 Hz), 3.98, 3.97 (2s, 2′-OCH_3, 3′-OCH_3), 3.94 (s, 4′-OCH_3), 3.94–3.86 (m, 2H, CO–CH_2), 3.19 (t, 2H, H-4, J_{4-5} = 10.0 Hz).^{13}C NMR (75.49 MHz, $CDCl_3$) δ: 169.81 (CO), 154.17 (C-3), 153.30 (C-4′), 152.57 (C-3′), 147.15 (C-6′), 143.70 (C-2′), 135.64 (C-1″), 129.64 (C-3″, C-5″), 128.57 (C-2″, C-6″), 126.81 (C-4″), 116.73 (C-1′), 104.63 (C-5′), 62.36, 61.48

(2′-OCH_3, 3′-OCH_3), 46.83 (4′-OCH_3), 44.53 (C-5), 40.96 (CO–CH_2), 36.71 (C-4). MS (LSIMS): $[M+H]^+$ = 400.4031.

4.1.4.18. 3-(6-Nitro-2,3,4-trimethoxyphenyl)-1-phenylpropanoyl-4,5-dihydro-1*H*-pyrazole (34r). Mp: 104–106 °C. Yield: 22%; ^1H NMR (400.17 MHz, $CDCl_3$) δ: 7.30–6.97 (m, 6H, H-5′, H-2″ to H-6″), 4.10 (t, 2H, J_{5-4} = 10.0 Hz, H-5), 3.97, 3.95 (2s, 2′-OCH_3, 3′-OCH_3), 3.87 (s, 4′-OCH_3), 3.19 (t, 2H, J_{4-5} = 10.0 Hz, H-4), 3.00–2.94 (m, 4H, –CO–CH_2–CH_2). ^{13}C NMR (125.69 MHz, $CDCl_3$) δ: 180.21 (CO), 156.59 (C-3), 155.79 (C-4′), 154.94 (C-3′), 149.52 (C-6′), 143.92 (C-2′), 142.97 (C-1″), 131.18 (C-2″, C-6″), 131.97 (C-3″, C-5″), 128.96 (C-4″), 119.05 (C-1′), 107.03 (C-5′), 62.23, 61.29 (2′-OCH_3, 3′-OCH_3), 46.86 (4′-OCH_3), 44.27 (C-5), 38.45 (C-4), 35.85 (CO–CH_2–CH_2), 32.21 (CO–CH_2–CH_2). MS (LSIMS): $[M+H]^+$ = 414.1604.

4.1.5. Preparation of 1-acyl-3-(2-aminophenyl-substituted)-4,5-dihydro-1*H*-pyrazoles (3a–n) and 1-acy-3-(6-aminophenyl-2,3,4-trimethoxy-)-4,5-dihydro-1*H*-pyrazole (3o–r) general method

A mixture of nitroarene (0.309 mmol) and $SnCl_2$ (350 mg) was dissolved on ethanol and was stirred under reflux for 2 h. The solution was quenched to pH = 7 with saturated $NaHCO_3$ water solution, extracted with ethyl acetate (2 × 15 mL), and dried (Na_2SO_4). Evaporation of the solvent gave a residue of the corresponding amino-derivative that was purified by column chromatography (EtOAc/hexane 1:3).

4.1.5.1. 3-(2-Aminophenyl)-1-phenylacetyl-4,5-dihydro-1*H*-pyrazole (3a). Mp: 196–198 °C. Yield: 70%; ^1H NMR (300.20 MHz, $CDCl_3$) δ: 7.39–7.20 (m, 7H, H-2″ to H-6″, H-4′, H-6′), 6.77–6.72 (m, 2H, H-3′, H-5′), 5.71 (sa, 2H, NH_2), 4.08 (s, 2H, CO–CH_2), 4.02 (t, 2H, J_{5-4} = 10 Hz, H-5), 3.34 (t, 2H, H-4, J_{4-5} = 10 Hz). ^{13}C NMR (75.49 MHz, $CDCl_3$) δ: 168.89 (CO), 157.87 (C-3), 146.99 (C-2′), 135.58 (C-1″), 131.30 (C-4″), 129.78 (C-6′), 129.28, 128.82 (C-2″, C-3″, C-5″, C-6″), 126.99 (C-4″), 117.05 (C-5′), 116.24 (C-3′), 112.95 (C-1′), 42.93 (C-5), 41.64 (CO–CH_2), 33.41 (C-4). MS (LSIMS): $[M+Na]^+$ = 302.1267.

4.1.5.2. 3-(2-Aminophenyl)-1-phenylpropanoyl-4,5-dihydro-1*H*-pyrazole (3b). Mp: 145–147 °C. Yield: 74%; ^1H NMR (300.20 MHz, $CDCl_3$) δ: 7.33–7.11 (m, 7H, H-2″ to H-6″, H-4′, H-6′), 6.78–6.73 (m, 2H, H-3′, H-5′), 5.76 (sa, 2H, NH_2), 4.00 (t, 2H, J_{5-4} = 10 Hz, H-5), 3.34 (t, 2H, J_{4-5} = 10 Hz, H-4), 3.10–3.03 (m, 4H, CO–CH_2–CH_2). ^{13}C NMR (75.49 MHz, $CDCl_3$) δ: 170.29 (CO), 157.67 (C-3), 146.98 (C-2′), 141.64 (C-1″), 131.24 (C-4′), 129.75 (C-6′), 128.72, 128.67 (C-2″, C-3″, C-5″, C-6″), 126.34 (C-4″), 117.04 (C-5′), 116.24 (C-3′), 113.53 (C-1′), 42.79 (C-5), 36.37 (CO–CH_2–CH_2), 33.26 (C-4), 31.23 (CO–CH_2–CH_2). MS (LSIMS): $[M+Na]^+$ = 316.1416.

4.1.5.3. 3-(2-Amino-5-chlorophenyl)-1-phenylacetyl-4,5-dihydro-1*H*-pyrazole (3c). Mp: 152–154 °C. Yield: 68%; ^1H NMR: (400.17 MHz, $CDCl_3$) δ: 7.33–7.26 (m, 5H, H-2″ to H-6″), 7.15–7.11 (m, 2H, H-4′, H-6′), 6.65 (d, 1H, $J_{3'-4'}$ = 8.6 Hz, H-3′), 4.02–3.96 (m, 4H, H-5, CO–CH_2), 3.27 (t, 2H, J_{4-5} = 10 Hz, H-4). ^{13}C NMR (75.49 MHz, $CDCl_3$) δ: 168.94 (–CO–), 156.65 (C-3), 145.45 (C-2′), 135.35 (C-1″), 130.99 (C-4′), 129.20 (C-6′), 128.91 (C-2″ to C-6″), 121.39 (C-5′), 117.43 (C-3′), 114.60 (C-1′), 43.05 (C-5), 41.61 (CO–CH_2), 33.25 (C-4). MS (LSIMS): $[M+Na]^+$ = 336.0884.

4.1.5.4. 3-(2-Amino-5-chlorophenyl)-1-phenylpropanoyl-4,5-dihydro-1*H*-pyrazole (3d). Mp: 165–167 °C. Yield: 69%; ^1H NMR: (400.17 MHz, $CDCl_3$) δ: 7.30–7.19 (m, 5H, H-2″ to H-6″), 7.16–7.10 (m, 2H, H-4′, H-6′), 6.66 (d, 1H, $J_{3'-4'}$ = 8.6 Hz, H-3′), 3.97 (t, 2H, J_{5-4} = 10.1 Hz, H-5), 3.26 (t, 2H, J_{4-5} = 10.1 Hz, H-4), 3.05–2.98 (m, 4H, CO–CH_2–CH_2). ^{13}C NMR (125.69 MHz, $CDCl_3$) δ: 170.33 (CO), 156.41 (C-3), 145.44 (C-2′), 141.48 (C-1″), 130.93 (C-4′), 128.88 (C-6′), 128.62 (C-2″, C-3″, C-5″, C-6″), 126.36 (C-4″), 121.39 (C-5′), 117.42 (C-3′), 114.60 (C-1′), 42.90 (C-5), 36.27 (CO–CH_2–CH_2), 33.11 (C-4), 31.14 (CO–CH_2–CH_2). MS (LSIMS): $[M+Na]^+$ = 350.1036.

4.1.5.5. 3-(2-Amino-4,5-dichlorophenyl)-1-cyclopropylcarbonyl-4,5-dihydro-1*H*-pyrazole (3e). Mp: 148–149 °C. Yield: 80%; ^1H NMR (400.17 MHz, $CDCl_3$) δ: 7.27 (s, 1H, H-3′), 6.85 (s, 1H, H-6′), 3.99 (t, 2H, J_{5-4} = 10.2, H-5), 3.27 (t, 2H, J_{4-5} = 10.2, H-4), 2.30–2.36 (m, 1H, H-1″), 1.11–0.80 (m, H-2″, H-3″). ^{13}C NMR (125.69 MHz, $CDCl_3$) δ: 178.07 (CO), 158.29 (C-3), 141.23 (C-2′), 130.50 (C-4′), 125.78 (C-6′), 125.26 (C-5′), 115.32 (C-1′), 112.41 (C-3′), 35.89 (C-5), 28.30 (C-4), 7.43 (C-1″), 3.73 (C-2″, C-3″). MS (LSIMS): $[M+Na]^+$ = 321.0414.

4.1.5.6. 3-(2-Amino-4,5-dichlorophenyl)-1-benzoyl-4,5-dihydro-1*H*-pyrazole (3f). Mp: 220–223 °C. Yield: 92%; ^1H NMR (400.17 MHz, DMSO) δ: 7.68 (d, 2H, $J_{2''-3''} = J_{6''-5''}$ = 8.0 Hz, H-2″, H-6″), 7.52–7.42 (m, 3H, H-3″, H-4″, H-5″), 7.40 (s, 1H, H-6′), 6.89 (s, 1H, H-3′), 3.99 (t, 2H, J_{5-4} = 9.9 Hz, H-5), 3.36 (t, 2H, J_{4-5} = 9.9 Hz, H-4). ^{13}C NMR (75.49 MHz, $CDCl_3$) δ: 168.07 (CO), 157.69 (C-3), 147.69 (C-2′), 135.81 (C-1″), 133.36 (C-4′), 131.49 (C-6′), 129.08–128.60 (C-2″, C-6″, C-3″, C-5″), 131.29 (C-4″), 116.57 (C-3′), 113.40 (C-1′), 116.76 (C-5′), 44.15 (C-5), 31.38 (C-4). MS (ESI): $[M+H]^+$ = 334.0514.

4.1.5.7. 3-(2-Amino-4,5-dichlorophenyl)-1-phenylacetyl-4,5-dihydro-1*H*-pyrazole (3g). Mp: 155–160 °C. Yield: 90%; ^1H NMR (400.17 MHz, $CDCl_3$) δ: 7.30 (m, 6H, H-6′, H-2″ to H-6″), 6.88 (s, 1H, H-3′), 4.04–3.98 (m, 4H, $COCH_2$, H-5); 3.25 (t, 2H, J_{4-5} = 10.5 Hz, H-4).^{13}C NMR (75.49 MHz, $CDCl_3$) δ: 168.88 (CO), 155.38 (C-3), 145.32 (C-2′), 142.68 (C-1″), 134.66 (C-4′), 130.43 (C-6′), 129.00–128.70 (C-2″, C-6″, C-3″, C-5″), 126.93 (C-4″), 122.23 (C-5′), 117.31 (C-3′), 113.05 (C-1′), 43.07 (C-5), 41.48 (CO–CH_2), 33.06 (C-4). MS (ESI): $[M+Na]^+$ = 370.0490.

4.1.5.8. 3-(2-Amino-4,5-dichlorophenyl)-1-phenylpropanoyl-4,5-dihydro-1*H*-pyrazole (3h). Mp: 175–178 °C. Yield: 93%; ^1H NMR (300.20 MHz, $CDCl_3$) δ: 7.26 (m, 6H, H-6′, H-2″ to H-6″), 6.92 (s, 1H, H-3′), 5.05 (sa, 2H, NH_2), 4.02 (t, 2H, J_{5-4} = 10.3 Hz, H-5), 3.28 (t, 2H, J_{4-5} = 10.3 Hz, H-4), 3.05–2.98 (m, 4H, CO–CH_2–CH_2).^{13}C NMR (75.49 MHz, $CDCl_3$) δ: 170.47 (CO), 155.54 (C-3), 144.60 (C-2′), 141.39 (C-1″), 134.81 (C-4′), 130.61 (C-6′), 128.75, 128.67 (C-2″, C-6″, C-3″, C-5″, C-5′), 126.43 (C-4″), 120.51 (C-1′), 118.05 (C-3′), 43.03 (C-5), 36.22 (CO–CH_2–CH_2), 33.09 (C-4), 31.14 (CO–CH_2–CH_2). MS (ESI): $[M+H]^+$ = 362.0812.

4.1.5.9. 3-(2-Amino-5-methoxyphenyl)-1-phenylacetyl-4,5-dihydro-1*H*-pyrazole (3i). Mp: 177–180 °C. Yield: 71%; ^1H NMR (400.17 MHz, $CDCl_3$) δ: 7.36–7.21 (m, 5H, H-2″ to H-6″), 6.85 (dd, 1H, $J_{4'-3'}$ = 8.8 Hz, $J_{4'-6'}$ = 2.9 Hz, H-4′), 6.75–6.71 (m, 2H, H-3′, H-6′), 4.04 (s, 2H, CO–CH_2), 3.99 (t, 2H, J_{5-4} = 8.8 Hz, H-5), 3.76 (s, 3H, OCH_3), 3.28 (t, 2H, J_{4-5} = 8.8 Hz, H-4). ^{13}C NMR (125.69 MHz, $CDCl_3$) δ: 171.40 (CO), 159.83 (C-5′), 154.02 (C-3), 143.18 (C-2′), 137.91 (C-1″), 131.70, 131.21 (C-2″, C-3″, C-5″, C-6″), 129.39 (C-4″), 120.64 (C-4′), 120.19 (C-3′), 116.82 (C-6′), 113.72 (C-1′), 58.70 (OCH_3), 45.44 (C-5), 43.98 (CO–CH_2), 35.83 (C-4). MS (ESI): $[M+Na]^+$ = 332.1374.

4.1.5.10. 3-(2-Amino-5-methoxyphenyl)-1-phenylpropanoyl-4,5-dihydro-1*H*-pyrazole (3j). Mp: 155–157 °C. Yield: 75%; ^1H NMR (400.17 MHz, $CDCl_3$) δ: 7.31–7.24 (m, 4H, H-2″, H-3″, H-5″, H-6″), 7.20–7.18 (m, 1H, H-4″), 6.86 (dd, 1H, J'_{4-3} = 8.8 Hz,

J'_{4-6} = 3.1 Hz, H-4′), 6.76–6.72 (m, 2H, H-3′, H-6′), 3.97 (t, 2H, J_{5-4} = 10.3 Hz, H-5), 3.77 (s, 3H, OCH_3), 3.29 (t, 2H, J_{4-5} = 10.3 Hz, H-4), 3.08–2.97 (m, 4H, $COCH_2$–CH_2) ^{13}C NMR (125.69 MHz, $CDCl_3$) δ: 172.80 (CO), 159.61 (C-5′), 154.07 (C-3), 143.99 (C-2′), 143.04 (C-1″), 131.07 (C-2″, C-3″, C-5″, C-6″), 128.72 (C-4″), 120.52 (C-4′), 120.23 (C-3′), 116.83 (C-6′), 113.50 (C-1′), 58.69 (OCH_3), 45.30 (C-5), 38.70 (CO–CH_2–CH_2), 35.69 (C-4), 33.60 (CO–CH_2–CH_2). MS (ESI): $[M+Na]^+$ = 346.1531.

4.1.5.11. 3-(2-Amino-4,5-dimethoxyphenyl)-1-cyclopropylcarbonyl-4,5-dihydro-1*H*-pyrazole (3k). Mp: 128–130 °C. Yield: 90%; ^{1}H NMR (400.17 MHz, $CDCl_3$) δ: 6.71 (s, 1H, H-6′), 6.32 (s, 1H, H-3′), 3.97 (t, 2H, J_{5-4} = 9.6, H-5), 3.88 (s, 3H, 5′-OCH_3), 3.82 (s, 3H, 4′-OCH_3), 3.29 (t, 2H, J_{4-5} = 9.6, H-4), 2.43 (m, 1H, H-1″), 1.10–0.84 (m, 2H, H-2″, H-3″). ^{13}C NMR (75.49 MHz, $CDCl_3$) δ: 171.43 (CO), 157.14 (C-3), 152.41 (C-4′), 142.58 (C-5′), 141.35 (C-2′), 113.21 (C-6′), 105.87 (C-1′), 100.10 (C-3′), 57.32 (4′-OCH_3), 56.06 (5′-OCH_3), 43.07 (C-5), 33.40 (C-4), 12.17 (C-1″), 8.25 (C-2″, C-3″). MS (LSIMS): $[M+Na]^+$ = 312.1324.

4.1.5.12. 3-(2-Amino-4,5-dimethoxyphenyl)-1-benzoyl-4,5-dihydro-1*H*-pyrazole (3l). Mp: 128–130 °C. Yield: 66%; ^{1}H NMR (300.20 MHz, $CDCl_3$) δ: 7.90–7.87 (m, 2H, H-2″, H-6″), 7.47–7.43 (m, 3H, H-3″-H-5″), 6.78 (s, 1H, H-6′), 6.72 (s, 1H, H-3′), 4.21 (t, 2H, J_{5-4} = 10.1 Hz, H-5), 3.89 (s, 3H, 5′-OCH_3), 3.87 (s, 3H, 4′-OCH_3), 3.38 (t, 2H, J_{4-5} = 10.1 Hz, H-4). ^{13}C NMR (75.49 MHz, $CDCl_3$) δ: 165.38 (CO), 155.46 (C-3), 150.60 (C-4′), 145.23 (C-5′), 141.06 (C-2′), 133.34 (C-1″), 129.25 (C-3″, C-5″), 126.45 (C-2″, C-6″), 126.37 (C-4″), 115.06 (C-1′), 111.18 (C-6′), 101.65 (C-3′), 55.48 (4′-OCH_3), 54.56 (5′-OCH_3), 42.10 (C-5), 31.21 (C-4). MS (ESI): $[M+Na]^+$ = 348.1330.

4.1.5.13. 3-(2-Amino-4,5-dimethoxyphenyl)-1-phenylacetyl-4,5-dihydro-1*H*-pyrazole (3m). Mp: 185–186 °C. Yield: 89%; ^{1}H NMR (400.17 MHz, $CDCl_3$) δ: 7.35–7.26 (m, 4H, H-2″, H-3″, H-5″, H-6″), 7.23–7.20 (m, 1H, H-4″), 6.69 (s, 1H, H-6′), 6.53 (s, 1H, H-3′), 4.04 (s, 2H, CO-CH_2), 3.98 (t, 2H, J_{5-4} = 10.2 Hz, H-5), 3.85 (s, 3H, 5′-OCH_3), 3.82 (s, 3H, 4′-OCH_3), 3.26 (t, 2H, J_{4-5} = 10.2 Hz, H-4). ^{13}C NMR (125.69 MHz, $CDCl_3$) δ: 171.21 (CO), 159.39 (C-3), 154.74 (C-4′), 145.24 (C-5′), 141.38 (C-2′), 137.99 (C-1″), 129.16 (C-3″, C-5″), 128.69 (C-2″, C-6″), 126.83 (C-4″), 115.37 (C-1′), 112.78 (C-6′), 101.65 (C-3′), 57.05 (4′-OCH_3), 56.02 (5′-OCH_3), 42.79 (C-5), 41.16 (CO–CH_2), 33.31 (C-4). MS (LSIMS): $[M+H]^+$ = 340.1661.

4.1.5.14. 3-(2-Amino-4,5-dimethoxyphenyl)-1-phenylpropanoyl-4,5-dihydro-1*H*-pyrazole (3n). Mp: 176–179 °C. Yield: 60%; ^{1}H NMR (400.17 MHz, $CDCl_3$) δ: 7.27–7.25 (m, 4H, H-2″, H-3″, H-5″, H-6″), 7.17–7.15 (m, 1H, H-4″), 6.70 (s, 1H, H-6′), 6.52 (s, 1H, H-3′), 3.96 (t, 2H, J_{5-4} = 10.0 Hz, H-5), 3.86 (s, 3H, 5′-OCH_3), 3.83 (s, 3H, 4′-OCH_3), 3.26 (t, 2H, J_{4-5} = 10.0 Hz, H-4), 3.05–2.98 (m, 4H, CO–CH_2–CH_2). ^{13}C NMR (75.49 MHz, $CDCl_3$) δ: 165.43 (CO), 152.08 (C-3), 147.57 (C-4′), 145.24 (C-5′), 138.02 (C-2′), 136.89 (C-1″), 123.98, 123.95 (C-2″, C-3″, C-5″, C-6″), 121.55 (C-4″), 113.93 (C-1′), 108.20 (C-6′), 97.01 (C-3′), 52.48 (4′-OCH_3), 51.44 (5′-OCH_3), 38.04 (C-5), 31.50 (C-4), 30.70 (CO–CH_2–CH_2), 25.66 (CO–CH_2–CH_2). MS (LSIMS): $[M+H]^+$ = 354.1817.

4.1.5.15. 3-(6-Amino-2,3,4-trimethoxyphenyl)-1-cyclopropylcarbonyl-4,5-dihydro-1*H*-pyrazole (3o). Mp: 176–179 °C. Yield: 65%; ^{1}H-NMR: (400.17 MHz, $CDCl_3$) δ: 6.02 (s, H-5′), 3.93 (t, 2H, J_{5-4} = 10.0 Hz, H-5), 3.87, 3.84 (2s, 6H, 2′-OCH_3, 3′-OCH_3), 3.76 (s, 3H, 4′-OCH_3), 3.42 (t, 2H, J_{4-5} = 10.0 Hz, H-4), 2.42–2.39 (m, 1H, H-1″), 1.08–0.83 (m, 2H, H-2″, H-3″). ^{13}C NMR (75.49 MHz, $CDCl_3$) δ: 173.83 (CO), 159.15 (C-3), 158.13 (C-4′), 157.01 (C-2′), 146.95 (C-6′), 136.53 (C-3′), 104.58 (C-1′), 97.56 (C-5′), 63.79, 63.64 (2′-OCH_3, 3′-OCH_3), 58.36 (4′-OCH_3), 45.78 (C-5), 38.51 (C-4), 14.49 (C-1″), 10.51 (C-2″, C-3″). MS (LSIMS): $[M+H]^+$ = 320.1504.

4.1.5.16. 3-(6-Amino-2,3,4-trimethoxyphenyl)-1-benzoyl-4,5-dihydro-1*H*-pyrazole (3p). Mp: 155–157 °C. Yield: 60%; ^{1}H NMR (400.17 MHz, $CDCl_3$) δ: 7.81–7.79 (m, 2H, H-2″, H-6″), 7.39–7.37 (m, 3H, H-3″-H-5″), 5.29 (s, 1H, H-6′), 4.13 (t, 2H, J_{5-4} = 11.7 Hz, H-5), 3.92 (1s, 3H, 3′-OCH_3), 3.83, 381 (2s, 6H, 2′-OCH_3, 4′-OCH_3), 3.51 (t, 2H, J_{4-5} = 11.7 Hz, H-4).^{13}C NMR(75.49 MHz, $CDCl_3$) δ: 167.12 (CO), 156.14 (C-3), 155.54 (C-4′), 154.43 (C-2′), 144.65 (C-6′), 134.93 (C-3′), 133.34 (C-1″), 130.71 (C-3″, C-5″), 128.12 (C-2″, C-6″), 126.87 (C-4″), 110.31 (C-1′), 77.18 (C-5′), 61.48, 61.01 (2′-OCH_3, 3′-OCH_3), 56.26 (4′-OCH_3), 43.90 (C-5), 35.64 (C-4). MS (LSIMS): $[M+H]^+$ = 356.1561.

4.1.5.17. 3-(6-Amino-2,3,4-trimethoxyphenyl)-1-phenylacetyl-4,5-dihydro-1*H*-pyrazole (3q). Mp: 158–160 °C. Yield: 60%; ^{1}H NMR (400.17 MHz, $CDCl_3$) δ: 7.33–7.21 (m, 5H, H-2″ to H-6″), 5.97 (s, 1H, H-5′), 4.00–3.85 (m, 4H, H-5, CO–CH_2), 3.86, 3.82 (2s, 6H, 2′-OCH_3, 3′-OCH_3), 3.74 (s, 3H, 4′-OCH_3), 3.40 (t, 2H, J_{4-5} = 10 Hz, H-4). ^{13}C NMR (75.49 MHz, $CDCl_3$) δ: 168.66 (CO), 157.20 (C-3), 155.89 (C-4′), 154.62 (C-2′), 144.69 (C-6′), 135.79 (C-3′), 133.97 (C-1″), 129.20 (C-3″, C-5″), 128.80 (C-2″, C-6″), 126.90 (C-4″), 104.99 (C-1′), 94.97 (C-5′), 61.26 (2′-OCH_3, 3′-OCH_3), 55.95 (4′-OCH_3), 43.09 (C-5), 41.70 (CO–CH_2), 36.33 (C-4). MS (LSIMS): $[M+H]^+$ = 370.1703.

4.1.5.18. 3-(6-Amino-2,3,4-trimethoxyphenyl)-1-phenypropanoyl-4,5-dihydro-1*H*-pyrazole (3r). Mp: 158–160 °C. Yield: 68%; ^{1}H NMR (400.17 MHz, $CDCl_3$) δ: 7.28–7.27 (m, 5H, H-2″ to H-6″), 6.03 (s, 1H, H-5′), 3.95 (t, 2H, J_{5-4} = 10 Hz, H-5), 3.87, 3.84 (2s, 6H, 2′-OCH_3, 3′-OCH_3), 3.76 (s, 3H, 4′-OCH_3), 3.44 (t, 2H, J_{4-5} = 10 Hz, H-4), 3.04–2.96 (m, 4H, CO–CH_2–CH_2). ^{13}C NMR (75.49 MHz, $CDCl_3$) δ: 166.11 (CO), 158.19 (C-3), 152.96 (C-4′), 151.89 (C-1′), 144.70 (C-6′), 141.29 (C-3′), 137.79 (C-1″), 124.75 (C-2″, C-3″, C-5″, C-6″), 122.36 (C-4″), 98.09 (C-1′), 91.30 (C-5′), 57.89, 57.32 (2′-OCH_3, 3′-OCH_3), 52.05 (4′-OCH_3), 39.00 (C-5), 32.38 (C-4), 32.28 (CO–CH_2–CH_2), 27.36 (CO–CH_2–CH_2). MS (LSIMS): $[M+H]^+$ = 384.1832.

4.2. In vitro nNOS and iNOS activities determination

L-Arginine, L-citrulline, *N*-(2-hydroxymethyl)piperazine-*N*′-(2-ethanesulfonic acid) (HEPES), DL-dithiothreitol (DTT), hypoxantine-9-β-D-ribofuranosid (inosine), ethylene glycol-bis-(2-aminoethylether)-*N*,*N*,*N*′,*N*′-tetraacetic acid (EGTA), bovine serum albumin (BSA), Dowex-50 W (50 × 8–200), FAD, NADPH and 5,6,7,8-tetrahydro-L-biopterin dihydrocloride (H_4-biopterin) were obtained from Sigma–Aldrich Química (Spain). L-[^{3}H]-arginine (54 Ci/mmol) was obtained from Amersham (Amersham Biosciences, Spain). Tris-(hydroxymethyl)-aminometane (Tris–HCl) and calcium chloride were obtained from Merck (Spain). Calmodulin from bovine brain, and recombinant iNOS and nNOS were obtained from Alexis Biochemicals (Enzo Life Sciences, Grupo Taper, Seville, Spain).

The nNOS activity was measured by the Bredt and Snyder[34] method, monitoring the conversion of L-[^{3}H]-arginine to L-[^{3}H]-citrulline. The final incubation volume was 100 μL and consisted of 10 μL of an aliquot of recombinant nNOS (specific activity 21.05 nmol/min/mg protein) added to a buffer with a final concentration of 25 mM Tris–HCl, 1 mM DTT, 4 μM H_4-biopterin, 10 μM FAD, 0.5 mM inosine, 0.5 mg/mL BSA, 0.1 mM $CaCl_2$, 10 μM L-arginine, and 50 nM L-[^{3}H]-arginine, at pH 7.6. The reaction was started by the addition of 10 μL of NADPH (0.75 mM final) and 10 μL of each 4,5-dihydro-1*H*-pyrazole derivative in ethanol to give a final

concentration of 1 mM. The tubes were vortex and incubated at 37 °C for 30 min. Control incubations were performed by the omission of NADPH. The reaction was halted by the addition of 400 μL of cold 0.1 M HEPES, 10 mM EGTA, and 0.175 mg/mL L-citrulline, pH 5.5. The reaction mixture was decanted into a 2 mL column packet with Dowex-50 W ion-exchange resin (Na^+ form) and eluted with 1.2 mL of water. L-[^{3}H]-citrulline was quantified by liquid scintillation spectroscopy. The retention of L-[^{3}H]-arginine in this process was greater than 98%. Specific enzyme activity was determined by subtracting the control value, which usually amounted to less than 1% of the radioactivity added. The nNOS activity was expressed as picomoles of L-[^{3}H]-citrulline produced (/mg of protein/min).

For iNOS activity determination, the procedure was essentially the same as for nNOS, excepting that an aliquot of 10 μL recombinant iNOS (specific activity of 0.7 nmol/min/mg protein) was used instead of nNOS, and the mixture was incubated in the absence of calmodulin.

4.3. Statistical analysis

Data are expressed as the mean ± SEM. One-way analysis of variance, followed by the Newmane–Keuls multiple range test was used. A $P < 0.05$ was considered statistically significant.

Acknowledgments

This word was partially supported by Grants from the Junta de Andalucía (P06-CTS-01941 and P07-CTS-03135) and from the Vicerrectorado de Política Científica e Investigación de la Universidad de Granada (GENIL/GREIB and GREIB.PYR_2010_03).

Supplementary data

Supplementary data associated with this article can be found, in the online version, at http://dx.doi.org/10.1016/j.bmc.2013.05.016.

References and notes

1. Mustafa, A. K.; Gadalla, M. M.; Sydner, S. H. *Sci. Signaling* **2009**, *2*, 1.
2. Alderton, W. K.; Cooper, C. E.; Knowles, R. G. *Biochem. J.* **2001**, *357*, 593.
3. Rosen, G. M.; Tsai, P.; Pou, S. *Chem. Rev.* **2002**, *102*, 1191.
4. Stuehr, D. J.; Santolini, J.; Wang, Z. Q.; Wei, C. C.; Adak, S. *J. Biol. Chem.* **2004**, *279*, 36167.
5. Hierholzer, C.; Harbrecht, B.; Menezes, J. M.; Kane, J.; MacMicking, J.; Nathan, C. F.; Peitzman, A. B.; Billiar, T. R.; Tweardy, D. J. *J. Exp. Med.* **1998**, *187*, 1.
6. Ghafourifar, P.; Cadenas, E. *Trends Pharmacol. Sci.* **2005**, *26*, 190.
7. Escames, G.; León, J.; Macías, M.; Khadly, H.; Acuña-Castroviejo, D. *FASEB J.* **2003**, *17*, 932.
8. Escames, G.; López, L. C.; Ortiz, F.; López, A.; García, J. A.; Ros, E.; Acuña-Castroviejo, D. *FEBS J.* **2007**, *274*, 2135.
9. Erdal, E. P.; Litzinger, E. A.; Seo, J.; Zhu, y.; Li, H.; Silverman, R. B. *Curr. Top. Med. Chem.* **2005**, *5*, 603.
10. Vallance, P.; Leiper, J. *Nat. Rev. Drug Disc.* **2002**, *1*, 939.
11. Ramnauth, J.; Speed, J.; Maddaford, S. P.; Dove, P.; Annedi, S. C.; Renton, P.; Rakhit, S.; Andrews, J.; Silverman, S.; Mladenova, G.; Zinghini, S.; Nair, S.; Catalano, C.; Lee, D. K. H.; De Felice, M.; Porreca, F. *J. Med. Chem.* **2011**, *54*, 5562.
12. Calabrese, V.; Mancuso, C.; Calvani, M.; Rizzarelli, E.; Butterfield, A. D.; Stella, A. M. G. *Nat. Rev. Neurosci.* **2007**, *8*, 766.
13. Wilcock, D. M.; Lewis, M. R.; Van Nostrand, W. E.; Davis, J.; Previti, M. L.; Gharkholonarehe, N.; Vitek, M. P.; Colton, C. A. *J. Neurosci.* **2008**, *28*, 1537.
14. Levy, D.; Zochodne, D. W. *Pain Pract.* **2004**, *4*, 11.
15. Wu, J.; Fang, L.; Lin, Q.; Willis, W. D. *Pain* **2001**, *94*, 47.
16. Dehmer, T.; Lindenau, J.; Haid, S.; Dichgan, J.; Schulz, J. B. *J. Neurochem.* **2000**, *74*, 2213.
17. Tapias, V.; Escames, G.; López, L. C.; López, A.; Camacho, E.; Carrión, M. D.; Entrena, E.; Gallo, M. A.; Espinosa, A.; Acuña-Castroviejo, D. *J. Neurochem.* **2009**, *87*, 3002.
18. Camacho, M. E.; León, J.; Carrión, M. D.; Entrena, A.; Escames, G.; Khaldy, H.; Acuña-Castroviejo, D.; Gallo, M. A.; Espinosa, A. *J. Med. Chem.* **2002**, *45*, 263.
19. Entrena, A.; Camacho, M. E.; Carrión, M. D.; López-Cara, L. C.; Velasco, G.; León, J.; Escames, G.; Acuña-Castroviejo, D.; Tapias, V.; Gallo, M. A.; Vivó, A.; Espinosa, A. *J. Med. Chem.* **2005**, *48*, 8174.
20. Camacho, M. E.; León, J.; Entrena, A.; Velasco, G.; Carrión, M. D.; Escames, G.; Vivó, A.; Acuña-Castroviejo, D.; Gallo, M. A.; Espinosa, A. *J. Med. Chem.* **2004**, *47*, 5641.
21. Carrión, M. D.; Camacho, M. E.; León, J.; Escames, G.; Tapias, V.; Acuña-Castroviejo, D.; Gallo, M. A.; Espinosa, A. *Tetrahedron* **2004**, *60*, 4051.
22. Carrión, M. D.; López-Cara, L. C.; Camacho, M. E.; Espinosa, A.; Gallo, M. A.; Tapias, V.; Escames, G.; Acuña-Castroviejo, D.; Entrena, A. *Eur. J. Med. Chem.* **2008**, *43*, 2579.
23. López-Cara, L. C.; Camacho, M. E.; Carrión, M. D.; Tapias, V.; Gallo, M. A.; Escames, G.; Acuña-Castroviejo, D.; Espinosa, A.; Entrena, A. *Eur. J. Med. Chem.* **2009**, *44*, 2655.
24. López-Cara, L. C.; Carrión, M. D.; Entrena, A.; Gallo, M. A.; Espinosa, A.; López, A.; Escames, G.; Acuña-Castroviejo, A.; Camacho, M. E. *Eur. J. Med. Chem.* **2012**, *50*, 129.
25. Zhu, A.; Lippa, B.; Townsend, L. B. *J. Org. Chem.* **1999**, *64*, 4159.
26. Shen, B.; Löffler, D.; Reischl, G.; Machulla, H.; Zeller, K. *J. Fluorine Chem.* **2009**, *130*, 216.
27. Ottl, J.; Gabriel, D.; Marriott, G. *Bioconjugate Chem.* **1998**, *9*, 143.
28. Bellamy, F. D.; Ou, K. *Tetrahedron Lett.* **1984**, *25*, 839.
29. Fedorov, R.; Hartmann, E.; Ghosh, D. K.; Schlichting, I. *J. Biol. Chem.* **2003**, *278*, 45818.
30. Schrödinger Suite 2012 Update 2.
31. Schrödinger Suite 2012 Protein Preparation Wizard; Epik version 2.3, Schrödinger, LLC, New York, NY, 2012; Impact version 5.8, Schrödinger, LLC, New York, NY, 2012; Prime version 3.1, Schrödinger, LLC, New York, NY, 2012.
32. LigPrep, version 2.5, Schrödinger, LLC, New York, NY, 2012.
33. Figures were built using the PyMOL Molecular Graphics System, Version 1.4, Schrödinger, LLC.
34. Bredt, D. S.; Snyder, S. H. *Proc. Natl. Acad. Sci. U.S.A.* **1990**, *87*, 682.

3.2 Artículo 2

ChemPubSoc Europe

DOI: 10.1002/cmdc.201500007

CHEMMEDCHEM Full Papers

Development of Urea and Thiourea Kynurenamine Derivatives: Synthesis, Molecular Modeling, and Biological Evaluation as Nitric Oxide Synthase Inhibitors

Mariem Chayah,[a] M. Dora Carrión,[a] Miguel A. Gallo,[a] Rosario Jiménez,[b] Juan Duarte,[b] and M. Encarnación Camacho*[a]

Herein we describe the synthesis of a new family of kynurenamine derivatives with a urea or thiourea moiety, together with their in vitro biological evaluation as inhibitors of both neuronal and inducible nitric oxide synthases (nNOS and iNOS, respectively), enzymes responsible for the biogenesis of NO. These compounds were synthesized from a 5-substituted-2-nitrophenyl vinyl ketone scaffold in a five-step procedure with moderate to high chemical yields. In general, the assayed compounds show greater inhibition of iNOS than of nNOS, with 1-[3-(2-amino-5-chlorophenyl)-3-oxopropyl]-3-ethylurea (compound **5n**) being the most potent iNOS inhibitor in the series and the most iNOS/nNOS-selective compound. In this regard, we performed molecular modeling studies to propose a binding mode for this family of compounds to both enzymes and, thereby, to elucidate the differential molecular features that could explain the observed selectivity between iNOS and nNOS.

Introduction

Nitric oxide (NO) is an important second-messenger molecule that regulates several physiological functions in the nervous, immune, and cardiovascular systems.[1] A family of nitric oxide synthase (NOS) enzymes catalyze the biosynthesis of NO using L-arginine (L-Arg) as a substrate. Native NOS is a homodimeric enzyme. Each monomer consists of an N-terminal oxygenase domain with a catalytic heme active site and a cofactor tetrahydrobiopterin binding site, and a C-terminal electron-donating reductase domain binding flavin adenine dinucleotide (FAD), flavin mononucleotide (FMN), and nicotinamide adenine dinucleotide (NADPH).[2,3] The linker between the two functional domains is a calmodulin binding motif that enables electron flow from the oxygenase domain to the reductase domain, catalyzing the oxidation of L-Arg to L-citrulline with concomitant production of NO.[4]

Three similar isoforms of NOS have been identified in mammals.[5] Neuronal NOS (nNOS) and endothelial NOS (eNOS) are constitutive and regulated by intracellular Ca^{2+}/calmodulin. They continually produce low levels of NO used for nerve function and blood regulation, respectively. Conversely, inducible NOS (iNOS) is expressed by macrophages and microglia, produces large toxic bursts of NO to fight pathogens, and is not Ca^{2+}-dependent.[6,7]

To exert appropriate functions, NO synthesis by the three isozymes is under tight regulation. The overproduction of NO by nNOS or iNOS and the underproduction by eNOS have been associated with several pathological processes, including neurodegenerative diseases such as Alzheimer's,[8] Parkinson's[9] or Huntington's,[10] as well as amyotrophic lateral sclerosis[11] and chronic inflammatory[12] and autoimmune diseases such as rheumatoid arthritis, multiple sclerosis, colitis,[13] hypertension,[14] and atherosclerosis.[15]

Accordingly, inhibition of nNOS or iNOS, but not of eNOS, could provide an effective therapeutic approach. Moreover, selective inhibitors could be useful pharmacological tools to investigate other biological functions of NO. The research objective of our group is to develop potent and selective nNOS or iNOS inhibitors. To this end, we have carried out the publication of several families of inhibitors, some with good inhibition and selectivity.

In previous experiments, we demonstrated that melatonin **1**, the hormone secreted by the pineal gland, produces inhibitory effects on the CNS in rats and humans.[16] These effects could be interpreted as resulting from the inhibition of NOS. In particular, it has been shown that melatonin inhibits the nNOS isoform in a dose-dependent and calmodulin-dependent manner.[17]

In addition, we have described several compounds with kynurenine **2**,[18] kynurenamine **3**,[19] and 4,5-dihydro-1*H*-pyrazole **4**[20] structures as nNOS inhibitors. The last compounds are rigid analogues of the main brain metabolite of melatonin, *N*-acetyl-5-methoxykynurenamine (**3**, $R^1 = OCH_3$, $R^2 = CH_3$), which also inhibits the iNOS in sepsis associated with Parkinson's dis-

[a] M. Chayah, Dr. M. D. Carrión, Prof. M. A. Gallo, Dr. M. E. Camacho
Departamento de Química Farmacéutica y Orgánica
Facultad de Farmacia, Universidad de Granada (Spain)
E-mail: ecamacho@ugr.es

[b] Dr. R. Jiménez, Prof. J. Duarte
Departamento de Farmacología
Facultad de Farmacia, Universidad de Granada (Spain)

Supporting information for this article is available on the WWW under http://dx.doi.org/10.1002/cmdc.201500007: characterization data for compounds **9b–c**, **9e**, **9g–h**, **9j**, **9l–m**, **9o**, **10b–c**, **10e**, **10g–h**, **10j**, **10l–m**, **10o**, **5b–c**, **5e**, **5g–h**, **5j**, **5l–m**, and **5o**.

ChemPubSoc Europe

CHEMMEDCHEM Full Papers

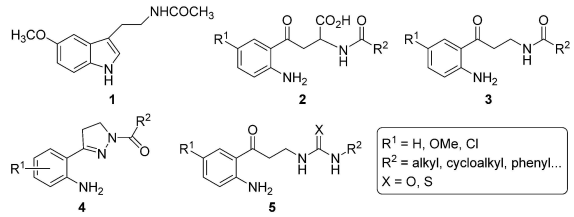

Figure 1. Melatonin and NOS inhibitors synthesized by our research group.

ease.[21] We have demonstrated that these pyrazole derivatives behave as nNOS/iNOS-selective inhibitors[22] (Figure 1).

In this paper, we report the synthesis and biological evaluation of a series of more flexible compounds (**5**). These products were designed from kynurenamine derivatives **3**, carrying a urea or thiourea substituted group, isosteric to the final guanidine moiety of the L-Arg, in order to find potent and selective inhibitors of NOS.

Results and Discussion

Chemistry

The synthesis of derivatives **5a**–**o** was carried out using the general methodology shown in Scheme 1. Compounds **7a**–**c** were synthesized as previously reported[19] from 2-nitrophenyl, 5-methoxy-2-nitrophenyl, and 5-chloro-2-nitrophenyl vinyl ketones **6a**–**c** by treatment with phthalimide in the presence of sodium methoxide to afford the *N*-(3-(2-nitro-5-substituted-phenyl)-3-oxopropyl)phthalimides. Protection of the resultant ketones by reaction with ethylene glycol in the presence of *p*-toluenesulfonic acid yielded dioxolane derivatives **7a**–**c**, respectively. Reaction of these derivatives with hydrazine opened the phthalimide moiety to give intermediates 2-(2-(5-substituted-2-nitrophenyl)-1,3-dioxolan-2-yl)-ethanamines (**8a**–**c**). Nucleophilic addition of either alkyl isocyanate or alkyl isothiocyanate[23] to these derivatives gave intermediates **9a**–**o** (60–96% yield) with an alkyl urea or thiourea residue, which led to ketones **10a**–**o** after acidification (61–94% yield). Finally, reduction of the nitro group belonging to the aromatic ring with Fe/$FeSO_4$ results in final kynurenamine derivatives **5a**–**o** (64–95% yield).

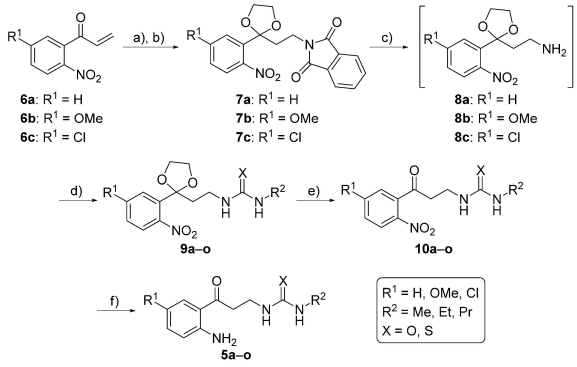

Scheme 1. Synthesis of kynurenamine derivatives **5a**–**o**. *Reagents and conditions*: a) Phthalimide, NaOMe, DMSO, RT, 2 h; b) $(CH_2OH)_2$, *p*-TsOH, toluene, reflux, 10 h; c) NH_2NH_2, dry EtOH, reflux, 4.5 h; d) $XCNR^2$, anhyd CH_2Cl_2, RT, overnight; e) HCl, CH_2Cl_2, RT, 4 h; f) Fe/$FeSO_4$, H_2O, 95 °C, 3 h.

Inhibition of iNOS and nNOS

The biological activity of new compounds **5a**–**o** as inhibitors of both iNOS and nNOS has been evaluated by means of in vitro assays using recombinant isoenzymes. The assays were performed with each compound at 1 mM to identify the most potent and selective derivatives. Furthermore, the IC_{50} values were measured for the most interesting compounds. Table 1 illustrates the inhibition percentages versus iNOS and nNOS (kynurenamine **3a**, previously described,[19] was introduced as a reference), and Figure 2 shows the percentages of residual activity of both isoforms in the presence of each compound. To interpret these biological results properly, we separately studied the effect of each substituent (R^1, R^2, and X) on the potency and/or selectivity of all resulting compounds.

In general, all compounds show better inhibition values for iNOS than for nNOS, with the chlorinated series having the most active compounds. Molecules with neutral (R^1=H) or electron-donating (R^1=OCH_3) phenyl substituents have lower inhibitory activity, indicating that an electron withdrawing group such as chloride is more suitable for the inhibition of both isoforms. Derivatives with a methylthiourea moiety (**5a**, **5f**, and **5k**) have, in general, good inhibition versus both isoforms, independently of the R^1 substituent.

When we compare urea and thiourea derivatives with the same R^2 substituent, the iNOS inhibitory effect decreases when the R^2 volume increases in series with R^1=H (**5b**–**c** and **5d**–**e**) and R^1=Cl (**5l**–**m** and **5n**–**o**), while in the series with R^1=OMe, iNOS inhibition increases

ChemPubSoc Europe

CHEMMEDCHEM Full Papers

Table 1. In vitro iNOS and nNOS inhibition observed in the presence of compounds **5a–o**.

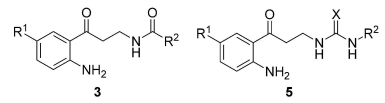

3 **5**

Compd	R^1	R^2	X	Inhibition [%][a] iNOS	nNOS
3a	OMe	Me	–	30.90 ± 2.92	65.36 ± 5.60[b]
5a	H	Me	S	71.71 ± 2.43	77.67 ± 1.02
5b	H	Et	S	45.83 ± 1.73	12.93 ± 3.45
5c	H	Pr	S	38.88 ± 3.59	47.48 ± 2.97
5d	H	Et	O	50.93 ± 3.85	11.80 ± 0.39
5e	H	Pr	O	38.03 ± 3.72	18.25 ± 0.87
5f	OMe	Me	S	78.20 ± 2.43	46.04 ± 2.85
5g	OMe	Et	S	17.71 ± 2.74	40.30 ± 0.32
5h	OMe	Pr	S	39.30 ± 0.99	47.21 ± 1.23
5i	OMe	Et	O	22.08 ± 1.57	0.47 ± 3,34
5j	OMe	Pr	O	55.28 ± 1.24	14.64 ± 0.65
5k	Cl	Me	S	51.29 ± 1.32	60.84 ± 0.82
5l	Cl	Et	S	77.86 ± 1.08	69.78 ± 1.05
5m	Cl	Pr	S	51.91 ± 1.28	53.42 ± 1.46
5n	Cl	Et	O	78.63 ± 1.34	9.86 ± 3.17
5o	Cl	Pr	O	59.58 ± 2.34	74.08 ± 1.04

[a] Values are the mean ± SEM of the percentage of iNOS and nNOS inhibition produced by each compound at 1 mM, determined from three experiments performed in triplicate using recombinant iNOS and nNOS enzymes. [b] Kynurenamine **3a** was used as a reference; see ref. [19].

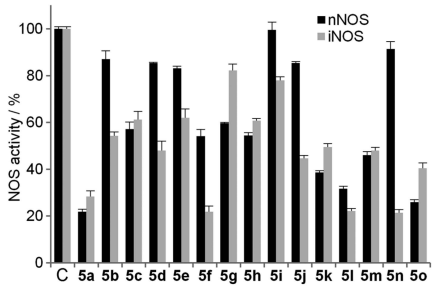

Figure 2. Residual activities of nNOS and iNOS in the presence of tested kynurenamine derivatives (compounds **5a–o**) at 1 mM, as compared with those of untreated samples (C). Each value is the mean ± SEM of three experiments performed in triplicate using recombinant iNOS and nNOS enzymes.

with the volume of R^2 (**5g–h** and **5i–j**). On the other hand, nNOS inhibition values increase with the volume of the R^2 substituent from an ethyl to a propyl group, with the exception of **5l–m**, for which the opposite is true.

In this new family of kynurenamines, the urea residue plays an important role in compound selectivity. All compounds with a urea group inhibit iNOS to a greater extent than nNOS, except **5o**. This effect can be observed clearly in compound **5n** which, besides having very good inhibitory activity, had eightfold selectivity for iNOS over nNOS. Table 2 shows the IC_{50} values of the most interesting synthesized kynurenamine derivatives for both isoenzymes. Compounds **5f** and **5n** had the best results versus iNOS, confirming the potency and selectivity of **5n**. With respect to nNOS, **5a** showed the best IC_{50} value.

Table 2. Inhibition of nNOS and iNOS activity by compounds **5a**, **5f**, **5l**, **5n**, and **5o**.

Compd	IC_{50} [mM][a] nNOS	iNOS
5a	0.18	0.58
5f	–[b]	0.11
5l	0.59	0.59
5n	–[b]	0.10
5o	0.43	0.86

[a] Data obtained by measuring percent inhibition with at least five inhibitor concentrations. [b] Not tested.

Effects of 5n on LPS-induced vascular hyporeactivity to noradrenaline (NA) and eNOS inhibition

The most interesting compound in this family was **5n.** To test functional evidence and to ensure the iNOS selectivity of this compound, we performed a pharmacological essay, using descending thoracic aortic rings. LPS inhibited agonist-induced contractions of isolated vascular preparations.[24] This effect is related to NO overproduction from the induction of iNOS in vascular smooth muscle. In fact, aminoguanidine, a preferential inhibitor of iNOS, reverses the blunted phenylephrine-evoked contraction of endothelium-denuded aortic rings from LPS-treated rats or rings exposed to LPS in vitro. Aminoguanidine did not impair the relaxation of aortic rings with endothelium to acetylcholine, a known stimulator of eNOS.[25] As shown in Figure 3a, incubation of endotoxin decreased the contractile responses elicited by NA in aortic rings without endothelium. Incubation of aortic rings with the NOS inhibitor L-NAME significantly restored NA responses from the LPS group, showing that NO is involved in the attenuated vascular reactivity to NA induced by endotoxin (Figure 3b). Furthermore, the presence of **5n** partially prevented endotoxin-induced NA contractile hyporesponsiveness.

We also carried out an eNOS inhibitory activity assay for **5n**, using human umbilical vein endothelial cells (HUVECs) incubated with 1 mM of **5n** or vehicle and measuring the NO production stimulated by the known eNOS activator A23187. This agent increased NO production in a time-dependent manner. No significant differences ($p > 0.05$) were observed in A23187 stimulated NO production in the presence of **5n**, showing that this compound did not inhibit eNOS (Figure 3c). Moreover, the endothelium-dependent relaxation by acetylcholine was not affected by **5n** (Figure 3d), confirming the absence of eNOS inhibition by this compound.

ChemPubSoc Europe

CHEMMEDCHEM Full Papers

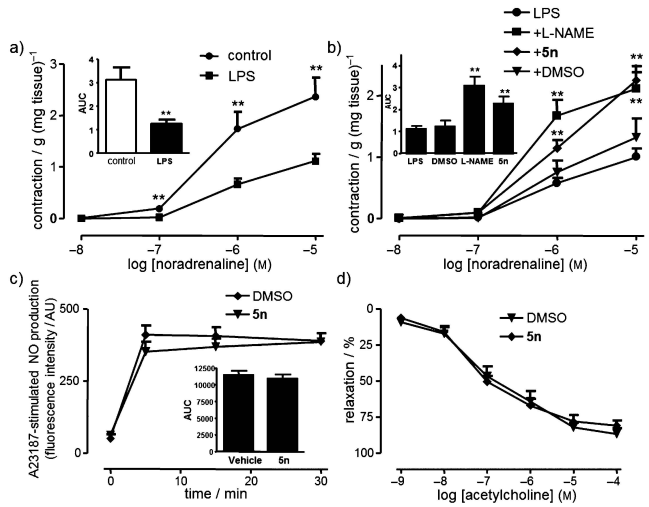

Figure 3. Effects of **5n** on NA-induced contraction in LPS-treated rings and eNOS activation. NA-evoked contraction of rat aortic rings ($n=6$–8) without endothelium treated in vitro: a) with or without LPS (1 $\mu g\,mL^{-1}$, 20 h), or b) in the presence or absence of L-NAME (3×10^{-4} M), **5n** (10^{-4} M), or DMSO, 30 min before NA. c) A23187-dependent NO production in HUVECs incubated with DMSO or **5n** (1 mM) for 30 min ($n=12$). d) Acetylcholine-evoked relaxation in aortic rings with endothelium contracted with 1 μM NA in the presence of DMSO or **5n** (1 mM) for 30 min ($n=5$). Data are expressed as the mean $\pm$SEM of n experiments; $^{**}p<0.01$ versus LPS group.

Molecular modeling

To propose a binding mode for these new kynurenamine derivatives (**5a–o**) to i/nNOS, we performed docking and molecular dynamics (MD) simulation studies. The main descriptive pose obtained by docking for this family of compounds within iNOS (PDB ID: 3NW2)[26] is illustrated in Figure 4a with compound **5n**. According to this pose, interactions with the protein occur in three ways: 1) each urea nitrogen is hydrogen bonded to a carboxylate moiety of the heme group, 2) the 2"-NH_2 group of **5n** interacts with the Glu371 side chain by means of two hydrogen bonds, and 3) the phenyl ring is situated below the heme group, establishing a π–cation interaction, and is surrounded by hydrophobic residues such as Phe363, Val346, and Pro344.

On the other hand, Figure 4b shows the main pose adopted by most compounds within nNOS (PDB ID: 1QW6).[27] In this case, only one hydrogen bond is formed between the urea amine group of **5n** and the carboxylate group of Glu592. The urea moiety is surrounded by a polar environment formed by three arginine residues (Arg596, Arg603 and Arg481). It is noteworthy that the phenyl is now located below the heme group in a different position with respect to that observed in iNOS, allowing the chloride atom of the phenyl group to interact with Trp587.

With regard to the differences found within the series of compounds **5a–o**, the major variations observed in their interaction with the binding site are in the π–cation interaction between the aromatic ring and the heme group, together with the hydrogen bonding network involving the urea moiety. In particular, those compounds bearing a phenyl group with an orientation that is too inclined with respect to the heme group lose activity. In addition, the establishment of two hydrogen bonds through the urea moiety reinforces the interaction and hence, the activity.

Next, we performed molecular dynamics (MD) simulations of iNOS and nNOS in complex with compound **5n** to take into account the flexibility of the protein (Figure 5). The analysis of the trajectory (Figure 5a) showed that those interactions described previously between the NH_2 group of **5n** and Glu371 from one side, and between the heme carboxylate moiety with the **5n** urea moiety from the other side, were retained during the MD simulations. However, Figure 5b shows new hydrogen bonds between the urea residue and the heme carboxylate moiety. Furthermore, the main differences between the MD simulations of both isoforms with **5n** were essentially the new additional stabilizing interactions that **5n** establishes with residues Gln257 and Arg260 (iNOS), located at the entrance of the binding site, together with stacking with the heme group. In particular, the conformation of Gln257 is controlled by the Arg260 side chain orientation which, in turn, depends on the mutation of Thr277 in iNOS and Asn498 in nNOS.[28] These interactions, detected from the simulation process, could explain the iNOS selectivity shown by compounds like **5n** and the good nNOS inhibition observed for some compounds.

The binding of **5n** to iNOS was more favorable than to nNOS (-31.8 ± 0.8 versus -27.3 ± 2.2 kcal mol^{-1}, respectively), due to the great contribution of the π-stacking interaction with the heme group. Finally, the binding energy per residue (Table 3) observed for Gln478 and Arg481 (nNOS) with **5n** was less favorable than for the corresponding residues in iNOS (Gln257 and Arg260).

Conclusions

Herein we report the synthesis of fifteen novel urea and thiourea kynurenamine derivatives **5**, each with different substituents in the aromatic ring and the urea or thiourea moiety. In addition, we evaluate the nNOS and iNOS activity of these new structures. In general, the compounds had better inhibitory ac-

ChemPubSoc Europe

CHEMMEDCHEM Full Papers

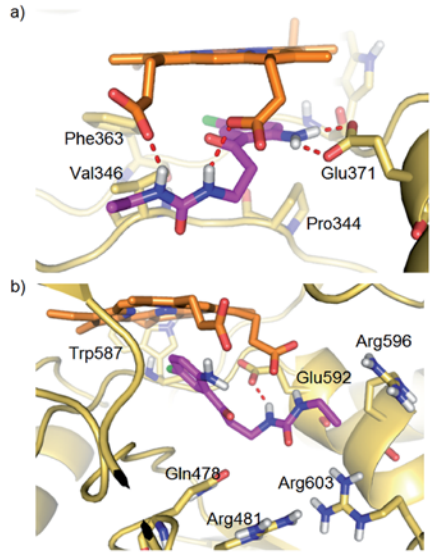

Figure 4. Detailed view of the main poses obtained for compound **5n** in the a) iNOS and b) nNOS binding sites. Dotted lines indicate hydrogen bond interactions between the ligand and residues of the enzyme.

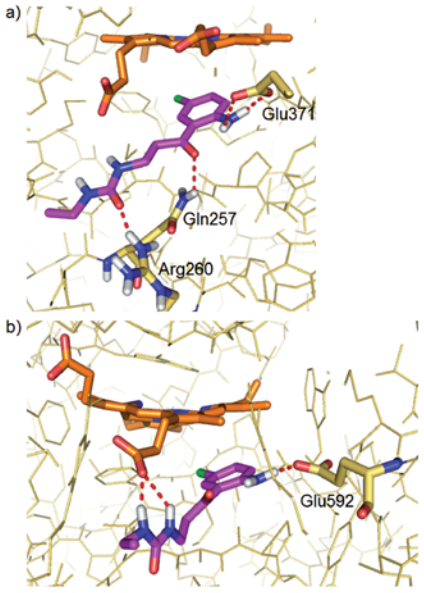

Figure 5. Image of a) **5n**–iNOS and b) **5n**–nNOS complexes taken from both average structures obtained from each MD simulation. Dotted lines indicate hydrogen bond interactions between the ligand and the residues of the enzyme.

Table 3. Calculated binding energy per residue of iNOS/nNOS with compound **5n**.[a]

iNOS		nNOS	
Residue	E [kcal mol^{-1}]	Residue	E [kcal mol^{-1}]
Heme	−11.8 ± 0.4	Heme	−6.2 ± 0.5
Pro 344	−2.5 ± 0.1	Pro 565	−2.6 ± 0.1
Glu 371	−2.5 ± 0.1	Glu 592	−6.5 ± 0.2
Gln 257	−2.5 ± 0.1	Gln 478	−0.6 ± 0.7
Val 346	−2.0 ± 0.1	Val 567	−1.3 ± 0.1
Arg 260	−1.3 ± 0.1	Arg 481	−0.4 ± 0.2
Trp 366	−0.9 ± 0.0	Trp 587	−1.2 ± 0.1
Gly 365	−0.7 ± 0.1	Gly 586	−0.7 ± 0.0
Phe 363	−0.7 ± 0.1	Phe 584	−0.9 ± 0.0

[a] Data are the mean ± SD of the calculated binding energies along the MD simulation (single run).

tivity against iNOS than nNOS, and derivatives with a withdrawing substituent in the aromatic ring were the best inhibitors. Thioureas similarly inhibited both isoenzymes, while ureas selectively inhibited iNOS. The urea **5n** was the most potent iNOS inhibitor and the most iNOS/nNOS-selective. This was confirmed by docking and MD simulations studies, which showed the more favorable orientation of **5n** in iNOS establishing good interactions with the enzyme. Also, this compound did not inhibit eNOS, demonstrating the selectivity necessary to avoid the adverse effects of hypertension. Consequently, this derivative could be an interesting starting point to find new therapeutic alternatives for inflammatory diseases.

Experimental Section

Chemistry

Melting points were determined using an Electrothermal-1 A-6301 apparatus and are uncorrected. Analytical thin layer chromatography was performed using Merck Kieselgel 60 F_{254} aluminum sheets, with the spots developed with UV light ($\lambda = 254$ nm). Flash chromatography was carried out using silica gel 60, 230–240 mesh (Merck), and the solvent mixture reported within parentheses was used as the eluent. ^{1}H NMR and ^{13}C NMR spectra were recorded on a Varian Inova Unity 300 spectrometer operating at 300.20 MHz for ^{1}H and 75.479 MHz for ^{13}C, on a Varian direct drive 400 spectrometer operating at 400.17 MHz for ^{1}H and 125.69 MHz for ^{13}C, and on a Varian direct drive 600 spectrometer operating at 600.24 MHz for ^{1}H and 150.95 MHz for ^{13}C in $CDCl_3$, CD_3OD, $(CD_3)_2CO$, and $(CD_3)_2SO$ at room temperature. The peaks are reported in ppm (δ) and are referenced to the residual solvent peak. High-resolution nano-assisted laser desorption/ionization (HR-NALDI) or electrospray ionization mass spectra (ESI-MS) were carried out on a Bruker Autoflex or a Waters LCT Premier mass spectrometer, respectively.

General method for the preparation of 1-(2-(2-(5-substituted-2-nitrophenyl)-1,3-dioxolan-2-yl)ethyl)-3-alkylthioureas and alkyl-

ChemPubSoc Europe

CHEMMEDCHEM Full Papers

ureas, 9a–o: Hydrazine (95%, 6.18 mmol) was added to a solution of the corresponding phthalimide **7a–c** (2.06 mmol) in dry EtOH (60 mL). The mixture was held at reflux for 4.5 h, then cooled to room temperature and filtered, and the solvent was removed by evaporation. The crude residue was diluted with water (30 mL), basified with KOH, and extracted with EtOAc. The organic layer was dried over anhydrous Na_2SO_4, filtered, and concentrated to give amines **8a–c**. These intermediates were dissolved in anhydrous CH_2Cl_2 (9 mL) under argon atmosphere, and the corresponding alkylisocyanate or alkylisothiocyanate (4.12 mmol) was added dropwise. The reaction mixture was stirred overnight at room temperature. The crude mixture was concentrated and purified by flash chromatography (EtOAc/hexane, 1:2).

1-(2-(2-(2-Nitrophenyl)-1,3-dioxolan-2-yl)ethyl)-3-methylthiourea, 9a: Yellow solid (1.96 mmol, 95%); mp: 122–123 °C; ^{1}H NMR (600 MHz, $CDCl_3$): δ = 2.48 (t, 2H), 2.95 (s, 3H), 3.64–3.70 (m, 4H), 3.99–4.06 (m, 2H), 7.42–7.43 (m, 2H), 7.51 (ddd,1H), 7.59 ppm (d, 1H); ^{13}C NMR (150 MHz, $CDCl_3$): δ = 30.3, 38.1, 40.0, 65.0, 109.7, 123.5, 128.4, 129.8, 131.6, 134.7, 149.5, 180.8 ppm; HRMS *m/z* $[M+H]^+$ calcd for $C_{13}H_{18}N_3O_4S$: 312.1018, found: 312.1016.

1-(2-(2-(2-Nitrophenyl)-1,3-dioxolan-2-yl)ethyl)-3-ethylurea, 9d: White solid (1.46 mmol, 71%); mp: 168–169 °C; ^{1}H NMR (300 MHz, $CDCl_3$): δ = 1.12 (t, 3H), 2.36 (t, 2H), 3.17 (q, 2H), 3.36 (t, 2H), 3.62–3.67 (m, 2H), 3.96–4.02 (m, 2H), 7.37–7.42 (m, 2H), 7.45–7.52 (m, 1H), 7.55–7.60 ppm (m, 1H); ^{13}C NMR (75 MHz, $CDCl_3$): δ = 15.6, 35.7, 39.4, 65.1, 109.5, 123.4, 128.6, 129.7, 131.5, 135.2, 149.7, 158.5 ppm; HRMS *m/z* $[M+H]^+$ calcd for $C_{14}H_{20}N_3O_5$: 332.1228, found: 332.1222.

1-(2-(2-(5-Methoxy-2-nitrophenyl)-1,3-dioxolan-2-yl)ethyl)-3-methylthiourea, 9f: Yellow oil (1.48 mmol, 72%); ^{1}H NMR (300 MHz, $CDCl_3$): δ = 2.50–2.55 (m, 2H), 2.95 (d, 3H), 3.65–3.73 (m, 4H), 3.85 (s, 3H), 3.99–4.04 (m, 2H), 5.97 (bs), 6.43 (bs), 6.86 (dd, 1H), 7.06 (d, 1H), 7.48 ppm (d, 1H); ^{13}C NMR (75 MHz, $CDCl_3$): δ = 30.5, 38.0, 40.4, 56.2, 65.1, 109.5, 113.4, 114.3, 126.2, 137.7, 143.0, 161.9, 182.2 ppm; HRMS *m/z* $[M+Na]^+$ calcd for $C_{14}H_{19}N_3O_5SNa$: 364.0940, found: 364.0943.

1-(2-(2-(5-Methoxy-2-nitrophenyl)-1,3-dioxolan-2-yl)ethyl)-3-ethylurea, 9i: Yellow oil (1.38 mmol, 67%); ^{1}H NMR (300 MHz, $CDCl_3$): δ = 0.92 (t, 3H), 2.72 (t, 2H), 3.30 (q, 2H), 3.36 (t, 2H), 3.63–3.67 (m, 1H), 3.84 (s, 3H), 4.15–4.20 (m, 2H), 6.48 (bs, 2H), 6.84 (dd, 1H), 7.13 (d, 1H), 7.46 ppm (d, 1H); ^{13}C NMR (75 MHz, $CDCl_3$): δ = 15.5, 35.6, 39.0, 41.8, 55.6, 64.8, 109.5, 113.2, 114.1, 125.7, 137.6, 144.9, 158.6, 161.4 ppm; HRMS *m/z* $[M+H]^+$ calcd for $C_{15}H_{22}N_3O_6$: 340.1416, found: 340.1427.

1-(2-(2-(5-Chloro-2-nitrophenyl)-1,3-dioxolan-2-yl)ethyl)-3-methylthiourea, 9k: Yellow solid (1.40 mmol, 68%); mp: 164–165 °C; ^{1}H NMR (300 MHz, $CDCl_3$): δ = 2.45–2.49 (m, 2H), 2.95 (s, 3H), 3.67–3.73 (m, 4H), 4.02–4.06 (m, 2H), 7.39–7.40 (m, 2H), 7.57–7.59 ppm (m, 1H); ^{13}C NMR (75 MHz, $CDCl_3$): δ = 30.5, 38.1, 40.1, 65.3, 109.1, 125.2, 128.6, 130.0, 137.2, 137.9, 147.9, 181.7 ppm; HRMS *m/z* $[M+Na]^+$ calcd for $C_{13}H_{16}N_3O_4SClNa$: 346.0839, found: 346.0826.

1-(2-(2-(5-Chloro-2-nitrophenyl)-1,3-dioxolan-2-yl)ethyl)-3-ethylurea, 9n: Yellow oil (1.26 mmol, 61%); ^{1}H NMR (400 MHz, $CDCl_3$): δ = 1.10 (t, 3H), 2.35 (t, 2H), 3.17 (q, 2H), 3.29 (t, 2H), 3.65–3.67 (m, 2H), 4.02–4.04 (m, 2H), 7.36 –7.37 (m, 2H), 7.57–7.59 ppm (m, 1H); ^{13}C NMR (125 MHz, $CDCl_3$): δ = 15.3, 35.4, 35.4, 42.4, 64.9, 108.9, 124.7, 128.4, 129.4, 137.2, 137.3, 147.7, 158.8 ppm; HRMS *m/z* $[M+H]^+$ calcd for $C_{14}H_{19}N_3O_5Cl$: 344.7523, found: 344.7528.

General method for the preparation of 1-(3-(5-substituted-2-nitrophenyl)-3-oxopropyl)-3-alkylthioureas and alkylureas, 10a–o: A solution of concentrated HCl (13.5 mL, 12 N) was added to a solution of the corresponding dioxolane precursor **9a–o** (0.995 mmol) in CH_2Cl_2 (6.8 mL). The mixture was stirred for 4 h at room temperature and then quenched with an aqueous saturated solution of KOH until achieving a basic pH. The former aqueous phase was extracted with CH_2Cl_2 (3×15 mL), and the organic layers were washed with brine (1×15 mL), dried on anhydrous Na_2SO_4, filtered, and concentrated under vacuum. The crude mixture was purified by flash chromatography (EtOAc/hexane, 1:1).

1-(3-(2-Nitrophenyl)-3-oxopropyl)-3-methylthiourea, 10a: Yellow oil (0.61 mmol, 61%); ^{1}H NMR (400 MHz, $CDCl_3$): δ = 2.94 (s, 3H), 3.16–3.23 (m, 2H), 4.01–4.09 (m, 2H), 6.51 (bs, 2H), 7.42 (d, 1H), 7.57–7.61 (m, 1H), 7.69–7.71 (m, 1H), 8.06 ppm (d, 1H); ^{13}C NMR (125 MHz, $CDCl_3$): δ = 32.8, 39.5, 42.5, 124.5, 127.3, 131.1, 134.5, 137.2, 145.8, 181.5, 202.5 ppm; HRMS *m/z* $[M+H]^+$ calcd for $C_{11}H_{14}N_3O_3S$: 267.3049, found: 267.3052.

1-(3-(2-Nitrophenyl)-3-oxopropyl)-3-ethylurea, 10d: Yellow solid (0.61 mmol, 61%); mp: 133–134 °C; ^{1}H NMR (300 MHz, $CDCl_3$): δ = 1.10 (t, 3H), 3.03 (t, 2H), 3.17 (q, 2H), 3.62 (t, 2H), 7.40 (dd, 1H), 7.55–7.61 (m, 1H), 7.67–7.73 (m, 1H), 8.07 ppm (d, 1H); ^{13}C NMR (75 MHz, $CDCl_3$): δ = 15.6, 35.4, 35.6, 43.4, 124.7, 127.5, 131.0, 134.5, 137.6, 145.9, 158.5, 202.6 ppm; HRMS *m/z* $[M+Na]^+$ calcd for $C_{12}H_{15}N_3O_4Na$: 288.0954, found: 288.0960.

1-(3-(5-Methoxy-2-nitrophenyl)-3-oxopropyl)-3-methylthiourea, 10f: Yellow solid (0.83 mmol, 84%); mp: 176–180 °C; ^{1}H NMR (300 MHz, $(CD_3)_2CO$): δ = 2.92 (d, 3H), 3.15 (t, 2H), 3.87–3.93 (m, 2H), 3.96 (s, 3H), 6.91 (bs, 1H), 6.96 (bs, 1H), 7.06 (d, 1H), 7.16 (dd, 1H), 8.13 ppm (d, 1H); ^{13}C NMR (75 MHz, $(CD_3)_2CO$): δ = 30.2, 39.4, 42.4, 56.4, 112.5, 115.6, 127.2, 138.6, 140.8, 164.7, 184.3, 201.3 ppm; HRMS *m/z* $[M+Na]^+$ calcd for $C_{12}H_{15}N_3O_6SNa$: 320.0680, found: 320.0681.

1-(3-(5-Methoxy-2-nitrophenyl)-3-oxopropyl)-3-ethylurea, 10i: Yellow solid (0.73 mmol, 73%); mp: 146–147 °C; ^{1}H NMR (300 MHz, $CDCl_3$): δ = 1.14 (t, 3H), 2.99 (t, 2H), 3.21 (q, 2H), 3.65 (t, 2H), 3.90 (s, 3H), 6.75 (d, 1H), 6.98 (dd, 1H), 8.13 ppm (d, 1H); ^{13}C NMR (75 MHz, $CDCl_3$): δ = 15.4, 35.5, 35.9, 43.5, 56.6, 112.0, 115.4, 127.4, 138.2, 140.6, 158.7, 164.7, 202.6 ppm; HRMS *m/z* $[M+Na]^+$ calcd for $C_{13}H_{17}N_3O_5Na$: 318.1072, found: 318.1066.

1-(3-(5-Chloro-2-nitrophenyl)-3-oxopropyl)-3-methylthiourea, 10k: Yellow solid (0.61 mmol, 61%); mp: 129–130 °C; ^{1}H NMR (300 MHz, $CDCl_3$): δ = 2.96 (s, 3H), 3.17 (t, 2H), 4.07 (t, 2H), 7.36 (d, 1H), 7.56 (dd, 1H), 8.07 ppm (d, 1H); ^{13}C NMR (75 MHz, $CDCl_3$): δ = 29.9, 39.7, 42.6, 126.4, 127.5, 131.1, 138.9, 141.7, 144.0, 181.8, 201.1 ppm; HRMS *m/z* $[M+Na]^+$ calcd for $C_{11}H_{12}N_3O_5SClNa$: 324.0185, found: 324.0186.

1-(3-(5-Chloro-2-nitrophenyl)-3-oxopropyl)-3-ethylurea, 10n: White solid (0.62 mmol, 62%); mp: 149–150 °C; ^{1}H NMR (300 MHz, $CDCl_3$): δ = 1.14 (t, 3H), 3.04 (t, 2H), 3.20 (q, 2H), 3.64 (t, 2H), 4.87 (bs, 2H), 7.36 (d, 1H), 7.54 (dd, 1H), 8.06 ppm (d, 1H); ^{13}C NMR (75 MHz, $CDCl_3$): δ = 16.5, 36.7, 37.1, 44.5, 127.4, 128.8, 132.1, 142.8, 145.1, 160.0, 202.0; HRMS *m/z* $[M+H]^+$ calcd for $C_{12}H_{13}N_3O_4Cl$: 300.0760, found: 300.0751.

General method for the preparation of 1-(3-(2-aminophenyl-5-substituted)-3-oxopropyl)-3-alkylthioureas and alkylureas, 5a–o: A mixture of nitro precursor **10a–o** (0.93 mmol), iron powder (9.3 mmol), and $FeSO_4$ (0.93 mmol) in water (19.5 mL) was stirred and heated for 3 h at 95 °C. Next, the suspension was filtered through Celite and thoroughly washed with CH_2Cl_2. The aqueous phase was extracted with CH_2Cl_2 (3×15 mL). The merged organic layer was washed with brine (1×15 mL), dried (Na_2SO_4), filtered,

ChemPubSoc Europe

CHEMMEDCHEM Full Papers

and evaporated under vacuum. The crude mixture was purified by flash chromatography (EtOAc/hexane, 1:1).

1-(3-(2-Aminophenyl)-3-oxopropyl)-3-methylthiourea, 5a: Yellow solid (0.76 mmol, 82%); mp: 127–128 °C; ^{1}H NMR (300 MHz, $CDCl_3$): δ = 2.96 (s, 3H), 3.35 (t, 2H), 3.98–4.04 (m, 2H), 5.30 (bs, 2H), 6.30 (bs, 1H), 6.51 (bs, 1H), 6.64–6.72 (m, 2H), 7.28–7.34 (m, 1H), 7.73 ppm (dd, 1H); ^{13}C NMR (75 MHz, $CDCl_3$): δ = 30.3, 38.5, 40.1, 116.3, 117.5, 117.6, 131.2, 135.0, 150.3, 182.2, 201.9 ppm; HRMS *m/z* $[M+Na]^+$ calcd mass for $C_{11}H_{15}N_3OSNa$: 260.0834, found: 260.0838; Anal. calcd for $C_{11}H_{15}N_3OS$: C 55.67, H 6.37, N 17.71, found: C 55.35, H 6.31, N 17.58.

1-(3-(2-Aminophenyl)-3-oxopropyl)-3-ethylurea, 5d: White solid (0.74 mmol, 80%); mp: 139–141 °C; ^{1}H NMR (300 MHz, $CDCl_3$): δ = 1.09 (t, 3H), 3.11–3.19 (m, 4H), 3.57 (t, 2H), 4.77 (bs, 4H), 6.59–6.66 (m, 2H), 7.24 (ddd, 1H), 7.69 ppm (dd, 1H); ^{13}C NMR (75 MHz, $CDCl_3$): δ = 15.4, 35.4, 35.5, 39.4, 116.1, 117.4, 117.9, 131.2, 134.6, 150.2, 158.8, 202.0 ppm; HRMS *m/z* $[M+Na]^+$ calcd mass for $C_{12}H_{17}N_3O_2Na$: 258.1218, found: 258.1227. Anal. calcd for $C_{12}H_{17}N_3O_2$: C 61.26, H 7.28, N 17.86, found: C 61.53, H 7.55; N 17.46.

1-(3-(2-Amino-5-methoxyphenyl)-3-oxopropyl)-3-methylthiourea, 5f: Yellow solid (0.87 mmol, 94%); mp: 125–126 °C; ^{1}H NMR (300 MHz, $CDCl_3$): δ = 2.90 (d, 3H), 3.27 (t, 2H), 3.74 (s, 3H), 3.93–4.01(m, 2H), 5.95 (bs, 2H), 6.27 (bs, 1H), 6.47 (bs, 1H), 6.60 (d, 1H), 6.95 (dd, 1H), 7.12 ppm (d, 1H); ^{13}C NMR (75 MHz, $CDCl_3$): δ = 30.4, 38.9, 40.3, 56.3, 113.2, 117.5, 119.1, 124.6, 145.4, 150.5, 182.4, 201.6 ppm; HRMS *m/z*: $[M+Na]^+$ calcd mass for $C_{12}H_{17}N_3O_2SNa$: 290.0939, found: 290.0940. Anal. calcd for $C_{12}H_{17}N_3O_2S$: C 53.91, H 6.41, N 15.72, S 11.99, found: C 53.55; H 6.79, N 15.11, S 11.73.

1-(3-(2-Amino-5-methoxyphenyl)-3-oxopropyl)-3-ethylurea, 5i: Yellow solid (0.83 mmol, 89%); mp: 115–117 °C; ^{1}H NMR (300 MHz, $CDCl_3$): δ = 1.06 (t, 3H), 3.10–3.18 (m, 4H), 3.57 (t, 2H), 3.74 (s, 3H), 5.21 (bs, 4H), 6.73 (d, 1H), 6.95 (dd, 1H), 7.16 ppm (d, 1H); ^{13}C NMR (75 MHz, $CDCl_3$): δ = 15.6, 35.6, 35.6, 39.9, 56.2, 113.8, 119.3, 120.1, 123.5, 142.8, 151.5, 158.6, 201.9 ppm; HRMS *m/z* $[M+Na]^+$ calcd mass for $C_{13}H_{19}N_3O_3Na$: 288.1324, found: 288.1329. Anal. calcd for $C_{13}H_{19}N_3O_3$: C 58.85, H 7.22, N 15.84, found: C 59.17, H 7.55, N 15.57.

1-(3-(2-Amino-5-chlorophenyl)-3-oxopropyl)-3-methylthiourea, 5k: Yellow solid (0.65 mmol, 70%); mp: 166–168 °C; ^{1}H NMR (300 MHz, $(CD_3)_2SO$): δ = 2.76 (s, 3H), 3.16 (t, 2H), 3.61–3.63 (m, 2H), 6.76 (d, 1H), 7.24 (dd, 1H), 7.40 (bs, 2H), 7.75 ppm (d, 1H); ^{13}C NMR (75 MHz, $(CD_3)_2SO$): δ = 31.1, 38.8, 40.0, 117.8, 119.7, 121.7, 130.8, 134.7, 150.5, 181.4, 200.6 ppm; HRMS *m/z* $[M+H]^+$ calcd mass for $C_{11}H_{15}N_3OSCl$: 272.0624, found: 272.0609. Anal. calcd for $C_{11}H_{14}N_2OS$: C 48.61, H 5.19, N 15.46, found: C 53.63, H 6.20, N 12.57.

1-(3-(2-Amino-5-chlorophenyl)-3-oxopropyl)-3-ethylurea, 5n: Yellow solid (0.70 mmol, 75%); mp: 157–160 °C; ^{1}H NMR (300 MHz, $CDCl_3$): δ = 1.10 (t, 3H), 3.13–3.21 (m, 4H), 3.58 (t, 2H), 4.59 (bs, 4H), 6.60 (d, 1H), 7.19 (dd, 1H), 7.63 ppm (d, 1H); ^{13}C NMR (75 MHz, $CDCl_3$): δ = 15.5, 35.8, 35.8, 39.6, 118.6, 119.2, 120.8, 130.5, 135.0, 148.8, 158.6, 201.2 ppm; HRMS *m/z* $[M+Na]^+$ calcd mass for $C_{12}H_{16}N_3O_2ClNa$: 292.0829, found: 292.0835. Anal. calcd for $C_{12}H_{16}N_3O_2Cl$: C 53.43, H 5.98, N 15.58 found: C 53.11, H 5.64, N 15.36.

Biological assays

In vitro nNOS and iNOS activity determination: L-Arginine, L-citrulline, *N*-(2-hydroxymethyl)piperazine-*N*'-(2-ethanesulfonic acid) (HEPES), D,L-dithiothreitol (DTT), hypoxanthine-9-β-D-ribofuranoside (inosine), (ethylene glycol)-bis-(2-aminoethylether)-*N*,*N*,*N*',*N*'-tetraacetic acid (EGTA), bovine serum albumin (BSA), Dowex-50W (50×8–200), FAD, NADPH, and 5,6,7,8-tetrahydro-L-biopterin dihydrochloride (H_4-biopterin), tris-(hydroxymethyl)aminomethane (Tris·HCl), and calcium chloride were obtained from Sigma–Aldrich Química (Spain). L-[^{3}H]arginine (47.4 Ci mmol^{-1}) was obtained from PerkinElmer (Spain). Calmodulin from bovine brain and recombinant iNOS and nNOS were obtained from Enzo Life Sciences (Spain).

i/nNOS activity was measured by the Bredt and Snyder method,[29] monitoring the conversion of L-[^{3}H]arginine to L-[^{3}H]citrulline. The final incubation volume was 100 µL and consisted of 10 µL of an aliquot of recombinant i/nNOS added to a buffer with a final concentration of 25 mM Tris·HCl, 1 mM DTT, 4 µM H_4-biopterin, 10 µM FAD, 0.5 mM inosine, 0.5 mg mL^{-1} BSA, 0.1 mM $CaCl_2$, 10 µM L-arginine, 10 µg mL^{-1} calmodulin (only for nNOS), and 50 nM L-[^{3}H]arginine, at pH 7.6 and 7.0 for iNOS and nNOS, respectively. The reaction was started by the addition of 10 µL of 7.5 mM NADPH and 10 µL of each kynurenamine derivative in EtOH (20%) to give a final concentration of 1 mM. The tubes were vortexed and incubated at 37 °C for 30 min. Control incubations were performed by the omission of NADPH. The reaction was halted by the addition of 400 µL of cold 0.1 M HEPES, 10 mM EGTA, and 0.175 mg mL^{-1} L-citrulline, pH 5.5. The reaction mixture was decanted into a 2 mL column packet with Dowex-50W ion-exchange resin (Na^+ form) and eluted with 1.2 mL water. L-[^{3}H]Citrulline was quantified by liquid scintillation spectroscopy. The retention of L-[^{3}H]arginine in this process was greater than 98%. Specific enzyme activity was determined by subtracting the control value, which usually amounted to less than 1% of the radioactivity added. The nNOS activity was expressed as pmol L-[^{3}H]citrulline produced per mg protein per min.

Tissue preparation and measurement of tension: This investigation conformed to the Guide for the Care and Use of Laboratory Animals published by the U.S. National Institutes of Health (NIH Publication No. 85–23, revised 1996) and with the principles outlined in the Declaration of Helsinki and approved by our institutional review board. Male Wistar rats (250–300 g), obtained from Harlam Laboratories SA (Barcelona, Spain), were euthanized by a quick blow on the head followed by exsanguination. The descending thoracic aortic rings were dissected, and the endothelium was removed mechanically and incubated in Krebs solution (118 mM NaCl, 4.75 mM KCl, 25 mM $NaHCO_3$, 1.2 mM $MgSO_4$, 2 mM $CaCl_2$, 1.2 mM KH_2PO_4, and 11 mM glucose) at 37 °C and gassed with 95% O_2 and 5% CO_2 for 20 h in a cell culture incubator in the absence or presence of *Escherichia coli* 055:B5 lipopolysaccharide (LPS, 1 µg mL^{-1}) (Sigma–Aldrich, Spain). Rings were then mounted in organ chambers filled with Krebs solution and were stretched to 2 g of resting tension by means of two L-shaped stainless steel wires inserted into the lumen and attached to the chamber and to an isometric force-displacement transducer (UF-1, Cibertec, Spain) and recorded in a recording and analysis system (MacLab AD Instruments), as described previously.[30] After equilibration of aortic rings, concentration–response curves for noradrenaline (NA, 10^{-9}–10^{-5} M) were performed by increasing the concentration in the organ chamber in cumulative increments after a steady-state response was reached with each increment. In some experiments, the non-selective NOS inhibitor, NG-nitro-arginine methyl ester (L-

NAME, 3×10^{-4} M), compound **5n** (10^{-4} M), or vehicle (DMSO) alone were added to the organ chamber 30 min before the addition of NA. The rings were then removed from the organ chambers, air-dried for 24 h, and weighed. The contraction was expressed in grams of force per milligram of dried tissue. The area under the concentration–response curve (AUC) was measured.

In another experiment, aortic rings with a functional endothelium were incubated with vehicle or **5n** (1 mM) for 30 min and contracted with NA (1 μM). Once a plateau contraction was reached, a concentration–response curve was constructed by cumulative addition of acetylcholine. Results are expressed as percentage of NA-evoked contraction. *n* reflects the number of aortic rings from different rats.

Quantification of NO in human umbilical vein endothelial cells (HUVECs): Endothelial cells were isolated from human umbilical cord veins using a previously reported method with several modifications.[31] The cells were cultured in Medium 199 with 20% fetal bovine serum and penicillin/streptomycin (2 mM), amphotericin B (2 mM), glutamine (2 mM), HEPES (10 mM), endothelial cell growth supplement (30 μg mL^{-1}), and heparin (100 mg mL^{-1}) under 5% CO_2 at 37 °C. HUVECs were then used to measure NO production by diaminofluorescein-2 (DAF-2) fluorescence, as described previously.[31] Briefly, cells were incubated for 30 min in the presence of **5n** at a concentration of 1 mM. After this period, cells were washed with PBS and then were pre-incubated with L-arginine (100 μM in PBS for 5 min at 37 °C). Subsequently, DAF-2 (0.1 μM) was incubated for 2 min, then the calcium ionophore calimycin (A23187, 1 μM) was added for 30 min, and cells were incubated in the dark at 37 °C. Fluorescence (arbitrary units) was then measured using a spectrofluorimeter (Fluorostart, BMG Labtechnologies, Offenburg, Germany). The auto-fluorescence was subtracted from each value. The area under the time–fluorescence curve (AUC) was measured.

Statistical analysis: Data are expressed as the mean ± SEM. Statistically significant differences between groups were calculated by Students' t test for unpaired observations or for multiple comparisons. ANOVA, followed by the Newmane–Keuls multiple range test, was used. A $p<0.05$ was considered statistically significant.

Docking and molecular dynamics (MD) simulations

The Maestro suite of programs (Schrödinger, LCC[32]) was used for the docking studies. The Cartesian coordinates for the two proteins, iNOS and nNOS, were obtained from the Protein Data Bank and treated with the Protein Preparation Wizard module[33] of Maestro. The 3D structures of the conformers of compounds **5a–o** were generated using the program LigPrep[34] after taking their structures from fragment libraries and optimizing using the Macromodel module. Rigid docking was performed using Glide with a Standard Precision (SP) protocol. Figure were built using PyMOL.[35]

Unrestrained MD simulations were carried out with the AMBER 12 software suite[36] in explicit solvent using the AMBER force field leaprc.ff10. The PDB2PQR tool[37,38] was used to estimate the most probable protonation states of titratable residues in the proteins at pH 7.0 and also to add all missing hydrogen atoms. Parameters for the prosthetic heme group were obtained from Giammona.[39] Parameters for compound **5n** as well as for H_4B were calculated using the antechamber module and the generalized AMBER force field with AM1-BCC charges.

Each enzyme–inhibitor complex was immersed in a cubic box of TIP3P water molecules with a minimum distance of 12 Å from any atom to the edge. The system was neutralized by incorporating the necessary amount of sodium ions. Particle Mesh Ewald method for long-range electrostatic interactions, together with standard periodic boundary conditions, were used. The SHAKE algorithm was applied to reach an integration step of 2.0 fs.

Before the simulation, the system was energetically minimized with a protocol of: 2000 steps of steepest descent, followed by 3000 steps of conjugate gradient. In this protocol, hydrogen atoms were first optimized, freezing the rest of the system, then only the water molecules were allowed to move, and finally the whole system was allowed to move. Next, the system was heated to 300 K in 20 ps at 1 atm using the Berendsen thermostat and a restraint constant on the alpha carbon of protein residues, ligands, and cofactors. The restraint was then decreased slowly in the equilibration step. Finally, 2 ns of production simulation were performed, collecting the coordinates of the system at each 1 ps. The binding free energy was calculated using the MM-ISMSA model,[40] and the estimated error was obtained with the block averaging method implemented in the *g analyse* tool of the GROMACS suite.[41]

Acknowledgements

This work was supported in part by the Instituto de Salud Carlos III through grant FI11/00432 and project RIC RD12/0042/0011.

Keywords: biological activity · inhibitors · kynurenamines · molecular modeling · nitric oxide synthase

[1] S. Moncada, R. M. Palmer, E. A. Higgs, *Pharmacol. Rev.* **1991**, *43*, 109–142.
[2] O. W. Griffith, D. J. Stuehr, *Annu. Rev. Physiol.* **1995**, *57*, 707–734.
[3] L. J. Roman, P. Martásek, B. S. Masters, *Chem. Rev.* **2002**, *102*, 1179–1189.
[4] R. G. Knowles, S. Moncada, *Biochem. J.* **1994**, *298*, 249–258.
[5] W. K. Alderton, C. E. Cooper, R. G. Knowles, *Biochem. J.* **2001**, *357*, 593–615.
[6] J. T. Groves, C. C. Wang, *Curr. Opin. Chem. Biol.* **2000**, *4*, 687–695.
[7] F. Aktan, *Life Sci.* **2004**, *75*, 639–653.
[8] M. A. Smith, M. Vasak, M. Knipp, R. J. Castellani, G. Perry, *Free Radical Biol. Med.* **1998**, *25*, 898–902.
[9] G. T. Liberatore, V. Jackson-Lewis, S. Vukosavic, A. S. Mandir, M. Vila, W. G. McAuliffe, V. L. Dawson, T. M. Dawson, S. Przedborski, *Nat. Med.* **1999**, *5*, 1403–1409.
[10] P. J. Norris, H. J. Waldvogel, R. L. Faull, D. R. Love, P. C. Emson, *Neuroscience* **1996**, *72*, 1037–1047.
[11] N. K. Wong, M. J. Strong, *Eur. J. Cell Biol.* **1998**, *77*, 338–343.
[12] C. O. Bingham III, *J. Rheumatol. Suppl.* **2002**, *65*, 3–9.
[13] K. D. Kröncke, K. Fehsel, V. Kolb-Bachofen, *Clin. Exp. Immunol.* **1998**, *113*, 147–156.
[14] S. Taddei, A. Virdis, L. Ghiadoni, I. Sudano, A. Salvetti, *J. Cardiovasc. Pharmacol.* **2001**, *38*, S11–S14.
[15] C. Napoli, F. de Nigris, S. Williams-Ignarro, O. Pignalosa, V. Sica, L. J. Ignarro, *Nitric Oxide* **2006**, *15*, 265–279.
[16] J. León, F. Vives, E. Crespo, E. Camacho, A. Espinosa, M. A. Gallo, G. Escames, D. Acuña-Castroviejo, *J. Neuroendocrinol.* **1998**, *10*, 297–302.
[17] J. León, M. Macías, G. Escames, E. Camacho, H. Khaldy, M. Martín, A. Espinosa, M. A. Gallo, D. Acuña-Castroviejo, *Mol. Pharmacol.* **2000**, *58*, 967–975.
[18] E. Camacho, J. Leon, A. Carrion, A. Entrena, G. Escames, H. Khaldy, D. Acuña-Castroviejo, M. A. Gallo, A. Espinosa, *J. Med. Chem.* **2002**, *45*, 263–274.

[19] A. Entrena, M. E. Camacho, M. D. Carrión, L. C. López-Cara, G. Velasco, J. León, G. Escames, D. Acuña-Castroviejo, V. Tapias, M. A. Gallo, A. Vivó, A. Espinosa, *J. Med. Chem.* **2005**, *48*, 8174–8181.
[20] M. E. Camacho, J. León, A. Entrena, G. Velasco, M. D. Carrión, G. Escames, A. Vivó, D. Acuña-Castroviejo, M. A. Gallo, A. Espinosa, *J. Med. Chem.* **2004**, *47*, 5641–5650.
[21] V. Tapias, G. Escames, L. C. López, A. López, E. Camacho, M. D. Carrión, A. Entrena, M. A. Gallo, A. Espinosa, D. Acuña-Castroviejo, *J. Neurosci. Res.* **2009**, *87*, 3002–3010.
[22] M. D. Carrión, M. Chayah, A. Entrena, A. López, M. A. Gallo, D. Acuña-Castroviejo, M. E. Camacho, *Bioorg. Med. Chem.* **2013**, *21*, 4132–4142.
[23] J. S. Fortin, J. Lacroix, M. Desjardins, A. Patenaude, E. Petitclerc, R. C. Gaudreault, *Bioorg. Med. Chem.* **2007**, *15*, 4456–4469.
[24] C. Szabó, J. A. Mitchell, C. Thiemermann, R. J. Vane, *Br. J. Pharmacol.* **1993**, *108*, 786–792.
[25] A. L. Weigert, E. M. Higa, M. Niederberger, I. F. McMurtry, M. Reynolds, R. W. Schrier, *J. Am. Soc. Nephrol.* **1995**, *5*, 2067–2072.
[26] U. Grädler, T. Fuchss, W.-R. Ulrich, R. Boer, A. Strub, C. Hesslinger, C. Anézo, K. Diederichs, A. Zaliani, *Bioorg. Med. Chem. Lett.* **2011**, *21*, 4228–4232.
[27] R. Fedorov, E. Hartmann, D. K. Ghosh, I. Schlichting, *J. Biol. Chem.* **2003**, *278*, 45818–45825.
[28] L. C. López-Cara, M. D. Carrión, A. Entrena, M. A. Gallo, A. Espinosa, A. López, G. Escames, D. Acuña-Castroviejo, M. E. Camacho, *Eur. J. Med. Chem.* **2012**, *50*, 129–139.
[29] D. S. Bredt, S. H. Snyder, *Proc. Natl. Acad. Sci. USA* **1990**, *87*, 682–685.
[30] J. Duarte, M. A. Ocete, F. Pérez-Vizcaino, A. Zarzuelo, J. Tamargo, *Eur. J. Pharmacol.* **1997**, *338*, 25–33.
[31] R. Jiménez, M. Sánchez, M. J. Zarzuelo, M. Romero, A. M. Quintela, R. López-Sepúlveda, P. Galindo, M. Gómez-Guzmán, J. M. Haro, A. Zarzuelo, F. Pérez-Vizcaino, J. Duarte, *J. Pharmacol. Exp. Ther.* **2010**, *332*, 554–561.
[32] Schrödinger Suite **2012**: Update 2.
[33] Schrödinger Suite **2012**: Protein Preparation Wizard, Epik version 2.3; Impact version 5.8; Prime version 3.1, Schrödinger LLC, New York, NY (USA).
[34] Lig Prep version 2.5, Schrödinger LLC, New York, NY (USA), **2012**.
[35] PyMOL Molecular Graphics System, version 1.4, Schrödinger LLC, New York, NY (USA).
[36] AMBER 12: D. A. Case, T. A. Darden, T. E. Cheatham III, C. L. Simmerling, J. Wang, R. E. Duke, R. Luo, R. C. Walker, W. Zhang, K. M. Merz, B. Roberts, S. Hayik, A. Roitberg, G. Seabra, J. Swails, A. W. Goetz, I. Kolossvai, K. F. Wong, F. Paesani, J. Vanicek, R. M. Wolf, J. Liu, X. Wu, S. R. Brozell, T. Steinbrecher, H. Gohlke, Q. Cai, X. Ye, J. Wang, M. J. Hsieh, G. Cui, D. R. Roe, D. H. Mathews, M. G. Seetin, R. Salomon-Ferrer, C. Sagui, V. Babin, T. Luchko, S. Gusarov, A. Kovalenko, P. A. Kollman, University of California, San Francisco, **2012**.
[37] T. J. Dolinsky, P. Czodrowski, H. Li, J. E. Nielsen, J. H. Jensen, G. Klebe, N. A. Baker, *Nucleic Acids Res.* **2007**, *35*, W522–W525.
[38] T. J. Dolinsky, J. E. Nielsen, J. A. McCammon, N. A. Baker, *Nucleic Acids Res.* **2004**, *32*, W665–W667.
[39] Parameters around the iron atom are appropriate for a six-coordinate (ligand bound) hemoglobin/myoglobin. Force field parameters were adapted from D. A. Giammona, PhD thesis, University of California, Davis, **1984**.
[40] J. Klett, A. Núñez-Salgado, H. G. Dos Santos, A. Cortés-Cabrera, A. Perona, R. Gil-Redondo, D. Abia, F. Gago, A. Morreale, *J. Chem. Theory Comput.* **2012**, *8*, 3395–3408.
[41] S. Pronk, S. Páll, R. Schulz, P. Larsson, P. Bjelkmar, R. Apostolov, M. R. Shirts, J. C. Smith, P. M. Kasson, D. Van der Spoel, B. Hess, *Bioinformatics* **2013**, *29*, 845–854.

Received: January 9, 2015
Published online on March 20, 2015

CHEMMEDCHEM
Chemistry & Drug Discovery

Supporting Information

Development of Urea and Thiourea Kynurenamine Derivatives: Synthesis, Molecular Modeling, and Biological Evaluation as Nitric Oxide Synthase Inhibitors

Mariem Chayah,[a] M. Dora Carrión,[a] Miguel A. Gallo,[a] Rosario Jiménez,[b] Juan Duarte,[b] and M. Encarnación Camacho*[a]

cmdc_201500007_sm_miscellaneous_information.pdf

Supporting Information

Characterisation data of 1-(2-(2-(5-substituted-2-nitrophenyl)-1,3-dioxolan-2-yl)ethyl)-3-alkylthioureas and alkykureas, 9b-c, 9e, 9g-h, 9j, 9l-m and 9o.

1-(2-(2-(2-Nitrophenyl)-1,3-dioxolan-2-yl)ethyl)-3-ethylthiourea, 9b. (1.62 mmol, 79%); ^{1}H NMR (300 MHz, $CDCl_3$): δ = 1.23 (t, 3H), 2.47 (t, 2H), 3.28–3.41 (m, 2H), 3.60–3.75 (m, 4H), 3.98–4.06(m, 2H), 7.40–7.45 (m, 2H), 7.48–7.54 (m, 1H), 7.57–7.62 ppm (m, 1H); ^{13}C NMR (75 MHz, $CDCl_3$): δ = 14.28, 38.18, 38.73, 40.09, 65.14, 109.46, 123.59, 128.48, 129.93, 131.70, 134.79, 149.64, 180.92 ppm; HRMS m/z $[M + H]^+$ calcd for $C_{14}H_{20}N_3O_4$: 326.3832, found: 326.3864.

1-(2-(2-(2-Nitrophenyl)-1,3-dioxolan-2-yl)ethyl)-3-propylthiourea, 9c. (1.98 mmol, 96%); ^{1}H NMR (300 MHz, $CDCl_3$): δ = 0.97 (t, 3H), 1.55–1.69 (m, 2H), 2.47 (t, 2H), 3.26 (t, 2H), 3.64–3.73 (m, 4H), 3.98–4.05 (m, 2H), 7.39–7.44 (m, 2H), 7.48–7.53 (m, 1H), 7.56–7.60 ppm (m, 1H); ^{13}C NMR (75 MHz, $CDCl_3$): δ = 11.44, 22.16, 37.98, 39.96, 45.60, 64.93, 109.23, 123.37, 128.29, 129.72, 131.47, 134.56, 149.46, 180.39 ppm; HRMS m/z $[M + H]^+$ calcd for $C_{15}H_{22}N_3O_4S$: 340.1334 , found: 340.1331.

1-(2-(2-(2-Nitrophenyl)-1,3-dioxolan-2-yl)ethyl)-3-propylurea, 9e. (1.71 mmol, 83%); ^{1}H NMR (300 MHz, $CDCl_3$): δ = 0.91 (t, 3H),1.46–1.56 (m, 2H), 2.37 (t, 2H), 3.10 (t, 2H), 3.37 (t, 2H), 3.62–3.67 (m, 2H), 3.98–4.03 (m, 2H), 4.58 (s, 2H), 7.38–7.42 (m, 2H), 7.46–7.52 (m, 1H), 7.56–7.60 ppm (m, 1H); ^{13}C NMR (75 MHz, $CDCl_3$): δ = 11.36, 23.26, 35.59, 39.04, 42.56, 64.88, 109.24, 123.20, 128.42, 129.52, 131.29, 149.46, 158.54 ppm; HRMS m/z $[M + H]^+$ calcd for $C_{15}H_{22}N_3O_5$: 324.1550, found: 324.1559.

1-(2-(2-(5-Methoxy-2-nitrophenyl)-1,3-dioxolan-2-yl)ethyl)-3-ethylthiourea, 9g. (1.34 mmol, 65%); ^{1}H NMR (300 MHz, $CDCl_3$): δ = 1.24 (t, 3H), 2.49–2.59 (m, 2H), 3.27–3.42 (m, 2H), 3.64–3.72 (m, 4H), 3.85 (s, 3H), 3.98–4.05 (m, 2H), 6.51 (bs, 2H), 6.86 (dd, 1H), 7.07 (d, 1H), 7.49 ppm (d, 1H); ^{13}C NMR (75 MHz, $CDCl_3$): δ = 22.65, 37.95, 40.31, 42.25, 56.14, 65.12, 109.43, 113.33, 114.29, 126.22, 137.42, 143.14, 161.72, 182.98 ppm; HRMS m/z $[M + H]^+$ calcd for $C_{15}H_{22}N_3O_5S$: 355.4564, found: 355.4593.

1-(2-(2-(5-Methoxy-2-nitrophenyl)-1,3-dioxolan-2-yl)ethyl)-3-propylthiourea, 9h. (1.77 mmol, 86%); ^{1}H NMR (300 MHz, $CDCl_3$): δ = 0.96 (t, 3H), 1.59–1.65 (m, 2H), 2.49–2.54 (m, 2H), 3.20–3.33 (m, 2H), 3.64–3.73 (m, 4H), 3.85 (s, 3H), 3.98–4.02 (m, 2H), 5.88 (bs, 1H), 6.38 (bs, 1H), 6.85 (dd, 1H), 7.06 (d, 1H), 7.48 ppm (d, 1H); ^{13}C NMR (75 MHz, $CDCl_3$): δ = 11.63, 22.39, 37.94, 40.28, 45.78, 56.16, 65.13, 109.54, 113.38, 114.27, 126.19, 137.6, 143.05, 161.92, 181.34 ppm; HRMS m/z $[M + Na]^+$ calcd for $C_{16}H_{23}N_3O_5SNa$: 392.1258, found: 392.1256.

1-(2-(2-(5-Methoxy-2-nitrophenyl)-1,3-dioxolan-2-yl)ethyl)-3-propylurea, 9j. (1.75 mmol, 85%); ^{1}H NMR (400 MHz, $CDCl_3$): δ = 0.90 (t, 3H), 1.46–1.52 (m, 2H), 2.41 (t, 2H), 3.08 (m, 2H), 3.35–3.37 (m, 2H), 3.63–3.66 (m, 2H), 3.83 (s, 3H), 3.96–4.00 (m, 2H), 4.42 (bs, 1H), 4.90 (bs, 1H), 6.84 (dd, 1H), 7.05 (d, 1H), 7.44 ppm (d, 1H); ^{13}C NMR (125 MHz, $CDCl_3$): δ = 11.44, 23.50, 35.57, 39.01, 42.49, 55.94, 64.91, 109.46,

113.26, 114.00, 125.76, 137.79, 142.97, 158.40, 161.58 ppm; HRMS m/z $[M + Na]^+$ calcd for $C_{16}H_{23}N_3O_5SNa$: 376.1479, found: 376.1485.

1-(2-(2-(5-Chloro-2-nitrophenyl)-1,3-dioxolan-2-yl)ethyl)-3-ethylthiourea, 9l. (1.24 mmol, 60%); ^1H NMR (300 MHz, $CDCl_3$): δ = 1.29 (t, 3H), 2.50–2.55 (m, 2H),3.39 (q, 2H), 3.73–3.77 (m, 4H), 4.07–4.11 (m, 2H), 7.44–7.45 (m, 2H), 7.63–7.64 ppm (m, 1H); ^{13}C NMR (75 MHz, $CDCl_3$): δ = 14.26, 38.09, 38.80, 39.98, 65.32, 109.06, 125.16, 128.59, 129.99, 137.18, 137.90, 147.86, 180.68 ppm; HRMS m/z $[M + H]^+$ calcd for $C_{14}H_{19}N_3O_4SCl$: 360.0783, found: 360.0785.

1-(2-(2-(5-Chloro-2-nitrophenyl)-1,3-dioxolan-2-yl)ethyl)-3-propylthiourea, 9m. (1.24 mmol, 60%); ^1H NMR (300 MHz, $CDCl_3$): δ = 0.96 (t, 3H), 1.60–1.67 (m, 2H), 2.48 (t, 2H), 3.26 (t, 2H), 3.67–3.73 (m, 4H), 4.01–4.07 (m, 2H), 7.39–7.40 (m, 2H), 7.57–7.58 ppm (m, 1H); ^{13}C NMR (75 MHz, $CDCl_3$): δ = 11.66, 22.37, 38.10, 40.07, 45.80, 65.33, 109.07, 125.16, 128.59, 130.00, 137.18, 137.89, 147.88, 180.79 ppm; HRMS m/z $[M + H]^+$ calcd for $C_{15}H_{21}N_3O_4SCl$: 374.8558, found: 374.8564.

1-(2-(2-(5-Chloro-2-nitrophenyl)-1,3-dioxolan-2-yl)ethyl)-3-propylurea, 9o. (1.24 mmol, 60%); ^1H NMR (400 MHz, $CDCl_3$): δ = 0.91 (t, 3H), 1.48–1.53 (m, 2H), 2.36 (t, 2H), 3.10 (t, 2H), 3.37 (t, 2H), 3.66–3.68 (m, 2H), 4.01–4.03 (m, 2H), 7.37–7.38 (m, 2H), 7.57–7.58 ppm (m, 1H); ^{13}C NMR (125 MHz, $CDCl_3$): δ = 11.31, 23.34, 35.25, 39.02, 42.39, 64.97, 108.89, 124.66, 128.44, 129.48, 137.26, 137.35, 147.61, 158.78 ppm; HRMS m/z $[M + H]^+$ calcd for $C_{15}H_{21}N_3O_5Cl$: 358.1164, found: 358.1170.

Characterisation data of 1-(3-(5-substituted-2-nitrophenyl)-3-oxopropyl)-3-alkylthioureas and alkylureas, 10b-c, 10e, 10g-h, 10j, 10l-m and 10o.

1-(3-(2-Nitrophenyl)-3-oxopropyl)-3-ethylthiourea, 10b. (0.79 mmol, 79%); ^1H NMR (300 MHz, $CDCl_3$): δ = 1.20 (t, 3H), 3.17 (t, 2H), 3.35 (q, 2H), 4.03 (t, 2H), 6.42 (bs, 2H), 7.41 (d, 1H), 7.57–7.62 (m, 1H), 7.69–7.71 (m, 1H), 8.07 ppm (d, 1H); ^{13}C NMR (75 MHz, $CDCl_3$): δ = 14.22, 38.75, 39.71, 42.51, 124.81, 127.45, 131.19, 134.61, 137.23, 145.91, 181.54, 202.64 ppm; HRMS m/z $[M + H]^+$ calcd for $C_{12}H_{16}N_3O_3S$: 282.0956, found: 282.0939.

1-(3-(2-Nitrophenyl)-3-oxopropyl)-3-propylthiourea, 10c. (0.84 mmol, 84%); ^1H NMR (300 MHz, $CDCl_3$): δ = 0.95 (t, 3H), 1.57–1.65 (m, 2H), 3.19 (t, 2H), 3.27 (t, 2H), 4.03 (t, 2H), 7.42 (dd, 1H), 7.57–7.62 (m, 1H), 7.69–7.74 (m, 1H), 8.07 ppm (dd, 1H); ^{13}C NMR (75 MHz, $CDCl_3$): δ = 11.43, 22.13, 39.52, 42.30, 45.62, 124.60, 127.27, 130.99, 134.39, 137.01, 145.73, 180.70, 202.38 ppm; HRMS m/z $[M + H]^+$ calcd for $C_{13}H_{18}N_3O_3S$: 296.1071, found: 296.1069.

1-(3-(2-Nitrophenyl)-3-oxopropyl)-3-propylurea, 10e. (0.94 mmol, 94%); ^1H NMR (300 MHz, CD_3OD): δ = 0.99 (t, 3H), 1.51–1.58 (m, 2H), 3.11 (t, 2H), 3.36–3.38 (m, 2H), 3.57–3.59 (m, 2H), 7.64 (dd, 1H), 7.72–7.78 (m, 1H), 7.84–7.89 (m, 1H), 8.17 ppm (dd, 1H); ^{13}C NMR (75 MHz, CD_3OD): δ = 10.46, 23.27, 34.82, 34.86, 41.66, 124.29, 127.64, 131.01, 134.21, 137.25, 146.22, 160.00, 202.03 ppm; HRMS m/z $[M + H]^+$ calcd for $C_{13}H_{18}N_3O_4$: 280.1215, found: 280.1217.

1-(3-(5-Methoxy-2-nitrophenyl)-3-oxopropyl)-3-ethylthiourea, 10g. (0.69 mmol, 69%); ^{1}H NMR (300 MHz, $(CD_3)_2SO$): δ = 1.05 (t, 3H), 3.12 (t, 2H), 3.31 (m, 2H), 3.70–3.72 (m, 2H), 3.92 (s, 3H), 7.15 (d, 1H), 7.21 (dd, 1H), 7.37 (bs, 1H), 7.50 (bs, 1H), 8.17 ppm (d, 1H); ^{13}C NMR (75 MHz, $(CD_3)_2SO$): δ = 15.09, 38.93, 39.41, 42.63, 57.31, 113.20, 116.31, 127.86, 138.43, 140.64, 164.70, 182.37, 201.95 ppm; HRMS m/z [M + Na]$^+$ calcd for $C_{13}H_{17}N_3O_4SNa$: 334.0826, found: 334.0837.

1-(3-(5-Methoxy-2-nitrophenyl)-3-oxopropyl)-3-propylthiourea, 10h. (0.71 mmol, 71%); ^{1}H NMR (300 MHz, $CDCl_3$): δ = 0.95 (t, 3H), 1.57–1.65 (m, 2H), 3.10 (t, 2H), 3.23–3.31 (m, 2H), 3.90 (s, 3H), 4.02–4.08 (m, 2H), 6.11 (bs, 1H), 6.34 (bs, 1H), 6.74 (d, 1H), 6.98 (dd, 1H), 8.13 ppm (d, 1H); ^{13}C NMR (75 MHz, $CDCl_3$): δ = 11.64, 22.32, 39.86, 42.73, 45.68, 56.63, 112.06, 115.49, 127.50, 138.26, 140.44, 164.75, 181.83, 202.74 ppm; HRMS m/z [M + Na]$^+$ calcd for $C_{14}H_{19}N_3O_4SNa$: 348.0993, found: 348.0994.

1-(3-(5-Methoxy-2-nitrophenyl)-3-oxopropyl)-3-propylurea, 10j. (0.65 mmol, 65%); ^{1}H NMR (300 MHz, $CDCl_3$): δ = 0.90 (d, 3H), 1.44–1.53 (m, 2H), 3.00 (t, 2H), 3.06 (t, 2H), 3.53 (t, 2H), 3.94 (s, 3H), 6.97 (d, 1H), 7.14 (dd, 1H), 8.17 ppm (d, 1H); ^{13}C NMR (75 MHz, $CDCl_3$): δ = 10.46, 23.27, 34.94, 41.68, 43.09, 55.85, 112.31, 115.04, 126.99, 138.31, 140.68, 160.01, 164.82, 202.23 ppm; HRMS m/z [M + Na]$^+$ calcd for $C_{14}H_{19}N_3O_5Na$: 332.1221, found: 332.1222.

1-(3-(5-Chloro-2-nitrophenyl)-3-oxopropyl)-3-ethylthiourea, 10l. (0.63 mmol, 63%); ^{1}H NMR (300 MHz, $CDCl_3$): δ = 1.26 (t, 3H), 3.18 (t, 2H), 3.36 (q, 2H), 4.04 (t, 2H), 7.38 (d, 1H), 7.56 (dd, 1H), 8.07 ppm (d, 1H); ^{13}C NMR (75 MHz, $CDCl_3$): δ = 14.21, 38.73, 39.64, 42.64, 126.34, 127.53, 131.07, 138.86, 141.68, 143.96, 181.43, 201.15 ppm; HRMS m/z [M + Na]$^+$ calcd for $C_{12}H_{14}N_3O_3SClNa$: 338.0423, found: 338.0420.

1-(3-(5-Chloro-2-nitrophenyl)-3-oxopropyl)-3-propylthiourea, 10m. (0.69 mmol, 69%); ^{1}H NMR (300 MHz, $CDCl_3$): δ = 0.96 (t, 3H), 1.58–1.67 (m, 2H), 3.18 (t, 2H), 3.27 (t, 2H), 4.04 (t, 2H), 7.37 (d, 1H), 7.55 (dd, 1H), 8.06 ppm (d, 1H); ^{13}C NMR (75 MHz, $CDCl_3$): δ = 11.65, 22.33, 39.66, 42.65, 45.75, 126.32, 127.54, 131.06, 138.87, 141.66, 143.96, 181.60, 201.16 ppm; HRMS m/z [M + Na]$^+$ calcd for $C_{13}H_{16}N_3O_3SClNa$: 330.0678, found: 330.0679.

1-(3-(5-Chloro-2-nitrophenyl)-3-oxopropyl)-3-propylurea, 10o. (0.70 mmol, 70%); ^{1}H NMR (300 MHz, $CDCl_3$): δ = 0.93 (t, 3H), 1.49–1.56 (m, 2H), 3.04 (t, 2H), 3.12 (t, 2H), 3.64 (t, 2H), 4.67 (bs, 2H), 7.54 (dd, 1H), 8.06 ppm (d, 1H); ^{13}C NMR (75 MHz, $CDCl_3$): δ = 11.53, 23.27, 35.58, 42.92, 43.35, 126.30, 127.58, 131.00, 139.03, 141.69, 143.92, 158.99, 200.91 ppm; HRMS m/z [M + Na]$^+$ calcd for $C_{12}H_{15}N_3O_4ClNa$: 336.0719, found: 336.0727.

Characterisation data of 1-(3-(2-aminophenyl-5-substituted)-3-oxopropyl)-3-alkylthioureas and alkylureas, 5b-c, 5e, 5g-h, 5j, 5l-m and 5o.

1-(3-(2-Aminophenyl)-3-oxopropyl)-3-ethylthiourea, 5b. Yellow solid (0.79 mmol, 85%); mp: 130–132 ºC; ^{1}H NMR (300 MHz, $CDCl_3$): δ = 1.18 (t, 3H), 3.22–3.38 (m, 4H), 3.93–3.99 (m, 2H), 6.18 (bs, 1H), 6.48 (bs, 1H), 6.57–6.66 (m, 2H), 7.21–7.29 (m, 1H), 7.67 (dd, 1H) ppm; ^{13}C NMR (75 MHz, $CDCl_3$): δ = 14.23, 38.70, 40.19, 116.42, 117.65, 117.77, 131.43, 135.16, 150.60, 181.34, 202.14 ppm; HRMS m/z $[M + Na]^+$ calcd. mass for $C_{12}H_{17}N_3OSNa$: 274.0990, found: 274.0985; Anal. calc. for $C_{12}H_{17}N_3OS$: C 57.34, H 6.82, N 16.72, S 12.76, found: C 57.42, H 7.15, N 16.56, S 12.47.

1-(3-(2-Aminophenyl)-3-oxopropyl)-3-propylthiourea, 5c. Yellow solid (0.88 mmol, 95%); mp: 58–60 ºC; ^{1}H NMR (400 MHz, CD_3OD): δ = 0.99 (t, 3H), 1.60–1.66 (m, 2H), 3.33 (t, 2H), 3.35–3.39 (m, 2H), 3.90–3.94 (m, 2H), 6.65 (ddd, 1H), 6.79 (dd, 1H), 7.29 (ddd, 1H), 7.85 (dd, 1H) ppm; ^{13}C NMR (125 MHz, CD_3OD): δ = 11.66, 23.55, 39.76, 41.11, 46.70, 116.42, 118.48, 118.77, 132.57, 135.68, 152.83, 182.36, 202.76 ppm; HRMS m/z $[M + H]^+$ calcd. mass for $C_{13}H_{20}N_3OS$: 266.1327, found: 266.1320. Anal. calc. for $C_{13}H_{19}N_3OS$: C 58.84, H 7.22, N 15.83, found: C 58.72, H 7.34, N 15.61.

1-(3-(2-Aminophenyl)-3-oxopropyl)-3-propylurea, 5e. White solid (0.76 mmol, 82%); mp: 130–132 ºC; ^{1}H NMR (300 MHz, $CDCl_3$): δ = 0.86 (t, 3H), 1.39–1.50 (m, 2H), 3.06 (t, 2H), 3.15 (t, 2H), 3.56 (t, 2H), 5.51 (bs, 4H), 6.60–6.68 (m, 2H), 7.24 (ddd, 1H), 7.67 (dd, 1H) ppm; ^{13}C NMR (75 MHz, $CDCl_3$): δ = 11.59, 23.56, 35.88, 39.71, 42.62, 116.79, 117.94, 118.48, 131.43, 134.88, 149.87, 158.85, 202.16 ppm; HRMS m/z $[M + H]^+$ calcd. mass for $C_{13}H_{20}N_3O_2$: 250.1556, found: 250.1555. Anal. calc. for $C_{13}H_{19}N_3O_2$: C 62.63, H 7.68, N 16.85, found: C 62.38, H 7.86, N 16.45.

1-(3-(2-Amino-5-methoxyphenyl)-3-oxopropyl)-3-ethylthiourea, 5g. Yellow solid (0.84 mmol, 90%); mp: 141–143 ºC; ^{1}H NMR (300 MHz, $CDCl_3$): δ = 1.17 (t, 3H), 3.25 (t, 2H), 3.31–3.34 (m, 2H), 3.73 (s, 3H), 3.95–3.97 (m, 2H), 5.47 (bs, 2H), 6.23 (bs, 1H), 6.53 (bs, 1H), 6.63 (d, 1H), 6.95 (dd, 1H), 7.11 (d, 1H) ppm; ^{13}C NMR (75 MHz, $CDCl_3$): δ = 14.23, 38.93, 40.18, 56.29, 113.30, 117.89, 119.39, 124.44, 144.74, 150.74, 181.36, 201.69 ppm; HRMS m/z $[M + Na]^+$ calcd. mass for $C_{13}H_{19}N_3O_2SNa$: 304.1096, found: 304.1099. Anal. calc. for $C_{13}H_{19}N_3O_2S$: C 55.49, H 6.81, N 14.93, S11.40, found: C 55.23, H 7.03, N 14.42, S 11.70.

1-(3-(2-Amino-5-methoxyphenyl)-3-oxopropyl)-3-propylthiourea, 5h. Yellow solid (0.78 mmol, 84%); mp: 115–117 ºC; ^{1}H NMR (300 MHz, $CDCl_3$): δ = 0.92 (t, 3H), 1.51–1.62 (m, 2H), 3.18–3.23 (m, 2H), 3.27 (t, 2H), 3.74 (s, 3H), 3.95–4.00 (m, 2H), 5.95 (bs, 2H), 6.14 (bs, 1H), 6.43 (t, 1H), 6.61 (d, 1H), 6.96 (dd, 1H), 7.13 (d, 1H) ppm; ^{13}C NMR (75 MHz, $CDCl_3$): δ = 11.66, 22.32, 38.89, 40.29, 45.74, 56.30, 113.23, 117.51, 119.13, 124.61, 145.45, 150.52, 181.56, 201.67 ppm; HRMS m/z $[M + Na]^+$ calcd. mass for $C_{14}H_{21}N_3O_2SNa$: 318.1252, found: 318.1252. Anal. calc. for $C_{14}H_{21}N_3O_2S$: C 56.92, H 7.17, N 14.22, S 10.85, found: C 57.16, H 7.64, N 13.98, S 11.16.

1-(3-(2-Amino-5-methoxyphenyl)-3-oxopropyl)-3-propylurea, 5j. Yellow solid (0.75 mmol, 80%); mp: 112–114 ºC; ^{1}H NMR (300 MHz, $CDCl_3$): δ = 0.87 (t, 3H), 1.46 (m, 2H), 3.07 (c, 2H), 3.14 (t, 2H), 3.54–3.60 (m, 2H), 3.74 (s, 3H), 4.46 (bs, 1H), 5.02 (bs, 1H), 5.95 (bs, 2H), 6.60 (d, 1H), 6.94 (dd, 1H), 7.14 (d, 1H) ppm; ^{13}C NMR (75 MHz, $CDCl_3$): δ = 11.58, 23.61, 35.73, 39.81, 42.63, 56.25, 113.47, 117.90, 119.04, 124.13,

145.29, 150.48, 158.49, 201.76 ppm; HRMS m/z $[M + Na]^+$ calcd. mass for $C_{14}H_{21}N_3O_3Na$: 302.1400, found: 302.1408. Anal. calc. for $C_{14}H_{21}N_3O_3$: C 60.20, H 7.58, N 15.04, found: C 60.55, H 7.54, N 14.62.

1-(3-(2-Amino-5-chlorophenyl)-3-oxopropyl)-3-ethylthiourea, 5l. Yellow solid (0.60 mmol, 65%); mp: 151–154 ºC; ^{1}H NMR (300 MHz, $CDCl_3$): δ = 1.19 (t, 3H), 3.27 (t, 2H), 3.32–3.35 (m, 2H), 3.96 (t, 2H), 6.63 (d, 1H), 7.21 (d, 1H), 7.65 (s,1H) ppm; ^{13}C NMR (75 MHz, $CDCl_3$): δ = 14.22, 38.78, 40.01, 118.59, 119.31, 121.13, 130.50, 135.13, 148.55, 181.40, 201.23 ppm; HRMS m/z $[M + H]^+$ calcd. mass for $C_{12}H_{17}N_3OSCl$: 286.0781, found: 286.0787. Anal. calc. for $C_{12}H_{16}N_3OS$: C 50.43, H 5.64, N 14.70, found: C 53.17, H 6.08, N 13.34.

1-(3-(2-Amino-5-chlorophenyl)-3-oxopropyl)-3-propylthiourea, 5m. Yellow solid (0.66 mmol, 71%); mp: 148–150 ºC; ^{1}H NMR (300 MHz, $CDCl_3$): δ = 0.96 (t, 3H), 1.52–1.65 (m, 2H), 3.21–3.30 (m, 4H), 3.99 (t, 2H), 5.95 (bs, 4H), 6.69 (d, 1H), 7.23 (dd, 1H), 7.67 (d, 1H) ppm; ^{13}C NMR (75 MHz, $CDCl_3$): δ = 11.67, 22.35, 38.85, 40.00, 45.82, 119.03, 119.62, 121.65, 130.52, 135.11, 147.84, 181.52, 201.24 ppm; HRMS m/z $[M + H]^+$ calcd. mass for $C_{13}H_{19}N_3OSCl$: 300.0937, found: 300.0939. Anal. calc. for $C_{13}H_{18}N_3OSCl$: C 52.08, H 6.05, N 14.02, found: C 53.17, H 6.15, N 13.90.

1-(3-(2-Amino-5-chlorophenyl)-3-oxopropyl)-3-propylurea, 5o. Yellow solid (0.59 mmol, 64%); mp: 115–117 ºC; ^{1}H NMR (300 MHz, $CDCl_3$): δ = 0.91 (t, 3H), 1.46–1.54 (m, 2H), 3.09 (t, 2H), 3.14 (t, 2H), 3.58 (t, 2H), 5.18 (bs, 4H), 6.62 (d, 1H), 7.19 (dd, 1H), 7.62 (d, 1H) ppm; ^{13}C NMR (75 MHz, $CDCl_3$): δ = 11.57, 23.42, 35.86, 39.56, 42.80, 118.63, 119.28, 120.93, 130.45, 134.99, 148.70, 158.88, 201.06 ppm; HRMS m/z $[M + Na]^+$ calcd. mass for $C_{13}H_{18}N_3O_2ClNa$: 306.0985, found: 306.0982 . Anal. calc. for $C_{13}H_{18}N_3O_2$: C 55.03, H 6.39, N 14.81, found: C 59.85, H 7.05, N 10.44.

3.3 Artículo 3

Letter - spectral assignments

MRC

Received: 11 May 2015 Revised: 12 June 2015 Accepted: 18 June 2015 Published online in Wiley Online Library

(wileyonlinelibrary.com) DOI 10.1002/mrc.4295

NMR assignments and structural characterization of new thiourea and urea kynurenamine derivatives nitric oxide synthase inhibitors

Mariem Chayah,[a] M. Dora Carrión,[a] Miguel A. Gallo,[a] Duane Choquesillo-Lazarte[b] and M. Encarnación Camacho[a]*

Introduction

The bioactive molecule of nitric oxide (NO) is an important second messenger that participates in regulation of cardiovascular, nervous and immune systems.[1] NO synthases (NOS) catalyze the oxidation of the amino acid L-arginine to L-citrulline and NO with NADPH and molecular oxygen as cosubstrates.[2] In mammalians, three isoforms of NOS have been identified: neuronal (nNOS), endothelial and inducible NOS.[3] These isoenzymes are involved in important biological processes and are implicated in many pathological diseases. Thus, overproduction of NO by nNOS has been associated with neurodegenerative disorders in Alzheimer's, Parkinson's or Huntington's diseases,[4–6] and the inducible isoform seems to be responsible for the massive NO production in pathologies such as arthritis, colitis, tissue damage, cancer or several inflammatory states.[7–9] In this way, many authors have focused their interest in the development of NOS selective inhibitors.

In a recent paper, the synthesis and biological evaluation of a novel family of kynurenamine derivatives bearing a thiourea or urea fragment **31–45**, which were designed and evaluated as NOS inhibitor agents, have been described.[10]

Although the structures of these derivatives have been determined by means of standard spectroscopic techniques (^{1}H and ^{13}C NMR and MS), a detailed NMR study has been performed in some of them, in order to unequivocally corroborate their structures.

The present study reports the unambiguous assignment of each signal in the ^{1}H and ^{13}C NMR spectra in compounds **31–45**, using one-dimensional and two-dimensional resonance techniques. The spectra of nitro derivatives **1–30**, the precursors in the synthetic pathway, are also included.

Experimental

NMR spectra

Nuclear magnetic resonance spectra were recorded on 300-MHz ^{1}H NMR and 75-MHz ^{13}C NMR Agilent Varian Direct Drive, 400-MHz ^{1}H NMR and 100-MHz ^{13}C NMR Agilent Varian Direct Drive and 600-MHz ^{1}H NMR and 150-MHz ^{13}C NMR Agilent Varian Direct Drive spectrometers at 298 K. The following parameters were used in DEPT experiments: pulse width (PW) (135°), 9.0 ms; recycle time, 1 s; 0.5 J (CH) = 4 ms; 65 536 data points acquired and transformed from 1024 scans; spectral width, 15 KHz; and line broadening, 1.3 Hz. Chemical shifts (δ) are quoted in parts per million (ppm) and are referenced to the residual solvent peak: $CDCl_3$, $\delta = 7.26$ ppm (^{1}H), $\delta = 77.4$ ppm (^{13}C); $(CD_3)_2CO$, $\delta = 2.05$ ppm (^{1}H), $\delta = 29.84$ ppm (^{13}C); $(CD_3)_2SO$, $\delta = 2.50$ ppm (^{1}H), $\delta = 39.52$ ppm (^{13}C); and CD_3OD, $\delta = 3.31$ ppm (^{1}H), $\delta = 49.00$ ppm (^{13}C). Spin multiplicities are given as s (singlet), bs (broad singlet), d (doublet), dd (doublet doublet), ddd (doublet, doublet doublet), t (triplet), q (quadruplet) and m (multiplet). Coupling constant (J) are given in hertz.

The HMBC spectra were measured with a pulse sequence gc2hmbc (standard sequence, Agilent Vnmrj_3.2A software) optimized for 8 Hz (inter-pulse delay for the evolution of long-range couplings: 62.5 ms). The HSQC spectra were measured with a pulse sequence gc2hsqcse (standard sequence, Agilent Vnmrj_3.2A software).

Nuclear Overhauser spectra were recorded on an Agilent Varian Direct Drive spectrometer, operating at 600 MHz, with a spectral widths of 4.96 KHz in both F2 and F1 domains; 744 × 200 data points were acquired with 16 scans per increment and relaxation delays of 1.0 s. The mixing time in NOESY experiments was 0.5 s. Data processing was performed on a 1 × 1 K data matrix.

Molecular dynamics simulations

Unrestricted molecular dynamics (MD) simulations were carried out with the AMBER 12 software suite[11] in explicit solvent using the AMBER force field leaprc ff12SB. Geometry of compound **39** was optimized using RHF/6-31G* as implemented in Gaussian 09 (Gaussian, Inc., Wallingford, CT). Charges were then assigned to

* *Correspondence to: M. Encarnación Camacho. Departamento de Química Farmacéutica y Orgánica, Facultad de Farmacia, Universidad de Granada, c/ Campus de Cartuja, s/n 18071 Granada, Spain. E-mail: ecamacho@ugr.es*

a *Departamento de Química Farmacéutica y Orgánica, Facultad de Farmacia, Universidad de Granada, Granada, Spain*

b *Laboratorio de Estudios Cristalográficos, IACT-CSIC, Armilla, Granada, Spain*

individual atoms by fitting the quantum mechanically calculated (RHF/6-31G*//RHF/3-21G*) molecular electrostatic potential to a point charge model. Compound **39** was immersed in a cubic box of $CHCl_3$ molecules (CL3 model) with a minimum distance of 12 Å from any atom to the edge. The particle mesh Ewald method for long-range electrostatic interactions together with standard periodic boundary conditions was used. SHAKE algorithm was applied to reach an integration step of 2.0 fs. The followed MD simulation protocol was the same as previously described.[10] Distances and conformational clustering were performed using the program cpptraj implemented in Amber Tools 14.

Table 1. Structural data of the intermediate (**1–30**) and final (**31–45**) compounds

Compound	R_1	R_2	X	Compound	R_1	R_2	X
1, 16, 31	H	Me	S	**10, 25, 40**	H	Et	O
2, 17, 32	H	Et	S	**11, 26, 41**	H	Pr	O
3, 18, 33	H	Pr	S	**12, 27, 42**	OMe	Et	O
4, 19, 34	OMe	Me	S	**13, 28, 43**	OMe	Pr	O
5, 20, 35	OMe	Et	S	**14, 29, 44**	Cl	Et	O
6, 21, 36	OMe	Pr	S	**15, 30, 45**	Cl	Pr	O
7, 22, 37	Cl	Me	S				
8, 23, 38	Cl	Et	S				
9, 24, 39	Cl	Pr	S				

X-ray crystallography

A yellow crystal of compound **39** was mounted on a MiTeGen Micromounts, and this sample was used for data collection. Data were collected with a Bruker D8 Venture diffractometer. Data were processed with APEX[12] and corrected for absorption using SADABS.[13] The structures were solved by direct methods,[14] which revealed the position of all non-hydrogen atoms. These atoms were refined on F^2 by a full-matrix least-squares procedure using anisotropic displacement parameters.[14] All hydrogen atoms were located in different Fourier maps and included as fixed contributions riding on attached atoms with isotropic thermal displacement parameters that are 1.2 times those of the respective atom. Crystallographic data for the structural analysis have been deposited with the Cambridge Crystallographic Data Centre, CCDC 1063097.

Results and discussion

Scheme 1 represents the previously reported synthetic pathway followed in the preparation of final compounds **31–45**,[10] and Table 1 shows the structural data of all the intermediate and final compounds synthesized.

Structural elucidation of these compounds has been made by routine ^1H and ^{13}C techniques. Nevertheless, a definitive assignment of all signals needs the use of several NMR techniques as follows: (i) DEPT experiments to determine the number of protons attached to each carbon atom; (ii) HSQC spectra to determine the ^{13}C resonances of the tertiary, secondary and primary carbons; (iii) HMBC sequences to assign the signals of quaternary carbons via two-bond and three-bond interactions; and (iv) NOESY experiments to determinate the preferred conformation in solution.

Tables 2–4 show the ^1H NMR signals of each proton for compounds **1–45**, whereas Tables 5–7 show the corresponding ^{13}C NMR chemical shifts for the same molecules. NMR spectra of all compounds were carried out in $CDCl_3$ solution, except for compound **19**, which was registered in $(CD_3)_2CO$, **20** and **37** in $(CD_3)_2SO$ and **26** and **33** in CD_3OD. For this reason, some significant variations are observed in the chemical shifts according to the solvent.

The ^1H NMR and ^{13}C NMR signals of the aromatic ring (H-1"–H-6", C-1"–C-6") and C-3' are similar in the three families of compounds: 1-(2-(2-(5-substituted-2-nitrophenyl)-1,3-dioxolan-2-yl)ethyl)-3-alkylthioureas and alkylureas **1–15**, 1-(3-(5-substituted-2-nitrophenyl)-3-oxopropyl)-3-alkylthioureas and alkylureas **16–30**, and 1-(3-(2-aminophenyl-5-substituted)-3-oxopropyl)-3-alkylthioureas and alkylureas **31–45**. However, signals corresponding to the linear chain (H-1', H-2', C-2, C-1' and C-2') are influenced by the thiourea or urea residue of each family of compounds. Finally, H-1 and H-3 signals, linked to nitrogen atoms, do not follow the same pattern and sometimes are not visible.

Heteronuclear single-quantum correlation and HMBC experiments were performed on some compounds of each series, and the results of these experiments have been extrapolated to the other compounds. Table 8 shows the HSQC correlations for some representative compounds, whereas Fig. 1 shows the more important connectivities found in the HMBC spectra.

Heteronuclear single-quantum correlation experiments performed on compounds **1**, **6**, **9** and **11** allow the assignment of

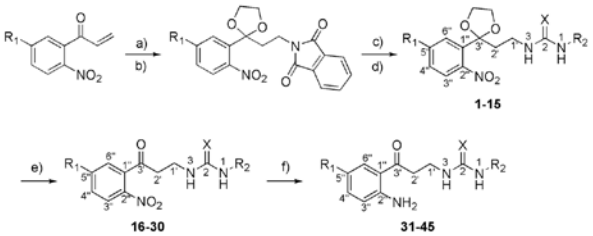

Scheme 1. General synthetic pathway followed in the preparation of final compounds **31–45**. (a) Phthalimide, NaOMe, DMSO; room temperature (RT), 2 h; (b) $(CH_2OH)_2$, *p*-TsOH; toluene, reflux, 10 h; (c) NH_2NH_2, dry EtOH, reflux, 4.5 h; (d) $XCNR_2$, anhyd CH_2Cl_2, RT, overnight; (e) HCl, CH_2Cl_2, RT, 4 h; (f) Fe/$FeSO_4$, H_2O, 95 °C, 3 h.

MRC

Table 3. ^{1}H NMR signal assignments of compounds **16–30**

Compound	H-1	H-3	H-1′	H-2′	H-3″	H-4″	H-5″	H-6″	OCH_3
16	6.51 (bs)	6.51 (bs)	4.05 (m)	3.19 (m)	8.06 (d, 8.1)	7.57 (m)	7.70 (m)	**7.42** (d, 7.5)	—
17	6.42 (bs)	6.42 (bs)	4.03 (t, 5.5)	3.17 (t, 5.5)	8.07 (d, 8.2)	7.59 (m)	7.70 (m)	**7.41** (d, **1.2**, 7.5)	—
18	n.o.	n.o.	4.03 (t, 5.5)	3.19 (t, 5.5)	8.07 (dd, 1.2, 8.2)	7.59 (m)	7.71 (m)	**7.42** (dd, 1.4, 7.5)	—
19[a]	6.96 (bs)	6.91 (bs)	3.90 (m)	3.15 (t, 6.4)	8.13 (d, 9.2)	7.16 (dd, 2.8, 9.2)	—	7.06 (d, 2.8)	3.96 (s)
20[b]	7.50 (bs)	7.37 (bs)	3.71 (m)	3.12 (t, 6.6)	8.17 (d, 9.1)	7.21 (dd, 2.7, 9.1)	—	7.15 (d, 2.7)	3.92 (s)
21	6.34 (bs)	6.11 (bs)	4.05 (m)	3.10 (t, 5.5)	8.13 (d, 9.2)	6.98 (dd, 2.7, 9.2)	—	6.74 (d, 2.7)	3.90 (s)
22	n.o.	n.o.	4.07 (5.3)	3.17 (t, 5.3)	8.07 (d, 8.8)	7.56 (dd, 2.2, 8.8)	—	7.36 (d, 2.2)	—
23	n.o.	n.o.	4.04 (t, 5.4)	3.18 (t, 5.4)	8.07 (d, 8.8)	7.56 (dd, 2.2, 8.8)	—	7.38 (d, 2.2)	—
24	n.o.	n.o.	4.04 (t, 5.5)	3.18 (t, 5.5)	8.06 (d, 8.8)	7.55 (dd, 2.2, 8.8)	—	7.37 (d, 2.2)	—
25	n.o.	n.o.	3.62 (t, 5.6)	**3.03** (t, 5.6)	8.07 (d, 8.2)	7.58 (m)	7.70 (m)	7.40 (dd, 1.4, 7.5)	—
26[c]	n.o.	n.o.	3.58 (m)	3.37 (m)	8.17 (dd, 1.2, 8.1)	7.75 (m)	7.86 (m)	7.64 (dd, 1.4, 7.5)	—
27	n.o.	n.o.	3.65 (t, 5.6)	**2.99** (t, 5.6)	8.13 (d, 9.2)	6.98 (dd, 2.7, 9.2)	—	6.75 (d, 2.7)	3.90 (s)
28	5.02 (bs)	4.46 (bs)	3.53 (t, 6.2)	**3.00** (t, 6.2)	8.17 (d, 9.2)	7.14 (dd, 2.7, 9.2)	—	6.97 (d, 2.7)	3.94 (s)
29	4.87 (bs)	4.87 (bs)	3.64 (t, 5.6)	**3.04** (t, 5.6)	8.06 (d, 8.8)	7.54 (dd, 2.2, 8.8)	—	7.36 (d, 2.2)	—
30	4.67 (bs)	4.67 (bs)	3.64 (t, 5.6)	**3.04** (t, 5.6)	8.06 (d, 8.8)	7.54 (dd, 2.2, 8.8)	—	7.35 (d, 2.2)	—

[a]Solvent used $(CD_3)_2CO$.
[b]Solvent used $(CD_3)_2SO$.
[c]Solvent used CD_3OD.
Chemical shifts (in $CDCl_3$) are reported in δ (in ppm) relative to $CDCl_3$ multiplicities and coupling constants (Hz) are given in parentheses.
^{1}H signals for the R_2 substituent: **16**, CH_3: 2.96 (s); **17**, CH_2CH_3: 3.35 (q, 7.1), 1.20 (t, 7.1); **18**, $CH_2CH_2CH_3$: 3.27 (t, 7.0), 1.61 (m), 0.95 (t, 7.4); **19**, CH_3: 2.92 (d, 4.7); **20**, CH_2CH_3: 3.31 (m), 1.05 (t, 7.2); **21**, $CH_2CH_2CH_3$: 3.27 (m), 1.61 (m), 0.95 (t, 7.4); **22**, CH_3: 2.96 (s); **23**, CH_2CH_3: 3.36 (m), 1.26 (t, 7.3); **24**, $CH_2CH_2CH_3$: 3.27 (t, 7.0), 1.63 (m), 0.96 (t, 7.4); **25**, CH_2CH_3: 3.17 (q, 7.2), 1.10 (t, 7.2); **26**, $CH_2CH_2CH_3$: 3.11 (t, 7.1), 1.54 (m), 0.99 (t, 7.4); **27**, CH_2CH_3: 3.21 (q, 7.2), 1.14 (t, 7.2); **28**, $CH_2CH_2CH_3$: 3.06 (t, 7.0), 1.49 (m), 0.90 (d, 7.5); **29** CH_2CH_3: 3.20 (q, 7.2), 1.14 (t, 7.2); **30**, $CH_2CH_2CH_3$: 3.12 (t, 7.0), 1.52 (m), 0.93 (t, 7.4).
n.o., not observable; s, singlet; bs, broad singlet; d, doublet; dd, doublet doublet; t, triplet; q, quadruplet; m, multiplet.

Table 4. ^{1}H NMR signal assignments of compounds **31–45**

Compound	H-1	H-3	H-1′	H-2′	H-3″	H-4″	H-5″	H-6″	$-NH_2$	OCH_3
31	6.51 (bs)	6.30 (bs)	4.01 (m)	3.35 (t, 5.5)	6.70 (m)	7.31 (m)	6.67 (m)	7.73 (dd, 1.5, 8.4)	5.30 (bs)	—
32	6.48 (bs)	6.18 (bs)	3.96 (m)	3.30 (m)	6.62 (m)	7.25 (m)	6.62 (m)	7.67 (dd, 1.2, 8.5)	n.o.	—
33[b]	6.48 (bs)	6.18 (bs)	3.92 (m)	3.33 (t, 6.3)	6.79 (dd, 1.1, 8.4)	7.29 (ddd, 1.4, 7.0, 8.4)	6.65 (ddd, 1.1, 7.0, 8.4)	7.85 (dd, 1.4, 8.4)	n.o.	—
34	6.47 (bs)	6.27 (bs)	3.97 (m)	3.27 (t, 5.5)	6.60 (d, 9.0)	6.95 (dd, 2.9, 9.0)	—	7.12 (d, 2.9)	5.95 (bs)	3.74 (s)
35	6.53 (bs)	6.23 (bs)	3.96 (m)	3.25 (t, 5.5)	6.63 (d, 9.0)	6.95 (dd, 2.9, 9.0)	—	7.11 (d, 2.9)	5.47 (bs)	3.73 (s)
36	6.43 (t, 5.7)	6.14 (bs)	3.97 (m)	3.27 (t, 5.5)	6.61 (d, 9.0)	6.96 (dd, 2.9, 9.0)	—	7.13 (d, 2.9)	5.95 (bs)	3.74 (s)
37[a]	7.40 (bs)	7.40 (bs)	3.62 (m)	3.16 (t, 6.8)	6.76 (d, 9.0)	7.24 (dd, 2.4, 9.0)	—	7.75 (d, 2.4)	n.o.	—
38	n.o.	n.o.	3.96 (t, 5.2)	3.27 (t, 5.2)	6.63 (d, 9.0)	7.21 (d, 9.0)	—	7.65 (s)	n.o.	—
39	5.95 (bs)	5.95 (bs)	3.99 (t, 5.5)	3.26 (m)	6.69 (d, 8.8)	7.23 (dd, 2.3, 8.8)	—	7.67 (d, 2.3)	5.95 (bs)	—
40	4.77 (bs)	4.77 (bs)	3.57 (t, 5.5)	3.15 (m)	6.62 (m)	7.24 (ddd, 1.3, 7.1, 8.4)	6.62 (m)	7.69 (dd, 1.3, 8.4)	4.77 (bs)	—
41	5.51 (bs)	5.51 (bs)	3.56 (t, 5.6)	3.15 (t, 5.6)	6.64 (m)	7.24 (ddd, 1.5, 6.9, 7.9)	6.64 (m)	7.67 (dd, 1.5, 8.4)	5.51 (bs)	—
42	5.21 (bs)	5.21 (bs)	3.57 (t, 5.5)	3.14 (m)	6.73 (d, 9.0)	6.95 (dd, 2.8, 9.0)	—	7.16 (d, 2.9)	5.21 (bs)	3.74 (s)
43	5.02 (bs)	4.46 (bs)	3.57 (m)	3.14 (t, 5.7)	6.60 (d, 8.9)	6.94 (dd, 2.8, 8.9)	—	7.14 (d, 2.8)	5.95 (bs)	3.74 (s)
44	4.59 (bs)	4.59 (bs)	3.58 (t, 5.2)	3.17 (m)	6.60 (d, 8.8)	7.19 (dd, 2.2, 8.8)	—	7.63 (d, 2.2)	4.59 (bs)	—
45	5.18 (bs)	5.18 (bs)	3.58 (t, 5.6)	3.14 (t, 5.6)	6.62 (d, 8.8)	7.19 (dd, 2.4, 8.8)	—	7.62 (d, 2.4)	5.18 (bs)	—

[a]Solvent used $(CD_3)_2SO$.
[b]Solvent used CD_3OD.
Chemical shifts (in $CDCl_3$) are reported in δ (in ppm) relative to $CDCl_3$; multiplicities and coupling constants (**Hz**) are given in parentheses.
^{1}H signals for the R_2 substituent: **31**, CH_2: 2.90 (s); **32**, CH_2CH_2: 3.30 (m), 1.18 (t, 7.2); **33**, $CH_2CH_2CH_2$: 3.37 (m), 1.63 (m), 0.99 (t, 7.4); **34**, CH_2: 2.09 (d, 4.9); **35**, CH_2CH_2: 3.33 (m), 1.17 (t, 7.2); **36**, $CH_2CH_2CH_2$: 3.21 (m), 1.57 (m), 0.92 (t, 7.4); **37**, CH_2: 2.76 (s); **38**, CH_2CH_2: 3.33 (m), 1.19 (t, 7.2); **39**, $CH_2CH_2CH_2$: 3.26 (m), 1.58 (m), 0.96 (t, 7.4); **40**, CH_2CH_2: 3.16 (m), 1.09 (t, 7.2); **41**, $CH_2CH_2CH_2$: 3.06 (t, 7.1), 1.45 (m), 0.86 (t, 7.4); **42**, CH_2CH_2: 3.14 (m), 1.06 (t, 7.2); **43**, $CH_2CH_2CH_2$: 3.07 (q, 6.8), 1.46 (m), 0.87 (t, 7.4); **44** CH_2CH_2: 3.17 (m), 1.10 (t, 7.2); **45**, $CH_2CH_2CH_2$: 3.09 (t, 7.2), 1.50 (m), 0.91 (t, 7.4).
n.o., not observable; s, singlet; bs, broad singlet; d, doublet; dd, doublet doublet; ddd, doublet, doublet doublet; t, triplet; q, quadruplet; m, multiplet.

Table 5. ^{13}C NMR chemical shifts of compounds **1–15**

Compound	C-2	C-1′	C-2′	C-3′	C-1″	C-2″	C-3″	C-4″	C-5″	C-6″	2xC_{diox}	OCH_3
1	180.82	40.04	38.06	109.28	134.66	149.51	131.61	129.82	123.48	128.38	65.04	
2	180.92	40.09	38.18	109.46	134.79	149.64	131.70	129.93	123.59	128.48	65.14	—
3	180.39	39.96	37.98	109.23	134.56	149.46	131.47	129.72	123.37	128.29	64.93	—
4	182.19	40.35	37.97	109.54	137.65	143.01	126.24	114.28	161.94	113.38	65.14	56.17
5	181.98	40.31	37.95	109.43	137.42	143.14	126.22	114.29	161.72	113.33	65.12	56.14
6	181.34	40.28	37.94	109.54	137.61	143.05	126.19	114.27	161.92	113.38	65.13	56.16
7	181.66	40.06	38.12	109.06	137.21	147.85	125.18	130.00	137.91	128.59	65.33	—
8	180.68	39.98	38.09	109.06	137.18	147.86	125.16	129.99	137.90	128.59	65.32	—
9	180.79	40.07	38.10	109.07	137.18	147.88	125.16	130.00	137.89	128.59	65.33	—
10	158.50	35.66	39.37	109.51	135.15	149.66	131.47	129.68	123.38	128.63	65.07	—
11	158.54	35.59	39.04	109.24	135.07	149.46	131.29	129.52	123.20	128.42	64.88	—
12	158.57	35.59	39.01	109.45	137.62	144.92	125.74	114.08	161.42	113.21	64.83	55.62
13	158.40	35.57	39.01	109.46	137.79	142.97	125.76	114.00	161.58	113.26	64.91	55.94
14	158.77	35.43	42.39	108.93	137.20	147.69	124.70	129.43	137.30	128.41	64.87	—
15	158.78	35.25	42.39	108.89	137.26	147.61	124.66	129.48	137.35	128.44	64.97	—

δ (in ppm) relative to $CDCl_3$. ^{13}C signals for the R_2 substituent: **1**, CH_3: 32.81; 30.29; **2**, CH_2CH_3: 38.18, 14.28; **3**, $CH_2CH_2CH_3$: 45.60, 22.16, 11.44; **4**, CH_3: 30.50; **5**, CH_2CH_3: 42.25, 22.65; **6**, $CH_2CH_2CH_3$: 45.78, 22.39, 11.63; **7**, CH_3: 30.47; **8**, CH_2CH_3:38.80, 14.26; **9**, $CH_2CH_2CH_3$: 45.80, 22.37, 11.66; **10**, CH_2CH_3: 35.66, 15.64; **11**, $CH_2CH_2CH_3$: 42.56, 23.26, 11.36; **12**, CH_2CH_3: 41.79, 15.47; **13**, $CH_2CH_2CH_3$: 42.49, 23.50, 11.44; **14** CH_2CH_3: 35.35, 15.31; **15**, $CH_2CH_2CH_3$: 39.02, 23.34, 11.31.

Table 6. ^{13}C NMR chemical shifts of compounds **16–30**

Compound	C-2	C-1′	C-2′	C-3′	C-1″	C-2″	C-3″	C-4″	C-5″	C-6″	OCH_3
16	181.50	39.50	42.50	202.54	137.20	145.76	124.50	131.09	134.50	127.30	—
17	181.54	39.71	42.51	202.64	137.23	145.91	124.81	131.19	134.61	127.45	—
18	180.70	39.51	42.30	202.38	137.01	145.73	124.60	130.99	134.39	127.27	—
19[a]	184.29	39.44	42.36	201.28	138.56	140.82	127.21	115.60	164.71	112.51	56.36
20[b]	182.37	39.41	42.63	201.95	138.43	140.64	127.86	116.31	164.70	113.20	57.31
21	181.83	39.86	42.73	202.74	138.26	140.44	127.50	115.49	164.75	112.06	56.63
22	181.76	39.70	42.64	201.09	138.87	143.95	126.35	131.07	141.70	127.51	—
23	181.43	39.64	42.64	201.15	138.86	143.96	126.34	131.07	141.68	127.53	—
24	181.60	39.66	42.65	201.16	138.87	143.96	126.32	131.06	141.66	127.54	—
25	158.53	35.64	43.43	202.55	137.58	145.92	124.74	130.99	134.53	127.50	—
26[c]	160.00	34.82	41.66	202.03	137.25	146.22	124.29	131.01	134.21	127.64	—
27	158.73	35.54	43.47	202.55	138.18	140.59	127.43	115.43	164.72	112.04	56.61
28	160.01	34.94	43.09	202.23	138.31	140.68	126.99	115.04	164.82	112.31	55.85
29	159.95	36.65	44.52	202.02	140.24	145.07	127.42	132.11	142.80	128.75	—
30	158.99	35.58	43.35	200.91	139.03	143.92	126.30	131.00	141.69	127.58	—

[a]Solvent used $(CD_3)_2CO$.
[b]Solvent used $(CD_3)_2SO$.
[c]Solvent used CD_3OD.
δ (in ppm) relative to $CDCl_3$. ^{13}C signals for the R_2 substituent: **16**, CH_3: 32.80; **17**, CH_2CH_3: 38.75, 14.22; **18**, $CH_2CH_2CH_3$: 45.62, 22.13, 11.43; **19**, CH_3: 30.20; **20**, CH_2CH_3: 38.93, 15.09; **21**, $CH_2CH_2CH_3$: 45.68, 22.32, 11.64; **22**, CH_3: 29.93; **23**, CH_2CH_3:38.73, 14.21; **24**, $CH_2CH_2CH_3$: 45.75, 22.33, 11.65; **25**, CH_2CH_3: 35.35, 15.61; **26**, $CH_2CH_2CH_3$: 34.86, 23.27, 10.46; **27**, CH_2CH_3: 35.88, 15.35; **28**, $CH_2CH_2CH_3$: 41.68, 23.27, 10.46; **29** CH_2CH_3: 37.07, 16.52; **30**, $CH_2CH_2CH_3$: 42.92, 23.27, 11.53.

the secondary carbon atoms C-1′ and C-2′ chemical shifts, and the tertiary carbon atoms C-3″, C-4″, C-5″ and C-6″ chemical shifts in the dioxolane derivatives **1–15**. These atoms show signals in ranges of 35.25–40.35 (C-1′), 37.94–42.39 (C-2′), 124.66-131.70 (C-3″), 114.00–130.00 (C-4″), 123.20–161.94 (C-5″) and 113.21–128.63 (C-6″).

Similar HSQC experiments performed on compounds **18**, **21**, **23**, **27** and **30** indicate that the ^{13}C NMR signals for the analogue secondary and tertiary carbon atoms in the intermediate nitrophenyl derivatives **16–30** are in the following ranges: 34.82–39.86 (C-1′), 41.66–44.52 (C-2′), 124.29–127.86 (C-3″), 115.04–132.11 (C-4″), 134.21–164.82 (C-5″) and 112.04–128.75 (C-6″).

In the same way, HSQC experiments performed on compounds **32**, **35**, **39**, **41**, **43** and **45** confirm that the peaks corresponding to the analogue secondary and tertiary carbon atoms in the final aminophenyl derivatives **31–45** appear around 35.54–41.11 (C-1′), 38.47–39.93 (C-2′), 117.38–120.05 (C-3″), 123.54–135.68 (C-4″), 116.13–151.54 (C-5″) and 113.23–132.57 (C-6″).

To confirm the signals corresponding to quaternary carbons, HMBC spectra on the intermediate (**1**, **6**, **11**, **18**, **21** and **30**) and final

Table 7. ^{13}C NMR chemical shifts of compounds **31–45**

Compound	C-2	C-1′	C-2′	C-3′	C-1″	C-2″	C-3″	C-4″	C-5″	C-6″	OCH_3
31	182.21	40.06	38.47	201.92	117.62	150.38	117.47	134.97	116.26	131.22	—
32	181.34	40.19	38.70	202.14	117.77	150.60	117.65	135.16	116.42	131.43	—
33[b]	182.86	41.11	39.76	202.76	118.77	152.83	118.48	135.68	116.42	132.57	
34	182.41	40.31	38.87	201.61	117.51	145.44	119.13	124.60	150.51	113.24	56.30
35	181.36	40.18	38.93	201.69	117.89	144.74	119.39	124.44	150.74	113.30	56.29
36	181.56	40.29	38.89	201.67	117.51	145.45	119.13	124.61	150.52	113.23	56.30
37[a]	181.43	39.99	38.82	200.61	117.76	150.52	119.67	134.73	121.65	130.84	—
38	181.40	40.01	38.78	201.23	118.59	148.55	119.31	135.13	121.13	130.50	—
39	181.52	40.00	38.85	201.24	119.03	147.84	119.62	135.11	121.65	130.52	—
40	158.82	35.54	39.41	201.96	117.91	150.16	117.38	134.61	116.13	131.20	—
41	158.85	35.88	39.71	202.16	118.48	149.87	117.94	134.88	116.79	131.43	—
42	158.57	35.64	39.93	201.91	119.33	142.75	120.05	123.54	151.54	113.83	56.24
43	158.49	35.73	39.81	201.76	117.90	145.29	119.04	124.13	150.48	113.47	56.25
44	158.62	35.80	39.59	201.15	118.59	148.82	119.19	134.98	120.83	130.49	—
45	158.88	35.86	39.56	201.06	118.63	148.70	119.28	134.99	120.93	130.45	—

[a]Solvent used $(CD_3)_2SO$.
[b]Solvent used CD_3OD.
δ (in ppm) relative to $CDCl_3$. ^{13}C signals for the R_2 substituent: **31**, CH_3: 30.25; **32**, CH_2CH_3: 38.70, 14.23; **33**, $CH_2CH_2CH_3$: 39.76, 23.55, 11.66; **34**, CH_3: 30.42; **35**, CH_2CH_3: 38.93, 14.23; **36**, $CH_2CH_2CH_3$: 45.74, 22.32, 11.66; **37**, CH_3: 31.12; **38**, CH_2CH_3:38.78, 14.22; **39**, $CH_2CH_2CH_3$: 45.82, 22.35, 11.67; **40**, CH_2CH_3: 35.35, 15.38; **41**, $CH_2CH_2CH_3$: 42.62, 23.56, 11.59; **42**, CH_2CH_3: 35.55, 15.63; **43**, $CH_2CH_2CH_3$: 42.63, 23.61, 11.58; **44** CH_2CH_3: 35.82, 15.49; **45**, $CH_2CH_2CH_3$: 42.80, 23.42, 11.57.

Table 8. HSQC correlations found for compounds **1**, **6**, **9**, **11**, **18**, **21**, **23**, **27**, **30**, **33**, **35**, **39**, **41**, **43** and **45**

$^1H/^{13}C$	Compound														
	1	**6**	**9**	**11**	**18**	**21**	**23**	**27**	**30**	**32**	**35**	**39**	**41**	**43**	**45**
H-1′	3.67	3.68	3.70	3.37	4.03	4.05	4.04	3.65	3.64	3.96	3.96	3.99	3.56	3.57	3.58
C-1′	40.04	40.28	40.07	35.50	39.51	39.86	39.64	35.54	35.58	40.19	40.18	40.00	35.88	35.73	35.86
H-2′	2.48	2.52	2.48	2.37	3.19	3.10	3.18	2.99	3.04	3.30	3.25	3.26	3.15	3.14	3.14
C-2′	38.06	37.94	38.10	39.04	42.30	42.72	42.64	43.47	43.35	38.70	38.93	38.85	39.71	39.81	39.56
H-3″	7.51	7.48	7.40	7.49	8.07	8.13	8.07	8.13	8.06	6.62	6.63	6.69	6.64	6.60	6.62
C-3″	131.61	126.19	125.16	131.29	124.60	127.50	126.34	127.43	126.30	117.65	119.39	119.62	117.44	119.04	119.28
H-4″	7.43	6.85	7.40	7.40	7.59	6.98	7.56	6.98	7.54	7.25	6.95	7.23	7.24	6.94	7.19
C-4″	129.82	114.27	130.00	129.52	130.99	115.49	131.07	115.43	131.00	135.16	124.44	135.11	134.88	124.13	134.99
H-5″	7.43			7.40	7.71					6.62			6.64		
C-5″	123.48			123.20	134.39					116.42			116.79		
H-6″	7.79	7.06	7.58	7.58	7.42	6.74	7.38	6,75	7.35	7.67	7.11	7.67	7.67	7.14	7.62
C-6″	128.38	113.38	128.59	128.42	127.27	112.06	127.53	112.04	127.58	131.43	113.30	130.52	131.43	113.47	130.45

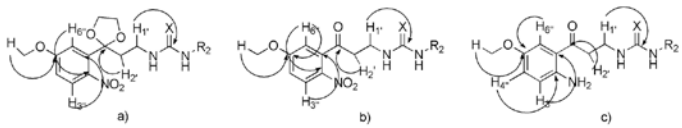

Figure 1. Important connectivities found in the HMBC spectra of compounds (a) **1–15**, (b) **16–30** and (c) **31–45**.

(**35**, **39**, **41** and **45**) compounds were recorded (Fig. 1). Correlations in compound **1** between H-6″ (δ 7.59 ppm) and the ^{13}C signal at 149.51 ppm, H-3″ (δ 7.51 ppm) and the ^{13}C signal at 134.66 ppm and H-2″ (δ 2.48 ppm) and the ^{13}C signal at 109.28 ppm allow the unequivocal assignment of C-2″, C-1″ and C-3′, respectively. In addition, compound **6** HMBC analysis indicates a correlation between OCH_3 (δ 3.85) and the ^{13}C signal at 161.92 ppm, which can be attributed to C-5″. Also, correlation between H-1′ (δ 3.37) in compound **11** and the peak at 158.54 ppm shows that this signal corresponds to C-2.

Heteronuclear multiple-bond correlation experiment performed on compound **18** indicates that the signal at δ 8.07 (H-3″) is correlated with the ^{13}C signal at 137.01 ppm, which can be assigned to C-1″, whereas H-6″ signal (δ 7.42) is correlated with the ^{13}C signal

at 145.73 ppm; accordingly, this signal corresponds to C-2". Furthermore, a correlation between H-1' signal (δ 4.03) and ^{13}C signal at 180.70 ppm has been observed, and this signal can be designated as C-2 of thiourea. Finally, H-2' (δ 3.19) is correlated with a signal at δ 202.38 that can be assigned to C-3'. In addition, similar experiment of compound **21** indicates a correlation between the OCH_3 (δ 3.90) and the ^{13}C signal at 164.75 ppm that is identified as C-5". Lastly, HMBC experiment on the urea **30** demonstrates that H-6" signal (δ 7.35) is correlated with the ^{13}C signal at 141.69 ppm, and this signal corresponds to C-5", whereas correlation between H-1' (δ 3,64) and a signal at 158.99 ppm indicates that this signal corresponds to C-2 of urea.

Heteronuclear multiple-bond correlation spectrum of compound **35** denotes that H-3" (δ 6.63) and OCH_3 (δ 3.73) are correlated with the ^{13}C signals at 117.89 and 150.74 ppm, which are assigned to C-1" and C-5", respectively. In compound **39**, the signal of ^{13}C at 147.84 ppm can be assigned to C-2" because of its correlation with H-4" (δ 7.23), whereas H-1' (δ 3.99) is correlated with the ^{13}C signal at 182.52 ppm, and consequently, this peak is identified as C-2 of the thiourea. Also, H-2' of the urea **41** (δ 3.15) is correlated with a ^{13}C signal at 202.16 that is assigned to C-3'. Finally, in compound **45,** the H-6" (δ 7.62) and H-1' (δ 3.58) are correlated with the ^{13}C signals at 120.93 and 158.88 ppm that are designed to C-5" and C-2 of the urea, respectively.

These compounds have been designed from a series of *N*-(3-(2-amino-5-substitutedphenyl)-3-oxopropyl)alkylamide derivatives previously synthesized by our research group,[15] by substitution of the main chain alkylamide for an alkylurea or alkylthiourea ones. The main differences between the ^{13}C chemical shifts of the previously kynurenamine derivatives[15] and the new kynurenamine-ureas and thioureas are the ^{13}C signals of the main chain (C-1 atom of the amides and the equivalent C-2 atom of the ureas or thioureas). The amide C-1 atom shows signals in a range of 167.4–176.4, whereas for the equivalent urea C-2 atom, the signals appear in a range of 158.5–160.0, and for the thiourea C-2 atom, the range is 180.7–184.3 ppm, according to similar compounds described in literature.[16,17]

Nuclear Overhauser spectroscopy experiments performed on compound **39** (R_1 = Cl, R_2 = Pr, X = S) (Fig. 2) demonstrate a correlation between H-6" and H-2' and vice versa, which proves that they have close distance in space. These NOE effects are possible if the molecule adopts a conformation where there is an intramolecular hydrogen bond between the carbonyl group of the linear chain and the amino group in 2"-position of the aromatic ring.

To explore the conformational behavior of this molecule in solution, we performed an unrestricted MD simulation (100 ns) of compound **39** in similar conditions to those where NOESY spectra were recorded (box of $CHCl_3$ molecules and 300 K) (Fig. 3(a)). In the three calculated conformational clusters of **39** along the MD simulation, a permanent intramolecular hydrogen bond between the carbonyl oxygen and the amino group of the phenyl ring is observed. In this regard, the distance between $\underline{NH}_2$ and $\underline{O}$=C remains under 2.8 Å along the MD simulation (Fig. 3(b)). As a consequence, hydrogen atoms H-2' and H-6" are close in space (2.0–2.5 Å), which is in line with the experimental NOEs. Finally, the major differences between the three groups of conformers are due to the

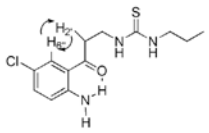

Figure 2. Selected NOESY correlations for compound **39**.

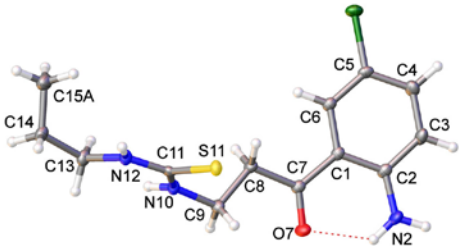

Figure 4. Asymmetric unit in the crystal of compound **39**. Only one of the disordered positions of the propyl group is depicted for clarity.

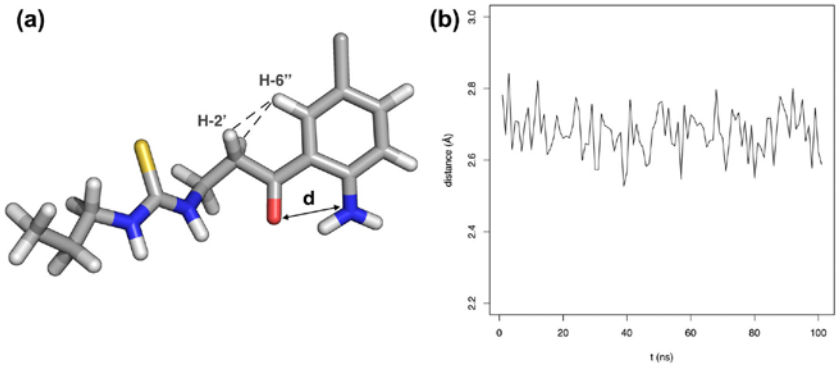

Figure 3. Molecular dynamics (MD) simulation of **39** in a box of $CHCl_3$ molecules. (a) Representative structure of the major conformer of **39** and (b) distance evolution between carbonyl oxygen and the amino group calculated along the 100-ns MD simulation. Spatial proximity of H-2" and H-6" atoms is indicated as dotted lines.

relative orientation of the thiourea side chain to the ring due to the rotation of C2–C1 bonds in the chain.

Derivative **39** has been crystallized with the object of confirming the preferred conformation of these molecules in solid state, and its 3D structure has been determined using X-ray diffraction. This compound crystallizes in the triclinic system, space group P-1. The asymmetric unit consists of one molecule (Fig. 4) where the mean planes of the aromatic ring and the thiourea moiety defines a dihedral angle of 75.44°. In this conformation, one intramolecular H-bond is observed involving aromatic-NH_2 and CO groups (N–H···O: 2.683 A 129.0°). The propyl group is disordered over two alternative positions, with site-occupancy factors 0.52:0.48. In the crystal lattice, pairs of adjacent molecules are symmetrically connected by intermolecular H-bonds that involve aromatic-NH_2 and CO groups (N–H···O: 3.184 A 154.0°). The aforementioned pairs of molecules are further associated by additional intermolecular H-bonding interactions where aromatic Cl and thiourea groups are involved, building a 3D H-bonded network.

Acknowledgement

This work was partially supported by the Instituto de Salud Carlos III through the grant FI11/00432.

References

[1] W. K. Alderton, C. E. Cooper, R. G. Knowles. *Biochem. J.* **2001**, *357*, 593–615.
[2] G. M. Rosen, P. Tsai. *S. Pou. Chem. Rev.* **2002**, *102*, 1191–1199.
[3] L. Zhou, D. Y. Zhu. *Nitric Oxide* **2009**, *20*, 223–230.
[4] D. M. Wilcock, M. R. Lewis, W. E. Van Nostrand, J. Davis, M. L. Previti, N. Gharkholonarehe, M. P. Vitek, C. A. Colton. *J. Neurosci.* **2008**, *28*, 1537–1545.
[5] V. Calabrese, C. Mancuso, M. Calvani, E. Rizzarelli, D. A. Butterfield, A. M. Stella. *Nat. Rev. Neurosci.* **2007**, *8*, 766–775.
[6] A. W. Deckel. *J. Neurosci. Res.* **2001**, *64*, 99–107.
[7] K. D. Kroncke, K. Fehsel, V. Kolb-Bachofen. *Clin. Exp. Immunol.* **1998**, *113*, 147–146.
[8] M. Lechner, P. Lirk, J. Rieder. *Semin Cancer Biol* **2005**, *15*, 277–89.
[9] R. Zamora, Y. Vodovotz, T. R. Billiar. *Mol. Med.* **2000**, *6*, 347–373.
[10] M. Chayah, M. D. Carrión, M. A. Gallo, R. Jiménez, J. Duarte, M. E. Camacho. *ChemMedChem* **2015**, *10*, 874–882.
[11] D. A. Case, T. A. Darden, T. E. Cheatham III, C. L. Simmerling, J. Wang, R. E. Duke, R. Luo, R. C. Walker, W. Zhang, K. M. Merz, B. Roberts, S. Hayik, A. Roitberg, G. Seabra, J. Swails, A. W. Goetz, I. Kolossvai, K. F. Wong, F. Paesani, J. Vanicek, R. M. Wolf, J. Liu, X. Wu, S. R. Brozell, T. Steinbrecher, H. Gohlke, Q. Cai, X. Ye, J. Wang, M. J. Hsieh, G. Cui, D. R. Roe, D. H. Mathews, M. G. Seetin, R. Salomon-Ferrer, C. Sagui, V. Babin, T. Luchko, S. Gusarov, A. Kovalenko, P. A. Kollman, *AMBER 12*, University of California, San Francisco, **2012**.
[12] APEX2 Software, v2014.11. Bruker AXS Inc., Madison, Wisconsin, USA **2014**.
[13] G. M. Sheldrick, *SADABS, Program for Empirical Absorption Correction of Area Detector Data*, University of Göttingen, Göttingen, **2012**.
[14] G. Sheldrick. *Acta Crystallogr.* **2008**, *A64*, 112–122.
[15] A. Entrena, M. E. Camacho, M. D. Carrión, L. C. López-Cara, G. Velasco, J. León, G. Escames, D. Acuña-Castroviejo, V. Tapias, M. A. Gallo, A. Vivó, A. Espinosa. *J. Med. Chem.* **2005**, *48*, 8174–8188.
[16] G. Heinisch, P. Lukavsky, B. Matuszczak, D. Rakowitz. *Magn. Reson. Chem.* **1997**, *35*, 653–655.
[17] A. R. Katritzky, S. Sobiak, C. M. Marson. *Magn. Reson. Chem.* **1988**, *26*, 665–670.

3.4 Artículo 4

N,N'-disubstituted thiourea and urea derivatives: Design, synthesis, docking studies and biological evaluation against nitric oxide synthase

***MedChemComm* (submitted)**

Mariem Chayah[a], M. Encarnación Camacho[a]*, M. Dora Carrión[a]*, Miguel A. Gallo[a], Miguel Romero[b], Juan Duarte[b].

[a]Departamento de Química Farmacéutica y Orgánica, Facultad de Farmacia, Universidad de Granada (Spain).

[b]Departamento de Farmacología, Facultad de Farmacia, Universidad de Granada (Spain).

*Correspondig authors: Dr. M. Encarnación Camacho. Tel.: +34-958-243844; E-mail: ecamacho@ugr.es and Dr. M. Dora Carrión. Tel.: +34-958-240728; E-mail: dcarrion@ugr.es

Abstract

The synthesis and biological evaluation of a new type of *N,N'*-disubstituted thiourea and urea derivatives as inhibitors of both neuronal and inducible nitric oxide synthase (nNOS and iNOS) are described. These compounds have been designed by reduction of the carbonyl group in the thiourea and urea kynurenamine derivatives **3** previously synthesized by our research group. The synthetic route performed to this new family also allows us to obtain the molecules **3** with less synthetic steps and higher global yield. Regarding the biological results, in general, the new derivatives **4** inhibit better the neuronal NOS isoform than the inducible one. Furthermore, thioureas exhibit higher inhibition than ureas for both isoenzymes. Among all the tested compounds, **4g** shows significant nNOS (80.6%) and iNOS (76.6%) inhibition values without inhibiting eNOS. This molecule could be an interesting starting point for the design of new inhibitors with application in neurological disorders where both isoenzymes are implicated such as Parkinson.

Introduction

Nitric oxide synthase (NOS) is a family of isoenzymes that converts *L*-arginine to *L*-citrulline with nitric oxide (NO) release. There are three human NOS isoforms: endothelial NOS (eNOS) which regulates blood pressure and flow, inducible NOS (iNOS) involved in immune response, and neuronal NOS (nNOS) essential for neurotransmission.[1] Nonetheless, several studies demonstrated the implication of NOS in many neurodegenerative,[2-7] chronic inflammatory[8,9] and cardiovascular[10,11] diseases. Indeed, NO overproduction, by nNOS or iNOS, leads to cellular and tissue damage through nitrosative and oxidative stress.[12-16] The underproduction of NO by eNOS can affect the vascular tone and blood flow controls and cause hypertension. Therefore the inhibition of nNOS and iNOS but not eNOS is a viable therapeutic strategy to treat and prevent disorders and pathologies as previously mentioned.

A comparison of the NOSs structures reveals a huge similarity especially in their substrate binding sites.[17] This fact represents a real challenge in designing selective NOS inhibitors.

In previous efforts to find selective and potent i/nNOS inhibitors, our research group has synthesized and published several families of compounds. Figure 1 shows some of them with analogous structures: the kynurenine **1**,[18] kynurenamine **2**,[19] and kynurenamine-urea and thiourea **3**[20] derivatives. These last ones have mostly better inhibition results versus iNOS. Docking and molecular dynamic studies demonstrated the urea group implication especially in the selectivity process. Also both, the aromatic ring and the amine group, interact with the enzyme through π-cation interaction and hydrogen bonds, respectively. However, any clear role was observed for the carbonyl group. Therefore we decided to act at this point, changing this hydrogen bond acceptor residue by another donor such as hydroxyl.

This way, herein we present a new series of compounds **4** where the carbonyl group, present in the three families of the above derivatives, has been replaced by a hydroxyl one, waiting increased interaction with the enzyme and improved inhibition. This change involved the development of a new synthetic pathway. Subsequent biological assays and docking studies were performed in this new family of compounds to evaluate the results.

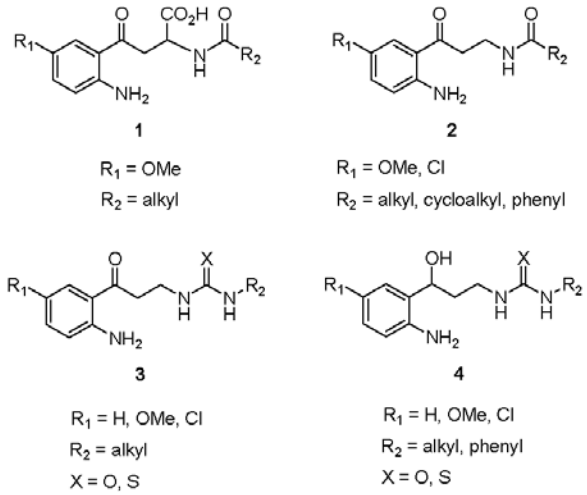

Figure 1. Some kynurenamine derivatives as NOS inhibitors synthesized by our research group.

Results and discussion

Chemistry

The general synthetic pathway of all the final compounds **4a-q** is represented in Scheme 1. 5-Methoxy-2-nitrobenzaldehyde **5b** (synthesized from 5-hydroxy-2-nitrobenzaldehyde by reaction with MeI in the presence of K_2CO_3/THF),[21] the commercially available 2-nitrobenzaldehyde **5a** and 5-chloro-2-nitrobenzaldehyde **5c** were transformed into the β-hydroxynitriles **6a-c** by treatment with BuLi and acetonitrile in dry THF[22] (70-90% yield). The nitrile group of these last intermediates was reduced selectively with borane in THF[23] to give the 3-amino-1-(2-nitrophenyl)propan-1-ol derivatives **7a-c**. Nucleophilic addition of either alkyl isothiocyanate or alkyl isocyanate *in situ*, using microwave (MW) technique, gives the intermediates **8a-q** with good yields (70-85%). The introduction of an urea or thiourea moiety in kynurenamine derivatives has been described using MW assisted synthesis, shortening the reaction time from 18

h[20,24] to 20 min. Finally, reduction of the phenyl nitro group, with Pd/C in the flow hydrogenator, results in the final derivatives **4a-q** (75-91% yield).

On the other hand, this new synthetic route is useful to obtain urea and thiourea kynurenamines **3**. Thereby, as an example, we have carried out the oxidation of the hydroxyl group to a carbonyl one in the derivative **8o** (R_1 = Cl, R_2 = Et, X = O), using the Jones reagent followed by the nitro reduction to amino group[20] (Scheme 1). This alternative synthesis improves the previously described one[20] by shortening the synthetic route (from 8 to 5 steps) and doubling the global yield.

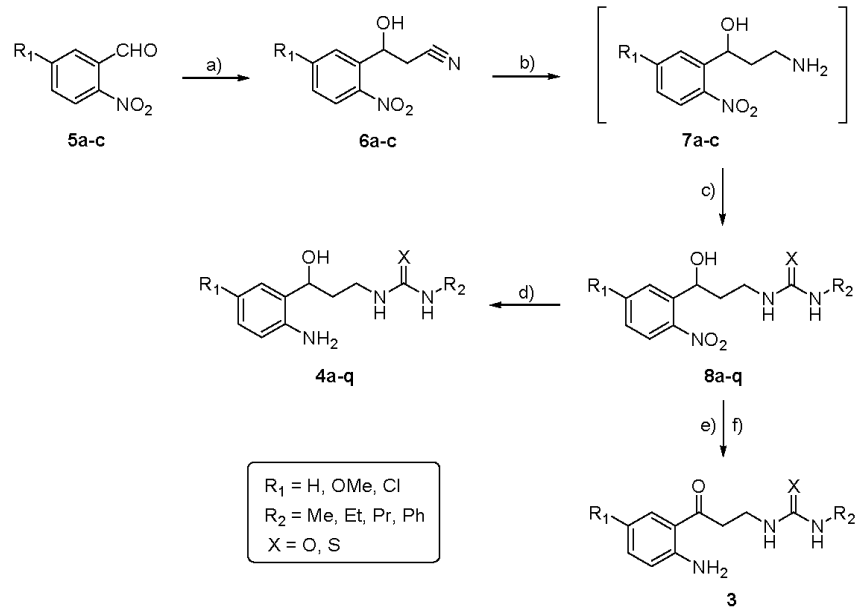

Scheme 1. Synthesis of *N,N'*-disubstituted thiourea and urea derivatives **4a-q**. a) CH_3CN, BuLi, THF, -78ºC, then RT; b) BH_3-THF, 0ºC, then 4h RT; c) $XCNR_2$, CH_2Cl_2, 20 min (MW); d) 10% Pd/C, MeOH (flow hydrogenation), 60ºC, 60 bar; e) CrO_3, CH_3COCH_3, H_2SO_4, 10 min; f) $Fe/FeSO_2$, H_2O, 95ºC, 3h.

Results and discussion

iNOS and nNOS inhibition

Compounds **4a-q** have been evaluated *in vitro* as inhibitors of iNOS and nNOS using recombinant isoenzymes. The assays were made at 1mM concentration of each compound in order to identify the more active and selective derivatives. Besides, IC_{50} values were measured for the most interesting compounds.

Table 1 illustrates the inhibition percentages versus iNOS and nNOS (the kynurenamine derivatives **3a-b**, previously described,[20] was introduced as reference).

Table 1. *In vitro* iNOS and nNOS inhibition (%) observed in the presence of 1 mM concentration of compounds **3a-b** and **4a-q**.

Compound	R_1	R_2	X	% iNOS inhibition[a]	% nNOS inhibition[a]
3a[b]	OMe	Me	S	78.20 ± 2.43	46.04 ± 2.85
3b[b]	Cl	Et	O	78.63 ± 1.34	9.86 ± 3.17
4a	H	Me	S	20.74 ± 1.15	70.17 ± 0.77
4b	H	Et	S	19.36 ± 3.33	44.84 ± 0.02
4c	H	Pr	S	31.10 ± 0.55	51.74 ± 1.35
4d	H	Et	O	18.34 ± 0.43	7.81 ± 3.06
4e	H	Pr	O	19.04 ± 1.45	7.00 ± 0.32
4f	H	Ph	O	27.86 ± 1.15	17.69 ± 1.32
4g	OMe	Me	S	76.55 ± 0.33	80.55 ± 2.29
4h	OMe	Pr	S	25.39 ± 1.71	6.02 ± 1.61
4i	OMe	Et	O	26.64 ± 2.05	43.02 ± 0.48
4j	OMe	Pr	O	14.66 ± 0.19	15.81 ± 1.03
4k	OMe	Ph	O	12.33 ± 1.30	12.10 ± 1.08
4l	Cl	Me	S	22.13 ± 0.28	70.53 ± 4.60
4m	Cl	Et	S	60.42 ± 2.31	70.61 ± 3.54
4n	Cl	Pr	S	54.98 ± 3.21	32.40 ± 2.24
4o	Cl	Et	O	33.85 ± 1.86	15.22 ± 2.33
4p	Cl	Pr	O	19.61 ± 3.04	23.81 ± 1.34
4q	Cl	Ph	O	3.11 ± 2.36	38.62 ± 1.63

[a]Values are the mean ±SEM of the percentage of iNOS and nNOS inhibition produced by 1 mM concentration of each compound. Each value is the mean of three experiments performed by triplicate using recombinant iNOS and nNOS enzymes. [b]**3a-b** were used as reference.[20]

In general, compounds **4a-q** show better values of inhibition versus nNOS than iNOS, since five compounds exhibit good nNOS percentage inhibition (**4g**, 80.6%; **4m**, 70.6%; **4l**, 70.5%, **4a**, 70.2% and **4c**, 51.7%) and only three compounds show good inhibitory activity versus iNOS (**4g**, 76.6%, **4m**, 60.4% and **4n**, 55.0%). Regarding the R_1 radical, no clear structure-activity relationship can be concluded. Independently of the substituent nature (neutral (R_1 = H), electron-donating (R_1 = OCH_3) or electron withdrawing (R_1 = Cl)) different inhibition levels can be observed. It seems that the inhibitory activity depends more on X and R_2. Thus, derivatives with a thiourea residue (X = S) show better inhibition data for both isoenzymes than those bearing urea (X = O). In addition, compounds with methyl substituent in R_2 produce higher inhibition for iNOS as **4g** and for nNOS such as **4a**, **4g** and **4l**. It is noteworthy that compound **4m** shows good inhibition having a R_2 = Et. Finally, **4g** stands out as the best inhibitor of both isoforms.

Furthermore, Table 2 shows the iNOS inhibition values of kynurenamines previously synthesized **2a-l** (not published before), as well as their nNOS values already described[19] in order to compare them with the new *N,N'*-disubstituted thioureas and ureas **4**. These last compounds were designed from the kynurenamines **2**, introducing two structural modifications: replacement of the terminal acyl group by a thiourea or urea one, isosteric to the final guanidine moiety of the NOS substrate (*L*-Arg); and substitution of the carbonyl group with a hydroxyl residue.

The best nNOS inhibitors of derivatives **2a-l** were **2a** (R_1 = OMe, R_2 = Me, 65.4%), and **2b** (R_1 = OMe and R_2 = Et, 50.9%); however, no compounds with relevant iNOS inhibition values was found, so they can be considered as selective inhibitors of nNOS

versus iNOS. Kynurenamine **2a**, the N^1-methyl-5-methoxykynurenamine, is the main brain metabolite of melatonin hormone in mammalians, that intermediates some of the actions of this indolamine. Both of them inhibited nNOS activity *in vitro* in a dose-related manner.[25]

If we compare the derivatives **4** with the kynurenamines **2**, we can see that both series inhibit better nNOS than iNOS (compounds **4** having greater potency), unlike the corresponding **3** showing better iNOS inhibition values. Besides, the best inhibitors of the two first families carry a methoxy group in R_1 and a methyl in R_2 (urea **4g** and kynurenamine **2a**, respectively), while the urea-kynurenamine **3b** which has a chlorine in R_1 and a ethyl in R_2 is the best inhibitor of this family and the most selective one. Finally, **4g** has the highest percentage of inhibition of all the tested derivatives with similar structures.

Table 2. *In vitro* iNOS and nNOS inhibition (%) observed in the presence of 1 mM concentration of compounds **2a-l**.

Compound	R_1	R_2	% iNOS inhibition[a]	% nNOS inhibition[b]
2a	OMe	Me	30.74 ± 2.92	65.36 ± 5.6
2b	OMe	Et	0.24 ± 1.95	50.87 ± 1.9
2c	OMe	Pr	7.35 ± 4.48	42.81 ± 1.9
2d	OMe	Bu	14.11 ± 0.89	39.68 ± 1.17
2e	OMe	*c*-C_3H_5	2.66 ± 1.4	40.44 ± 1.84
2f	OMe	*c*-C_4H_7	0.01 ± 1.52	33.75 ± 1.39
2g	OMe	*c*-C_5H_9	0.61 ± 2.49	45.04 ± 1.97
2h	OMe	*c*-C_6H_{11}	9.24 ± 2.1	48.24 ± 2.42
2i	OMe	Ph	10.86 ± 3.73	46.47 ± 2.36
2j	Cl	Me	19.70 ± 0.57	17.70 ± 1.13
2k	Cl	*c*-C_3H_5	5.37 ± 2.59	9.66 ± 4.17
2l	Cl	Ph	26.60 ± 4.52	7.20 ± 1.29

[a]Values are the mean ±SEM of the percentage of iNOS and nNOS inhibition produced by 1 mM concentration of each compound. Each value is the mean of three experiments performed by triplicate using recombinant iNOS and nNOS enzymes. [b]See Ref. 19.

Table 3 includes the IC_{50} data of the most interesting derivatives **4**. Compound **4g** stands out the best values of inhibition, 130 and 180 μM, versus nNOS and iNOS, respectively, confirming the potency of this molecule.

Table 3. IC_{50} values (mM) for the inhibition of nNOS and iNOS activity by the compounds **4a**, **4c**, **4g**, **4l**, **4m** and **4n**.

IC_{50}[a]	4a	4c	4g	4l	4m	4n
nNOS	0.35	0.88	0.13	0.71	0.77	>1
iNOS	>1	>1	0.18	>1	0.80	0.86

[a]Data were obtained by measuring percentage of inhibition with at least five concentrations of inhibitor.

eNOS inhibition

We carried out the eNOS inhibitory activity of compound **4g**, using HUVECs incubated with 100 µmol/L of **4g** or vehicle and measuring the NO production stimulated by the known eNOS activator A23187. This agent increased in a time dependent manner NO production. No significant differences ($p>0.05$) were observed in A23187-stimulated NO production in the presence of **4g**, showing that this compound did not inhibit eNOS (Figure 2a). Moreover, the endothelium-dependent relaxation to acetylcholine was not affected by **4g** (Figure 2b), confirming the absence of eNOS inhibition of this compound. However, L-NAME suppressed this NO-dependent relaxant response.

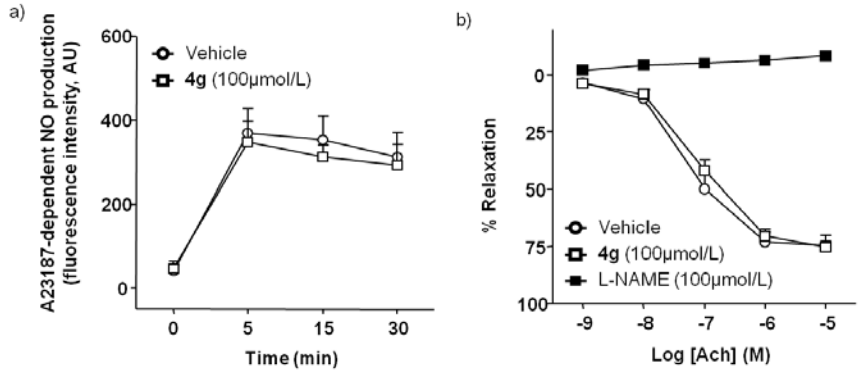

Figure 2. Effects of **4g** on eNOS activity. A23187-dependent NO production in HUVECs incubated with DMSO or **4g** (100 µmol/L) for 30 min (n = 12) (c). Acetylcholine-evoked relaxation in aortic rings with endothelium contracted with 1 µM noradrenaline in the presence of DMSO, **4g** (100 µmol/L), or L-NAME (100 µmol/L) for 30 min (n = 5). Data are expressed as means ±SEM mean of n experiment.

Docking studies

Docking studies were performed to propose and understand the binding mode of *N,N'*-disubstituted thiourea and urea derivatives **4a-q** inside nNOS and iNOS.

Figure 3 illustrates the main poses obtained for these compounds in the nNOS (PDB id: 1QW6)[26] binding site. All the ligands interact with the Glu592 and a carboxylate moiety of the heme group through the hydroxyl group and both thiourea/urea nitrogens, respectively. Compound **4a** (Figure 3a) shows additional interactions of the amino group, forming two more hydrogen bonds, one with residue Trp587 and one with Glu592. Moreover **4a** have a good orientation in the binding site: the phenyl ring points to the lipophilic region (Phe584 and Pro565) being situated below the heme group establishing a π-cation interaction, the aliphatic chain is directed to Val575 establishing VdW interactions and the thiourea moiety is oriented to a polar pocket formed by three arginines (Arg596, Arg603 and Arg481). In addition, more VdW interactions are established with Gln478.

On the other hand, compound **4j** (Figure 3b) shows no additional hydrogen bonds in the binding site. Despite it presents a similar orientation to **4a**, being longer adopts a more constricted conformation which results more unstable and reduce the π-cation interaction, due to the inclination of the aromatic ring respect to the heme group. This fact can explain the loss of activity of some compounds.

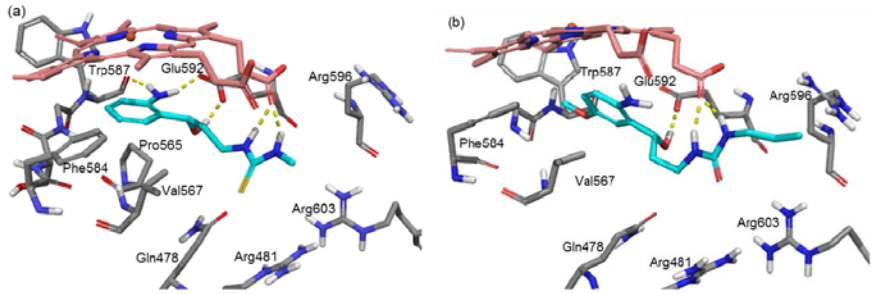

Figure 3. Detailed view of the main poses obtained for compound **4a** (a) and **4j** (b) in the nNOS binding site. Dotted lines indicate hydrogen bond interactions between the ligand and the residues of the enzyme.

Figure 4 shows the most common poses obtained for hydroxypropyl derivatives in the iNOS binding site. Compound **4g** (Figure 4a) forms three hydrogen bonds, one with Glu371 through the hydroxyl group and two with a heme propionate moiety through both thiourea nitrogens. It is noteworthy that, although **4a** have more favourable H-bond contribution inside nNOS, **4g** seems to have higher VdW stabilising contribution insite iNOS. This contribution is performed through the aliphatic chain which interacts with the nearby residues Val346, Pro344 and Gln257, and especially through the thiourea moiety which is oriented to Gln257 and to the arginines pocket.

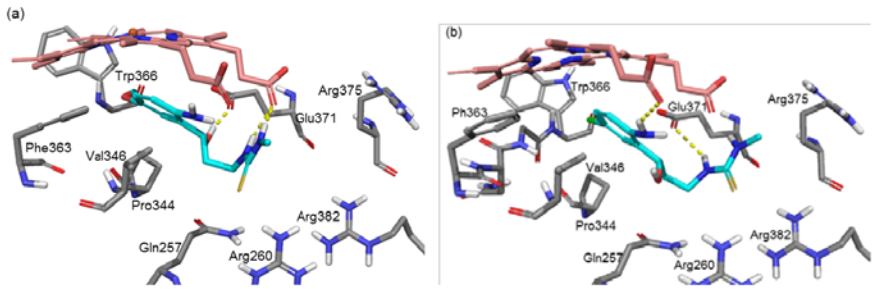

Figure 4. Detailed view of the main poses obtained for compound **4g** (a) and **4l** (b) in the iNOS binding site. Dotted lines indicate hydrogen bond interactions between the ligand and the residues of the enzyme.

Other compounds such as **4l** (Figure 4b) demonstrate weaker interaction with the iNOS (PDB id: 3NW2)[27] binding site. In this case, two hydrogen bonds are established, one between the amino group and a propionate of the heme group, and the other between ~~one~~ a thiourea nitrogen and Glu371. Moreover, the conformation adopted by **4l** moves away the phenyl ring and the thiourea moiety reducing the π-cation interaction with the heme group and the VdW interactions which decrease the stability and efficiency of the binding process.

Conclusions

In summary, we have designed and successfully synthesized a series of novel *N*,*N*'-disubstituted thiourea and urea derivatives. The synthetic pathway of these new compounds can be used to prepare kynurenamine-thioureas and ureas easier, in less synthetic steps and higher global yield than the previously described route. Their biological evaluation was performed versus nNOS and iNOS isoforms for all

compounds and versus eNOS isoform for **4g**. In general, compounds **4** inhibit better the neuronal NOS isoform than the inducible one, exhibiting the thioureas higher inhibition than the ureas. The derivatives **4a** and **4g** are the most active compounds with an IC_{50} values of 350 and 130 µM, respectively, versus nNOS, and 180 µM versus iNOS for the second compound. In addition, **4g** does not inhibit eNOS which is necessary to avoid the hypertension. Both *in silico* and *in vitro* studies reveal promising properties for these compounds which could be a reference to design new nNOS and iNOS inhibitors without adverse vascular effect, useful in neurodegenerative disorders such as Parkinson, where both isoforms are involved.

Experimental section

Chemistry

Melting points were determined using a capillary melting point apparatus and are uncorrected. Analytical thin layer chromatography was performed using Merck Kieselgel 60 F254 aluminum sheets and the spots were developed with UV light (λ = 254 nm). Flash chromatography was carried out using silica gel 60, 230-240 mesh (Merck), and the eluents used are reported within parentheses. ^{1}H NMR and ^{13}C NMR spectra were recorded on a Varian Inova Unity 300 spectrometer operating at 300.20 for ^{1}H and 75.49 MHz for ^{13}C, on a Varian direct drive 400 spectrometer operating at 400.57 MHz for ^{1}H and 100.73 MHz for ^{13}C, on a Varian Inova Unity 500 spectrometer operating at 499.79 for ^{1}H and 125.68 MHz for ^{13}C and on a Varian direct drive 600 spectrometer operating at 600.25 MHz for ^{1}H and 150.95 MHz for ^{13}C in the deuterated solvents indicated at ambient temperature. Chemical shifts are reported in ppm (δ) and are referenced to the residual solvent peak. High-resolution mass spectromatry (HRMS) was carried out on a Waters LCT Premier Mass Spectrometer. Elemental analyses were within ±0.4% of the theoretical values.

General synthetic method of 3-hydroxy-3-(2-nitro-5-substitutedphenyl)propanenitrile, 6a-c.

BuLi (1.6 M/hexane, 20.3 mL) was added to dry THF (37.5 mL) cooled to -78 ºC under argon. Then, a solution of acetonitrile (1.7 mL) in dry THF (4.9 mL) was added dropwise. The mixture was stirred at -78 ºC for 1 h. Afterward a solution of the corresponding benzaldehyde **5a-c** (16.16 mmol) in dry THF (4.9 mL) was added dropwise. The mixture was stirred again at -78 ºC for 30 min and afterward warmed to RT. The reaction was agitated for 15 min at RT and was quenched with cold water (25 mL), diluted with diethyl ether (30 mL) and washed with 2% aqueous HCl (15 mL). The aqueous layer was extracted with diethyl ether (3 x 15 mL). Finally the organic phase was washed with $NaHCO_3$ saturated solution (10 mL) and brine (15 mL), dried over anhydrous Na_2SO_4, filtered and concentrated under vacuum. The crude mixture was purified by flash chromatography (EtOAc/hexane, 1:2).

3-Hydroxy-3-(2-nitrophenyl)propanenitrile, 6a. Yellow solid (70%).[28]

3-Hydroxy-3-(5-methoxy-2-nitrophenyl)propanenitrile, 6b. Yellow solid (90%); mp: 88 - 90 ºC; ^{1}H NMR (300 MHz, $CDCl_3$) δ 8.13 (d, 1H), 7.47 (d, 1H), 6.94 (dd, 1H), 5.81 - 5.70 (m, 1H), 3.94 (s, 3H), 3.07 (dd, 1H), 2.85 (dd, 1H); ^{13}C NMR (125 MHz, $CDCl_3$) δ 164.39, 140.30, 139.65, 127.97, 117.03, 114.49, 112.73, 65.50, 56.15, 27.27; HRMS m/z 245.0540 $[M + Na]^+$, calcd. mass for $C_{10}H_{10}N_2O_4Na$: 245.0538.

3-(5-Chloro-2-nitrophenyl)-3-hydroxypropanenitrile, 6c. Yellow solid (70%); mp: 63 - 64 ºC; ^{1}H NMR (500 MHz, $CDCl_3$) δ 8.05 (d, 1H), 8.01 (d, 1H), 7.51 (dd, 1H), 5.69 (dd, 1H), 3.08 (dd, 1H), 2.87 (dd, 1H); ^{13}C NMR (125 MHz, $CDCl_3$) δ 145.07, 141.37,

138.95, 129.63, 128.61, 126.52, 116.64, 65.18, 27.41; HRMS m/z 249.0047 $[M + Na]^+$, calcd. mass for $C_9H_7N_2O_3NaCl$: 249.0045.

General synthetic method of 3-amino-1-(2-nitro-5-substitutedphenyl)propan-1-ol, 7a-c.

3-Hydroxy-3-(2-nitro-5-substitutedphenyl)propanenitrile derivatives **6a-c** (1.7 mmol) were treated dropwise with a solution of BH_3 (12.3 mL) in THF at 0 ºC under argon. The mixture was stirred during 4h at RT. Afterward the reaction mixture was cooled to 0 ºC and an ice-cold solution of 6 N HCl (7.5 mL) was added carefully. The THF was evaporated and the aqueous phase was basified with 4 N NaOH to pH = 10, and extracted with EtOAc (3 x 15 mL). The organic phase was washed with brine, dried over Na_2SO_4 and concentrated. The crude was used for the next step without purification.

General synthetic method of *N*-alkyl or aryl-*N'*-[3-Hydroxy-3-(2-nitro-5-substituted phenyl)propyl]-thioureas and ureas, 8a-q.

Thioisocianate or isocianate (0.9 mmol) was added, under argon, to a solution of 3-amino-1-(2-nitro-5-substitutedphenyl)propan-1-ol derivatives **7a-c** (0.6 mmol) in dry CH_2Cl_2. The reaction mixture was irradiated under microwave conditions at 90 ºC for 20 min. The crude mixture was purified by flash chromatography (EtOAc/hexane, 1:1).

***N*-[3-Hydroxy-3-(2-nitrophenyl)propyl]-*N'*-methylthiourea, 8a.** Yellow solid (0.42 mmol, 70%); mp: 40 ºC; ^{1}H NMR (300 MHz, $CDCl_3$) δ 7.98 - 7.90 (m, 2H), 7.70 - 7.63 (m, 1H), 7.44 - 7.35 (m, 1H), 5.37 (d, 1H), 4.36 (bs, 1H), 3.59 - 3.42 (m, 1H), 3.03 (s, 3H), 2.89 - 2.83 (m, 1H), 2.14 - 1.97 (m, 2H), 1.88 - 1.73 (m, 1H); ^{13}C NMR (150 MHz, $CDCl_3$) δ 182.69, 146.98, 140.26, 134.13, 128.09, 128.26, 124.61, 66.09, 42.09, 38.92, 27.41; HRMS m/z 270.0916 $[M + H]^+$, calcd. mass for $C_{11}H_{16}N_3O_3S$: 270.0912.

***N*-Ethyl-*N'*-[3-hydroxy-3-(2-nitrophenyl)propyl]thiourea, 8b.** Yellow oil (0.42 mmol, 70%); ^{1}H NMR (300 MHz, CD_3OD) δ 8.05 - 7.82 (m, 2H), 7.82 - 7.61 (m, 1H), 7.59 - 7.42 (m, 1H), 5.38 - 5.20 (m, 1H), 3.76 - 3.59 (m, 1H), 3.52 - 3.39 (m, 1H), 3.37 - 3.28 (m, 2H), 2.34 - 2.08 (m, 1H), 2.04 - 1.86 (m, 1H), 1.39 - 1.24 (m, 3H); ^{13}C NMR (125 MHz, CD_3OD) δ 185.83, 147.37, 140.47, 133.30, 128.00, 127.72, 123.87, 66.13, 44.33, 38.48, 36.70, 11.78; HRMS m/z 284.1064 $[M + H]^+$, calcd. mass for $C_{12}H_{18}N_3O_3S$: 284.1069.

***N*-[3-Hydroxy-3-(2-nitrophenyl)propyl]-*N'*-propylthiourea, 8c.** Yellow oil (0.43 mmol, 73%); ^{1}H NMR (500 MHz, $CDCl_3$) δ 7.94 (dd, 1H), 7.90 (dd, 1H), 7.67 - 7.63 (m, 1H, H-4"), 7.42 - 7.39 (m, 1H), 6.25 (bs, 1H), 6.15 (bs, 1H), 5.35 (d, 1H), 4.35 - 4.26 (m, 2H), 3.52 - 3.47 (m, 2H), 3.34 - 3.31 (m, 2H), 2.09 - 2.02 (m, 1H), 1.85 - 1.76 (m, 1H), 1.69 - 1.62 (m, 2H), 0.99 (t, 3H); ^{13}C NMR (125 MHz, CD_3OD) δ 181.91, 147.10, 140.18, 134.07, 128.24, 128.12, 124.60, 66.26, 45.65, 42.16, 38.83, 22.20, 11.55; HRMS m/z 282.1460 $[M + H]^+$, calcd. mass for $C_{13}H_{20}N_3O_4$: 282.1454.

***N*-Ethyl-*N'*-[3-hydroxy-3-(2-nitrophenyl)propyl]urea, 8d.** Yellow oil (0.48 mmol, 81%); ^{1}H NMR (600 MHz, $CDCl_3$) δ 7.93 - 7.87 (m, 2H), 7.65 - 7.60 (m, 1H), 7.40 - 7.35 (m, 1H), 5.30 (dd, 1H), 3.82 - 3.75 (m, 1H), 3.24 - 3.14 (m, 3H), 2.01 - 1.94 (m, 1H), 1.68 - 1.61 (m, 1H), 1.14 (t, 3H); ^{13}C NMR (150 MHz, $CDCl_3$) δ 159.61, 147.06, 140.46, 133.70, 128.18, 127.65, 124.18, 65.91, 39.70, 36.96, 35.56, 15.27; HRMS m/z 268.1302 $[M + H]^+$, calcd. mass for $C_{12}H_{18}N_3O_4$: 268.1297.

***N*-[3-Hydroxy-3-(2-nitrophenyl)propyl]-*N'*-propylurea, 8e.** Yellow oil (0.45 mmol, 76%); ^{1}H NMR (500 MHz, $CDCl_3$) δ 7.93 - 7.88 (m, 2H), 7.64 - 7.61 (m , 1H), 7.39 -

7.36 (m, 1H), 5.30 (dd, 1H), 4.78 (bs, 2H), 3.83 - 3.77 (m, 1H), 3.19 - 3.14 (m, 1H), 3.12 (t, 2H), 2.01 - 1.94 (m, 1H), 1.67 - 1.61 (m, 1H), 1.55 - 1.49 (m, 2H), 0.91 (t, 3H); ^{13}C NMR (125 MHz, $CDCl_3$) δ 159.87, 147.28, 140.61, 133.82, 128.35, 127.78, 124.32, 66.05, 42.67, 39.95, 37.11, 23.43, 11.42; HRMS m/z 298.1222 $[M + H]^+$, calcd. mass for $C_{13}H_{20}N_3O_3S$: 298.1225.

***N*-[3-Hydroxy-3-(2-nitrophenyl)propyl]-*N'*-phenylurea, 8f.** Yellow oil (0.42 mmol, 70%); ^{1}H NMR (500 MHz, $CDCl_3$) δ 7.93 - 7.86 (m, 2H), 7.63 - 7.60 (m, 1H), 7.51 - 7.44 (m, 1H), 7.39 - 7.36 (m, 2H), 7.25 - 7.20 (m, 2H), 7.04 - 6.99 (m, 1H), 5.34 (dd, 1H), 3.82 - 3.77 (m, 1H), 3.24 - 3.21 (m, 1H), 2.02 - 1.96 (m, 1H), 1.72 - 1.66 (m, 1H); ^{13}C NMR (125 MHz, $CDCl_3$) δ 157.62, 147.07, 140.20, 137.84, 133.75, 129.36, 128.42, 127.82, 124.30, 121.81, 121.04, 66.39, 39.07, 37.20; HRMS m/z 316.1292 $[M + H]^+$, calcd. mass for $C_{16}H_{18}N_3O_4$: 316.1297.

***N*-[3-Hydroxy-3-(5-methoxy-2-nitrophenyl)propyl]-*N'*-methylthiourea, 8g.** Yellow oil (0.43 mmol, 72%); ^{1}H NMR (500 MHz, $CDCl_3$) δ 8.09 (d, 1H), 7.43 (d, 1H), 6.87 (dd, 1H), 5.51 (d, 1H), 4.39 (bs, 1H), 3.94 (s, 3H), 3.91 - 3.89 (m, 1H), 3.56 - 351 (m, 1H), 3.05 (s, 3H), 2.11 - 2.04 (m, 1H), 1.79 - 1.74 (m, 1H); ^{13}C NMR (75 MHz, $CDCl_3$) δ 181.77, 164.22, 144.04, 139.51, 127.70, 113.55, 111.97, 66.22, 55.98, 42.04, 38.62, 30.31; HRMS m/z 300.1021 $[M + H]^+$, calcd. mass for $C_{12}H_{18}N_3O_4S$: 300.1018.

***N*-[3-Hydroxy-3-(5-methoxy-2-nitrophenyl)propyl]-*N'*-propylthiourea, 8h.** Yellow oil (0.46 mmol, 77%); ^{1}H NMR (500 MHz, $CDCl_3$) δ 8.07 (d, 1H), 7.40 (d, 1H), 6.84 (dd, 1H), 6.21 (bs, 1H), 6.14 (bs, 1H), 5.48 (d, 1H), 4.42 - 4.35 (m, 2H), 3.91 (s, 3H), 3.52 - 3.46 (m, 1H), 3.36 - 3.30 (m, 2H), 2.07 - 2.00 (m, 1H), 1.76 - 1.70 (m, 1H), 1.66 (q, 2H), 0.99 (t, 3H); ^{13}C NMR (125 MHz, $CDCl_3$) δ 182.16, 164.61, 144.37, 139.96, 128.09, 113.93, 112.37, 66.60, 56.36, 45.88, 42.41, 39.08, 22.46, 11.81; HRMS m/z 326.1159 $[M + H]^+$, calcd. mass for $C_{14}H_{20}N_3O_4S$: 326.1175.

***N*-ethyl-*N'*-[3-Hydroxy-3-(5-methoxy-2-nitrophenyl)propyl]urea, 8i.** Yellow oil (0.44 mmol, 74%); ^{1}H NMR (500 MHz, $CDCl_3$) δ 8.03 (d, 1H), 7.41 (d, 1H), 6.82 (dd, 1H), 5.45 (dd, 1H), 3.90 (s, 3H), 3.87 - 3.80 (m, 1H), 3.24 - 3.15 (m, 3H), 2.01 - 1.94 (m, 1H), 1.61 - 1.55 (m, 1H), 1.15 (t, 3H); ^{13}C NMR (125 MHz, $CDCl_3$) δ 164.23, 159.78, 144.63, 139.86, 127.57, 113.59, 112.02, 66.35, 56.06, 39.73, 37.17, 35.77, 15.43; HRMS m/z 296.1254 $[M + H]^+$, calcd. mass for $C_{13}H_{18}N_3O_5$: 296.1246.

***N*-[3-Hydroxy-3-(5-methoxy-2-nitrophenyl)propyl]-*N'*-propylurea, 8j.** Yellow oil (0.45 mmol, 75%); ^{1}H NMR (500 MHz, $CDCl_3$) δ 8.08 (d, 1H), 7.41 (d, 1H), 6.85 (dd, 1H), 5.45 (d, 1H), 4.73 (bs, 2H), 3.89 (s, 3H), 3.83 - 3.72 (m, 1H),3.26 - 3.18 (m, 1H), 3.14 (t, 2H), 2.04 - 1.89 (m, 1H), 1.65 - 1.48 (m, 3H), 0.92 (t, 3H); ^{13}C NMR (75 MHz, $CDCl_3$) δ 164.05, 159.77, 144.46, 139.70, 127.39, 113.38, 111.95, 66.39, 55.89, 42.61, 39.28, 37.29, 23.15, 11.23; HRMS m/z 312.1571 $[M + H]^+$, calcd. mass for $C_{14}H_{22}N_3O_5$: 312.1559.

***N*-[3-Hydroxy-3-(5-methoxy-2-nitrophenyl)propyl]-*N'*-phenylurea, 8k.** Yellow solid (0.48 mmol, 80%); mp: 77 - 78 ºC; ^{1}H NMR (400 MHz, $CDCl_3$) δ 8.02 (d, 1H), 7.38 (d, 1H), 7.34 - 7.24 (m, 4H), 7.09 - 7.04 (m, 1H), 6.80 (dd, 1H), 5.49 (dd, 1H), 3.87 (s, 3H), 3.84 - 3.77 (m, 1H), 3.23 - 3.17 (m, 1H), 2.01 - 1.93 (m, 1H), 1.65 - 1.56 (m, 1H); ^{13}C NMR (100 MHz, $CDCl_3$) δ 164.10, 157.52, 144.30, 139.62, 138.15, 129.28, 127.52, 124.12, 121.52, 113.42, 111.91, 66.53, 55.89, 39.07, 37.04; HRMS m/z 368.1214 $[M + H]^+$, calcd. mass for $C_{17}H_{19}N_3O_5Na$: 368.1222.

***N*-[3-(5-Chloro-2-nitrophenyl)-3-hydroxypropyl]-*N'*-methylthiourea, 8l.** Yellow oil (0.45 mmol, 75%); ^{1}H NMR (300 MHz, $CDCl_3$) δ 7.96 - 7.90 (m, 2H), 7.36 (dd, 1H), 6.33 (bs, 2H), 5.38 (dd, 1H), 4.36 (bs, 1H), 3.54 - 3.41 (m, 2H), 3.01 (s, 3H), 2.06 - 1.95

(m, 1H), 1.78 - 1.65 (m, 1H); ^{13}C NMR (125 MHz, $CDCl_3$) δ 182.41, 144.83, 142.57, 140.79, 128.44, 128.07, 126.15, 66.67, 41.79, 38.84, 30.29; HRMS m/z 304.0522 [M + H]$^+$, calcd. mass for $C_{11}H_{15}N_3O_3SCl$: 304.0523.

***N*-[3-(5-Chloro-2-nitrophenyl)-3-hydroxypropyl]-*N'*-ethylthiourea, 8m.** Yellow oil (0.42 mmol, 70%); ^{1}H NMR (300 MHz, $CDCl_3$) δ 7.99 - 7.82 (m, 2H), 7.35 (dd, 1H), 6.37 (bs, 2H), 5.38 (d, 1H), 4.34 (bs, 1H), 3.75 - 3.42 (m, 4H), 2.06 - 1.97 (m, 1H), 1.87 - 1.56 (m, 1H), 1.32 - 1.20 (m, 3H); ^{13}C NMR (75 MHz, $CDCl_3$) δ 181.45, 144.90, 142.53, 140.71, 128.44, 128.02, 126.09, 66.69, 41.75, 38.80, 38.68, 13.99; HRMS m/z 318.0672 [M + H]$^+$, calcd. mass for $C_{12}H_{17}N_3O_3SCl$: 318.0679.

***N*-[3-(5-Chloro-2-nitrophenyl)-3-hydroxypropyl]-*N'*-propylthiourea, 8n.** Yellow oil (0.45 mmol, %); ^{1}H NMR (300 MHz, $CDCl_3$) δ 8.00 - 7.90 (m, 2H), 7.38 (dd, 1H), 6.36 (bs, 2H), 5.41 (d, 1H), 4.38 (bs,1H), 3.81 - 3.30 (m, 4H), 2.12 - 1.96 (m, 1H), 1.80 - 1.62 (m, 3H), 1.01 (t, 3H); ^{13}C NMR (125 MHz, $CDCl_3$) δ 181.57, 144.88, 142.58, 140.72, 128.46, 128.02, 126.10, 66.65, 45.67, 41.76, 38.89, 22.10, 11.41; HRMS m/z 332.0833 [M + H]$^+$, calcd. mass for $C_{13}H_{19}N_3O_3SCl$: 332.0836.

***N*-[3-(5-Chloro-2-nitrophenyl)-3-hydroxypropyl]-*N'*-ethylurea, 8o.** Yellow oil (0.51 mmol, 85%); ^{1}H NMR (500 MHz, $CDCl_3$) δ 7.93 (d, 1H), 7.90 (d, 1H), 7.34 (dd,1H), 5.33 (dd, 1H), 4.94 (bs, 2H), 4.30 (bs, 1H), 3.85 - 3.79 (m, 1H), 3.24 - 3.15 (m, 3H), 1.99 - 1.92 (m, 1H), 1.61 - 1.55 (m, 1H), 1.15 (t, 3H); ^{13}C NMR (125 MHz, $CDCl_3$) δ 159.65, 145.07, 142.88, 140.53,128.53, 127.80, 125.89, 65.66, 39.76, 36.86, 35.65, 15.25; HRMS m/z 302.0903 [M + H]$^+$, calcd. mass for $C_{12}H_{17}N_3O_4Cl$: 302.0908.

***N*-[3-(5-Chloro-2-nitrophenyl)-3-hydroxypropyl]-*N'*-propylurea, 8p.** Yellow oil (0.42 mmol, 70%); ^{1}H NMR (500 MHz, $CDCl_3$) δ 7.94 (d, 1H), 7.90 (d, 1H), 7.38 (dd, 1H), 5.32 (dd, 1H), 3.86 - 3.80 (m, 1H), 3.20 - 3.15 (m, 1H), 3.13 (t, 2H), 1.99 - 1.92 (m, 1H), 1.61 - 1.55 (m, 1H), 1.56 - 1.51 (m, 2H), 0.93 (t, 3H); ^{13}C NMR (125 MHz, $CDCl_3$) δ 159.75, 145.07, 142.85, 140.54, 128.52, 127.79, 125.89, 65.63, 42.60, 39.81, 36.86, 23.25, 11.27; HRMS m/z 316.1056 [M + H]$^+$, calcd. mass for $C_{13}H_{19}N_3O_4Cl$: 316.1064.

***N*-[3-(5-Chloro-2-nitrophenyl)-3-hydroxypropyl]-*N'*-phenylurea, 8q.** Yellow solid (0.42 mmol, 70%); mp: 53ºC; ^{1}H NMR (400 MHz, $CDCl_3$) δ 7.92 - 7.88 (m, 2H), 7.35 - 7.28 (m, 5H), 7.13 - 7.08 (m, 1H), 5.37 (dd, 1H), 3.87 - 3.80 (m, 1H), 3.20 - 3.15 (m, 1H), 1.98 - 1.90 (m, 1H), 1.64 - 1.56 (m, 1H); ^{13}C NMR (100 MHz, $CDCl_3$) δ 157.65, 144.98, 142.67, 140.61, 137.76, 129.43, 128.44, 127.91, 126.00, 124.64, 122.09, 65.90, 39.32, 36.89; HRMS m/z 372.0722 [M + H]$^+$, calcd. mass for $C_{16}H_{16}N_3O_4NaCl$: 372.0727.

General synthetic method of *N*-alkyl or aryl-*N'*-[3-(2-amino-5-substitutedphenyl)-3-hydroxypropyl]-thioureas and ureas, 4a-q.

A solution of nitro precursor **8a-q** (0.5 mmol) in MeOH (10 mL) was passed through the Flow-hydrogenator under the following conditions: 60ºC, 60 bar, 0.2 mL/min flow rate and 10% Pd/C as catalyst. After evaporation of the solvent, the crude mixture was purified by recrystallization (diethyl ether) or by Flash chromatography (EtOAc or EtOAc/hexane, 1:1).

***N*-[3-(2-Aminophenyl)-3-hydroxypropyl]-*N'*-methylthiourea, 4a.** Yellow oil (0.37 mmol, 75%); ^{1}H NMR (600 MHz, CD_3OD) δ 7.06 (d, 1H), 6.96 - 6.93 (m, 1H), 6.66 (d, 1H), 6.63 - 6.60 (m, 1H), 4.72 (dd, 1H), 3.53 - 3.24 (m, 2H), 2.90 (s, 3H), 2.02 - 1.96 (m, 2H); ^{13}C NMR (150 MHz, CD_3OD) δ 181.71, 147.42, 130.83, 130.29, 129.13, 120.45, 119.16, 72.55, 42.10, 38.53, 32.02; HRMS m/z 240.1176 [M + H]$^+$, calcd. mass

for $C_{11}H_{18}N_3OS$: 240.1171; Anal. calcd for $C_{11}H_{17}N_3OS$: C 55.20, H 7.16, N 17.56, found: C 54.81, H 7.16, N 17.17.

***N*-[3-(2-Aminophenyl)-3-hydroxypropyl]-*N'*-ethylthiourea, 4b.** Yellow oil (0.37 mmol, 75%); ^{1}H NMR (500 MHz, $CDCl_3$) δ 7.09 - 7.04 (m, 2H), 6.73 - 6.70 (m,1H), 6.64 (dd, 1H), 6.43 (bs, 1H), 6.15 (bs, 1H), 4.78 (dd, 1H), 3.92 (m, 1H), 3.49 - 3.33 (m, 1H), 3.35 - 3.30 (m, 2H), 2.21 - 2.15 (m, 1H), 1.98 - 1.91 (m, 1H), 1.19 (t, 3H); ^{13}C NMR (125 MHz, $CDCl_3$) δ 181.25, 144.70, 128.67, 127.12, 127.08, 118.54, 116.96, 71.12, 42.09, 38.87, 34.69, 14.18; HRMS m/z 254.1175 $[M + H]^+$, calcd. mass for $C_{12}H_{20}N_3OS$: 254.1171; Anal. calcd for $C_{12}H_{19}N_3OS$: C 56.89, H 7.56 , N 16.58, found: C 57.26, H 7.91, N 16.22.

***N*-[3-(2-Aminophenyl)-3-hydroxypropyl]-*N'*-propylthiourea, 4c.** Yellow solid (0.40 mmol, 80%); mp: 50 ºC; ^{1}H NMR (500 MHz, $CDCl_3$) δ 7.09 - 7.03 (m, 2H), 6.74 - 6.69 (m, 1H), 6.64 (d, 1H), 6.38 (bs, 1H), 6.15 (bs, 1H), 4.81 - 4.75 (m, 1H), 4.07 - 3.76 (m, 2H), 3.53 - 3.44 (m, 1H), 3.32 - 3.17 (m, 2H), 2.22 - 2.15 (m, 1H), 1.98 - 1.90 (m, 1H), 1.62 - 1.55 (m, 2H), 0.94 (t, 3H); ^{13}C NMR (125 MHz, $CDCl_3$) δ 181.61, 144.91, 128.83, 127.22, 127.18, 118.62, 117.06, 71.35, 46.03, 42.13, 34.82, 22.31, 11.55; HRMS m/z 268.1469 $[M + H]^+$, calcd. mass for $C_{13}H_{22}N_3OS$: 268.1484; Anal. calcd for $C_{13}H_{21}N_3OS$: C 58.39, H 7.92, N 15.71, found: C 58.14, H 8.12, N 15.41.

***N*-[3-(2-Aminophenyl)-3-hydroxypropyl]-*N'*-ethylurea, 4d.** White solid (0.41 mmol, 83%); mp: 115 ºC; ^{1}H NMR (400 MHz, CD_3OD) δ 7.09 (d, 1H), 7.03 - 6.98 (m, 1H), 6.71 (d, 1H), 6.69 - 6.65 (td, 1H), 4.75 (dd, 1H), 3.31 (bs, 1H), 3.29 - 3.18 (m, 2H), 3.13 (q, 2H), 2.03 - 1.88 (m, 2H), 1.09 (t, 3H); ^{13}C NMR (150 MHz, CD_3OD) δ 159.98, 144.89, 128.19, 127.56, 126.54, 117.67, 116.47, 70.07, 37.00, 35.90, 34.41, 14.34; HRMS m/z 238.1475 $[M + H]^+$, calcd. mass for $C_{12}H_{20}N_3O_2$: 238.1477; Anal. calcd for $C_{12}H_{19}N_3O_2$: C 60.74, H 8.07, N 17.71, found: C 60.86, H 8.34, N 17.41.

***N*-[3-(2-Aminophenyl)-3-hydroxypropyl]-*N'*-propylurea, 4e.** Yellow solid (0.45 mmol, 90%); mp: 108 - 109 ºC; ^{1}H NMR (600 MHz, CD_3OD) δ 7.11 (d, 1H), 7.03 - 7.01 (m, 1H), 6.71 (d, 1H), 6.70 - 6.67 (m, 1H), 4.76 (dd, 1H), 3.31 - 3.26 (m, 1H), 3.24 - 3.19 (m, 1H), 3.08 (t, 2H), 2.04 - 1.98 (m, 1H), 1.97 - 1.91(m, 1H), 1.53 - 1.48 (m, 2H), 0.93 (t, 3H); ^{13}C NMR (150 MHz, CD_3OD) δ 161.53, 146.32, 129.61, 128.99, 127.97, 119.09, 117.90, 71.52, 42.88, 38.43, 37.35, 24.47, 11.62; HRMS m/z 252.1701 $[M + H]^+$, calcd. mass for $C_{13}H_{22}N_3O_2$: 252.1712; Anal. calcd for $C_{13}H_{21}N_3O_2$: C 62.13, H 8.42, N 16.72, found: C 62.23, H 8.44, N 16.41.

***N*-[3-(2-Aminophenyl)-3-hydroxypropyl]-*N'*-phenylurea, 4f.** White solid (0.35 mmol, 70%); mp: 95ºC; ^{1}H NMR (500 MHz, CD_3OD) δ 7.36 - 7.32 (m, 2H), 7.26 - 7.21 (m, 2H), 7.12 (d, 1H), 7.03 - 7.01 (m, 1H), 6.99 - 6.94 (m, 1H), 6.72 (dd, 1H), 6.69 - 6.66 (m, 1H), 4.80 (dd, 1H), 3.39 - 3.34 (m, 1H), 3.28 - 3.26 (m, 1H), 2.09 - 1.95 (m, 2H); ^{13}C NMR (125 MHz, CD_3OD) δ 160.84, 148.58, 143.26, 132.04, 131.92, 131.30, 130.27, 125.67, 122.55, 121.42, 120.22, 74.02, 40.65, 39.40; HRMS m/z 286.1560 $[M + H]^+$, calcd. mass for $C_{16}H_{20}N_3O_2$: 286.1556; Anal. calcd for $C_{16}H_{19}N_3O_2$: C 67.35, H 6.71, N 14.73, found: C 67.49, H 7.09, N 14.63.

***N*-[3-(2-Amino-5-methoxyphenyl)-3-hydroxypropyl]-*N'*-methylthiourea, 4g.** Yellow solid (0.37 mmol, 75%); mp: 50 ºC; ^{1}H NMR (300 MHz, CD_3OD) δ 6.98 (d, 1H), 6.93 (d, 1H), 6.83 (dd, 1H), 4.92 (d, 1H), 3.82 (s, 3H), 3.80 - 3.78 (m, 2H), 2.98 (s, 3H), 2.12 - 2.06 (m, 2H); ^{13}C NMR (150 MHz, CD_3OD) δ 182.41, 155.80, 134.34, 131.26, 121.11, 115.91, 114.99, 72.27, 57.35, 38.38, 36.51, 31.05; HRMS m/z 270.1280 $[M + H]^+$, calcd. mass for $C_{12}H_{20}N_3O_2S$: 270.1276; Anal. calcd for $C_{12}H_{19}N_3O_2S$: C 53.51, H 7.11, N 15.60, found: C 53.50, H 7.55, N 15.50.

***N*-[3-(2-Amino-5-methoxyphenyl)-3-hydroxypropyl]-*N'*-propylthiourea, 4h.** Yellow solid (0.38 mmol, 76%); mp: 45 ºC; ^{1}H NMR (500 MHz, $CDCl_3$) δ 6.69 (d, 1H), 6.66 (dd, 1H), 6.62 (d, 1H), 6.50 (bs, 1H), 6.20 (bs, 1H), 4.77 (dd, 1H), 3.72 (s, 3H), 3.67 - 3.48 (m, 2H), 3.31 - 3.24 (m, 2H), 2.17 - 2.08 (m, 1H), 1.98 - 1.90 (m, 1H), 1.63 - 1.55 (m, 2H), 0.95 (t, 3H); ^{13}C NMR (125 MHz, $CDCl_3$) δ 181.63, 153.16, 137.56, 129.60, 118.71, 113.95, 113.07, 70.78, 55.92, 45.94, 42.21, 35.18, 22.33, 11.56; HRMS m/z 298.1580 $(M + H)^+$, calcd. mass for $C_{14}H_{24}N_3O_2S$: 298.1589; Anal. calcd for $C_{14}H_{23}N_3O_2S$: C 56.54, H 7.79, N 14.13, found: C 56.50, H 7.65, N 14.50.

***N*-[3-(2-Amino-5-methoxyphenyl)-3-hydroxypropyl]-*N'*-ehylurea, 4i.** Yellow solid (0.39 mmol, 78%); mp: 128 - 129 ºC; ^{1}H NMR (600 MHz, CD_3OD) δ 6.79 (d, 1H), 6.71 (d, 1H), 6.67 (dd, 1H), 4.76 (dd, 1H), 3.73 (s, 3H), 3.32 - 3.27 (m, 1H), 3.25 - 3.20 (m, 1H), 3.15 (q, 2H), 1.98 - 1.91 (m, 2H), 1.11 (t, 3H); ^{13}C NMR (150 MHz, CD_3OD) δ 161.40, 154.32, 139.07, 131.79, 119.39, 114.52, 113.66, 70.94, 56.09, 38.39, 37.67, 35.85, 15.76; HRMS m/z 268.1647 $(M + H)^+$, calcd. mass for $C_{13}H_{22}N_3O_3$: 268.1661; Anal. calcd for $C_{13}H_{21}N_3O_3$: C 58.41, H 7.92, N 15.72, found: C 58.50, H 7.63, N 15.75.

***N*-[3-(2-Amino-5-methoxyphenyl)-3-hydroxypropyl]-*N'*-propylurea, 4j.** White solid (0.37 mmol, 75%); mp: 130 ºC; ^{1}H NMR (300 MHz, CD_3OD) δ 6.83 (d, 1H), 6.76 (d, 1H), 6.71 (dd, 1H), 4.81 (dd, 1H), 3.78 (s, 3H), 3.36 - 3.25 (m, 2H), 3.13 (t, 2H), 2.04 - 1.95 (m, 2H), 1.61 - 1.50 (m, 2H), 0.98 (t, 3H); ^{13}C NMR (100 MHz, CD_3OD) δ 160.09, 152.88, 137.70, 130.33, 117.95, 113.13, 112.27, 69.55, 54.70, 41.47, 36.97, 36.26, 23.04, 10.19; HRMS m/z 282.1813 $(M + H)^+$, calcd. mass for $C_{14}H_{24}N_3O_3$: 282.1818; Anal. calcd for $C_{14}H_{23}N_3O_3$: C 59.77, H 8.24, N 14.94, found: C 59.79, H 8.40, N 14.75.

***N*-[3-(2-Amino-5-methoxyphenyl)-3-hydroxypropyl]-*N'*-phenylurea, 4k.** White solid (0.37 mmol, 75%); mp: 157 ºC; ^{1}H NMR (500 MHz, CD_3OD) δ 7.36 - 7.31 (m, 2H), 7.27 - 7.21 (m, 2H), 6.98 - 6.95 (m, 1H), 6.79 (d, 1H), 6.70 (d, 1H), 6.65 (dd, 1H), 4.79 (dd, 1H), 3.41 - 3.35 (m, 1H), 3.40 - 3.27 (m, 1H), 3.31 (s, 3H), 2.03 - 1.94 (m, 2H); ^{13}C NMR (125 MHz, CD_3OD) δ 157.13, 152.92, 139.55, 137.64, 130.37, 128.35, 121.99, 118.87, 118.02, 113.14, 112.25, 69.77, 54.67, 36.92, 36.01; HRMS m/z 316.1667 $[M + H]^+$, calcd. mass for $C_{17}H_{22}N_3O_3$: 316.1661; Anal. calcd for $C_{17}H_{21}N_3O_3$: C 64.74, H 6.71, N 13.32, found: C 64.72, H 6.57, N 13.52.

***N*-[3-(2-Amino-5-chlorophenyl)-3-hydroxypropyl]-*N'*-methylthiourea, 4l.** Yellow solid (0.39 mmol, 79%); mp: 55 ºC; ^{1}H NMR (400 MHz, CD_3OD) δ 7.18 (d, 1H), 7.02 (dd, 1H), 6.72 (d, 1H), 4.80 (dd, 1H), 3.37 - 3.35 (m, 2H), 2.97 (s, 3H), 2.08 - 2.03 (m, 2H); ^{13}C NMR (100 MHz, CD_3OD) δ 181.67, 143.62, 129.94, 127.15, 126.02, 121.99, 117.36, 69.08, 41.16, 34.81, 29.30; HRMS m/z 274.0775 $[M + H]^+$, calcd. mass for $C_{11}H_{17}N_3OSCl$: 274.0781; Anal. calcd for $C_{11}H_{16}N_3OSCl$: C 48.26, H 5.89, N 15.35, found: C 48.60, H 5.99, N 15.73.

***N*-[3-(2-Amino-5-chlorophenyl)-3-hydroxypropyl]-*N'*-ethylthiourea, 4m.** Yellow solid (0.36 mmol, 72%); mp: 48 ºC; ^{1}H NMR (500 MHz, $CDCl_3$) δ 7.05 (d, 1H), 7.02 - 6.98 (m, 1H), 6.56 (d, 1H), 4.76 (dd, 1H), 4.55 - 4.35 (m, 1H), 4.34 - 4.25 (m, 1H), 4.24 - 4.17 (m, 2H), 2.15 - 2.05 (m, 1H), 1.96 - 1.87 (m, 1H), 1.28 (t, 3H); ^{13}C NMR (125 MHz, $CDCl_3$) δ 182.70, 142.94, 128.98, 128.17, 126.75, 123.14, 118.03, 69.25, 46.39, 40.64, 34.73, 14.10; HRMS m/z 288.0941 $[M + H]^+$, calcd. mass for $C_{12}H_{19}N_3OSCl$: 288.0937; Anal. calcd for $C_{12}H_{18}N_3OSCl$: C 50.08, H 6.30, N 14.60, found: C 50.44, H 6.47, N 14.22.

***N*-[3-(2-Amino-5-chlorophenyl)-3-hydroxypropyl]-*N'*-propylthiourea, 4n.** White solid (0.40 mmol, 80%); mp: 130 ºC; ^{1}H NMR (400 MHz, CD_3OD) δ 7.13 (d, 1H), 6.96 (dd, 1H), 6.67 (d, 1H), 4.74 (dd, 1H), 3.71 - 3.60 (m, 1H), 3.56 - 3.46 (m, 1H), 3.45 - 3.42 (m, 2H), 2.03 - 1.97 (m, 2H), 1.62 - 1.55 (m, 2H), 0.94 (t, 3H); ^{13}C NMR (100 MHz,

CD_3OD) δ 181.17, 143.63, 129.93, 127.14, 126.02, 121.98, 117.35, 69.15, 45.56, 41.24, 34.85, 21.98, 10.20; HRMS m/z 302.1096 $[M + H]^+$, calcd. mass for $C_{13}H_{21}N_3OSCl$: 302.1094; Anal. calcd for $C_{13}H_{20}N_3OSCl$: C 51.73, H 6.68, N 13.92, found: C 51.51, H 7.16, N 13.54.

***N*-[3-(2-Amino-5-chlorophenyl)-3-hydroxypropyl]-*N'*-ethylurea, 4o.** Yellow solid (0.45 mmol, 91%); mp: 48 ºC; ^1H NMR (300 MHz, CD_3OD) δ 7.10 (d, 1H), 6.97 (dd, 1H), 6.67 (d, 1H), 4.71 (dd, 1H), 3.33 - 3.24 (m, 2H), 3.23 - 3.17 (m, 2H), 1.95 - 1.87 (m, 2H), 1.09 (t, 3H); ^{13}C NMR (100 MHz, CD_3OD) δ 159.97, 143.45, 130.15, 127.10, 126.11, 122.11, 117.48, 69.22, 36.91, 35.94, 34.43, 14.33; HRMS m/z 294.0982 $[M + Na]^+$, calcd. mass for $C_{12}H_{18}N_3O_2NaCl$: 294.0985; Anal. calcd for $C_{12}H_{18}N_3O_2NaCl$: C 53.04, H 6.68, N 15.46, found: C 53.38, H 7.02, N 15.52.

***N*-[3-(2-Amino-5-chlorophenyl)-3-hydroxypropyl]-*N'*-propylurea, 4p.** Yellow solid (0.41 mmol, 82%); mp: 137 ºC; ^1H NMR (300 MHz, CD_3OD) δ 7.03 (d, 1H), 6.96 (dd, 1H), 6.59 (d, 1H), 4.70 (dd, 1H), 3.39 - 3.03 (m, 4H), 1.93 - 1.71 (m, 2H), 1.53 - 1.46 (m, 2H), 0.92 (t, 3H); ^{13}C NMR (100 MHz, CD_3OD) δ 159.99, 143.54, 130.23, 127.15, 126.11, 122.15, 117.58, 69.32, 42.83, 36.92, 35.93, 22.58, 10.46; HRMS m/z 286.1318 $[M + H]^+$, calcd. mass for $C_{13}H_{21}N_3O_2Cl$: 286.1322; Anal. calcd for $C_{13}H_{20}N_3O_2Cl$: C 54.64, H 7.05, N 14.70, found: C 54.34, H 7.33, N 14.84.

***N*-[3-(2-Amino-5-chlorophenyl)-3-hydroxypropyl]-*N'*-phenylurea, 4q.** White solid (0.35 mmol, 71%); mp: 105 ºC; ^1H NMR (500 MHz, CD_3OD) δ 7.36 - 7.32 (m, 2H), 7.26 - 7.22 (m, 2H), 7.13 (d, 1H), 6.99 - 6.94 (m, 2H), 6.67 (d, 1H), 4.76 (dd, 1H), 3.41 - 3.35 (m, 1H), 3.31 - 3.27 (m, 1H), 2.01 - 1.92 (m, 2H); ^{13}C NMR (125 MHz, CD_3OD) δ 157.14, 143.71, 139.52, 130.01, 128.36, 127.13, 126.10, 122.02, 121.94, 118.90, 117.38, 69.44, 36.89, 35.65; HRMS m/z 320.1168 $[M + H]^+$, calcd. mass for $C_{16}H_{19}N_3O_2Cl$: 320.1166; Anal. calcd for $C_{16}H_{18}N_3O_2Cl$: C 60.09, H 5.67, N 13.14, found: C 60.21, H 5.96, N 13.38.

General synthetic method of *N*-[3-(2-amino-5-chlorophenyl)-3-oxopropyl]-*N'*-ethylurea 3b from *N*-[3-(5-chloro-2-nitrophenyl)-3-hydroxypropyl]-*N'*-ethylurea 8o.

The Jones reagent (0.418 mL), freshly prepared, (a mixture of 2.67 g chromic anhydride and 2.3 mL H_2SO_4 dissolved to 10 mL of water) was added to a solution of **8o** (0.742 mmol) in acetone (3 mL). After 10 min stirring, the reaction was quenched with ice-water (25 mL) and saturated $NaHSO_4$ solution (5 mL). The resulting mixture was extracted with ethyl acetate, filtered, dried (Na_2SO_4) and concentrated under vacuum. The crude mixture was purified by flash chromatography (EtOAc/hexane, 3:1). The next step is the nitro group reduction to amino one using $Fe/FeSO_4$ in water as previously described.[20]

***N*-[3-(5-Chloro-2-nitrophenyl)-3-oxopropyl]-*N'*-ethylurea.** Following the procedure described in this section, 200.1 mg of a white solid was obtained (90%). Spectroscopic data.[20]

***N*-[3-(2-Amino-5-chlorophenyl)-3-oxopropyl]-*N'*-ethylurea 3b.** Yellow solid (75%).[20]

Biological Procedures

***In vitro* nNOS and iNOS activities determination**

L-Arginine, *L*-citrulline, *N*-(2-hydroxymethyl)piperazine-*N'*-(2-ethanesulfonic acid) (HEPES), DL-dithiothreitol (DTT), hypoxantine-9-β-D-ribofuranosid (inosine), ethylene glycol-bis-(2-aminoethylether)-*N*,*N*,*N'*,*N'*-tetraacetic acid (EGTA), bovine serum

albumin (BSA), Dowex-50W (50 x 8-200), FAD, NADPH and 5,6,7,8-tetrahydro-L-biopterin dihydrocloride (H_4-biopterin), tris-(hydroxymethyl)-aminometane (Tris-HCl) and calcium chloride were obtained from Sigma-Aldrich Química (Spain). L-[^{3}H]-arginine (47.4 Ci/mmol) was obtained from Perkin Elmer (Spain). Calmodulin from bovine brain, and recombinant iNOS and nNOS were obtained from Enzo Life Sciences (Spain).

The i/nNOS activity was measured by the Bredt and Snyder method,[29] monitoring the conversion of *L*-[^{3}H]-arginine to *L*-[^{3}H]-citrulline. The final incubation volume was 100 µL and consisted of 10 µL of an aliquot of recombinant i/nNOS added to a buffer with a final concentration of 25 mM Tris-HCl, 1 mM DTT, 4 µM H_4-biopterin, 10 µM FAD, 0.5 mM inosine, 0.5 mg/mL BSA, 0.1 mM $CaCl_2$, 10 µM L-arginine, 10 µg/mL calmodulin (only for nNOS) and 50 nM*L*-[^{3}H]-arginine, at pH 7.6. The reaction was started by the addition of 10 µL of 7.5 mM NADPH and 10 µL of each derivative **4** in ethanol (10%) to give a final concentration of 1 mM. The tubes were vortex and incubated at 37 ºC for 30 min. Control incubations were performed by the omission of NADPH. The reaction was halted by the addition of 400 µL of cold 0.1 M HEPES, 10 mM EGTA, and 0.175 mg/mL L-citrulline, pH 5.5. The reaction mixture was decanted into a 2 mL column packet with Dowex-50W ion-exchange resin (Na^+ form) and eluted with 1.2 mL of water. *L*-[^{3}H]-citrulline was quantified by liquid scintillation spectroscopy. The retention of *L*-[^{3}H]-arginine in this process was greater than 98%. Specific enzyme activity was determined by subtracting the control value, which usually amounted to less than 1% of the radioactivity added. The nNOS activity was expressed as picomoles of *L*-[^{3}H]-citrulline produced (/mg of protein/min).

eNOS inhibition

Quantification of NO in human umbilical vein endothelial cells (HUVECs)

Endothelial cells were isolated from human umbilical cord veins using a previously reported method with several modifications.[30] The cells were cultured (Medium 199 + 20% fetal bovine serum + Penicillin/Streptomycin 2mmol/L + Amphotericin B 2 mmol/L + Glutamine 2 mmol/L + HEPES 10 mmol/L + endothelial cell growth supplement 30 µg/mL + Heparin 100 mg/mL) under 5% CO_2 at 37°C. HUVECs were then used to measure NO production by diaminofluorescein-2 (DAF-2) fluorescence, as described previously.[30] Briefly, cells were incubated during 30 min in the presence of the **4g** at the concentration of 100 µmol/L. After this period, cells were washed with PBS and then were pre-incubated with L-arginine (100 µmol/L in PBS, 5min, 37ºC). Subsequently, DAF-2 (0.1 µmol/L) was incubated for 2 min and then the calcium ionophore calimycin (A23187, 1 µmol/L) was added for 30 min and cells were incubated in the dark at 37ºC. Then the fluorescence (arbitrary units) was measured using a spectrofluorimeter (Fluorostart, BMG Labtechnologies, Offenburg, Germany). The auto-fluorescence was subtracted from each value. In some experiments, N^G-nitro-L-arginine methyl ester (L-NAME, 100 µmol/L) was added 15 min before the addition of L-arginine. The difference between fluorescence signal without and with L-NAME was considered NO production.

Tissue preparation and measurement of tension

The investigation conforms to the Guide for the Care and Use of Laboratory Animals published by the US National Institutes of Health (NIH Publication No. 85-23, revised 1996) and with the principles outlined in the Declaration of Helsinki and approved by our institutional review board. Male Wistar rats (250-300 g), obtained from Harlam Laboratories SA (Barcelona, Spain), were euthanized by a quick blow on the head followed by exsanguination. The descending thoracic aortic rings were dissected, and rings were then mounted in organ chambers filled with Krebs solution (composition in

mmol/L: NaCl, 118; KCl, 4.75; $NaHCO_3$, 25; $MgSO_4$, 1.2; $CaCl_2$, 2; KH_2PO_4, 1.2; and glucose, 11) and were stretched to 2 g of resting tension by means of two L-shaped stainless-steel wires inserted into the lumen and attached to the chamber and to an isometric force-displacement transducer (UF-1, Cibertec, Madrid, Spain), and recorded in a recording and analysis system (MacLab ADInstruments), as described previously.[30] After equilibration, aortic rings with a functional endothelium were incubated with vehicle (DMSO), **4g** (100 µmol/L), or L-NAME (100 µmol/L) for 30 min, and contracted with phenylephrine (1µmol/L). Once a plateau contraction was reached, a concentration-response curve was constructed by cumulative addition of acetylcholine. Results are expressed as percentage of phenylephrine-evoked contraction. Data are expressed as means ±SEM mean and n reflects the number of aortic rings from different rats.

Statistical analysis

Data are expressed as the mean ±SEM. Statistically significant differences between groups were calculated by Students´ t test for unpaired observations or for multiple comparisons by an ANOVA followed by a Newman Keuls test. $p<0.05$ was considered statistically significant.

Docking studies

The suite of programs Maestro (Schrödinger, LCC[31]) has been used for the docking studies. The Cartesian coordinates for the two proteins iNOS and nNOS were obtained from the Protein Data Bank and treated with the Protein Preparation Wizardmodule[32] of Maestro. The LigPrep[33] program was used to generate the 3D structures of the conformers of compounds **4** after taking their structures from fragment libraries and being optimized using the Macromodel module. Rigid docking was performed using the Glide with a Standard Precision (SP) protocol. Figures were built using PyMol.[34]

Acknowledgements

This work was partially supported by the Instituto de Salud Carlos III through the grant FI11/00432 and by Ministerio de Economía y Competitividad, Instituto de Salud Carlos III (RIC RD12/0042/0011).

Keywords

N,*N*'-disubstituted thiourea, *N*,*N*'-disubstituted urea, Inducible nitric oxide synthase (iNOS), Neuronal nitric oxide synthase (nNOS), Oxide nitric synthase (NOS) inhibitors.

References

1 R. G. Knowles and S. Moncada, *Biochem. J.* 1994, **298**, 249-258.

2 V. Calabrese, C. Mancuso, M. Calvani, E. Rizzarelli, D. A. Butterfield and A. M. Giuffrida Stella, *Neurosci.* 2007, **8**, 766-775.

3 D. Cho, T. Nakamura, J. Fang, P. Cieplak, A. Godzik, Z. Gu and S. A. Lipton, *Science* 2009, **324**, 102-105.

4 M. A. Smith, M. Vasak, M. Knipp, R. J. Castellani and G. Perry, *Free Radic. Biol. Med.* 1998, **25**, 898-902.

5 G. T. Liberatore, V. Jackson-Lewis, S. Vukosavic, A. S. Mandir, M. Vila, W. G. McAuliffe, V. L. Dawson, T. M. Dawson and S. Przedborski, *Nat. Med.* 1999, **5**, 1403-1409.

6 P. J. Norris, H. J. Waldvogel, R. L. Faull, D. R. Love and P. C. Emson, *Neuroscience* 1996, **72**, 1037-1047.

7 N. K. Wong and M. J. Strong, *Eur. J. Cell. Biol.* 1998, **77**, 338-343.

8 C. O. Bingham III, *J. Rheumatol. Suppl.* 2002, **65**, 3-9.

9 K. D. Kröncke, K. Fehsel and V. Kolb-Bachofen, *Clin. Exp. Immunol.* 1998, **113**, 147-156

10 S. Taddei, A. Virdis, L. Ghiadoni, I. Sudano and A. Salvetti, *J. Cardiovasc. Pharmacol.* 2001, **38** (Suppl.2), S11-S14.

11 Napolia, F. de Nigrisa, S. Williams-Ignarrod, O. Pignalosaa, V. Sicaa and L. J. Ignarroe, *Nitric Oxide* 2006, **15**, 265-279.

12 P. Pacher, J. S. Beckman and L. Liaudet, *Physiol. Rev.* 2007, *87*, 315-424.

13 F. Torreilles, S. Salman-Tabcheh, M. Guerin and J. Torreilles, *Brain Res. Rev.* 1999, **30**, 153-163.

14 D. G. Hirst and T. Robson, *Front. Biosci.* 2007, **12**, 3406-3418.

15 T. Uehara, T. Nakamura, D. Yao, Z. Q. Shi, Z. Gu, Y.Ma, E. Masliah, Y.Nomura and S. A. Lipton, *Nature* 2006, **441**, 513-517.

16 L. A. Ridnour, D. D. Thomas, D. Mancardi, M. G. Espey, K. M. Miranda, N. Paolocci, M. Feelisch, J. Fukuto and D. A. Wink, *Biol. Chem.* 2004, **385**, 1-10.

17 T. O. Fischmann, A. Hruza, X. D. Niu, J. D. Fossetta, C. A. Lunn, E. Dolphin, A. J. Prongay, P. Reichert, D. J. Lundell, S. K. Narula and P. C. Weber, *Nat. Struct. Biol.* 1999, **6**, 233-242.

18 E. Camacho, J. Leon, A. Carrión, A. Entrena, G. Escames, H. Khaldy, D. Acuña-Castroviejo, M. A. Gallo and A. Espinosa, *J. Med. Chem.* 2002, **45**, 263-274.

19 A. Entrena, M. E. Camacho, D. Carrión, L. C. López-Cara, G. Velasco, J. León, G. Escames, D. Acuña-Castroviejo, V. Tapias, M. A. Gallo, A. Vivó and A. Espinosa, *J. Med. Chem.* 2005, **48**, 8174-8181.

20 M. Chayah, M. D. Carrión, M. A. Gallo, R. Jiménez, J. Duarte and M. E. Camacho, *ChemMedChem* 2015, **10**, 874-882.

21 A. Fürstner, D. N. Jumbam and G. Seidel, *Chem. Ber.* 1994, **127**, 1125-1130.

22 D. A. Claremon, L. Zhuang, K. Leftheris, C. M. Tice, Z. Xu, Y. Ye, S. B. Singh, S. Cacatian, W. Zhao and F. Himmelsbach, Patent WO 2009017664 A1, 2009.

23 R. B. Silverman, G. R. Lawron, H. R. Ranaivo, L. K. Chico, J. Seo and D. M. Watterson, *Bioorg. Med. Chem.* 2009, **17**, 7593-7605.

24 J. S. Fortin, J. Lacroix, M. Desjardins, A. Patenaude, E. Petitclerc and R. C. Gaudreault, *Bioorg. Med. Chem.* 2007, **15**, 4456-4469.

25 J. León, G. Escames, M. I. Rodríguez, L. C. López, V. Tapias, A. Entrena, E. Camacho, M. D. Carrión, M. A. Gallo, A. Espinosa, D-X. Tan, R. J. Reiter, D. Acuña-Castroviejo, *J. Neurochem.* 2006, **98**, 2023-2033.

26 R. Fedorov, E. Hartmann, D. K. Ghosh and I. Schlichting, *J. Biol. Chem.* 2003, **278**, 45818-45825.

27 U. Grädler, T. Fuchß, W-R. Ulrich, R. Boer, A. Strub, C. Hesslinger, C. Anézo, K. Diederichs and A. Zaliani, *Bioorg. Med. Chem. Lett.* 2011, **21**, 4228-4232.

28 S. S. Labadie and J. K. Stille, *Tetrahedron* 1984, **40**, 2329-2336.

29 D. S. Bredt, S. H. Snyder, *Proc. Natl. Acad. Sci. U.S.A.* 1990, **87**, 682-685.

30 R. Jiménez, M. Sánchez, M. J. Zarzuelo, M. Romero, A. M. Quintela, R. López-Sepúlveda, P. Galindo, M. Gómez-Guzmán, J. M. Haro, A. Zarzuelo, F. Pérez-Vizcaíno and J. Duarte, *J. Pharmacol. Exp. Ther.* 2010, 332, 554-561.

31 Schrödinger Suite 2012 Update 2.

32 Schrödinger Suite 2012 Protein Preparation Wizard; Epik version 2.3, Schrödinger, LLC, New York, NY, 2012; Impact version 5.8, Schrödinger, LLC, New York, NY, 2012; Prime version 3.1, Schrödinger, LLC, New York, NY, 2012.

33 Lig Prep, version 2.5, Schrödinger, LLC, New York, NY, 2012.

34 PyMOL Molecular Graphics System, Version 1.4, Schrödinger. LLC.

3.5 Artículo 5

^{1}H and ^{13}C NMR spectral assignment of a novel group of bioactive *N,N'*-disubstituted thiourea and urea derivatives

MariemChayah[a], M. Encarnación Camacho[a]*, M. Dora Carrión[a]*, Miguel A. Gallo[a]

[a]Departamento de Química Farmacéutica y Orgánica, Facultad de Farmacia, Universidad de Granada (Spain).

*Correspondig authors: Dr. M. Encarnación Camacho. Tel.: +34-958-243844; E-mail: ecamacho@ugr.es and Dr. M. Dora Carrión. Tel.: +34-958-240728; E-mail: dcarrion@ugr.es

Abstract: The ^{1}H and ^{13}C NMR resonances of seventeen *N*-alkyl andaryl-*N'*-[3-hydroxy-3-(2-nitro-5-substitutedphenyl)propyl]-thioureas and ureas (**1-17**), and seventeen *N*-alkyl or aryl-*N'*-[3-(2-amino-5-substitutedphenyl)-3-hydroxypropyl]-thioureas and ureas (**18-34**) were assigned completely using the concerted application of one- and two-dimensional experiments (DEPT, HSQC and HMBC). NOESY experiments confirm the preferred conformation of these compounds.

Keywords: ^{1}H and^{13}C 1D NMR; ^{1}H and^{13}C 2D NMR (HSQC; HMBC); NOESY;*N,N'*-disubstituted thiourea and urea, hydroxypropylthioureas, hydroxypropylureas.

Introduction

Nitric oxide (NO) is an inorganic free radical and an important biomessenger that regulates several physiological functions in the nervous, immune, and cardiovascular systems.[1] NO is synthesized from the enzyme catalysis of L-arginine to L-citrulline in several cell types by a family of nitric oxide synthase (NOS) isoenzymes with consumption of molecular oxygen. In mammalians, three isoforms of NOS have been identified: neuronal (nNOS), endothelial (eNOS) and inducible NOS (iNOS).[2] nNOS and eNOS are constitutive and regulated by intracellular Ca/CaM. They continually produce low levels of NO used for nerve function and blood regulation, respectively. While, iNOS produces large toxic bursts of NO to fight pathogens, and is not Ca-dependent.[3,4]

To exert appropriate functions, NO synthesis by the three isozymes is under tight regulation. Thus, overproduction of NO by nNOS has been associated with neurodegenerative disorders such as Alzheimer's, Parkinson's or Huntington's diseases,[5-7] and the inducible isoform seems to be responsible for the massive NO production in pathologies such as arthritis, colitis, tissue damage, cancer or several inflammatory states.[8-10] The NO underproduction by eNOS has been associated with hypertension and atherosclerosis.[11,12] Accordingly, inhibition of nNOS or iNOS, but not of eNOS, could provide an effective therapeutic approach. Because of this, the development of NOS selective inhibitors is an important field of research.
In a recent paper, the synthesis and biological evaluation of a novel family of *N,N'*-disubstituted thiourea and urea derivatives **18-34**, which were designed and evaluated as NOS inhibitor agents, have been described.[13]

Although the structures of these derivatives have been determined by means of standard spectroscopic (^{1}H,^{13}C NMR) and spectrometric (MS) techniques, a detailed NMR study has been performed in some of them, in order to unequivocally corroborate their structures.

The present study reports the unambiguous assignment of each signal in the ^{1}H and ^{13}C NMR spectra in compounds **18-34**, using one-dimensional and two-dimensional resonance techniques. The spectra of nitro derivatives **1-17**, the precursors and their synthetic pathway are also included.

Experimental

NMR spectra

Nuclear magnetic resonance (NMR) spectra were recorded on a 300-MHz ^{1}H and 75-MHz ^{13}C NMR Agilent Varian Innova Unity, a400-MHz ^{1}H and 100 MHz ^{13}C NMR Agilent Varian Direct Drive, a 500-MHz ^{1}H and 125-MHz ^{13}C NMR Agilent Varian Innova Unity, and a 600-MHz ^{1}H and 150-MHz ^{13}C NMR Agilent Varian Direct Drive spectrometers at 298 K. The following parameters were used in DEPT experiments: pulse width (135°), 9.0ms; recycle time, 1 s; ½ J (CH) = 4 ms; 65 536 data points acquired and transformed from 1024 scans; spectral width, 15 KHz; and line broadening, 1.3 Hz. Chemical shifts (δ) are quoted in parts per million (ppm) and are referenced to the residual solvent peak: $CDCl_3$, δ = 7.26 ppm (^{1}H), δ = 77.4 ppm (^{13}C); CD_3OD, δ = 4.87 ppm (^{1}H), δ = 49.00 ppm (^{13}C). Spin multiplicities are given as s (singlet), bs (broad singlet), d (doublet), dd (doublet doublet), t (triplet), q (quadruplet), and m (multiplet). Coupling constant (J) are given in Hz.

The HMBC spectra were measured with a pulse sequence gc2hmbc (standard sequence, Agilent Vnmrj_3.2A software) optimized for 8 Hz (inter-pulse delay for the evolution of long-range couplings: 62.5 ms). The HSQC spectra were measured with a pulse sequence gc2hsqcse (Standard sequence, Agilent Vnmrj_3.2A software).

Nuclear Overhauser spectra was recorded on a Agilent Varian Direct Drive spectrometer, operating at 600 MHz, with a spectral widths of 4.96 KHz in both F2 and F1 domains; 744 x 200 data points was acquired with 16 scans per increment and relaxation delays of 1.0s. The mixing time in NOESY experiments was 0.5s. Data processing was performed on a 1K x 1K data matrix.

Results and Discussion

Scheme 1 represents the previously reported synthetic pathway followed in the preparation of final compounds **18-34**,[10] and Table 1 shows the structural data of all the synthesized intermediate and final compounds.

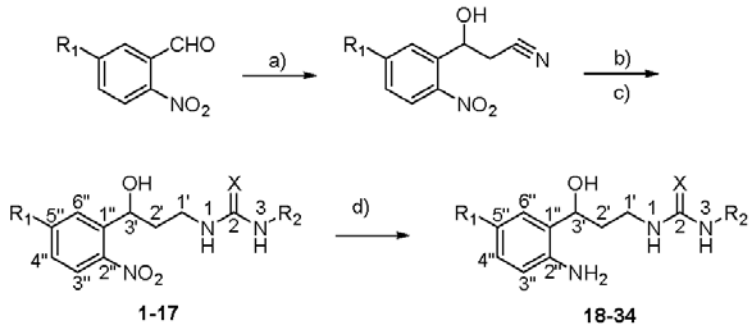

Scheme 1.Synthesis of *N,N'*-disubstitutedthiourea and urea derivatives **18-34**. a) CH_3CN, BuLi, THF, -78ºC, then RT; b) BH_3-THF, 0ºC, then 4h RT; c) $XCNR_2$, CH_2Cl_2, 20 min (MW); d) 10% Pd/C, MeOH (flow hydrogenation), 60ºC, 60 bar.

Table 1. Structural data of the intermediate (**1-17**) and final (**18-34**) compounds

Compound	R_1	R_2	X	Compound	R_1	R_2	X
1, 18	H	Me	S	**9, 26**	H	Et	O
2, 19	H	Et	S	**10, 27**	H	Pr	O
3, 20	H	Pr	S	**11, 28**	H	Ph	O
4, 21	OMe	Me	S	**12, 29**	OMe	Et	O
5, 22	OMe	Pr	S	**13, 30**	OMe	Pr	O
6, 23	Cl	Me	S	**14, 31**	OMe	Ph	O
7, 24	Cl	Et	S	**15, 32**	Cl	Et	O
8, 25	Cl	Pr	S	**16, 33**	Cl	Pr	O
				17, 34	Cl	Ph	O

Structural elucidation of these compounds has been made by routine ^{1}H and ^{13}C NMR techniques. Nevertheless, a definitive assignment of all signals needs the use of several NMR techniques as follows: i) DEPT experiments to determine the number of protons attached to each carbon atom; ii) HSQC spectra to determine the ^{13}C resonances of the tertiary, secondary and primary carbons; iii) HMBC sequences to assign the signals of quaternary carbons via two-bond and three-bond interactions; and iv) NOESY experiments to determinate the preferred conformation in solution.

Tables 2 and 3 show the ^{1}H NMR signals of each proton for compounds **1-34**, whereas Tables 4 and 5 show the corresponding ^{13}C NMR chemical shifts for the same molecules. The NMR spectra of the intermediate compounds were carried out in $CDCl_3$ solution, except for compound **2**, which was registered in CD_3OD. The NMR spectra of the final compounds were carried out in CD_3OD solution, except for compounds **19**, **20**, **22**, and **24**, which were accomplished in$CDCl_3$. For this reason, some significant variations are observed in the chemical shifts depending of the solvent.

Table 2. ^{1}H NMR signal assignments of compounds **1-17**

Comp	H-1	H-3	H-1'a	H-1'b	H-2'a	H-2'b	H-3'	H-3''	H-4''	H-5''	H-6''	OH	OCH_3
1	n.o.	n.o.	3.50 (m)	2.86 (m)	2.05 (m)	1.80 (m)	5.37 (d, 9.3)	7.94 (m)	7.66 (m)	7.40 (m)	7.94 (m)	4.36 (bs)	-
2[a]	n.o.	n.o.	3.67 (m)	3.45 (m)	2.21 (m)	1.95 (m)	5.29 (m)	7.93 (m)	7.72 (m)	7.50 (m)	7.93 (m)	n.o.	-
3	6.25 (bs)	6.15 (bs)	4.30 (m)	3.50 (m)	2.05 (m)	1.80 (m)	5.35 (d, 9.8)	7.94 (dd, 2.1, 8.2)	7.65 (m)	7.41 (m)	7.90 (dd, 1.1, 7.9)	4.30 (m)	-
4	n.o.	n.o.	3.90 (m)	3.53 (m)	2.07 (m)	1.77 (m)	5.51 (d, 9.7)	8.09 (d, 9.1)	6.87 (dd, 2.8, 9.1)	-	7.43 (d, 2.8)	4.39 (bs)	3.94(s)
5	6.21 (bs)	6.14 (bs)	4.38 (m)	3.49 (m)	2.03 (m)	1.73 (m)	5.48 (d, 10.3)	8.07 (d, 9.1)	6.84 (dd, 2.9, 9.1)	-	7.40 (d, 2.9)	4.38 (m)	3.91 (s)
6	6.33 (bs)	6.33 (bs)	3.47 (m)	3.47 (m)	2.01 (m)	1.71 (m)	5.38 (dd, 1.8, 10.1)	7.93 (m)	7.36 (dd, 2.1, 8.6)	-	7.93 (m)	4.36 (bs)	-
7	6.37 (bs)	6.37 (bs)	3.58 (m)	3.45 (m)	2.01 (m)	1.67 (m)	5.38 (d, 9.9)	7.90 (m)	7.35 (dd,2.4, 8.7)	-	7.90 (m)	4.34 (bs)	-
8	6.36 (bs)	6.36 (bs)	3.55 (m)	3.55 (m)	2.04 (m)	1.71 (m)	5.41 (d, 10)	7.95 (m)	7.38 (dd, 2.4, 8.7)	-	7.95 (m)	4.38 (bs)	-
9	n.o.	n.o.	3.78 (m)	3.50 (m)	1.97 (m)	1.65 (m)	5.30 (dd, 2.3, 10.2)	7.90 (m)	7.63 (m)	7.37 (m)	7.90 (m)	4.30 (m)	-
10	4.78 (bs)	4.78 (bs)	3.80 (m)	3.17 (m)	1.98 (m)	1.64 (m)	5.30 (dd, 2.1, 10.3)	7.90 (m)	7.62 (m)	7.38 (m)	7.90 (m)	n.o.	-
11	n.o.	n.o.	3.80 (m)	3.23 (m)	1.99 (m)	1.69 (m)	5.34 (dd, 2.2, 10.3)	7.90 (m)	7.61 (m)	7.48 (m)		n.o.	-
12	n.o.	n.o.	3.83 (m)	3.20 (m)	1.98 (m)	1.58 (m)	5.45 (dd, 2.1, 10.2)	8.03 (d, 9.2)	6.82 (dd, 2.8, 9.2)	-	7.41 (d, 2.8)	n.o.	3.90 (s)
13	4.73 (bs)	4.73 (bs)	3.77 (m)	3.22 (m)	1.97 (m)	1.56 (m)	5.45 (d, 9.4)	8.08 (d, 9.1)	6.85 (dd, 2.8, 9.1)	-	7.41 (d, 2.8)	n.o.	3.89 (s)
14	n.o.	n.o.	3.80 (m)	3.20 (m)	1.97 (m)	1.60 (m)	5.49 (dd, 2.0, 10.0)	8.02 (d, 9.1)	6.80 (dd, 2.8, 9.1)	-	7.38 (d,2.8)	n.o.	3.87 (s)
15	4.94 (bs)	4.94 (bs)	3.82 (m)	3.20 (m)	1.96 (m)	1.58 (m)	5.33 (dd, 2.0, 10.4)	7.90 (d, 8.7)	7.34 (dd, 2.4, 8.7)	-	7.93 (d, 2.4)	4.30 (bs)	-
16	n.o.	n.o.	3.83 (m)	3.18 (m)	1.96 (m)	1.58 (m)	5.32 (dd, 2.0, 10.4)	7.90 (d, 8.7)	7.34 (dd, 2.4, 8.7)	-	7.94 (d, 2.4)	n.o.	-
17	n.o.	n.o.	3.83 (m)	3.18 (m)	1.94 (m)	1.60 (m)	5.37 (dd, 2.1, 10.4)	7.89 (m)	7.34 (dd, 2.4, 8.7)	-	7.89 (m)	n.o.	-

[a]Solvent used CD_3OD.

Chemical shifts (in $CDCl_3$) are reported in δ (ppm) relative to $CDCl_3$; multiplicities and coupling constants (Hz) are given in parentheses.

^{1}H signals for the R_2 substituent: **1**, CH_3: 3.03 (s); **2**, CH_2CH_3: 3.33 (m), 1.30 (m); **3**, $CH_2CH_2CH_3$: 3.32 (m), 1.65 (m), 0.99 (t, 7.4); **4**, CH_3: 3.05 (s); **5**, $CH_2CH_2CH_3$: 3.33 (m), 1.66 (q, 7.4), 0.99 (t, 7.4); **6**, CH_3: 3.01 (s); **7**, CH_2CH_3: 3.58 (m), 1.26 (m); **8**,$CH_2CH_2CH_3$:3.55 (m), 1.71 (m), 1.01 (t, 7.4); **9** CH_2CH_3: 3.19 (m), 1.14 (t, 7.2); **10**, $CH_2CH_2CH_3$: 3.12 (t, 7.1), 1.52 (m), 0.91 (t, 7.4); **11**, Ph:7.37 (m), 7.22 (m), 7.02 (m); : **12**, CH_2CH_3: 3.20 (m), 1.15 (t, 7.2); **13**, $CH_2CH_2CH_3$: 3.14 (t, 7.4), 1.56 (m), 0.92 (t, 7.4); **14**,Ph:7.29 (m), 7.07 (m); **15**, CH_2CH_3: 3.20 (m), 1.15 (t, 7.2); **16**, $CH_2CH_2CH_3$: 3.13 (t, 7.0), 1.54 (m), 0.93 (t, 7.4); **17**, Ph:7.32 (m), 7.10 (m).

n.o., not observable; s, singlet; bs, broad singlet; d, doublet; dd, doublet doublet; t, triplet; m, multiplet.

Table 3. ^{1}H NMR signal assignments of compounds **18-34**

Comp	H-1	H-3	H-1'a	H-1'b	H-2'a	H-2'b	H-3'	H-3''	H-4''	H-5''	H-6''	OH	OCH_3
18[a]	n.o.	n.o.	3.38 (m)	3.38 (m)	1.99 (**m**)	1.99 (**m**)	4.72 (**dd**, 4.9, 8.6)	6.66 (d, 8)	6.95 (m)	6.61 (m)	7.06 (**d**, 7.6)	n.o.	-
19	6.43 (bs)	6.15 (bs)	3.92 (m)	3.41 (m)	2.18 (**m**)	1.95 (**m**)	4.78 (**dd**, 3.7, 9.9)	6.64 (**dd**, 1.2, 7.8)	7.06 (m)	6.71 (m)	7.06 (m)	n.o.	-
20	6.38 (bs)	6.15 (bs)	3.91 (m)	3.49 (m)	2.19 (**m**)	1.94 (**m**)	4.78 (m)	6.64 (**d**, 7.9)	7.06 (m)	6.71 (m)	7.06 (m)	3.91 (m)	-
21[a]	n.o.	n.o.	3.79 (m)	3.79 (m)	2.08 (**m**)	2.08 (**m**)	4.92 (d, 6.8)	6.83 (**d**, 8.7)	6.93 (dd, 2.8, 8.7)	-	6.98 (**d**, 2.8)	n.o.	3.82 (s)
22	6.50 (bs)	6.20 (bs)	3.58 (m)	3.58 (m)	2.13 (**m**)	1.94 (**m**)	4.77 (**dd**, 3.5, 9.8)	6.62 (**d**, 8.5)	6.66 (dd, 2.8, 8.5)	-	6.69 (**d**, 2.8)	n.o.	3.72 (s)
23[a]	n.o.	n.o.	3.36 (m)	3.36 (m)	2.05 (**m**)	2.05 (**m**)	4.80 (**dd**, 5.9, 7.4)	6.72 (**d**, 8.5)	7.02 (dd, 2.5, 8.5)	-	7.18 (**d**, 2.5)	n.o.	-
24	n.o.	n.o.	4.45 (m)	4.30 (m)	2.10 (**m**)	1.92 (**m**)	4.76 (**dd**, 3.2, 10.5)	6.56 (**d**, 8.5)	7.00 (m)	-	7.05 (**d**, 2.5)	n.o.	-
25[a]	n.o.	n.o.	3.66 (m)	3.51 (m)	2.00 (**m**)	2.00 (**m**)	4.74 (**dd**, 5.6, 7.8)	6.67 (**d**, 8.5)	6.96 (dd, 2.5, 8.5)	-	7.13 (**d**, 2.5)	n.o.	-
26[a]	n.o.	n.o.	3.24 (m)	3.24 (m)	1.95 (m)	1.95 (**m**)	4.75 (**dd**, 5.2, 8.6)	6.71 (**d**, 7.8)	7.01 (m)	6.67 (m)	7.09 (**d**, 7.4)	3.31 (**bs**)	-
27[a]	n.o.	n.o.	3.28 (m)	3.22 (m)	2.01 (**m**)	1.94 (**m**)	4.76 (**dd**, 5.0, 8.7)	6.71 (**d**, 7.8)	7.02 (m)	6.68 (m)	7.11 (**d**, 7.3)	n.o.	-
28[a]	n.o.	n.o.	3.37 (m)	3.27 (m)	2.02 (**m**)	2.02 (**m**)	4.80 (**dd**, 5.1, 8.6)	6.72 (**d**, 8.0)	7.02 (m)	6.68 (m)	7.12 (**d**, 7.6)	n.o.	-
29[a]	n.o.	n.o.	3.30 (m)	3.23 (m)	1.94 (**m**)	1.94 (**m**)	4.76 (**dd**, 5.1, 8.4)	6.71 (**d**, 8.6)	6.67 (dd, 2.9, 8.6)	-	6.79 (**d**, 2.9)	n.o.	3.73 (s)
30[a]	n.o.	n.o.	3.30 (m)	3.30 (m)	1.99 (**m**)	1.99 (**m**)	4.81 (**dd**, 5.6, 7.9)	6.76 (**d**, 8.5)	6.71 (dd, 2.7, 8.5)	-	6.83 (**d**, 2.7)	n.o.	3.78 (s)
31[a]	n.o.	n.o.	3.38 (m)	3.33 (m)	1.99 (**m**)	1.99 (**m**)	4.79 (**dd**, 5.4, 8.1)	6.70 (**d**, 8.6)	6.65 (dd, 2.8, 8.6)	-	6.79 (**d**, 2.8)	n.o.	3.31 (s)
32[a]	n.o.	n.o.	3.29 (m)	3.29 (m)	1.91 (**m**)	1.91 (**m**)	4.71 (**dd**, 5.9, 7.5)	6.67 (**d**, 8.5)	6.97 (dd, 2.5, 8.5)	-	7.10 (**d**, 2.5)	n.o.	-
33[a]	n.o.	n.o.	3.21(m)	3.21 (m)	1.83 (**m**)	1.83 (**m**)	4.70 (**dd**, 3.7, 10.1)	6.59 (**d**, 8.0)	6.96 (dd, 2.5, 8.0)	-	7.03 (**d**, 2.5)	n.o.	-
34[a]	n.o.	n.o.	3.38 (m)	3.29 (m)	1.97 (**m**)	1.97 (**m**)	4.76 (**dd**, 5.5, 8.0)	6.67 (**d**, 8.5)	6.97 (m)	-	7.13 (**d**, 2.5)	n.o.	-

[a]Solvent used CD_3OD.
Chemical shifts (in $CDCl_3$) are reported in δ (in ppm) relative to $CDCl_3$; multiplicities and coupling constants (Hz) are given in parentheses.
^{1}H signals for the R_2 substituent: **18**, CH_3: 2.90 (s); **19**, CH_2CH_3: 3.33 (m), 1.19 (t, 7.2); **20**, $CH_2CH_2CH_3$: 3.25 (**m**), 1.58 (m), 0.94 (t, 7.4); **21**, CH_3: 2.98 (s); **22**, $CH_2CH_2CH_3$: 3.27 (m), 1.59 (m), 0.95 (**t**, 7.4); **23**, CH_3: 2.97 (s); **24**, CH_2CH_3: 4.21 (m), 1.28 (t, 7.2); **25**, $CH_2CH_2CH_3$: 3.43 (m), 1.58 (**m**), 0.94 (t, 7.4); **26**, CH_2CH_3: 3.13 (q, 7.3), 1.09 (t, 7.2); **27**, $CH_2CH_2CH_3$: 3.08 (t, 7.1), 1.51 (m), 0.93 (**t**, 7.3); **28**, Ph: 7.34 (m), 7.23 (**m**), 6.97 (m); **29**, CH_2CH_3: 3.15 (q, 7.2), 1.11 (**t**, 7.2); **30**, $CH_2CH_2CH_3$: 3.13 (**t**, 7.1), 1.55 (**m**), 0.98 (t, 7.4); **31**, Ph: 7.33 (m), 7.24 (**m**), 6.96 (m); **32**, CH_2CH_3: 3.20 (m), 1.09 (t, 7.2); **33**, $CH_2CH_2CH_3$: 3.21 (m), 1.50 (**m**), 0.92 (t, 7.4); **34**, Ph: 7.34 (m), 7.24 (m), 6.97 (**m**).
n.o., not observable; **s**, singlet; **bs**, broad singlet; **d**, doublet; **dd**, doublet doublet; **t**, triplet; **q**, quadruplet; **m**, multiplet.

Table 4. ^{13}C NMR chemical shifts of compounds **1-17**

Compound	C-2	C-1'	C-2'	C-3'	C-1''	C-2''	C-3''	C-4''	C-5''	C-6''	OCH_3
1	182.69	42.09	38.92	66.09	146.98	140.26	124.61	134.13	128.09	128.26	-
2[a]	185.83	44.33	38.48	66.13	147.37	140.47	123.87	133.30	127.72	128.00	-
3	181.91	42.16	38.83	66.26	147.10	140.18	124.60	134.07	128.12	128.24	-
4	181.77	42.04	38.62	66.22	144.04	139.51	127.70	113.55	164.22	111.97	55.98
5	182.16	42.41	39.08	66.60	144.37	139.96	128.09	113.93	164.61	112.37	56.36
6	182.41	41.79	38.84	66.67	142.57	144.83	126.15	128.07	140.79	128.44	-
7	181.45	41.75	38.80	66.69	142.53	144.90	126.09	128.02	140.71	128.44	-
8	181.57	41.76	38.89	66.65	142.58	144.88	126.10	128.02	140.72	128.46	-
9	159.61	36.96	39.70	65.91	147.06	140.46	124.18	133.70	127.65	128.18	-
10	159.87	37.11	39.95	66.05	147.28	140.61	124.32	133.82	127.78	128.35	-
11	157.62	37.20	39.07	66.39	147.07	140.20	124.30	133.75	127.82	128.42	-
12	159.78	37.17	39.73	66.35	144.63	139.86	127.57	113.59	164.23	112.02	56.06
13	159.77	37.29	39.28	66.39	144.46	139.70	127.39	113.38	164.05	111.95	55.89
14	157.52	37.04	39.07	66.53	144.30	139.62	127.52	113.42	164.10	111.91	55.89
15	159.65	36.86	39.76	65.66	142.88	145.07	125.89	127.80	140.53	128.53	-
16	159.75	36.86	39.81	65.63	142.85	145.07	125.89	127.79	140.54	128.52	-
17	157.65	36.89	39.32	65.90	142.67	144.98	126.00	127.91	140.61	128.44	-

[a]Solvent used CD_3OD.

δ (ppm) relative to $CDCl_3$. ^{13}C signals for the R_2 substituent: **1**, CH_3:29.93; **2**, CH_2CH_3: 36.70, 11.87; **3**, $CH_2CH_2CH_3$: 45.65, 22.20, 11.55; **4**, CH_3: 30.31; **5**, $CH_2CH_2CH_3$: 45.88, 22.46, 11.81; **6**, CH_3: 30.29; **7**, CH_2CH_3: 38.68, 13.99; **8**, $CH_2CH_2CH_3$: 45.67, 22.10, 11.41; **9**, CH_2CH_3: 35.56, 15.27; **10**, $CH_2CH_2CH_3$: 42.67, 23.43, 11.42; **11**, Ph: 137.84, 129.36, 121.81, 121.04; **12**, CH_2CH_3: 35.77, 15.43; **13**, $CH_2CH_2CH_3$: 42.61, 23.15, 11.23; **14**, Ph: 138.15, 129.28, 124.12, 121.52; **15**, CH_2CH_3: 35.65, 15.25; **16**, $CH_2CH_2CH_3$: 42.60, 23.25, 11.27; **17**, Ph: 137.76, 129.43, 124.64, 122.09.

Table 5. ^{13}C NMR chemical shifts of compounds **18-34**

Compound	C-2	C-1'	C-2'	C-3'	C-1''	C-2''	C-3''	C-4''	C-5''	C-6''	OCH_3
18[a]	181.71	42.10	37.64	72.55	130.83	147.42	119.16	130.29	120.45	129.13	-
19	181.25	42.09	34.69	71.12	127.08	144.70	116.96	127.12	118.54	128.67	-
20	181.61	42.13	34.82	71.35	127.18	144.91	117.06	127.22	118.62	128.83	-
21[a]	182.41	38.38	36.51	72.27	131.26	134.34	121.11	115.91	155.80	114.99	57.35
22	181.63	42.21	35.18	70.78	129.60	137.56	118.71	113.95	153.16	113.07	55.92
23[a]	181.67	41.16	34.81	69.08	129.94	143.62	117.36	126.02	121.99	127.15	-
24	182.70	40.64	34.73	69.25	128.98	142.94	118.03	126.75	123.14	128.17	-
25[a]	181.17	41.24	34.85	69.15	129.93	143.63	117.35	126.02	121.98	127.14	-
26[a]	159.98	37.00	35.90	70.07	128.19	144.89	116.47	127.56	117.67	126.54	-
27[a]	161.53	38.43	37.35	71.52	129.61	146.32	117.90	128.99	119.09	127.97	-
28[a]	160.84	40.65	39.40	74.02	131.92	148.58	120.22	131.30	121.42	130.27	-
29[a]	161.40	38.39	37.67	70.94	131.79	139.07	119.39	114.52	154.32	113.66	56.09
30[a]	160.09	36.97	36.26	69.55	130.33	137.70	117.95	113.13	152.88	112.27	54.70
31[a]	157.13	36.92	36.01	69.77	130.37	137.64	118.02	113.14	152.92	112.25	54.67
32[a]	159.97	36.91	35.94	69.22	130.15	143.45	117.48	126.11	122.11	127.10	-
33[a]	159.99	36.92	35.93	69.32	130.23	143.54	117.58	126.11	122.15	127.15	-
34[a]	157.14	36.89	35.65	69.44	130.01	143.71	117.38	126.10	121.94	127.13	-

[a]Solvent used CD_3OD.

δ (ppm) relative to $CDCl_3$. ^{13}C signals for the R_2 substituent: **18**, CH_3: 32.02; **19**, CH_2CH_3: 38.87, 14.18; **20**, $CH_2CH_2CH_3$: 46.03, 22.31, 11.55; **21**,CH_3: 31.05; **22**, $CH_2CH_2CH_3$: 45.94, 22.33, 11.56; **23**, CH_3: 29.30; **24**,CH_2CH_3: 46.39, 14.10; **25**, $CH_2CH_2CH_3$: 45.56, 21.98, 10.20; **26**, CH_2CH_3: 34.41, 14.34; **27**, $CH_2CH_2CH_3$: 42.88, 24.47, 11.62; **28**, Ph: 143.26, 132.04, 125.67, 122.55; **29**, CH_2CH_3: 35.85, 15.76; **30**, $CH_2CH_2CH_3$: 41.47, 23.04, 10.19; **31**, Ph: 139.55, 128.35, 121.99, 118.87; **32**, CH_2CH_3: 34.43, 14.33; **33** ,$CH_2CH_2CH_3$: 42.83, 22.58, 10.46; **34**, Ph: 139.52, 128.36, 122.02, 118.90.

^{1}H NMR signals (H-1' and H-2') and ^{13}C NMR signals (C-2, C-1', C-2', C-4'' and C-6'') are similar in both, intermediate and final compounds: *N*-alkyl or aryl-*N*'-[3-hydroxy-3-(2-nitro-5-substitutedphenyl)propyl]-thioureas and ureas **1-17**, and *N*-alkyl and aryl-*N*'-[3-(2-amino-5-substitutedphenyl)-3-hydroxypropyl]-thioureas or ureas **18-34**; however, H-3', H-3''-H-6'', C-3', C-1''-C-3'' and C-5''are influenced by the activating and deactivating effects of the amine or nitro groups, respectively. C-2 of the main chain is influenced by the sulfur or oxygen atoms present in the thiourea or urea rest, but not by the nitro or amino group. Finally, H-1 and H-3 signals, linked to nitrogen atoms, do not follow the same pattern and sometimes are not visible.

HSQC and HMBC experiments were performed on some compounds of each series, and the results of these experiments have been extrapolated to the other compounds. Table 6 shows the HSQC correlations for compounds **3**, **5**, **8**, **9**, **12**, **15**, **19**, **22**, **24**, **26**, **30** and **32**, whereas Figure 1 shows the more important connectivities found in the HMBC spectra of compounds **5**, **9**, **12**, **18**, **29** and **32**.

HSQC experiments performed on compounds **3**, **5**, **8**, **9**, **12** and **15** allowed the assignment of the secondary carbon atoms chemical shifts C-1' and C-2', and the assignment of the tertiary carbon atoms chemical shifts C-3', C-3'', C-4'', C-5'' and C-6'' in the nitro derivatives **1-17**. These atoms show signals in ranges of 36.86-44.33 (C-1'), 38.48-39.95 (C-2'), 65.63-66.69 (C-3'), 123.87-128.09 (C-3''), 113.38-134.13 (C-4''), 127.65-164.61 (C-5'') and 111.91-128.53 (C-6'').

Similar HSQC experiments performed on compounds **19**, **22**, **24**, **26**, **30** and **32** indicate that the ^{13}C NMR signals for the analogue secondary and tertiary carbon atoms in the final amino-phenyl derivatives **18-34** are in the following ranges: 36.89-42.21 (C-1'), 34.69-39.40 (C-2'), 69.08-74.02 (C-3'), 117.06-121.11 (C-3''), 113.13-131.30 (C-4''), 117.67-155.80 (C-5'') and 112.25-130.27 (C-6'').

The quaternary carbons signals were confirmed by HMBC spectra on the intermediate (**5**, **9** and **12**) and final (**18**, **29** and **32**) compounds. For clarity, only some connectivities found in the HMBC spectra are illustrated in Figure 1. In compound **3**, correlations between H-6'' (δ 7.90) and H-5'' (δ 7.41), and the ^{13}C at 147.10 ppm, and between H-3'' (δ 7.94) and H-4'' (δ 7.65), and the ^{13}C signal at 140.18 ppm allowed the unequivocal assignment of C-1'' and C-2'', respectively. Correlation between H-1'b (δ 3.50) and the peak at 181.91 ppm allows the assignment of this shift to C-2. In addition, HMBC spectrum of compound **5** indicates a correlation between OCH_3 (δ 3.91) and the ^{13}C at δ 164.61 ppm, that can be assigned to C-5''. In a similar way, in compound **9**, the correlation of H-5'' (δ 7.37) and H-3' (δ 5.30) with ^{13}C at 147.06 indicated that this shift corresponds to C-1''. Also, when a ^{13}C at 140.46 ppm correlated with H-3'' (δ 7.90), H-4'' (δ 7.63) and H-3' (δ 5.30), it can be identified as C-2''. Regarding C-2, it corresponds to a signal appearing at 159.61 ppm due to the correlation with H-1'b (δ 3.50) and $C\underline{H}_2CH_3$ (δ 3.19). Moreover, in compound **12** spectrum, H-3'' (δ 8.03), H-6'' (δ 7.41) and OMe (δ 3.90) have a correlation with ^{13}C at 164.23 thus it can be assigned to C-5''.

Table 6. HSQC correlations found for compounds **3**, **5**, **8**, **9**, **12**, **15**, **19**, **22**, **24**, **26**, **30** and **32**

$^{1}H/^{13}C$	**3**	**5**	**8**	**9**	**12**	**15**	**19**	**22**	**24**	**26**	**30**	**32**
H-1'	3.50, 2.05	4.38, 3.49	3.55	3.78, 3.50	3.83, 3.20	3.82, 3.20	3.92, 3.41	3.58	4.45, 4.30	3.24	3.30	3.29
C-1'	42.16	42.41	41.76	36.96	37.17	36.86	42.09	42.21	40.64	37.00	36.97	36.91
H-2'	2.05, 1.80	2.03, 1.73	2.04, 1.71	1.97, 1.65	1.98, 1.58	1.96, 1.58	2.18, 1.95	2.13, 1.94	2.10, 1.92	1.95	1.99	1.91
C-2'	38.83	39.08	38.89	39.70	39.73	39.76	34.69	35.18	34.73	35.90	36.26	35.94
H-3'	5.35	5.48	5.41	5.30	5.45	5.33	4.78	4.77	4.76	4.75	4.81	4.71
C-3'	66.26	66.60	66.65	65.91	66.35	65.66	71.12	70.78	69.25	70.07	69.55	69.22
H-3''	7.94	8.07	7.95	7.90	8.03	7.90	6.64	6.62	6.56	6.71	6.76	6.67
C-3''	124.60	124.09	126.10	124.18	127.57	124.32	125.89	116.96	118.71	118.03	116.71	117.95	117.48
H-4''	7.65	6.84	7.38	7.63	6.82	7.34	7.06	6.66	7.00	7.01	6.71	6.97
C-4''	134.07	113.93	128.02	133.70	113.59	127.80	127.12	113.95	126.75	127.56	113.13	126.11
H-5''	7.41			7.37			6.71			6.67		
C-5''	128.12			127.65			118.54			117.67		
H-6''	7.90	7.40	7.95	7.90	7.41	7.93	7.06	6.69	7.05	7.09	6.83	7.10
C-6''	128.24	112.37	128.46	128.18	112.02	128.53	128.67	113.07	128.17	126.54	112.27	127.10

HMBC experiment performed on compound **18** indicates that the signals at δ 6.66 (H-3''), 6.61 (H-5") and 4.72 (H-3') are correlated with the ^{13}C signal at 130.83 ppm, which can be assigned to C-1'', whereas H-6" signal (δ 7.06) and H-4" signal (δ 6.95) are correlated with the ^{13}C signal at δ 147.42 ppm, thereby, this signal corresponds to C-2''. Besides, in compound **29**, correlations of H-3" signal (δ 6.71),H-3' signal (δ 4.76) and H-2' (δ 1.94) with ^{13}C signal at 131.79 ppm indicate that this signal can be designated as C-1". Similarly, correlations of H-6" (δ 6.79) and H-3' (δ 4.76) signals with ^{13}C signal at 139.07 ppm demonstrate that this signal corresponds to C-2". The correlation between OMe (δ 3.73) and ^{13}C signal at 56.09 ppm allowed the assignment of this peak to C-5". Finally, H-1'a (δ 3.30), H-1'b (δ 3.23) and $C\underline{H_2}CH_3$ (δ 3.15) are correlated with the peak at 161.40 ppm, thus is identified as C-2. Lastly, HMBC experiment on the urea **32** demonstrates that H-3" (δ 6.67), H-3' (δ 4.71) and H-2' (δ 1.91) are correlated with the ^{13}C at 130.15 which corresponds to C-1'', whereas H-6" (δ 7.10), H-4" (δ 6.97) and H-3' (δ 4.71) are correlated with the peak at 143.45 ppm that can be assigned to C-2". Moreover, correlations between H-6" (δ 7.10) and H-3" (δ 6.67), and a signal at 122.11 ppm indicates that this signal corresponds to C-5". Finally, the peak at 159.97 ppm which is correlated with H-1' (δ 3.29) and $C\underline{H_2}CH_3$ (δ 3.20) is identified as C-2.

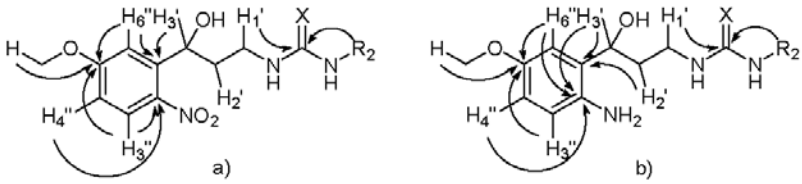

Figure 1. Important connectivities found in the HMBC spectra of compounds a) **1-17** and b) **18-34**.

These compounds have been designed from a series of 1-(3-(2-amino-5-substitutedphenyl)-3-oxopropyl)-3-alkylthioureas and ureas previously synthesized by our research group,[14] by substitution of the carbonyl group by a hydroxyl one. The main differences between the ^{13}C chemical shifts of the previous derivatives[14] and the new hydroxypropylthioureas and ureas are the ^{13}C signals of the propyl chain (C-1', C-2' and mainly C-3') and the C-1'' of the aromatic ring. The C-1' atom in the hydroxypropyl derivatives shows signals in range of 36.9-44.3 ppm, whereas for the oxopropyl compounds the range is 34.8-40.3 ppm; the C-2' atom in the first compounds appears between 38.5-39.9 ppm, and in the second compounds the range is between 38.5-44.5 ppm; the C-3' atom in the hydroxylpropyl derivatives shows signals in range of 65.6-66.7, and in the oxopropyl molecules fluctuates between 200.9-202.8 ppm, due to the change of a hydroxyl group by a carbonyl one; finally, the C-1'' in this new compounds appears in the range of 139.5-144.9 (in the nitro-derivatives) and between 127.1-131.9 (in the amine-derivatives), and in the structures with an oxopropyl residue the range is 134.5-137.8 (in the nitro-derivatives) and 117.5-119.9 (in the amine-derivatives).

2d-NOESY experiments performed on compound **25** (R_1 = Cl, R_2 = Pr, X = S) show the existence of the NOE effects between the aromatic H-6'' and the H-2' of the lineal chain, and vice versa. Also, another NOE effect is observed between H-6'' and H-3'. These NOE effects are only compatible with the formation of an intra-molecular hydrogen bond between the hydroxyl group of the C-3' and the amino group in 2''-position of the aromatic ring.

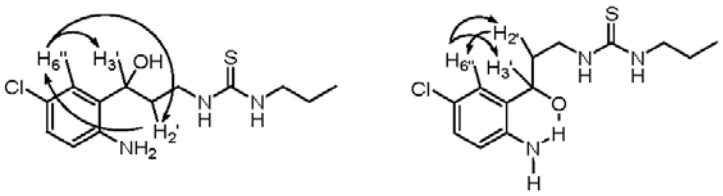

Figure 2. Selected NOESY correlations for **25**.

Acknowledgements

This work was partially supported by the Instituto de Salud Carlos III through the grant FI11/00432.

References

[1] S. R. M. J. Moncada, R. M. L. Palmer, E. Higgs. *Pharmacol. Rev.* **1991**, 43, 109-142.
[2] Zhou, L.; Zhu D-Y. *Nitric Oxide-Biol. Chem.* **2009**, 20, 223-230.
[3] J. T. Groves, C. C. Wang. *Curr. Opin. Chem. Biol.* **2000**, 4, 687-695.
[4] F. Aktan. *Life Sci.* **2004**, 75, 639-653.
[5] D. M. Wilcock, M. R. Lewis, W. E. Van Nostrand, J. Davis, M. L. Previti, N. Gharkholonarehe, M. P. Vitek, C. A.Colton. *J. Neurosci.* **2008**, 28, 1537-1545.
[6] V. Calabrese, C. Mancuso, M.Calvani, E.Rizzarelli, D. A. Butterfield, A. m. G. Stella. *Nat. Rev. Neurosci.***2007**, 8, 766-775.
[7] A. W. Deckel, *J. Neurosci. Res.* **2001**, 64, 99-107.
[8] K. D. Kröncke, K. Fehsel, V. Kolb-Bachofen. *Clin. Exp. Pharmacol. Physiol.* **1998**, 113, 147-156.
[9] M. Lechner, P. Lirk, J. Rieder. *Seminars in cancer biology* **2005**, Vol. 15, No. 4, 277-289. Academic Press.
[10] R. Zamora, Y. Vodovotz, T. R. Billiar. *Mol. Med.* **2000**, 6, 347-373.
[11] S. Taddei, A. Virdis, L. Ghiadoni, I. Sudano, A. Salvetti. *J. Cardiovasc. Pharmacol.* **2001**, 38, S11-S14.
[12] C. Napoli, F. de Nigris, S. Williams-Ignarro, O. Pignalosa, V. Sica, L. J. Ignarro. *Nitric oxide* **2006**, 15, 265-279.
[13] M. Chayah, M. E. Camacho, M. D. Carrión, M. A. Gallo, M. Romero, J. Duarte. *MedChemComm* **2015**. (submited)
[14] M. Chayah, M. D, Carrión, M. A. Gallo, R. Jiménez, J. Duarte, M. E. Camacho. *ChemMedChem* **2015**, 10, 874-882.

4. CONCLUSIONES, LIMITACIONES Y PERSPECTIVAS DE FUTURO

4.1 Conclusiones

El aumento de la incidencia de las enfermedades relacionadas con el NO, como Párkinson, Alzheimer, esclerosis lateral amiotrofica, corea de Huntington, choque séptico o artritis reumatoide, entre otras, hace imprescindible y urgente la búsqueda de soluciones terapéuticas para tratar dichas patologías. En este contexto, esta investigación intenta contribuir a la búsqueda de dichas soluciones mediante la inhibición de la NOS, siendo sus principales conclusiones las siguientes:

1. En la presente tesis doctoral, se han diseñado, sintetizado y caracterizado de forma inequívoca, mediante el uso combinado de técnicas espectroscópicas de RMN (^{1}H, ^{13}C, DEPT y $^{1}H/^{13}C$), espectrometría de masas y análisis elemental, cincuenta compuestos finales que se distribuyen en tres familias estructurales:

   a. La primera familia incluye dieciocho compuestos finales con estructura pirazolínica, en la que los sustituyentes del anillo aromático (Cl, OCH_3) se han introducido en posiciones 5-, 4,5- y 2,3,4- y los sustituyentes de la cadena lateral fueron ciclopropilo, fenilo, bencilo y fenetilo.

   b. La segunda familia comprende quince compuestos finales con estructura kinurenamínica con restos de urea o tiourea. Los sustituyentes en R_1 (Cl, OCH_3) se han introducido en posición 5- del fenilo. En R_2 se ha introducido una cadena alquílica de Me, Et o Pr.

   c. La tercera familia engloba diecisiete compuestos finales derivados de 3-hidroxipropil urea y tiourea. Los sustituyentes en R_1 son los mismos que en la familia anterior, y en R_2 se han introducido restos de Me, Et, Pr y Ph.

2. Para la síntesis de los derivados de la tercera familia se ha puesto a punto una nueva ruta sintética que puede ser aplicada a los derivados kinurenamínicos con restos de urea y tiourea, lo que permite acortar la síntesis de 8 a 5 pasos y duplicar el rendimiento global.

3. La variación de metodología, mediante el uso de MW, para la formación de ureas y tioureas en la tercera familia ha permitido acortar el tiempo de reacción (de 18 h a 20 min) manteniendo un buen rendimiento (entre 70 y 90%), con respecto a la síntesis convencional llevada a cabo en la segunda serie de derivados.

4. Todos los productos finales sintetizados han sido ensayados *in vitro* como posibles inhibidores de las isoformas neuronal e inducible de la NOS. Los compuestos más interesantes de las dos últimas familias, **5n** y **4g**, han sido ensayados también frente a eNOS, demostrándose la ausencia de efectos adversos relacionados con la hipertensión.

5. Los resultados de las pruebas biológicas demuestran, en general, una moderada actividad inhibitoria de las tres familias frente a las isoformas nNOS e iNOS. Las conclusiones respecto a este punto se detallan, a continuación, para cada familia:

a. Los derivados pirazolínicos han demostado, en general, mejor inhibición frente a la isoforma neuronal. Esta inhibición se favorece con sustituyentes electrón-donantes (OCH_3) en R_1, siendo el compuesto **3r**, con tres grupos metoxilo en el anillo aromático, el mejor inhibidor con moderada selectividad hacia nNOS. El aumento del volumen y la flexibilidad de R_2 favorecen también esta inhibición.

b. Las kinurenamino-ureas y tioureas han presentado, generalmente, mayor afinidad por la isoforma inducible y, en concreto, las que llevan un

resto de urea. Los compuestos clorados han sido los más activos, destacando la urea 5n con una CI50 de 100 µM frente a iNOS y sin actividad frente a eNOS.

c. Principalmente, los compuestos de la tercera familia presentan mejores valores de inhibición frente a nNOS. Los derivados tioureicos han sido más activos que los ureicos, destacando **4g** con una CI_{50} de 130 y 180 µM frente a nNOS e iNOS, respectivamente, estando desprovisto de actividad frente a eNOS.

6. Los estudios de modelado molecular llevados a cabo sobre las tres familias permitieron entender mejor su posible interacción con la enzima y justificar así sus actividades biológicas:

a. Respecto a las nuevas pirazolinas, el estudio de docking ha permitido comprobar que el volumen de R_1 así como el volumen y longitud de R_2 influyen en la orientación y la disposición de los compuestos en el sitio de unión. Además, la conformación de Arg260 en iNOS y Arg481 en nNOS y, en consecuencia, la conformación de otros residuos en ambos centros activos, parecen ser decisivas en la interacción con la enzima, así como en la orientación de los compuestos en el sitio de unión.

b. Los estudios de docking y de dinámica molecular realizados en la segunda familia han demostrado la importancia del fenilo, del grupo amino unido a éste y de la urea en la interacción con la enzima a través de diferentes residuos del centro activo. Se ha comprobado también que la interacción del oxígeno de la urea con la Arg260 (iNOS) es fundamental para la selectividad en estos compuestos.

c. Los estudios de docking de los derivados de 3-hidroxipropil urea y tiourea han revelado que, además de la interacción del anillo aromático y

la del resto de tiourea con residuos del centro activo de nNOS, se establecen puentes de hidrógeno a través del grupo hidroxilo y el grupo amino, justificándose los mejores valores de inhibición que presentan algunos de estos derivados por dicha isoforma.

4.2 Limitaciones y perspectivas futuras

A pesar de que esta investigación permita mejorar los resultados obtenidos con anterioridad por nuestro grupo respecto a la inhibición de la NOS y ofrecer nuevas estrategias sintéticas, algunas limitaciones pueden destacarse y requieren futuras investigaciones para ser solventadas:

a. Aunque se ha supuesto que la inhibición ejercida por los compuestos descritos se produce a través de la interacción con el centro activo de la enzima, ningún experimento se ha llevado a cabo para confirmar esta hipótesis.

b. Los estudios computacionales representan una valiosa herramienta en el campo de la química farmacéutica pero aun así no dejan de ser estudios teóricos con cierto margen de error y su cumplimentación con estudios cristalográficos sería muy deseable para determinar realmente los puntos de interacción con la enzima y, en base a eso, realizar los cambios estructurales que se consideren oportunos.

c. Además de realizar los estudios computacionales con las isoformas neuronal e inducible, hubiera sido conveniente, también, llevarlos a cabo con la endotelial. Estos estudios aportarían más información respecto a la interacción de los compuestos con la enzima permitiendo analizar y explicar los resultados biológicos y establecer la influencia de la estructura en dicha interacción.

A pesar de estas limitaciones, los resultados obtenidos en este trabajo serán de gran ayuda para definir las líneas futuras de investigación. Continuar trabajando con el tipo de estructuras descritas, implica necesariamente determinar a qué nivel actúan, mediante estudios más profundos para encontrar moléculas no sólo más potentes sino también más selectivas de la nNOS, la iNOS o de ambas.

5. CONCLUSIONS, LIMITATIONS AND FUTURE PERSPECTIVES

5.1 Conclusions

1. In this thesis, fifty final products have been designed, synthesized and characterized by the combined use of NMR spectroscopy (^{1}H, ^{13}C, $^{1}H/^{13}C$) and mass spectrometry techniques as well as elemental analysis. They are divided into three structural families:

a. The first family includes eighteen final compounds with pirazoline structure in which the aromatic ring substituents (Cl, OCH_3) have been introduced in 5-, 4,5- and 2,3,4- positions, and the R_2 substituents were cycloprpyl, phenyl, benzyl and phenethyl.

b. The second family has fifteen final compounds with kynurenamine urea or thiourea structure. R_1 substituents (Cl, OCH_3) have been introduced in 5- position of the phenyl and an alkyl chain of Me, Et or Pr has been introduced as R_2.

c. The third family gathers seventeen final compounds 3-hydroxypropyl urea and thiourea based structure. R_1 is the same as for the previous family and R_2 can be a Me, Et, Pr or Ph group.

2. A new pathway has been reported for the synthesis of the third family. It can be applied to obtain kynurenamine-ureas and thioureas shortening the synthetic route from 8 to 5 steps and doubling the global yield.

3. The change of methodology using MW to form ureas and thioureas in the third family has shorten the reaction time (from 18h to 20 min) maintaining a good yield (70 to 90%), compared to the conventional synthesis carried out in the second series of derivatives and previous results described in literature.

4. All the synthesized final products have been tested *in vitro* as potential inhibitors of neuronal and inducible NOS isoforms. The most interesting compounds **5n** and **4g** have also been tested against eNOS demonstrating the absence of hypertension adverse effects.

5. The biological results show, in general, a moderate inhibitory activity against the three families against nNOS and iNOS isoforms. The findings on this point are detailed below for each family:

a. The pyrazoline derivatives have generally demonstrated better inhibition against the neuronal isoform. R_1 electron-donating substituents (OCH_3) improve this inhibition being the compound **3r**, with three methoxy groups, the best inhibitor with moderate selectivity for nNOS. Bulky and flexible R_2 also favor this inhibition.

b. The kynurenamine-urea and thiourea derivatives have mostly shown greater affinity for inducible isoform, in particular, the urea ones. Chlorinated compounds have been the most active. Among them, the urea **5n** stands with an IC_{50} of 100 µM being inactive against eNOS.

c. The third family of compounds has broadly shown more likely to inhibit nNOS. The thiourea derivatives have been more active than ureas, highlighting **4g** with an IC_{50} of 130 and 180 µM against nNOS and iNOS, respectively, and devoid of activity against eNOS.

6. Molecular modeling studies carried out on the three families allow understanding better their potential interactions with the enzyme and thus justifying their biological activities.

a. Regarding the new pyrazolines, docking study has shown that R_1 volume and R_2 volume and length influence the orientation and lay out of

the compounds in the binding site. Furthermore, the conformation of Arg260 and Arg481 in nNOS and iNOS, respectively, and therefore the conformation of other residues in both active sites appear to be crucial in the interaction with the enzyme as well as in the orientation of the compounds inside the binding site.

b. Regarding the new kynurenamines, docking study and molecular dynamics have shown the importance of the phenyl ring, the amino group and the urea in the interaction with the enzyme through different residues of the active site. It has also been found that the interaction of urea oxygen with Arg260 (iNOS) is essential for the selectivity in these compounds.

c. Docking studies of 3-hydroxypropyl urea and thiourea derivatives have revealed that, besides the interaction of the aromatic ring and the rest of thiourea with residues in the nNOS binding site, hydrogen bonds are established through the hydroxyl group and amino group, justifying the best inhibition values of several compounds versus this isoform.

5.2 Limitations and future perspectives

Despite this investigation improves the results previously obtained by our research group for NOS inhibition and offers new synthetic strategies, some limitations exist and require further research to be resolved:

a. Although it has been assumed that the inhibition exerted by the reported compounds occurs through interaction with the active site of the enzyme, no experiment has been conducted to confirm this hypothesis.

b. Computational studies are a valuable tool in the pharmaceutical chemistry field but even so they are still theoretical studies with a margin

of error. Thus, complementary crystallographic studies would be very desirable to actually determine the interaction spots with the enzyme and, based on that, make the structural changes deemed appropriate.

c. In addition to computational studies with neuronal and inducible isoforms, it would have been convenient, perform them also with the endothelial one. These studies would provide more information about the ligand-enzyme interaction allowing analyze and asses the biological results and establish the influence of the structure in such interaction.

Despite these limitations, the results obtained in this study will be helpful to define future research. Continue working with the reported structures types implies necessarily determine, by further studies, where they act, aiming to find not only more potent but also more selective molecules of nNOS, iNOS or both.

6. SUMMARY

6.1 Introduction

Nitric oxide (NO) is an inorganic free radical and an important biomessenger that regulates several physiological functions in the nervous, immune, and cardiovascular systems.[1]

NO is synthesized from the enzyme catalysis of L-arginine to L-citrulline in several cell types by a family of nitric oxide synthase (NOS) isoenzymes with consumption of molecular oxygen. Native NOS is a homodimeric enzyme. Each monomer consists of an *N*-terminal oxygenase domain with a catalytic heme active site and a cofactor tetrahydrobiopterin (BH_4) binding site, and a C-terminal electron-donating reductase domain binding flavin adenine dinucleotide (FAD), flavin mononucleotide (FMN), and nicotinamide adenine dinucleotide (NADPH).[2,3] The linker between the two functional domains is a calmodulin (CaM) binding motif that enables electron flow from the oxygenase domain to the reductase domain.[4]

In mammalians, three isoforms of NOS have been identified: neuronal (nNOS), endothelial (eNOS) and inducible NOS (iNOS)[5]. nNOS and eNOS are constitutive and regulated by intracellular Ca/CaM. They continually produce low levels of NO used for nerve function and blood regulation, respectively. While, iNOS produces large toxic bursts of NO to fight pathogens, and is not Ca-dependent.[6,7]

To exert appropriate functions, NO synthesis by the three isozymes is under tight regulation. Thus, overproduction of NO by nNOS has been associated with neurodegenerative disorders such as Alzheimer's, Párkinson's or Huntington's diseases,[8-10] and the inducible isoform seems to be responsible for the massive NO production in pathologies such as arthritis, colitis, tissue damage, cáncer or several inflammatory states.[11-13] The NO underproduction by eNOS has been associated with hypertension and atherosclerosis.[14,15]

Accordingly, inhibition of nNOS or iNOS, but not of eNOS, could provide an effective therapeutic approach.

Previously, our research group has described a series of nNOS inhibitors with a kynurenine **1**,[16] kynurenamine **2**,[17] or 4,5-dihydro-1H-pyrazole structure **3** (Figure 1).[18]

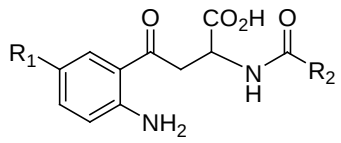

1

R_1 = OCH_3

R_2 = alkyl

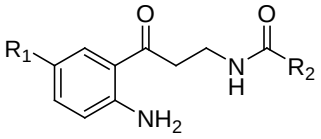

2

R_1 = Cl, OCH_3

R_2 = alkyl, cycloalkyl, phenyl

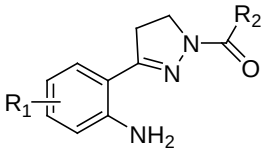

3

R_1 = H, Cl, OCH_3

R_2 = alkyl, cycloalkyl, phenyl

Figure 1. Derivatives synthesized by our research group.

6.2 Aims

The aim of this PhD dissertation is the development of potential NOS inhibitors. The design, synthesis and biological evaluation against the iNOS and nNOS isoforms of new pyrazolines and *N*,*N'*-disubstituted urea and thiourea derivatives is proposed.

The specific aims are the following:

1. Synthesis of the proposed compounds with their corresponding methodologies.

2. Unequivocally characterization of the synthesized molecules using one- and two-dimensional nuclear magnetic resonance (NMR) spectroscopy and high resolution mass spectrometry techniques (HRMS) as well as elemental analysis.

3. *In vitro* biological activity evaluation against nNOS and iNOS of all final products and against eNOS of the most active ones.

4. Assessment of the qualitative and quantitative structure-activity relationships (QSAR) of the three families of compounds.

5. Conducting molecular modeling studies to design and propose a binding mode for these new compounds to i/nNOS.

6.3 Results*

6.3.1 Pyrazoline derivatives

This family of compounds has been designed basing on the results of previous pyrazolines **3** (Figure 1) published by our group.[18] In these compounds, the activation and deactivation of the aromatic ring was increased, through R_1 substituents, keeping the cyclopropyl and phenyl groups in R_2, as well as changing the size and flexibility of the phenyl moiety (Figure 2)[19].

*In this section the compounds number used is the same that appears in the published articles corresponding to each family.

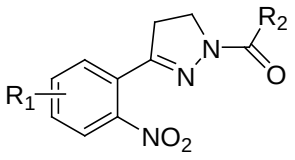

3

R_1 = H, 5-Cl, 4,5-Cl_2, 5-OMe, 4,5-$(OMe)_2$, 2,3,4-$(OMe)_3$

R_2 = *c*-C_3H_5, Ph, CH_2Ph, CH_2CH_2Ph

Figure 2. Pirazoline derivatives.

The *in vitro* biological results demonstrate that the increase of R_2 size substituent improves the iNOS, as well as the nNOS inhibitory activity. Nevertheless, regarding the R_1 substituent in the aromatic ring, electron-withdrawing groups enhance iNOS inhibition, whereas electron-donating substituents get better the nNOS inhibition. This fact is confirmed by docking studies which show the better orientation of **3h** (R_1 = 4,5-Cl_2, R_2 = CH_2CH_2Ph) in iNOS and **3r** (R_1 = 2,3,4-$(OMe)_3$, R_2 = CH_2CH_2Ph) in nNOS. This last derivative is the most active nNOS inhibitor of all the tested compounds (IC_{50} = 400 µM), with a good nNOS/iNOS selectivity.

6.3.2 Kynurenamine-urea and thiourea derivatives

These products were designed from kynurenamines **2**, carrying a urea or thiourea substituted group, isosteric to the final guanidine moiety of L-arginine, the natural substrate of NOS (Figure 3)[20,21].

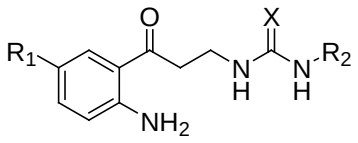

5

R_1 = H, OMe, Cl

R_2 = Me, Et, Pr

X = O, S

Figure 3. Kynurenamine-urea and thiourea derivatives.

In general, all compounds show, *in vitro*, better inhibition against iNOS than nNOS, being the chlorinated series the most active compounds. In addition, the urea residue seems to play an important role in compounds selectivity. Thioureas similarly inhibited both isoenzymes, while ureas selectively inhibited iNOS. The urea **5n** (R_1 = Cl, R_2 = Et, X = O) was the most active iNOS inhibitor with IC_{50} = 100. This was confirmed by docking and MD simulations studies, which showed the more favorable orientation of **5n** in iNOS establishing good interactions with the enzyme. Also, this compound did not inhibit eNOS, demonstrating the selectivity necessary to avoid the adverse effect of hypertension.

6.3.3 3-Hydroxypropyl urea and thiourea derivatives

These compounds have been designed by reduction of the kynurenamine-urea and thiourea derivatives carbonyl group **2** (Figure 4).

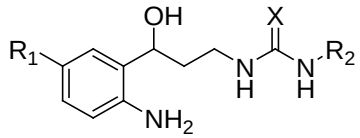

4

R_1 = H, OMe, Cl
R_2 = Me, Et, Pr, Ph
X = O, S

Figure 4. 3-hydroxypropyl urea and thiourea derivatives.

The synthetic route performed to this new family could also be applied to the last family allowing us to obtain the molecules **5** with less synthetic steps (from 8 to 5) and higher global yield (from 18% to 40%).

Moreover, using the MW, we could shorten the urea and thiourea formation time from 18h to 20 min with good yield ranging between 60 and 90%.

Regarding the biological results, this family mostly inhibits better the neuronal NOS isoform than the inducible one. Furthermore, thioureas exhibit

higher inhibition than ureas for both isoforms. Among all the tested compounds, **4g** (R_1 = OMe, R_2 = Me, X = S) shows the best nNOS (IC_{50} = 130 µM) and iNOS (IC_{50} = 180 µM) inhibition values without inhibiting eNOS. Such compound could be useful to fight pathologies where both i/nNOS are implicated such as neurodegenerative diseases.

6.4 References

1. Moncada, S. R. M. J.; Palmer, R. M. L.; Higgs, E. Nitric oxide: physiology, pathophysiology, and pharmacology. *Pharmacol. Rev.* **1991**, 43, 109-142.
2. Griffith, O. W.; Stuehr, D. J. Nitric Oxide Synthases: Properties and Catalytic Mechanism. *Annu. Rew. Physiol.* **1995**, 57, 707-736.
3. Roman, L. J.; Martásek, P.; Masters, B. S. S. Intrinsic and extrinsic modulation of nitric oxide synthase activity. *Chem. Rev.* **2002**, 102, 1179-1190.
4. Knowles, R. G.; Moncada, S. Nitric oxide synthases in mammals. *Biochem. J.* **1994**, 298(Pt 2), 249-258.
5. Zhou, L.; Zhu, D-Y. Neuronal nitric oxide synthase: structure, subcellular localization, regulation, and clinical implications. *Nitric Oxide-Biol. Chem.* **2009**, 20, 223-230.
6. Groves, J. T.; Wang, C. C. Nitric oxide synthase: models and mechanisms. *Curr. Opin. Chem. Biol.* **2000**, 4, 687-695.
7. Aktan, F. iNOS-mediated nitric oxide production and its regulation. *Life sci.* **2004**, 75, 639-653.
8. Wilcock, D. M.; Lewis, M. R.; Van Nostrand, W. E.; Davis, J.; Previti, M. L.; Gharkholonarehe, N.; Vitek, M. P.; Colton, C. A. Progression of amyloid pathology to Alzheimer's disease pathology in an amyloid

precursor protein transgenic mouse model by removal of nitric oxide synthase 2. *J. Neurosci.* **2008**, 28, 1537-1545.

9. Calabrese, V.; Mancuso, C.; Calvani, M.; Rizzarelli, E.; Butterfield, D. A.; Stella, A. M. G. Nitric oxide in the central nervous system: neuroprotection versus neurotoxicity. *Nat. Rev. Neurosci.* **2007**, 8, 766-775.

10. Deckel, A. W. Nitric oxide and nitric oxide synthase in Huntington's disease. *J. Neurosci. Res.* **2001**, 64, 99-107.

11. Kröncke, K. D.; Fehsel, K.; Kolb-Bachofen, V. Inducible nitric oxide synthase in human diseases. *Clin. Exp. Pharmacol. Physiol.* **1998**, 113, 147-156.

12. Lechner, M.; Lirk, P.; Rieder, J. Inducible nitric oxide synthase (iNOS) in tumor biology: the two sides of the same coin. *Seminars in cáncer biology* **2005**, Vol. 15, No. 4, 277-289. Academic Press.

13. Zamora, R.; Vodovotz, Y.; Billiar, T. R. Inducible nitric oxide synthase and inflammatory diseases. *Mol. Med.* **2000**, 6, 347.

14. Taddei, S.; Virdis, A.; Ghiadoni, L.; Sudano, I.; Salvetti, A. Endothelial dysfunction in hypertension. *J. Cardiovasc. Pharmacol.* **2001**, 38, S11-S14.

15. Napoli, C.; de Nigris, F.; Williams-Ignarro, S.; Pignalosa, O.; Sica, V.; Ignarro, L. J. Nitric oxide and atherosclerosis: an update. *Nitric oxide* **2006**, 15, 265-279.

16. Camacho, E.; León, J.; Carrión, A.; Entrena, A.; Escames, G.; Khaldy, H.; Acuña-Castroviejo, D.; Gallo, M. A.; Espinosa, A. Inhibition of nNOS activity in rat brain by synthetic kynurenines: Structure-activity dependence. *J. Med. Chem.* **2002**, 45, 263-274.

17. Entrena, A.; Camacho, M. E.; Carrión, M. D.; López-Cara, L. C.; Velasco, G.; León, J.; Escames, G.; Castroviejo-Acuña, D.; Tapias, V.; Gallo, M. A.; Vivó, A.; Espinosa, A. Kynurenamines as neural nitric oxide synthase inhibitors. *J. Med. Chem.* **2005**, 48, 8174-8181.

18. Camacho, M. E.; León, J.; Entrena, A.; Velasco, G.; Carrión, M. D.; Escames, G.; Vivó, A.; Acuña-Castroviejo, D.; Gallo, M. A.; Espinosa, A. 4, 5-Dihydro-1 H-pyrazole Derivatives with Inhibitory nNOS Activity in Rat Brain: Synthesis and Structure-Activity Relationships. *J. Med. Chem.* **2004**, 47, 5641-5650.

19. Carrión, M. D.; Chayah, M.; Entrena, A.; López, A.; Gallo, M. A.; Acuña-Castroviejo, D.; Camacho, M. E. Synthesis and biological evaluation of 4,5-dihydro-1*H*-pyrazole derivatives as potential nNOS/iNOS selective inhibitors. Part 2: Influence of diverse substituents in both the phenyl moiety and the acyl group. *Bioorg. Med. Chem.* **2013**, 21, 4132-4142.

20. Chayah, M.; Carrión, M. D.; Gallo, M. A.; Jiménez, R.; Duarte, J.; Camacho, M. E. Development of Urea and Thiourea Kynurenamine Derivatives: Synthesis, Molecular Modeling, and Biological Evaluation as Nitric Oxide Synthase Inhibitors. *ChemMedChem* **2015**, 10, 874-882.

21. Chayah, M.; Carrión, M. D.; Gallo, M. A.; Choquesillo-Lazarte D.; Camacho, M. E. NMR assignments and structural characterization of new thiourea and urea kynurenamine derivatives nitric oxide synthase inhibitors. *Magn. Reson. Chem.* 2015, DOI: 10.1002/mrc.4295.

7. BIBLIOGRAFÍA

1. a. Nobel Foundation. *Nobel lectures in physiology or medicine 1996-2000.* **2003**.

   b. Moncada, S; Palmer, R. M.; Higgs, E. A. Nitric oxide: physiology, pathophysiology, and pharmacology. *Pharmacol. Rev.* **1991**, 43, 109-142.

2. Aktan, F. iNOS-mediated nitric oxide production and its regulation. *Life Sci.* **2004**, 75, 639-653.
3. Wood, J.; Garthwaite, J. Models of the diffusional spread of nitric oxide: implications for neural nitric oxide signaling and its pharmacological properties. *Neuropharmacology* **1994**, 33, 1235-1244.
4. Snyder, S. H.; Bredt, D. S. Biological roles of nitric oxide. *Sci. Am.* **1992**, 266, 68-77.
5. Mariotto, S.; Menegazzi, M.; Suzuki, H. Biochemical aspects of nitric oxide. *Curr. Pharm. Design* **2004**, 10, 1627-1645.
6. Bogdan, C. Nitric Oxide and the Immune Response. *Nat. Immunol.* **2001**, 2, 907-916.
7. Furchgott, R. F.; Zawadzki, J. V. The obligatory role of endothelial cells in the relaxation of arterial smooth muscle by acetylcholine. *Nature* **1980**, 288, 373-376.
8. Lowenstein, C. J.; Dinerman, J. L.; Snyder, S. H. Nitric oxide: a physiologic messenger. *Ann. Intern. Med.* **1994**, 120, 227-237.
9. Moncada, S.; Higgs, E. A. Endogenous nitric oxide: physiology, pathology and clinical relevance. *Eur. J. Clin. Invest.* **1991**, 21, 361-374.
10. Moncada, S.; Higgs, E. A. The L-arginine-nitric oxide pathway. *N Engl. J. Med.* **1993**, 329, 2002-2012.
11. Bredt, D. S.; Snyder, S. H. Nitric oxide: a physiologic messenger molecule. *Annu. Rev. Biochem.* **1994**, 63, 175-195.
12. Kone, B. C.; Kuncewicz, T.; Zhang, W.; Yu, Z.-Y. Protein interactions with nitric oxide synthases: controlling the right time, the right place,

and the right amount of nitric oxide. *Am. J. Physiol-Renal* **2003**, 285, 178-190.

13. MacMicking, J.; Xie, Q.W.; Nathan, C. Nitric oxide and macrophage function. *Annu. Rev. Immunol.* **1997**, 15, 323-50.
14. Bogdan, C. Nitric oxide and the immune response. *Nat. Immunol.* **2001**, 2, 907-916.
15. Williams, S. B.; Cusco, J. A.; Roddy, M.; Johnstone, M. T.; Creager, M. A. Impaired nitric oxide-mediated vasodilation in patients with non-insulin-dependent diabetes mellitus. *J. Am. Coll. Cardiol.* **1996**, 27, 567-574.
16. Jayaraman, P.; Parikh, F.; Lopez-Rivera, E.; Hailemichael, Y.; Clark, A.; Ma, G.; Cannan, D.; Ramacher, M.; Kato, M.; Overwijk, W. W.; Chen, S.-H.; Umansky, V. Y.; Sikora, A. G. Modulation of vascular endothelial growth myeloid-derived suppressor cells through synthase controls induction of functional tumor-expressed inducible nitric oxide factor release. *J. Immunol.* **2012**, 188, 5365-5376.
17. Torrea, D.; Pugliesea, A.; Speranzaa, F. Role of nitric oxide in HIV-1 infection: friend or foe? *Lancet Infect. Dis.* **2002**, 2, 273-280.
18. Bredt, D. S.; Hwang, P. M.; Snyder, S. H. Localization of nitric oxide synthase indicating a neural role for nitric oxide. *Nature* **1990**, 347, 768-770.
19. Garthwaite, J.; Charles, S. L.; Chess-Williams, R. Endothelium-derived relaxing factor release on activation of NMDA receptors suggests role as intercellular messenger in the brain. *Nature* **1988**, 336, 385-388.
20. Snyder, S. H.; Bredt, D. S. Nitric oxide as a neuronal messenger. *Trends Pharmacol. Sci.* **1991**, 12,125-128.
21. O'Dell, T. J.; Hawkins, R. D.; Kandel, E. R.; Arancio, O. Tests of the roles of two diffusible substances in long-term potentiation: evidence for nitric oxide as a possible early retrograde messenger. *Proc. Natl. Acad. Sci. USA* **1991**, 88, 11285-11289.

22. Dawson, V. L.; Dawson, T. M. Nitric oxide in neurodegeneration. *Prog. Brain Res.* **1998**, 118, 215-229.
23. Palmer, R. M.; Rees, D. D.; Ashton, D. S.; Moncada, S. L-arginine is the physiological precursor for the formation of nitric oxide in endothelium-dependent relaxation. *Biochem. Biophys. Res. Com.* **1988**, 153, 1251-1256.
24. Bruckdorfer, R. The basics about Nitric Oxide. *Mol. Aspects Med.* **2005**, 26, 3-31.
25. Kwon, N. S.; Nathan, C. F.; Gilker, C.; Griffith, O. W.; Matthews, D. E.; Stuehr, D. J. L-citrulline production from L-arginine by macrophage nitric oxide synthase. The ureido oxygen derives from dioxygen. *J. Biol. Chem.* **1990**, 265, 13442-13445.
26. Stuehr, D. J.; Kwon, N. S.; Nathan, C. F.; Griffith, O. W.; Feldman, P. L.; Wiseman, J. *N*-omega-hydroxy-L-arginine is an intermediate in the biosynthesis of nitric oxide from L-arginine. *J. Biol. Chem.* **1991**, 266, 6259-6263.
27. Iyengar, R.; Stuehr, D. J.; Marletta, M. A. Macrophage synthesis of nitrite, nitrate, and *N*-nitrosamines: precursors and role of the respiratory burst. *Proc. Natl. Acad. Sci. USA* **1987**, 84, 6369-6373.
28. Marletta, M. A.; Yoon, P. S.; Iyengar, R.; Leaf, C. D.; Wishnok, J. S. Macrophage oxidation of L-arginine to nitrite and nitrate: nitric oxide is an intermediate. *Biochemistry* **1988**, 27, 8706-8711.
29. Griffith, O. W.; Stuehr, D. J. Nitric oxide synthases: properties and catalytic mechanism. *Annu. Rew. Physiol.* **1995**, 57, 707-736.
30. Kwon, N. S.; Nathan, C. F.; Stuehr, D. J. Reduced biopterin as a cofactor in the generation of nitrogen oxides by murine macrophages. *J. Biol. Chem.* **1989**, 264, 20496-20501.
31. Lundberg, J. O.; Weitzberg, E. Nitric oxide formation from inorganic nitrate and nitrite. *Nitric Oxide-Biol. Pathobiol.* **2010**, 539-553, Second Edition.

32. Lundberg, J. O.; Weitzberg, E. NO-synthase independent NO generation in mammals. *Biochem. Biophys. Res. Com.* **2010**, 396, 39-45.
33. Lundberg, J. O.; Weitzberg, E.; Gladwin, M. T. The nitrate-nitrite-nitric oxide pathway in physiology and therapeutics. *Nat. Rev. Drug Discov.* **2008**, 7, 156-167.
34. Krumenacker, J. S.; Hanafy, K. A.; Murad, F. Regulation of nitric oxide and soluble guanylyl cyclase. *Brain Res. Bull.* **2004**, 62, 505-515.
35. Haynes, V.; Elfering, S.; Traaseth, N.; Giulivi, C. Mitochondrial nitric-oxide synthase: enzyme expression, characterization, and regulation. *J. Bioenerg. Biomembr.* **2004**, 36, 341-346.
36. Giulivi, C.; Poderoso, J. J.; Boveris, A. Production of nitric oxide by mitochondria. *J. Biol. Chem.* **1998**, 273, 11038-11043.
37. Ghafourifar, P.; Richter C. Nitric oxide synthase activity in mitochondria. *FEBS Lett.* **1997**,418, 291-296.
38. Kato, K.; Giulivi C. Critical overview of mitochondrial nitric-oxide synthase. *Front. Biosci.* **2006**, 11, 2725-2738.
39. Alderton, W. K.; Cooper, C. E.; Knowles, R. G. Nitric oxide synthases: structure, function and inhibition. *Biochemical J.* **2001**, 357, 593-615.
40. Lamas, S.; Marsden, P. A.; Li, G. K.; Tempst, P.; Michel, T. Endothelial nitric oxide synthase: molecular cloning and characterization of a distinct constitutive enzyme isoform. *Proc. Natl. Acad. Sci. USA* **1992**, 89, 6348-6352.
41. Dawson, T. M.; Snyder, S. H. Gases as biological messengers: nitric oxide and carbon monoxide in the brain. *J. Neurosci.* **1994**, 14, 5147-5159.
42. Nathan, C.; Xie, Q. W. Nitric oxide synthases: roles, tolls and controls. *Cell* **1994**, 78, 915-918.
43. Blaise, G.; Gauvin, D.; Gangal, M.; Authier, S. Nitric oxide, cell signaling and cell death. *Toxicology* **2005**, 208, 177-192.

44. Conti, A.; Miscusi, M.; Cardali, S.; Germanò, A.; Suzuki, H.; Cuzzocrea, S.; Tomasello, F. Nitric oxide in the injured spinal cord: synthases crosstalk, oxidative stress and inflammation. *Brain Res. Rev.* **2007**, 54, 205-218.
45. Cho, H. J.; Xie, Q. W.; Calacay, J.; Mumford, R. A.; Swiderek, K. M.; Lee, T. D.; Nathan, C. Calmodulin is a subunit of nitric oxide synthase from macrophages. *J. Exp. Med.* **1992**, 176, 599-604.
46. Elfering, S. L.; Sarkela, T. M.; Giulivi, C. Biochemistry of mitochondrial nitric-oxide synthase. *J. Biol. Chem.* **2002**, 277, 38079-38086.
47. Ghafourifar, P.; Cadenas, E. Mitochondrial nitric oxide synthase. *TRENDS Pharmacol. Sci.* **2005**, 26, 190-195.
48. Geller, D. A.; Billiar, T. R. Molecular biology of nitric oxide synthases. *Cáncer Metast. Rev.* **1998**, 17, 7-23.
49. Li, H.; Poulos, T .L. Structure-function studies on nitric oxide synthases. *J. Inorg. Biochem.* **2005**, 99, 293-305.
50. Brenman, J. E.; Chao, D. S.; Xia, H.; Aldape, K.; Bredt, D. S. Nitric oxide synthase complexed with dystrophin and absent from skeletal muscle sarcolemma in Duchenne muscular dystrophy. *Cell* **1995**, 82, 743-752.
51. Wang, P.; Zhang, Q.; Tochio, H.; Fan, J. S.; Zhang, M. Formation of a native-like beta-hairpin finger structure of a peptide from the extended PDZ domain of neuronal nitric oxide synthase in aqueous solution. *Eur. J. Biochem. / FEBS* **2000**, 267, 3116-3122.
52. Hung, A. Y.; Sheng, M. PDZ Domains: Structural Modules for Protein Complex. *J. Biol. Chem.* **2002**, 277, 5699-5702.
53. Adams, V.; Krabbes, S.; Jiang, H.; Yu, J.; Rahmel, A.; Gielen, S.; Schuler, G.; Hambrecht, R. Complete coding sequence of inducible nitric oxide synthase from human heart and skeletal muscle of patients with chronic heart failure. *Nitric Oxide* **1998**, 2, 242-249.
54. Geller, D. A.; Lowenstein, C. J.; Shapiro, R. A.; Nussler, A. K.; Di Silvio, M.; Wang, S. C.; Nakayama, D. K.; Simmons, R. L.; Snyder, S.

H.; Billiar, T. R. Molecular cloning and expression of inducible nitric oxide synthase from human hepatocytes. *Proc. Natl. Acad. Sci. USA* **1993**, 90, 3491-3495.

55. Chen, P. F.; Tsai, A. L.; Wu, K. K. Cysteine 99 of endothelial nitric oxide synthase (NOS-III) is critical for tetrahydrobiopterin-dependent NOS-III stability and activity. *Biochem. Biophys. Res. Com.* **1995**, 215, 1119-1129.
56. Daff, S. NO synthase: structures and mechanisms. *Nitric Oxide-Biol. Chem.* **2010**, 23, 1-11.
57. Siddhanta, U.; Wu, C.; Abu-Soud, H. M.; Zhang, J.; Ghosh, D. K.; Stuehr, D. J. Heme iron reduction and catalysis by a nitric oxide synthase heterodimer containing one reductase and two oxygenase domains. *J. Biol. Chem.* **1996**, 271, 7309-7312.
58. Nishida, C. R.; Ortiz de Montellano, P. R. Control of electron transfer in nitric-oxide synthases. Swapping of autoinhibitory elements among nitric-oxide synthase isoforms. *J. Biol. Chem.* **2001**, 276, 20116-20124.
59. Nishida, C. R.; Ortiz de Montellano, P. R. Autoinhibition of endothelial nitric-oxide synthase. Identification of an electron transfer control element. *J. Biol. Chem.* **1999**, 274, 14692-14698.
60. Feng, C. Mechanism of nitric oxide synthase regulation: electron transfer and interdomain interactions. *Coordin. Chem. Rev.* **2012**, 256, 393-411.
61. Kone, B. C.; Kuncewicz, T.; Wenzheng, Z.; Zhi-Yuan, Y. Protein interactions with nitric oxide synthases: controlling the right time, the right place, and the right amount of nitric oxide. *Am. J. Physiol-Renal* **2003**, 285, 178-190.
62. a. Forstermann, U.; Munzel, T. Endothelial nitric oxide synthase in vascular disease: from marvel to menace. *Circulation* **2006**, 113, 1708-1714.

b. Mukherjee, P.; Cinelli, M. A.; Kang, S.; Silverman, R. B. Development of nitric oxide synthase inhibitors for neurodegeneration and neuropathic pain. *Chem. Soc. Rev.* **2014**, 43, 6814-6838.

63. Zhou, L.; Zhu D-Y. Neuronal nitric oxide synthase: structure, subcellular localization, regulation, and clinical implications. *Nitric Oxide-Biol. Chem.* **2009**, 20, 223-230.
64. Su, Z.; Blazing, M. A.; Fan, D.; George, S. E. the calmodulinnitric oxide synthase interaction. Critical role of the calmodulin latch domain in enzyme activation. *J. Biol. Chem.* **1995**, 270, 29117-29122.
65. Hobbs, A.; Higgs, J. A.; Moncada, S. Inhibition of nitric oxide synthase as a potential therapeutic target. *Annu. Rev. Pharmacol. Toxicol.* **1999**, 39, 191-220.
66. Bredt, D. S.; Snyder, S. H. Isolation of nitric oxide synthetase, a calmodulin-requiring enzyme. *Proc. Natl. Acad. Sci. USA* **1990**, 87, 682-685.
67. Förstermann, U.; Closs, E. I.; Pollock, J. S.; Nakane, M.; Schwarz, P.; Gath, I.; Kleinert, H. Nitric oxide synthase isozymes. Characterization, purification, molecular cloning, and functions. *Hypertension* **1994**, 23, 1121-1131.
68. Förstermann, U.; Boissel, J.-P.; Kleinert H. Expressional control of the ‘constitutive’ isoforms of nitric oxide synthase (NOS I and NOS III). *FASEB J.* **1998**, 12, 773-790.
69. Calabrese, V.; Mancuso, C.; Calvani, M.; Rizzarelli, E.; Butterfield, D. A.; Giuffrida Stella, A. M. Nitric oxide in the central nervous system: neuroprotection versus neurotoxicity. *Nat. Rev. Neurosci.* **2007**, 8, 766-775.
70. Nakane, M.; Schmidt, H. H.; Pollock, J. S.; Förstermann, U.; Murad, F. Cloned human brain nitric oxide synthase is highly expressed in skeletal muscle. *FEBS Lett.* **1993**, 316, 175-180.
71. Yang, C. C.; Alvarez, R. B.; Engel, W. K.; Haun, C. K.; Askanas, V. Immunolocalization of nitric oxide synthases at the postsynaptic

domain of human and rat neuromuscular junctions-light and electron microscopic studies. *Exp. Neurol.* **1997**, 148, 34-44.

72. Ponting, C. P.; Phillips, C.; Davies, K. E.; Blake, D. J. PDZ domains: targeting signalling molecules to sub-membranous sites. *BioEssays: News and Reviews in Molecular, Cellular and Developmental Biology* **1997**, 469-479.
73. Schepens, J.; Cuppen, E.; Wieringa, B.; Hendriks, W. The neuronal nitric oxide synthase PDZ motif binds to -G(D,E)XV* carboxyterminal sequences. *FEBS Lett.* **1997**, 409, 53-56.
74. Ricciardolo, F. L. M.; Nijkamp, F. P.; Folkerts, G. Nitric Oxide Synthase (NOS) as therapeutic target for asthma and chronic obstructive pulmonary disease. *Curr. Drug Targets* **2006**, 7, 721-735.
75. Li, H.; Förstermann, U. Nitric oxide in the pathogenesis of vascular disease. *J. Pathol.* **2000**, 190, 244-254.
76. Brahmajothi, M. V.; Campbell, D. L. Heterogeneous basal expression of nitric oxide synthase and superoxide dismutase isoforms in mammalian heart: implications for mechanisms governing indirect and direct nitric oxide-related effects. *Circ. Res.* **1999**, 85, 575-587.
77. Sessa, W. C. eNOS at a glance. *J. Cell Sci.* **2004**, 117, 2427-2429.
78. Michel, T.; Vanhoutte, P. M. Cellular signaling and NO production. *Eur J. Physiol.* **2010**, 459, 6, 807-816.
79. Rodrigo, J.; Alonso, D.; Bentura, M. L.; Castro-Blanco, S.; Encinas, J. M.; Fernandez, A. P.; Fernandez-Vizarra, P.; Richart, A.; Santacana, M.; Serrano J.; Martínez, A. Physiology and pathophysiology of nitric oxide in the nervous system, with special mention of the islands of Calleja and the circunventricular organs. *Histol. Histopathol.* **2002**, 17, 973-1003.
80. Chabrier, P. E.; Demerlé-Pallardy, C.; Auguet, M. Nitric Oxide Synthases: Targets for therapeutic strategies in neurological diseases. *Cell. Mol. Life Sci.* **1999**, 55, 1029-1035.

81. Oess, S.; Icking, A.; Fulton, D.; Govers, R.; Muller-Esterl, W. Subcellular targeting and trafficking of nitric oxide synthases. *Biochem. J*. **2006**, 396, 401-409.

82. Pautz, A.; Art, J.; Hahn, S.; Nowag, S.; Voss, C.; Kleinert, H. Regulation of the Expression of Inducible Nitric Oxide Synthase. *Nitric Oxide-Biol. Chem.* **2010**, 23, 75-93.

83. Casper, I.; Nowag, S.; Koch, K.; Hubrich, T.; Bollmann, F.; Henke, J.; Schmitz, K.; Kleinert, H.; Pautz, A. Post-transcriptional regulation of the human inducible nitric oxide synthase (iNOS) expression by the cytosolic poly(A)-binding protein (PABP). *Nitric Oxide* **2013**, 33, 6-17.

84. Govers, R.; Oess, S. To NO or Not to NO: 'Where?' Is the question. *Histol. Histopathol.* **2004**, 19, 585-605.

85. Ratovitski, E. A.; Alam, M. R.; Quick, R. A.; McMillan, A.; Bao, C.; Kozlovsky, C.; Hand, T. A.; Johnson, R. C.; Mains, R. E.; Eipper, B. A.; Lowenstein C. J. Kalirin inhibition of inducible nitric-oxide synthase. *J. Biol. Chem.* **1999**, 274, 993-999.

86. Fleming, I. Molecular mechanisms underlying the activation of eNOS. *Eur. J. Physiol.* **2010**, 459, 793-806.

87. Yoshida, M.; Xia, Y. Heat shock protein 90 as an endogenous protein enhancer of inducible nitric-oxide synthase. *J. Biol. Chem.* **2003**, 278, 36953-36958.

88. Fulton, D.; Fontana, J.; Sowa, G.; Gratton, J.- P.; Lin, M.; Li, K.-X.; Michell, B.; Kemp, B. E.; Rodman, D.; Sessa, W. C. Localization of endothelial nitric-oxide synthase phosphorylated on serine 1179 and nitric oxide in Golgi and plasma membrane defines the existence of two pools of active enzyme. *J. Biol. Chem.* **2002**, 277, 4277-4284.

89. Yun, H. Y.; Dawson, V. L.; Dawson, T. M. Nitric oxide in health and disease of the nervous system. *Mol. Psychiatr.* **1997**, 2, 300-310.

90. Kevil, C. G.; Lefer, D. J. Nitrite therapy for ischemic syndromes. *Nitric Oxide: Biology and Pathobiology* **2010**, 587-603, Second Edition.

91. Bogdan, C.; Rollinghoff, M.; Diefenbach, A. Reactive oxygen and reactive nitrogen intermediates in innate and specific immunity *Curr. Opin. Immunol.* **2000**, 12, 64-76.
92. MacMicking, J.; Xie, Q. W.; Nathan, C. Nitric oxide and macrophage function. *Annu. Rev. Immunol.* **1997**, 15, 323-350.
93. Kroncke, K. D.; Fehsel, K.; Kolb-Bachofen, V. Inducible nitric oxide synthase in human diseases. *Clin. Exp. Immunol.* **1998**, 113, 147-156.
94. Bohme, G. A.; Bon, C.; Stutzmann, J. M.; Doble, A.; Blanchard, J. C. Possible involvement of nitric oxide in longterm potentiation. *Eur. J. Pharmacol.* **1991**, 199, 379-381.
95. O'dell, T. J.; Hawkins, R. D.; Kandel, E. R.; Arancio, O. Tests of the roles of two di□usible substances in long-term potentiation: evidence for nitric oxide as a possible early retrograde messenger. *Proc. Natl. Acad. Sci. USA* **1991**, 88, 11285-11289.
96. Schuman, E. M.; Madison, D. V. A requirement for the intercellular messenger nitric oxide in long-term potentiation. *Science* **1991**, 254, 1503-1506.
97. Holscher, C.; Rose, S.P. An inhibitor of nitric oxide synthesis prevents memory formation in the chick. *Neurosci. Lett.* **1992**, 145, 165-167.
98. Bohme, G. A.; Bon, C.; Lemaire, M.; Reibaud, M.; Piot, O.; Stutzmann, J. M.; Doble, A.; Blanchard, J. C. Alered synaptic plasticity and memory formation in nitric oxide synthase inhibitor-treated rats. *Proc. Natl. Acad. Sci. USA* **1993**, 90, 9191-9194.
99. Kendrick, K. M.; Guevara Guzman, R.; Zorrilla, J.; Hinton, M. R.; Broad, K. D.; Mimmack, M.; Ohkura, S. Formation of olfactory memories mediated by nitric oxide. *Nature* **1997**, 388, 670-674.
100. Yamada, K.; Noda, Y.; Nakayama, S.; Komori, Y.; Sugihara, H.; Hasegawa, I.; Nabeshima, T. Role of nitric oxide in learning and memory and in monoamine metabolism in the rat brain. *Br. J. Pharmacol.* **1995**, 115, 852-858.

101. Contestabile, A. Roles of NMDA receptor activity and nitric oxide production in brain development. *Brain Res. Rev.* **2000**, 32, 476-509.
102. Okere, C. O.; Kaba, H. Increased expression of neuronal nitric oxide synthase mRNA in the accessory olfactory bulb during the formation of olfactory recognition memory in mice. *Eur. J. Neurosci.* **2000**, 12, 4552-4556.
103. Cudeiro, J.; Rivadulla, C. Sight and insight - on the physiological role of nitric oxide in the visual system. *Trends Neurosci.* **1999**, 22, 109-116.
104. Groll-Knapp, E.; Haider, M.; Kienzl, K.; Handler, A.; Trimmel, M. Changes in discrimination learning and brain activity (ERPs) due to combined exposure to NO and CO in rats. *Toxicology* **1988**, 49, 441-447.
105. Calapai, G.; Squadrito, F.; Altavilla, D.; Zingarelli, B.; Campo, G. M.; Cilia, M.; Caputi, A. P. Evidence that nitric oxide modulates drinking behaviour. *Neuropharmacology* **1992**, 31, 761-764.
106. De Luca, B.; Monda, M.; Sullo, A. Changes in eating behavior and thermogenic activity following inhibition of nitric oxide formation. *Am. J. Physiol.* **1995**, 268, 1533-1538.
107. Zhu, H.; Barr, G. A. Opiate withdrawal during development: are NMDA receptors indispensable? *Trends. Pharmacol. Sci.* **2001**, 22, 404-408.
108. Watanabe, A.; Ono, M.; Shibata, S.; Watanabe, S. E. Effect of a nitric oxide synthase inhibitor, N-nitro-L-arginine methylester, on light-induced phase delay of circadian rhythm of wheel-running activity in golden hamsters. *Neurosci. Lett.* **1995**, 192, 25-28.
109. Kapas, L.; Shibata, M.; Kimura, M.; Krueger, J. M. Inhibition of nitric oxide synthesis suppresses sleep in rabbits. *Am. J. Physiol.* **1994**, 266, 151-157.
110. Ling, L.; Karius, D. R.; Fiscus, R. R.; Speck, D. F. Endogenous nitric oxide required for an integrative respiratory function in the cat brain. *J. Neurophysiol.* **1992**, 68, 1910- 1912.

111. Nelson, R. J.; Demas, G. E.; Huang, P. L.; Fishman, M. C.; Dawson, V. L.; Dawson, T. M.; Snyder, S. H. Behavioural abnormalities in male mice lacking neuronal nitric oxide synthase. *Nature* **1995**, 378, 383-386.
112. Mao, J. NMDA and opioid receptors: their interactions in antinociception, tolerance and neuroplasticity. *Brain Res. Rev.* **1999**, 30, 289-304.
113. Esplugues, J. V. NO as a signalling molecule in the nervous system. *Br. J. Pharmacol.* **2002**, 135, 1079-1095.
114. Liberatore, G. T.; Jackson-Lewis, V.; Vukosavic, S.; Mandir, A. S.; Vila, M.; McAuliffe, W. G.; Dawson, V. L.; Dawson, T. M.; Przedborski, S. Inducible nitric oxide synthase stimulates dopaminergic neurodegeneration in the MPTP model of Párkinson disease. *Nat. Med.* **1999**, 5, 1403-1409.
115. Norris, P. J.; Waldvogel, H. J.; Faull, R. L.; Love, D. R.; Emson, P. C. Decreased neuronal nitric oxide synthase messenger RNA and somatostatin messenger RNA in the striatum of Huntington's disease. *Neurosci.* **1996**, 72, 1037-1047.
116. Smith, M. A.; Vasak, M.; Knipp, M.; Castellani, R. J.; Perry, G. Dimethylargininase, a nitric oxide regulatory protein, in Alzheimer disease. *Free Radical Biol. Med.* **1998**, 25, 898-902.
117. Wink, D. A.; Mitchell, J. B. Chemical biology of nitric oxide: insights into regulatory, cytotoxic and cytoprotective mechanisms of nitric oxide. *Free Radical Biol. Med.* **1998**, 434-456.
118. Waldman, S. A.; Murad, F. Cyclic GMP synthesis and function. *Pharmacol. Rew.* **1987**, 39, 163-196.
119. Stalmer, J. S.; Simon, D. I.; Osborne, J. A.; Mullins, M. E.; Jaraki, O.; Michel, T.; Singel, D. J.; Loscalzo, J. S-nitrosilation of proteins with nitric oxide: synthesis and characterization of biologically active compounds. *Proc. Natl. Acad. Sci. USA* **1992**, 89, 444-448.

120. Beckman, J. S.; Smith, C. M.; Koppenol, W. H. ALS, SOD and peroxynitrite. *Nature* **1993**, 364, 584.
121. Pryor, W. A.; Squadrito, G. L. The chemistry of peroxynitrite and peroxynitrous acid: products from the reaction of nitric oxide with superoxide. *Am. J. Phys.* **1996**, 268, 699-721.
122. Smith, M. A.; Richey Harris, P. L.; Sayre, L. M.; Beckman, J. S.; Perry, G. J. Widespread peroxynitrite-mediated damage in Alzheimer's disease. *J. Neurosc*. **1997**, 17, 2653-2657.
123. Good, P. G.; Hsu, A.; Werner, P.; Perl, D. P.; Olanow, C. W. J.; Protein nitration in Párkinson's disease. *Neuropathol. Exp. Neurol*. **1998**, 57, 338-342.
124. Abe, K.; Pan, L. H.; Watanabe, M.; Konno, H.; Kato, T.; Itoyama, Y.; *Neurol. Res.* **1997**, 19, 124-128.
125. Eliasson, M. J.; Sampei, K.; Mandir, A. S.; Hurn, P. D.; Traystman, R. J.; Bao, J.; Pieper, A.; Wang, Z. K.; Dawson, T. M.; Snyder, S. H.; Dawson, V. L. Poly (ADP-ribose) polymerase gene disruption renders mice resistant to cerebral ischemia. *Nat. Med*. **1997**, 3, 1089-1095.
126. Simic, G.; Lucassen, P. J.; Krsnik, Z.; Kruslin, B.; Kostovic, I.; Winblad, B.; Bogdanovi, N. nNOS expression in reactive astrocytes correlates with increased cell death related DNA damage in the hippocampus and entorhinal cortex in Alzheimer's disease. *Exp. Neurol*. **2000**, 165, 12-26.
127. Lu, F.; Selak, M.; O'Connor, J.; Croul, S.; Lorenzana, C.; Butunoi, C.; Kalman, B. Oxidative damage to mitochondrial DNA and activity of mitochondrial enzymes in chronic active lesions of multiple sclerosis. *J. Neurol. Sci*. **2000**, 177, 95-103.
128. Liu, Z.; Martin, L. J. Motor neurons rapidly accumulate DNA single-strand breaks after in vitro exposure to nitric oxide and peroxynitrite and in vivo axotomy. *J. Comp. Neurol*. **2001**, 432, 35-60.
129. Gross, S. S.; Wolin, M. S. Nitric oxide: pathological mechanisms. *Annu. Rev. Physiol.* **1995**, 57, 737-769.

130. Dorado, C.; Rugerio C. C.; Rivas, S. Estrés oxidativo y neurodegeneración. *Rev. Fac. Med. UNAM*, **2003**, 46, 229-325.
131. Segura, T.; Galindo, M. F.; Rallo-Gutierrez, B.; Ceña, V.; Jordan, J. Dianas farmacológicas en las enfermedades neurodegenerativas. *Rev. Neurol.* **2003**, 36, 11, 1047-1057.
132. De la Monte, S. M.; Sohn, Y. K.; Etienne, D.; Kraft, J.; Wands, J. R. Role of aberrant nitric oxide synthase-3 expression in cerebrovascular degeneration and vascular-mediated injury in Alzheimer's disease. *Ann. NY. Acad. Sci.* **2000**, 903, 61-71.
133. Eguchi, H.; Fujiwara, N.; Sakiyama, H.; Yoshihara, D.; Suzuki, K. Hydrogen peroxide enhances LPS-induced nitric oxide production via the expression of interferon beta in BV-2 microglial cells. *Neurosci. Lett.* **2011**, 494, 29-33.
134. Domenico, R. Pharmacology of nitric oxide: molecular mechanisms and therapeutic strategies. *Curr. Pharm. Des.* **2004**, 10, 1667-1676.
135. Lala, P. K.; Chakraborty, C. Role of nitric oxide in carcinogenesis and tumour progression. *Lancet Oncol.* **2012**, 3, 149-56.
136. Huang, P. L; Huang, Z.; Mashimo, H.; Bloch, K. D.; Moskowitz, M. A.; Bevan, J. A.; Fishman, M. C. Hypertension in mice lacking the gene for endothelial nitric oxide synthase. *Nature* **1995**, 377, 239-242.
137. Wei, X. Q.; Charles, I. G.; Smith, A.; Ure, J.; Feng, G. J.; Huang, F. P.; Xu, D.; Muller, W.; Moncada, S.; Liew, F. Y. Altered immune responses in mice lacking inducible nitric oxide synthase. *Nature* **1995**, 375, 408-411.
138. Ferriero, D. M.; Holtzman, D. M.; Black, S. M.; Sheldon, R. A. Neonatal mice lacking neuronal nitric oxide synthase are less vulnerable to hypoxic-ischemic injury. *Neurobiol. Dis.* **1996**, 3, 64-71.
139. Crane, B. R.; Arvai, A. S.; Gachhui, R.; Wu, C.; Ghosh, D. K.; Getzoff, E. D.; Stuehr D. J.; Tainer, J. A. The structure of nitric oxide synthase oxygenase domain and inhibitor complexes. *Science* **1997**, 278, 425-431.

140. Fischmann, T. O.; Hruza, A.; Niu, X. D.; Fossetta, J. D.; Lunn, C. A.; Dolphin, E.; Prongay, A. J.; Reichert, P.; Lundell, D. J.; Narula, S. K.; Weber, P. C. Structural characterization of nitric oxide synthase isoforms reveals striking active-site conservation. *Nat. Struct. Biol.* **1999**, 6, 233-242.

141. Raman, C. S.; Li, H.; Martásek, P.; Král, V.; Masters, B. L.; Poulos, T. L. Crystal structure of constitutive endothelial nitric oxide synthase: a paradigm for pterin function involving a novel metal center. *Cell* **1998**, 95, 939-950.

142. Li, H.; Shimizu, H.; Flinspach, M.; Jamal, J.; Yang, W.; Xian, M.; Cai, T.; Wen, E. Z.; Jia, Q.; Wang P. G.; Poulos, T. L. The novel binding mode of *N*-alkyl-*N'*-hydroxyguanidine to neuronal nitric oxide synthase provides mechanistic insights into no biosynthesis. *Biochemistry* **2002**, 41, 13868-13875.

143. Tinker, A. C.; Wallace, A. V. Selective inhibitors of inducible nitric oxide synthase: potential agents for the treatment of inflammatory diseases? *Curr. Top. Med. Chem.* **2006**, 6, 77-92.

144. Silverman, R. B. Design of selective neuronal nitric oxide synthase inhibitors for the prevention and treatment of neurodegenerative diseases. *Acc. Chem. Res.* **2009**, 42, 439-451.

145. Madaford, S.; Annedi, S. C.; Ramnauth, J.; Rakhit, S.; Advancements in the development of nitric oxide synthase inhibitors. *Ann. Rep. Med. Chem.* **2009**, 27-50. J. E. Macor, Ed. Elsevier.

146. Garcin, E. D.; Arvai, A. S.; Rosenfeld, R. J.; Kroeger, M. D.; Crane, B. R.; Andersson, G.; Andrews, G.; Hamley, P. J.; Mallinder, P. R.; Nicholls, D. J.; St-Gallay, S. A.; Tinker, A. C.; Gensmantel, N. P.; Mete, A.; Cheshire, D. R.; Connolly, S.; Stuehr, D. J.; Åberg, A.; Wallace, A. V.; Tainer, J. A.; Getzoff, E. D. Anchored plasticity opens doors for selective inhibitor design in nitric oxide synthase. *Nat. Chem. Biol.* **2008**, 4, 700-707.

147. Víteček, J.; Lojek, A.; Valacchi, G.; Kubala, L. Arginine-based inhibitors of nitric oxide synthase: therapeutic potential and challenges. *Mediat. Inflamm.* **2012**, Article ID 318087.
148. Mukherjee, P.; Cinelli, M. A.; Kang, S.; Silverman, R. B. Development of nitric oxide synthase inhibitors for neurodegeneration and neuropathic pain. *Chem. Soc. Rev.* **2014**, 43, 6814-6838.
149. Bedford, M. T.; Clarke, S. G. Protein arginine methylation in mammals: who, what, and why? *Mol. Cell* **2009**, 33, 1-13.
150. Sakuma, I.; Stuehr, D. J.; Gross, S. S.; Nathan, C.; Levi, R. Identification of arginine as a precursor of endotheliumderived relaxing factor. *Proc. Natl. Acad. Sci. USA* **1988**, 85, 8664-8667.
151. Aisaka, K.; Gross, S. S.; Griffith, O. W.; Levi, R. N^G- Methylarginine, an inhibitor of endothelium-derived nitric oxide synthesis, is a potent pressor agent in the guinea pig: does nitric oxide regulate blood pressure in vivo? *Biochem. Biophys. Res. Com.* **1989**, 160, 881-886.
152. Reif, D. W.; McCreedy, S. A. *N*-Nitro-L-arginine and *N*-monomethyl-L-arginine exhibit a different pattern of inactivation toward the three nitric oxide synthases. *Arch. Biochem. Biophys.* **1995**, 320, 170-176.
153. Lassen, L. H.; Ashina, M.; Christiansen, I.; Ulrich, V.; Grover, R.; Donaldson J.; Oleson, J. Nitric oxide synthase inhibition: a new principle in the treatment of migraine attacks. *Cephalgia* **1998**, 18, 27-32.
154. Baron, A. D.; Zhu, J. S.; Marshall, S.; Irsula, O.; Brechtel, G.; Keech, C. Insulin resistance after hypertension induced by the nitric oxide synthesis inhibitor L-NMMA in rats. *Am. J. Physiol.* **1995**, 269, 709-715.
155. López, A.; Lorente, J. A; Steingrub, J.; Bakker, J.; McLuckie, A.; Willatts, S.; Brockway, M.; Anzueto, A.; Holzapfel, H.; Breen, D.; Silverman, M. S.; Takala, J.; Donaldson, J.; Arneson, C.; Grove, G.; Grossman, S.; Grover, R. Multiple-center, randomized, placebo-controlled, double-blind study of the nitric oxide synthase inhibitor

546C88: effect on survival in patients with septic shock. *Crit. Care Med.* **2004**, 32, 21-30.

156. Moore, P. K.; Al-Swayeh, O. A.; Chong, N. W. S.; Evans, R. A.; Gibson, A. L-N^G-Nitroarginine (L-NOARG), a novel, L-arginine-reversible inhibitor of endothelium-dependent vasodilatation in vitro. *Br. J. Pharmacol.* **1990**, 99, 408-412.
157. Rees, D. D.; Palmer, R. M. J.; Schulz, R.; Hodson, H. F.; Moncada, S. Characterization of three inhibitors of endothelial nitric oxide synthase in vitro and in vivo. *Br. J. Pharmacol.* **1990**, 101, 746-752.
158. Griffith, O. W.; Kilbourn, R. G. Nitric oxide synthase inhibitors: amino acids. *Nitric oxide, part A: sources and detection of NO; NO synthase*. *Methods in Enzymology* **1996**, vol. 268, 375-392, A. G. Kartsatos, Ed. Academic Press, San Diego.
159. Furfine, E. S.; Harmon, M. F.; Paith, J. E.; Garvey, E. P. Selective inhibition of constitutive nitric oxide synthase by L-N^G-nitroarginine. *Biochemistry* **1993**, 32, 8512-8517.
160. Kobayashi, Y.; Ikeda, K.; Shinozuka, K.; Nara, Y.; Yamori, Y.; Hattori, K. L-nitroarginine increases blood pressure in the rat. *Clin. Exp. Pharmacol. Physiol.* **199**1, 18, 397-399.
161. Zhang, H. Q.; Fast, W.; Marletta, M. A.; Martasek, P.; Silverman, R. B. Potent and selective inhibition of neuronal nitric oxide synthase by N^{ω}-propyl-L-arginine. *J. Med. Chem*. **1997**, 40, 3869-3870.
162. Zhang, H. Q.; Dixon, R. P.; Marletta, M. A.; Nikolic, D.; Van Breemen, R.; Silverman, R. B. Mechanism of inactivation of neuronal nitric oxide synthase by N^{ω}-allyl-L-arginine. *J. Am. Chem. Soc.* **1997**, 119, 10888-10902.
163. Olken N. M.; Marietta, M. A. N^G-Allyl- and N^G-cyclopropyl-L-arginine: two novel inhibitors of macrophage nitric oxide synthase. *J. Med. Chem.* **1992**, 35, 1137-1144.
164. Fukuto, J. M.; Wood, K. S.; Byrns, R. E.; Ignarro, L. J. N^G-Amino-L-arginine: a new potent antagonist of L-arginine-mediated endothelium-

dependent relaxation. *Biochem. Biophys. Res. Com.* **1990**, 168, 458-465.

165. Gross, S. S.; Stuehr, D. J.; Aisaka, K.; Jaffe, E. A.; Levi, R.; Griffith, O. W. Macrophage and endothelial cell nitric oxide synthesis: cell-type selective inhibition by N^G-aminoarginine, N^G-nitroarginine and N^G-methylarginine. *Biochem. Biophys. Res. Com.* **1990**, 170, 96-103.
166. Wolff, D. J.; Lubeskie, A. Inactivation of nitric oxide synthase isoforms by diaminoguanidine and N^G-amino-L-arginine. *Arch. Biochem. Biophys.* **1996**, 325, 227-234.
167. Lebarbier, C.; Carreaux, F.; Carboni, B.; Boucher, J. L. Synthesis of boronic acid analogs of L-arginine as alternate substrates or inhibitors of nitric oxide synthase. *Bioorg. Med. Chem. Lett.* **1998**, 8, 2573-2576.
168. Narayanan, K.; Griffith, O. W. Synthesis of L-thiocitrulline, L-homothiocitrulline, and *S*-methyl-L-thiocitrulline: a new class of potent nitric oxide synthase inhibitors. *J. Med. Chem.* **1994**, 37, 885-887.
169. Ijuin, R.; Umezawa, N.; Nagai, S.; Higuchi, T. Evaluation of 3-substituted arginine analogs as selective inhibitors of human nitric oxide synthase isozymes. *Bioorg. Med. Chem. Lett.* **2005**, 15, 2881-2885.
170. Martell, J. D.; Li, H.; Doukov, T.; Martásek, P.; Roman, L. J.; Soltis, M.; Poulos, T. L.; Silverman, R. B. Heme-coordinating inhibitors of neuronal nitric oxide synthase. Iron−thioether coordination is stabilized by hydrophobic contacts without increased inhibitor potency. *J. Am. Chem. Soc.* **2010**, 132, 798-806.
171. Mukherjee, P.; Cinelli, M. A.; Kang, S.; Silverman, R. B. Development of nitric oxide synthase inhibitors for neurodegeneration and neuropathic pain. *Chem. Soc. Rev.* **2014**, 43, 6814-6838.
172. Park, J. M.; Higuchi, T.; Kikuchi, K.; Urano, Y.; Hori, H.; Nishino, T.; Aoki, J.; Inoue, K.; Nagano, T. Selective inhibition of human inducible nitric oxide synthase by *S*-alkyl-L-isothiocitrulline-containing dipeptides. *Br. J. Pharmacol.* **2001**, 132, 1876-1882.

173. Thiemermann, C.; Mustafa, M.; Mester, P. A.; Mitchell, J. A.; Hecker, M.; Vane, J. R. Inhibition of the release of endothelium-derived relaxing factor in vitro and in vivo by dipeptides containing N^G-nitro-L-arginine. *Br. J. Pharmacol.* **1991**, 104, 31-38.

174. Silverman, R. B.; Huang, H.; Marletta, M.; Martásek, P. Selective inhibition of neuronal nitric oxide synthase by N^{ω}-nitroarginine-and phenylalanine-containing dipeptides and dipeptide esters. *J. Med. Chem.* **1997**, 40, 2813-2817.

175. Hah, J.-M.; Roman, L. J.; Martásek, P.; Silverman, R. B. Reduced amide bond péptidomimetics. (4*S*)-*N*-(4-Amino-5-[aminoalkyl]aminopentyl)-*N'*-nitroguanidines, potent and highly selective inhibitors of neuronal nitric oxide synthase. *J. Med. Chem.* **2001**, 44, 2667-2670.

176. Gómez-Vidal, J. A.; Martásek, P.; Roman, L. J.; Silverman, R. B. Potent and selective conformationally restricted neuronal nitric oxide synthase inhibitors. *J. Med. Chem.* **2004**, 47, 703-710.

177. Seo, J.; Martásek, P.; Roman, L. J.; Silverman, R. B. Selective L-nitroargininylaminopyrrolidine and L-nitroargininylaminopiperidine neuronal nitric oxide synthase inhibitors. *Bioorg. Med. Chem.* **2007**, 15, 1928-1938.

178. Hah, J.-M.; Martásek, P.; Roman L. J.; Silverman, R. B. Aromatic reduced amide bond péptidomimetics as selective inhibitors of neuronal nitric oxide synthase. *J. Med. Chem.* **2003**, 46, 1661-1669.

179. Flinspach, M. L.; Li, H.; Jamal, J.; Yang, W.; Huang, H.; Hah, J.-M.; Gómez-Vidal, J. A.; Litzinger, E. A.; Silverman, R. B.; Poulos, T. L. Structural basis for dipeptide amide isoform-selective inhibition of neuronal nitric oxide synthase. *Nat. Struct. Mol. Biol.* **2004**, 11, 54-59.

180. McCall, T. B.; Feelisch, M.; Palmer, R. M. J.; Moncada, S. Identification of *N*-iminoethyl-L-ornithine as an irreversible inhibitor of nitric oxide synthase in phagocytic cells. *Br. J. Pharmacol.* **1991**, 102, 234-238.

181. McCall, T. B.; Feelisch, M.; Palmer, R. M. J.; Moncada, S. Identification of *N*-iminoethyl-L-ornithine as an irreversible inhibitor of nitric oxide synthase in phagocytic cells. *Br. J. Pharmacol.* **1991**, 102, 234-238.
182. Babu, B. R.; Griffith, O. W. *N*-5-(1-Imino-3-butenyl)-L-ornithine. A neuronal isoform selective mechanism-based inactivator of nitric oxide synthase. *J. Biol. Chem.* **1998**, 273, 8882-8889.
183. Hallinan, E. A.; Tsymbalov, S.; Finnegan, P. M.; Moore, W. M.; Jerome, G. M.; Currie, M. G.; Pitzele, B. S. Acetamidine lysine derivative, *N*-(5(*S*)-amino-6,7-dihydroxyheptyl)-ethanimidamide dihydrochloride: a highly selective inhibitor of human inducible nitric oxide synthase. *J. Med. Chem*. **1998**, 41, 775-777.
184. Young, R. J.; Beams, R. M.; Carter, K.; Clark, H. A. R.; Coe, D. M.; Chambers, C. L.; Davies, B. I.; Dawson, J.; Drysdale, M. J.; Franzman, K. W.; French, C.; Hodgson, S.T.; Hodson, H. F.; Kleanthous, S.; Rider, P.; Sanders, D.; Sawyer, D. A.; Scott, K. J.; Shearer, B. G.; Stocker, R.; Smith, S.; Tackley, M. C.; Knowles, R. G. Inhibition of inducible nitric oxide synthase by acetamidine derivatives of hetero-substituted lysine and homolysine. *Bioorg. Med. Chem. Lett*. **2000**, 10, 597-600.
185. Alderton, W. K.; Angell, A. D. R.; Craig, C.; Dawson, J.; Garvey, E.; Moncada, S.; Monkhouse, J.; Rees, D.; Russell, L. J.; Russell, R. J.; Schwartz, S.; Waslidge, N.; Knowles, R. G. GW274150 and GW273629 are potent and highly selective inhibitors of inducible nitric oxide synthase in vitro and in vivo. *Br. J. Pharmacol.* **2005**, 145, 301-312.
186. Ijuin, R.; Umezawa, N.; Higuchi, T. Design, synthesis, and evaluation of new type of L-amino acids containing pyridine moiety as nitric oxide synthase inhibitor. *Bioorg. Med. Chem.* **2006**, 14, 3563-3570.
187. Lee, Y.; Marletta, M. A.; Martasek, P.; Roman, L. J.; Masters, B. S. S.; Silvermann, R. B. Conformationally-restricted arginine analogues as

alternative substrates and inhibitors of nitric oxide synthases. *Bioorg. Med. Chem.* **1999**, 7, 1097-1104.

188. Ulhaq, S.; Chinje, E. C.; Naylor, M. A.; Jaffar, M.; Stratford, I. J.; Threadgill, M. D. S-2-Amino-5-azolylpentanoic acids related to L-ornithine as inhibitors of the isoforms of nitric oxide synthase (NOS). *Bioorg. Med. Chem.* **1998**, 6, 2139-2149.
189. Lee, Y.; Martásek, P.; Roman, L. J.; Masters, B. S. S.; Silverman, R. B. Imidazole-containing amino acids as selective inhibitors of nitric oxide synthases. *Bioorg. Med. Chem.* **1999**, 7, 1941-1951.
190. Shearer, B. G.; Lee, S.; Oplinger, J. A.; Frick, W.; Garvey, E. P.; Furfine, E. S. Substetuted *N*-phenylisothioureas: potent inhibitors of human nitric oxide synthase with neuronal isoform selectivity. *J. Med. Chem.* **1997**, 40, 1901-1905.
191. Garvey, E. P.; Oplinger, J. A.; Tanoury, G. J.; Sherman, P. A.; Fowler, M.; Marshall, S.; Harmon, M. F.; Furfine, E. S. Potent and selective inhibition of human nitri oxide synthase. Inhibition by non-amino acid isothioureas. *J. Biol. Chem.* **1994**, 269, 26669-26676.
192. Garvey, E. P.; Oplinger, J. A.; Furfine, E. S.; Kiff, R. J.; Laszlo, F.; Whittle, B.; Knowles, R. 1400W is a slow, tight binding, and highly selective inhibitor of inducible nitric oxide synthase in vitro and in vivo. *J. Biol. Chem.* **1997**, 272, 4959-4963.
193. Collins, J. L.; Shearer, B. G.; Oplinger, J. A.; Lee, S.; Garvey, E. P.; Salter, M.; Duffy, C.; Burnette, T. C.; Furfine, E. S. *N*- Phenylamidines as selective inhibitors of human neuronal nitric oxide synthase: structure-activity studies and demonstration of in vivo activity. *J. Med. Chem.* **1998**, 41, 2858-2871.
194. Maccallini, C.; Patruno, A.; Bešker, N.; Alì, J. I.; Ammazzalorso, A.; De Filippis, B.; Franceschelli, S.; Giampietro, L.; Pesce, M.; Reale, M.; Tricca, M. L.; Re, N.; Felaco, M.; Amoroso, R. Synthesis, biological evaluation, and docking studies of *N*-substituted acetamidines as

selective inhibitors of inducible nitric oxide synthase. *J. Med. Chem.* **2009**, 52, 1481-1485.

195. Fantacuzzi, M.; Maccallini, C.; Lannutti, F.; Patruno, A.; Masella, S.; Pesce, M.; Speranza, L.; Ammazzalorso, A.; De Filippis, B.; Giampietro, L.; Re, N.; Amoroso, R. Selective inhibition of iNOS by benzyl- and dibenzyl derivatives of *N*-(3-aminobenzyl)acetamidine. *ChemMedChem* **2011**, 6, 1203-1206.
196. Maccallini, C.; Montagnani, M.; Paciotti, R.; Ammazzalorso, A.; De Filippis, B.; Di Matteo, M.; Di Silvestre, S.; Fantacuzzi, M.; Giampietro, L.; Potenza, M. A.; Re, N.; Pandolfi, A.; Amoroso, R. Selective acetamidine-based nitric oxide synthase inhibitors: synthesis, docking and biological studies. *ACS Med. Chem. Lett.* **2015**, 6, 635-640.
197. Naka, M.; Nanbu, T.; Kobayashi, K.; Kamanaka, Y.; Komeno, M.; Yanase, R.; Fukutomi, T.; Fujimura, S.; Geuk Seo, H.; Fujiwara, N.; Ohuchida, S.; Suzuki, K.; Kondo, K.; Taniguchi, N. A Potent inhibitor of inducible nitric oxide synthase, ONO-1714, a cyclic amidine derivative. *Biochem. Biophys. Res. Com.* **2000**, 270, 663-667.
198. Moormanna, A. E.; Metza, s.; Totha, M. V.; Mooreb, W. M.; Jeromeb, G.; Kornmeierb, C.; Manningb, P.; Hansen Jr., D. W.; Pitzelec, B. S.; Webbera, R. K. Selective heterocyclic amidine inhibitors of human inducible nitric oxide synthase. *Bioorg. Med. Chem. Lett.* **2001**, 11, 2651-2653.
199. Tsymbalov, S.; Hagen, T. J.; Moore, W. M.; Jerome, G. M.; Connor, J. R.; Manning, P. T.; Pitzelea, B. S.; Hallinan, E. A. 3-Hydroxy-4-methyl-5-pentyl-2-iminopyrrolidine: a potent and highly selective inducible nitric oxide synthase inhibitor. *Bioorg. Med. Chem. Lett.* **2002**, 12, 3337-3339.
200. Hagmann, W. K.; Caldwell, C. G.; Chen, P.; Durette, P. L.; Esser, C. K.; Lanza, T. J.; Kopkaa, I. E.; Guthikondaa, R.; Shaha, S. K.; MacCossa, M.; Chabinb, R. M.; Fletcherd, D.; Grantb, S. K.; Greenb, B. G.; Humesc, J. L.; Kellyb, T. M.; Luelld, S.; Meurerd, R.; Moored, V.;

Pacholokc, S. G.; Paviab, T.; Williams, H. R.; Wong, K. K. Substituted 2-aminopyridines as inhibitors of nitric oxide synthases. *Bioorg. Med. Chem. Lett.* **2000**, 10, 1975-1978.

201. Beaton, H.; Hamley, P.; Nicholls, D. J.; Tinker, A. C.; Wallace, A. V. 3, 4-Dihydro-1-isoquinolinamines: a novel class of nitric oxide synthase inhibitors with a range of isoform selectivity and potency. *Bioorg. Med. Chem. Lett.* **2001**, 11, 1023-1026.
202. Beaton, H.; Boughton-Smith, N.; Hamley, P.; Ghelani, A.; Nicholls, D. J.; Tinker, A. C.; Wallace, A. V. Thienopyridines: Nitric oxide synthase inhibitors with potent in vivo activity. *Bioorg. Med. Chem. Lett.* ***2001***, 11, 1027-1030.
203. Tinker, A. C.; Beaton, H. G.; Boughton-Smith, N.; Cook, T. R.; Cooper, S. L.; Fraser-Rae, L.; Hallam , K.; Hamley , P.; McInally, T.; Nicholls , D. J.; Pimm , A. D.; Wallace, A. V. 1, 2-Dihydro-4-quinazolinamines: potent, highly selective inhibitors of inducible nitric oxide synthase which show antiinflammatory activity in vivo. *J. Med. Chem.* **2003**, 46, 913-916.
204. Ji, H.; Li, H.; Martásek, P.; Roman, L. J.; Poulos, T. L.; Silverman, R. B. Discovery of highly potent and selective inhibitors of neuronal nitric oxide synthase by fragment hopping. *J. Med. Chem.* **2009**, 52, 779-797.
205. Ji, H.; Delker, S. L.; Li, H.; Martásek, P.; Roman, L. J.; Poulos, T. L.; Silverman, R. B. Exploration of the active site of neuronal nitric oxide synthase by the design and synthesis of pyrrolidinomethyl 2-aminopyridine derivatives. *J. Med. Chem.* **2010**, 53, 7804-7824.
206. Xue, F.; Li, H.; Fang, J.; Roman, L. J.; Martásek, P.; Poulos, T. L.; Silverman, R. B. Peripheral but crucial: A hydrophobic pocket (Tyr 706, Leu 337, and Met 336) for potent and selective inhibition of neuronal nitric oxide synthase. *Bioorg. Med. Chem. Lett.* **2010**, 20, 6258-6261.
207. Ji, H.; Tan, S.; Igarashi, J.; Li, H.; Derrick, M.; Martásek, P.; Roman, L. J.; Vásquez-Vivar, J.; Poulos, T. L.; Silverman, R. B. Selective

neuronal nitric oxide synthase inhibitors and the prevention of cerebral palsy. *Ann. Neurol.* **2009**, 65, 209-217.

208. Xue, F.; Fang, J.; Lewis, W. W.; Martásek, P.; Roman, L. J.; Silverman, R. B. Potent and selective neuronal nitric oxide synthase inhibitors with improved cellular permeability. *Bioorg. Med. Chem. Lett.* **2010**, 20, 554-557.
209. Xue, F.; Li, H.; Delker, S. L.; Fang, J.; Martásek, P.; Roman, L. J.; Poulos, T. L.; Silverman, R. B. Potent, highly selective, and orally bioavailable gem-difluorinated monocationic inhibitors of neuronal nitric oxide synthase. *J. Am. Chem. Soc.* **2010**, 132, 14229-14238.
210. Labby, K. J.; Xue, F.; Kraus, J. M.; Ji, H.; Mataka, J.; Li, H.; Mártasek, P.; Roman, L. J.; Poulos, T. L.; Silverman, R. B. Intramolecular hydrogen bonding: a potential strategy for more bioavailable inhibitors of neuronal nitric oxide synthase. *Bioorg. Med. Chem.* **2012**, 20, 2435-2443.
211. Xue, F.; Huang, J.; Ji, H.; Fang, J.; Li, H.; Martásek, P.; Roman, L. J.; Poulos, T. L.; Silverman, R. B. Structure-based design, synthesis, and biological evaluation of lipophilic-tailed monocationic inhibitors of neuronal nitric oxide synthase. *Bioorg. Med. Chem.* **2010**, 18, 6526-6537.
212. Li, H.; Xue, F.; Kraus, J. M.; Ji, H.; Labby K. J.; Mataka, J.; Delker, S. L.; Martásek, P.; Silverman, R. B. Cyclopropyl- and methyl-containing inhibitors of neuronal nitric oxide synthase. *Bioorg. Med. Chem.* **2013**, 21, 1333-1343.
213. Silverman, R. B.; Lawton, G. R.; Ranaivo, H. R.; Chico, L. K.; Seo, J.; Watterson, D. M. Effect of potential amine prodrugs of selective neuronal nitric oxide synthase inhibitors on blood–brain barrier penetration. *Bioorg. Med. Chem.* **2009**, 17, 7593-7605.
214. Lawton, G. R.; Ji, H.; Martásek, P.; Roman, L. J.; Silverman, R. B. Synthesis and enzymatic evaluation of 2-and 4-aminothiazole-based

inhibitors of neuronal nitric oxide synthase. *Beilstein J. Org. Chem.* **2009**, 5 (1), 28.

215. Lawton, G. R.; Ranaivo, H. R.; Chico, L. K.; Ji, H.; Xue, F.; Martásek, P.; Roman, L. J.; Watterson, D. M.; Silverman, R. B. Analogues of 2-aminopyridine-based selective inhibitors of neuronal nitric oxide synthase with increased bioavailability. *Bioorg. Med. Chem.* **2009**, 17, 2371-2380.
216. Ji, H.; Li, H.; Martásek, P.; Roman, L. J.; Poulos, T. L.; Silverman, R. B. Discovery of highly potent and selective inhibitors of neuronal nitric oxide synthase by fragment hopping. *J. Med. Chem.* **2009**, 52, 779-797.
217. Xue, F.; Fang, J.; Lewis, W. W.; Martásek, P.; Roman, L. J.; Silverman, R. B. Potent and selective neuronal nitric oxide synthase inhibitors with improved cellular permeability. *Bioorg. Med. Chem. Lett.* **2010**, 20, 554-557.
218. Xue, F.; Fang, J.; Delker, S. L.; Li, H.; Martásek, P.; Roman, L. J.; Poulos, T. L.; Silverman, R. B. Symmetric double-headed aminopyridines, a novel strategy for potent and membrane-permeable inhibitors of neuronal nitric oxide synthase. *J. Med. Chem.* **2011**, 54, 2039-2048.
219. Huang, H.; Li, H.; Martásek, P.; Roman, L. J.; Poulos, T. L.; Silverman, R. B. Structure-guided design of selective inhibitors of neuronal nitric oxide synthase. *J. Med. Chem.* **2013**, 56, 3024-3032.
220. Yang, Y.; Yu, T.; Lian, Y. J.; Ma, R.; Yang, S.; Cho, J. Y. Nitric oxide synthase inhibitors: a review of patents from 2011 to the present. *Expert Opin. Ther. Patents* **2015**, 25, 49-68.
221. Jing, Q.; Li, H.; Roman, L. J.; Martásek, P.; Poulos, T. L.; Silverman, R. B. Accessible chiral linker to enhance potency and selectivity of neuronal nitric oxide synthase inhibitors. *ACS med. Chem. Lett.* **2013**, 5, 56-60.

222. Kang, S.; Tang, W.; Li, H.; Chreifi, G.; Martásek, P.; Roman, L. J.; Poulos, T. L.; Silverman, R. B. Nitric oxide synthase inhibitors that interact with both heme propionate and tetrahydrobiopterin show high isoform selectivity. *J. Med. Chem.* **2014***,* 57, 4382-4396.

223. Reif, D. W.; McCarthy, D. J.; Cregan, E.; Macdonald, J. E. Discovery and development of neuronal nitric oxide synthase inhibitors. *Free Radical Bio. Med.* **2000**, 28, 1470-1477.

224. Cheshire, D. R.; Åberg, A.; Andersson, G. M.; Andrews, G.; Beaton, H. G.; Birkinshaw, T. N.; Boughton-Smith, N.; Connolly, S.; Cook, T. R.; Cooper, A.; Cooper, S. L.; Cox, D.; Dixon, J.; Gensmantel, N.; Hamley, P. J.; Harrison, R.; Hartopp, P.; Käck, H.; Leeson, P. D.; Luker, T.; Mete, A.; Millichip, I.; Nicholls, D. J.; Pimm, A. D.; St-Gallay, S. A.; Wallace, A. V. The discovery of novel, potent and highly selective inhibitors of inducible nitric oxide synthase (iNOS). *Bioorg. Med. Chem. Lett.* **2011**, 21, 2468-2471.

225. Liang, G.; Neuenschwander, K.; Chen, X.; Wei, L.; Munson, R.; Francisco, G.; Scotese, A.; Shutske, G.; Black, M.; Sarhan, S.; Jiang, J.; Morize, I.; Vaz, R. J. Structure-based design, synthesis, and profiling of potent and selective neuronal nitric oxide synthase (nNOS) inhibitors with an amidinothiophene hydroxypiperidine scaffold. *MedChemComm* **2011**, 2, 201-205.

226. Ramnauth, J.; Speed, J.; Maddaford, S. P.; Dove, P.; Annedi, S. C.; Renton, P.; Rakhit, S.; Andrews, J.; Silverman, S.; Mladenova, G.; Zinghini, S.; Nair, S.; Catalano, C.; Lee, D. K. H.; De Felice, M.; Porreca, F. Design, synthesis, and biological evaluation of 3,4-dihydroquinolin-2(1*H*)-one and 1,2,3,4-tetrahydroquinoline-based selective human neuronal nitric oxide synthase (nNOS) inhibitors. *J. Med. Chem.* **2011**, 54, 5562-5575.

227. Ramnauth, J.; Renton, P.; Dove, P.; Annedi, S. C.; Speed, J.; Silverman, S.; Mladenova, G.; Maddaford, S. P.; Zinghini, S.; Rakhit, S.; Andrews, J.; Lee, D. K. H.; Zhang D.; Porreca, F. 1,2,3,4-

tetrahydroquinoline-based selective human neuronal nitric oxide synthase (nNOS) inhibitors: lead optimization studies resulting in the identification of N-(1-(2-(methylamino) ethyl)-1,2, 3,4-tetrahydroquinolin-6-yl)thiophene-2-carboximidamide as a preclinical development candidate. *J. Med. Chem.* **2012**, 55, 2882-2893.

228. Patman, J.; Bhardwaj, N.; Ramnauth, J.; Annedi, S. C.; Renton, P.;Maddaford, S. P.; Rakhit S.; Andrews, J. S. Novel 2-aminobenzothiazoles as selective neuronal nitric oxide synthase inhibitors. *Bioorg. Med. Chem. Lett.* **2007**, 17, 2540-2544.
229. Annedi, S. C.; Ramnauth, J.; Cossette, M.; Maddaford, S. P.; Dove, P.; Rakhit, S.; Andrews, J. S.; Porreca, F. Novel, druglike 1,7-disubstituted-2,3,4,5-tetrahydro-1*H*-benzo[b]azepine-based selective inhibitors of human neuronal nitric oxide synthase (nNOS). *Bioorg. Med. Chem. Lett.* **2012**, 22, 2510-2513.
230. Annedi, S. C.; Maddaford, S. P.; Ramnauth, J.; Renton, P.; Speed, J.; Rakhit, S.; Andrews J. S.; Porreca, F. 3,5-Disubstituted indole derivatives as selective human neuronal nitric oxide synthase (nNOS) inhibitors. *Bioorg. Med. Chem. Lett.* **2012**, 22, 1980-1984.
231. Annedi, S. C.; Maddaford, S. P.; Mladenova, G.; Ramnauth, J.; Rakhit, S.; Andrews, J. S.; Lee, D. H. K.; Zhang, D.; Porreca, F. Bunton D. and Christie, L. Discovery of N-(3-(1-methyl-1,2,3,6-tetrahydropyridin-4-yl)-1 H-indol-6-yl)thiophene-2-carboximidamide as a selective inhibitor of human neuronal nitric oxide synthase (nNOS) for the treatment of pain. *J. Med. Chem.* **2011**, 54, 7408-7416.
232. Maddaford, S.; Renton, P.; Speed, J.; Annedi, S. C.; Ramnauth, J.; Rakhit, S.; Andrews, J.; Mladenova, G.; Majuta L.; Porreca, F. 1,6-Disubstituted indole derivatives as selective human neuronal nitric oxide synthase inhibitors. *Bioorg. Med. Chem. Lett.* **2011**, 21, 5234-5238.
233. Renton, P.; Speed, J.; Maddaford, S.; Annedi, S. C.; Ramnauth, J.; Rakhit S.; Andrews, J. 1, 5-Disubstituted indole derivatives as selective

human neuronal nitric oxide synthase inhibitors. *Bioorg. Med. Chem. Lett.* **2011**, 21, 5301-5304.

234. Annedi, S. C.; Maddaford, S. P.; Ramnauth, J.; Renton, P.; Rybak, T.; Silverman, S.; Rakhit, S.; Mladenova, G.; Dove, P.; Andrews, J. S.; Zhang D.; Porreca, F.; Porreca, F. Discovery of a potent, orally bioavailable and highly selective human neuronal nitric oxide synthase (nNOS) inhibitor, N-(1-(piperidin-4-yl)indolin-5-yl)thiophene-2-carboximidamide as a pre-clinical development candidate for the treatment of migraine. *Eur. J. Med. Chem.* **2012**, 55, 94-107.
235. Annedi, S. C.; Ramnauth, J.; Maddaford, S. P.; Renton, P.; Rakhit, S.; Mladenova, G.; Dove, P.; Silverman, S.; Andrews, J. S.; De Felice, F.; Porreca, M. Discovery of cis-N-(1-(4-(methylamino) cyclohexyl)indolin-6-yl)thiophene-2-carboximidamide: a 1,6-disubstituted indoline derivative as a highly selective inhibitor of human neuronal nitric oxide synthase (nNOS) without any cardiovascular liabilities. *J. Med. Chem.* **2012**, 55, 943-955.
236. Grädler, U.; Fuchss, T.; Ulrich, W. R.; Boer, R.; Strub, A.; Hesslinger, C.; Anézo, C.; Diederichs, K.; Zaliani, A. Novel nanomolar imidazo[4,5-b]pyridines as selective nitric oxide synthase (iNOS) inhibitors: SAR and structural insights. *Bioorg. Med. Chem. Lett.* **2011**, 21, 4228-4232.
237. Moore, P. K.; Babbedge, R. C.; Wallace, P.; Gaffen, Z. A.; Hart, S. L. 7-Nitroindazole, an inhibitor of nitric oxide synthase, exhibits anti-nociceptive activity in the mouse without increasing blood pressure. *Br. J. Pharmacol.* **1993**, 108, 296-297.
238. Moore, P. K.; Wallace, P.; Gaffen, Z.; Hart, S. L.; Babbedge, R. C. Characterization of the novel nitric oxide synthase inhibitor 7-nitro indazole and related indazoles: antinociceptive and cardiovascular effects. *Br. J. Pharmacol.* **1993**, 110, 219-224.
239. Bland-Ward, P. A.; Moore, P. K. 7-Nitro indazole derivatives are potent inhibitors of brain, endothelium and inducible isoforms of nitric oxide synthase. *Life Sci.* **1995**, 57, PL131-135.

240. Handy, R. L. C.; Moore, P. K. Mechanism of the inhibition of neuronal nitric oxide synthase by 1-(2-trifluoromethylphenyl)imidazole (TRIM). *Life Sci.* **1997**, 60, PL389-394.

241. Sorrenti, V.; Salerno, L.; Di Giacomo, C.; Acquaviva, R.; Siracusa, M. A.; Vanella, A. Imidazole derivatives as antioxidants and selective inhibitors of nNOS. *Nitric Oxide* **2006**, 14, 45-50.

242. Werner, E.; Pitters, E.; Schmidt, K.; Wachter, H.; Werner-Felmayer, G.; Mayer, B. Identification of the 4-amino analogue of tetrahydrobiopterin as a dihydropteridine reductase inhibitor and a potent pteridine antagonist of rat neuronal nitric oxide synthase. *Biochem. J.* **1996**, 320, 193-196.

243. Fröhlich, L. G.; Kotsonis, P.; Traub, H.; Taghavi-Moghadam, S.; Al-Masoudi, N.; Hofmann, H.; Strobel, H.; Matter, H.; Pfleiderer W.; Schmidt, H. H. Inhibition of neuronal nitric oxide synthase by 4-amino pteridine derivatives: structure-activity relationship of antagonists of (6*R*)-5,6,7,8-tetrahydrobiopterin cofactor. *J. Med. Chem.* **1999**, 42, 4108-4121.

244. Palumbo, A.; d'Ischia, M.; Cioffi, F. A. 2-Thiouracil is a selective inhibitor of neuronal nitric oxide synthase antagonising tetrahydrobiopterin-dependent enzyme activation and dimerisation. *FEBS Lett.* **2000**, 485, 109-112.

245. McMillan, K.; Adler, M.; Auld, D. S.; Baldwin, J. J.; Blasko, E.; Browne, L. J.; Chelsky, D.; Davey, D.; Dolle, R. E.; Eagen, K. A.; Erickson, S.; Feldman, R. I.; Glaser, C. B.; Mallari, C.; Morrissey, M. M.; Ohlmeyer, M. H. J.; Pan, G.; Párkinson, J. F.; Phillips, G. B.; Polokoff, M. A.; Sigal, N. H.; Vergona, R.; Whitlow, M.; Young T. A.; Devlin, J. J. Allosteric inhibitors of inducible nitric oxide synthase dimerization discovered via combinatorial chemistry. *Proc. Natl. Acad. Sci. USA* **2000**, 97, 1506-1511.

246. Habisch, H. J.; Gorren, A. C.; Liang, H.; Venema, R. C.; Párkinson, J. F.; Schmidt, K.; Mayer, B. Pharmacological interference with

dimerization of human neuronal nitric-oxide synthase expressed in adenovirus-infected DLD-1 cells. *Mol. Pharmacol.* **2003**, 63, 682-689.

247. Bonnefous, C.; Payne, J. E.; Roppe, J.; Zhuang, H.; Chen, X.; Symons, K. T.; Nguyen, P. M.; Sablad, M.; Rozenkrants, N.; Zhang, Y.; Wang, L.; Severance, D.; Walsh, J. P.; Yazdani, N.; Shiau, A. K.; Noble, S. A.; Rix, P.; Rao, T. S.; Hassig, C. A.; Smith, N. D. Discovery of inducible nitric oxide synthase (iNOS) inhibitor development candidate KD7332, part 1: Identification of a novel, potent, and selective series of quinolinone iNOS dimerization inhibitors that are orally active in rodent pain models. *J. Med. Chem.* **2009**, 52, 3047-3062.
248. Payne, J. E.; Bonnefous, C.; Symons, K. T.; Nguyen, P. M.; Sablad, M.; Rozenkrants, N.; Zhang, Y.; Wang, L.; Yazdani, N.; Shiau, A. K.; Noble, S. A.; Rix, P.; Rao, T. S.; Hassig, C. A.; Smith, N. D. Discovery of dual inducible/neuronal nitric oxide synthase (iNOS/nNOS) inhibitor development candidate 4-((2-cyclobutyl-1*H*-imidazo[4,5-b]pyrazin-1-yl) methyl)-7,8-difluoroquinolin-2(1*H*)-one (KD7332) part 2: Identification of a novel, potent, and selective series of benzimidazole-quinolinone iNOS/nNOS dimerization inhibitors that are orally active in pain models. *J. Med. Chem.* **2010**, 53, 7739-7755.
249. Symons, K. T.; Nguyen, P. M.; Massari, M. E.; Anzola, J. V.; Staszewski, L. M.; Wang, L.; Yazdani, N.; Dorow, S.; Muhammad, J.; Sablad, M.; Rozenkrants, N.; Bonefous, C.; Payne, J. E.; Rix, P. J.; Shiau, A. K.; Noble, S. A.; Smith, N. D.; Hassig, C. A.; Zhang Y.; Rao, T. S. Pharmacological characterization of KLYP961, a dual inhibitor of inducible and neuronal nitric-oxide synthases. *J. Pharmacol. Exp. Ther.* **2011**, 336, 468-478.
250. Wolff, D. J.; Datto, G. A.; Samatovicz, R. A. The dual mode of inhibition of calmodulin-dependent nitric-oxide synthase by antifungal imidazole agents. *J. Biol. Chem.* **1993**, 268, 9430-9436.

251. Wolff, D. J.; Gribin, B. J. Interferon-γ-inducible murine macrophage nitric-oxide synthase: studies on the mechanism of inhibition by imidazole agents. *Arch. Biochem. Biophys.* **1994**, 311, 293-299.
252. Kuroda, S.; Nakai, A.; Kristían, T.; Siesjö, B. K. The calmodulin antagonist trifluoperazine in transient focal brain ischemia in rats anti-ischemic effect and therapeutic window. *Stroke* **1997**, 28, 2539-2544.
253. Sato, T.; Morishima, Y.; Sugimura, M.; Uchida, T.; Shirasaki, Y. DY-9760e, a novel calmodulin antagonist, reduces brain damage induced by transient focal cerebral ischemia. *Eur. J. Pharmacol.* **1999**, 370, 117-123.
254. Takagi, K.; Sato, T.; Shirasaki, Y.; Narita, K.; Tamura, A.; Sano, K. Post-ischemic administration of DY-9760e, a novel calmodulin antagonist, reduced infarct volume in the permanent focal ischemia model of spontaneously hypertensive rat. *Neurol. Res.* **2001**, 23, 662-668.
255. Marco, M.; Vicenzo, P.; Gilberto, S.; Tarzia, G. Medicinal chemistry feature molecule. Guest Editor: Matthew J. Dowd. *Curr. Med. Chem.* **1999**, 6, 501-518.
256. Pozo, D.; Reiter, R. J.; Calvo, J. R.; Guerrero, J. M. Physiological concentrations of melatonin inhibit nitric oxide synthase in rat cerebellum. *Life Sci.* **1994**, 55, 455-460.
257. Bettahi, I.; Pozo, D.; Osuna, C.; Reiter, R. J.; Acuña-Castroviejo, D.; Guerrero, J. Melatonin reduces nitric oxide synthase activity in rat hypothalamus. *J. Pineal Res.* **1996**, 20, 205-210.
258. Leon, J.; Vives, F.; Crespo, E.; Camacho, E.; Espinosa, A.; Gallo, M. A.; Escames, G.; Acuña-Castroviejo, D. Modification of nitric oxide synthase activity and neuronal response in rat striatum by melatonin and kynurenine derivatives. *J. Neuroendocrinol.* **1998**, 10, 297-302.
259. León, J.; Macias, M.; Escames, G.; Camacho, E.; Khaldy, H.; Martin, M.; Epinosa, A.; Gallo, M. A.; Acuña-Castroviejo, D. Structure-related inhibition of calmodulin-dependent neuronal nitric-oxide synthase

activity by melatonin and synthetic kynurenines. *Mol. Pharmacol.* **2000**, 58, 967-975.

260. Hirata, F.; Hayaishi, O.; Tokuyama, T.; Seno, S. In vitro and in vivo formation of two new metabolites of melatonin. *J. Biol. Chem.* **1974**, 249, 1311-1313.
261. Camacho, M. E.; León, J.; Carrión, M. D.; Entrena, A.; Escames, G.; Khaldy, H.; Castroviejo-Acuña, D.; Gallo, M. A.; Espinosa, A. Inhibition of nNOS activity in rat brain by synthetic kynurenines: Structure-activity dependence. *J. Med. Chem.* **2002**, 45, 263-274.
262. León, K.; Vives, F.; Gomez, I.; Camacho, E.; Gallo, M. A.; Epinosa, A.; Escames, G.; Acuña-Castroviejo, D. Modulation of rat striatal glutamatergic response in search for new neuroprotective agents: evaluation of melatonin and some kynurenine derivatives. *Brain. Res. Bull.* **1998**, 45, 525-530.
263. Entrena, A.; Camacho, M. E.; Carrión, M. D.; López-Cara, L. C.; Velasco, G.; León, J.; Escames, G.; Castroviejo-Acuña, D.; Tapias, V.; Gallo, M. A.; Vivó, A.; Espinosa, A. Kynurenamines as neural nitric oxide synthase inhibitors. *J. Med. Chem.* **2005**, 48, 8174-8181.
264. Camacho, M. E.; León, J.; Entrena, A.; Velasco, G.; Carrión, M. D.; Escames, G.; Vivó, A.; Acuña-Castroviejo, D.; Gallo, M. A.; Espinosa, A. 4,5-Dihydro-1-*H*-pyrazole derivatives with inhibitory nNOS activity in rat brain: synthesis and structure-activity relationships. *J. Med. Chem.* **2004**, 47, 5641-5650.
265. Carrión, M. D.; Camacho, M. E.; León, J.; Escames, G.; Tapias, V.; Acuña-Castroviejo, D.; Gallo, M. A.; Espinosa, A. Synthesis and iNOS/nNOS inhibitory activities of new benzoylpyrazoline derivatives. *Tetrahedron* **2004**, 60, 4051-4069.
266. Carrión, M. D.; López-Cara, L. C.; Camacho, M. E.; Tapias, V.; Escames, G.; Acuña-Castroviejo, D.; Espinosa, A.; Gallo, M. A.; Entrena, A. Pyrazoles and pyrazolines as neural and inducible nitric

oxide synthase (nNOS and iNOS) potential inhibitors (III). *Eur. J. Med. Chem.* **2008**, 43, 2579-2591.

267. López-Cara, L. C.; Camacho, M. E.; Carrión, M. D.; Tapias, V.; Gallo, M. A.; Escames, G.; Acuña-Castroviejo, D.; Espinosa, A.; Entrena, A. Phenylpyrrole derivatives as neural and inducible nitric oxide synthase (nNOS and iNOS) inhibitors. *Eur. J. Med. Chem.* **2009**, 44, 2655-2666.
268. López-Cara, L. C.; Carrión, M. D.; Entrena, A.; Gallo, M. A.; Espinosa, A.; López, A.; Escames, G.; Acuña-Castroviejo, D.; Camacho, M. E. 1,3,4-Thiadiazole derivatives as selective inhibitors of iNOS versus nNOS: Synthesis and structure-activity dependence. *Eur. J. Med. Chem.* **2012**, 50, 129-139.